# Advances in Clinical and Experimental Medicine

MONTHLY ISSN 1899-5276 (PRINT) ISSN 2451-2680 (ONLINE) www.advances.umw.edu.pl

2022, Vol. 31, No. 5 (May)

Impact Factor (IF) – 1.727
Ministry of Science and Higher Education – 70 pts
Index Copernicus (ICV) – 166.39 pts

Wroclaw Medical University

Advances
in Clinical and Experimental
Medicine

# Advances
# in Clinical and Experimental Medicine

ISSN 1899-5276 (PRINT) ISSN 2451-2680 (ONLINE) www.advances.umw.edu.pl

**MONTHLY 2022**
**Vol. 31, No. 5**
**(May)**

Advances in Clinical and Experimental Medicine (*Adv Clin Exp Med*) publishes high-quality original articles, research-in-progress, research letters and systematic reviews and meta-analyses of recognized scientists that deal with all clinical and experimental medicine.

**Editorial Office**
ul. Marcinkowskiego 2–6
50-368 Wrocław, Poland
Tel.: +48 71 784 12 05
E-mail: redakcja@umw.edu.pl

**Publisher**
Wroclaw Medical University
Wybrzeże L. Pasteura 1
50-367 Wrocław, Poland

Online edition is the original version of the journal

## Editorial Policy

Advances in Clinical and Experimental Medicine (Adv Clin Exp Med) is an independent multidisciplinary forum for exchange of scientific and clinical information, publishing original research and news encompassing all aspects of medicine, including molecular biology, biochemistry, genetics, biotechnology and other areas. During the review process, the Editorial Board conforms to the "Uniform Requirements for Manuscripts Submitted to Biomedical Journals: Writing and Editing for Biomedical Publication" approved by the International Committee of Medical Journal Editors (www.ICMJE.org). The journal publishes (in English only) original papers and reviews. Short works considered original, novel and significant are given priority. Experimental studies must include a statement that the experimental protocol and informed consent procedure were in compliance with the Helsinki Convention and were approved by an ethics committee.

For all subscription-related queries please contact our Editorial Office:
redakcja@umw.edu.pl

For more information visit the journal's website:
www.advances.umw.edu.pl

Pursuant to the ordinance No. 134/XV R/2017 of the Rector of Wroclaw Medical University (as of December 28, 2017) from January 1, 2018 authors are required to pay a fee amounting to 700 euros for each manuscript accepted for publication in the journal Advances in Clinical and Experimental Medicine.

Indexed in: MEDLINE, Science Citation Index Expanded, Journal Citation Reports/Science Edition, Scopus, EMBASE/Excerpta Medica, Ulrich's™ International Periodicals Directory, Index Copernicus

Typographic design: Piotr Gil, Monika Kolęda
DTP: Wydawnictwo UMW
Cover: Monika Kolęda
Printing and binding: Soft Vision Mariusz Rajski

# Advances
## in Clinical and Experimental Medicine

MONTHLY 2022, Vol. 31, No. 5 (May)

ISSN 1899-5276 (PRINT)
ISSN 2451-2680 (ONLINE)
www.advances.umw.edu.pl


# Contents

# Aging, depression and dementia: The inflammatory process

Maria del Pilar Carrera-González[1,2,A,C,D,F], Vanesa Cantón-Habas[1,A,B,D,F], Manuel Rich-Ruiz[1,3,A,D,F]

[1] Department of Nursing, Pharmacology and Physiotherapy, Faculty of Medicine and Nursing, University of Córdoba, Maimonides Institute of Biomedical Research of Córdoba (IMIBIC), Reina Sofia University Hospital, Spain
[2] Experimental and Clinical Physiopathology Research Group CTS-1039, Department of Health Sciences, Faculty of Health Sciences, University of Jaén, Spain
[3] Centro de Investigación Biomédica en Red Fragilidad y Envejecimiento Saludable (CIBERFES), Madrid, Spain

A – research concept and design; B – collection and/or assembly of data; C – data analysis and interpretation; D – writing the article; E – critical revision of the article; F – final approval of the article

Advances in Clinical and Experimental Medicine, ISSN 1899–5276 (print), ISSN 2451–2680 (online) *Adv Clin Exp Med*. 2022;31(5):469–473

**Address for correspondence**
Vanesa Cantón-Habas
E-mail: n92cahav@uco.es

**Funding sources**
None declared

**Conflict of interest**
None declared

Received on January 11, 2022
Reviewed on May 5, 2022
Accepted on May 9, 2022

Published online on May 12, 2022

## Abstract

Population aging that we are currently witnessing has led to an increase in chronic age-related diseases, with dementia and depression being highlighted. Several studies establish a relationship between dementia and depression, although without defining the mechanism that links them. Some studies establish depression as a prodrome of dementia, while others consider it a risk factor for dementia. One of the events that is common between dementia and depression is the inflammatory process. In depression, an increase in inflammatory cytokines has been described, which would justify the serotonergic, noradrenergic and dopaminergic dysfunction of depression. This increase entails altering the activity of the hypothalamic–pituitary–adrenal (HPA) axis, thus linking chronic stress to depression, and the consequent weakening of the blood–brain barrier (BBB), facilitating the passage of pro-inflammatory factors. In this line, recent studies suggest that inflammation could direct the development of the pathogenesis of dementia, particularly Alzheimer's disease (AD), once the pathology has begun. In addition, sustained exposure to pro-inflammatory cytokines characteristic of aging could alter the microglial function and the expression of enzymes responsible for amyloid peptide metabolism, aggravating the pathological process. In view of the involvement of the inflammatory process in both conditions, it is necessary to investigate the events which both conditions share, such as the inflammatory process, to know the involvement of the inflammatory process in both dementia and depression, possible relationship of these 2 conditions, and consequently, to establish the clinical approach to both conditions.

**Key words:** dementia, Alzheimer's disease, inflammation, depression

**Cite as**
Carrera-González MP, Cantón-Habas V, Rich-Ruiz M. Aging, depression and dementia: The inflammatory process. *Adv Clin Exp Med*. 2022;31(5):469–473. doi:10.17219/acem/149897

**DOI**
10.17219/acem/149897

## Introduction

Aging is an important contributing factor in the onset and development of various neurological disorders, such as cognitive impairment or dementia. However, dementia is not a natural or inevitable consequence of aging. In fact, other clinical conditions, in this case pathological processes, have been described as being associated with an increased risk of cognitive impairment/dementia, including depression, hypertension, diabetes, hypercholesterolemia, and obesity.[1]

During aging, the brain undergoes a progressive decline in energy use,[2] and according to the free radical theory of aging, free radicals and related oxidants, both environmental and derived from cellular metabolism, would be the main cause of cellular damage, also due to their accumulation over time. Thus, the changes in energy metabolism associated with aging would be responsible for the associated functional and structural cellular problems. In other words, during the last third of our lives, our brain accumulates structural and functional damage that reduces our adaptive homeostatic capacity,[3] which possibly makes it more susceptible to harmful stimuli.

In this context, one of the most affected cell types that are susceptible to such lesions are neurons, as well as different types of glial cells. Thus, in the aging brain, there is an increase in microglia, associated with a decrease in their function. Indeed, with aging, they lose their flexibility to move, which decreases their efficiency in defending the central nervous system (CNS),[4] as well as their ability to block exogenous invasion or endogenous metabolites such as β-amyloid peptides.[5,6] In this regard, one of the most relevant facts about aged microglia is the elevated expression of pro-inflammatory molecules, such as MHC-II, CD16/32 and CD86. Even the secretion of pro-inflammatory cytokines, such as tumor necrosis factor alpha (TNF-α), interferon gamma (IFN-γ), inducible nitric oxide synthase (iNOS), interleukin-6 (IL-6), and interleukin-1β (IL-1β), increases significantly in response to harmful stimuli.[7]

A possible interpretation of this shift from a microglial profile to an inflammatory or sensitization profile is based on 3 factors: 1) the increase in inflammatory markers and mediators; 2) the decrease in threshold and activation time; and 3) the increase in response and inflammation after this activation.[8,9]

In this regard, Chung et al.[10] established how age increases this sensitized state[10,11] – microglia develop an "alert, primed" phenotype, which contributes to the increased inflammatory state of the aging brain, as indicated by the increased inflammatory mediators and altered microglia phenotype (that occurs with age/aging). In this situation, results obtained in aged rodents following immune challenge, i.e., infection, show depressive-like behavioral complications and cognitive deficits.[12]

In the case of astrocytes, during aging, they also change their secretory phenotype to a pro-inflammatory phenotype under chronic stress. Even the aforementioned oxidative stress could induce astrocytes to secrete pro-inflammatory factors, such as IL-6, monocyte chemoattractant protein (MCP)-1 and metalloproteinase (MMP)-9, contributing to the inflammation in the senile brain, and altering the integrity of the blood–brain barrier (BBB).[13]

At this point, with the disruption of BBB integrity, it is important to note the enormous importance of the BBB in maintaining metabolic homeostasis in the CNS[14] and, consequently, the increased exposure of brain tissue to toxic molecules or inflammatory signals that circulate in the blood when BBB is disrupted.

Conditions associated with impaired BBB integrity include oxidative stress,[15] the presence of advanced glycation end products (AGEs) and their receptor (RAGE),[16] increased production of pro-inflammatory cytokines,[17] and vascular dysfunction, as well as chronic stress, depression or dementia.[18,19]

Having described the role of aging as a contributing factor in various neurological disorders, such as cognitive impairment or dementia, it is necessary to understand its relationship to various clinical situations or pathological processes, including depression and dementia.

In the case of depression and dementia, we must bear in mind that there is no single mechanism that explains both pathologies, although similar neurobiological changes or even a similar pattern of neuronal damage have been described for both conditions, thus deepening our understanding of a complex relationship between both pathologies. Cognitive changes are common in the context of depression, and mood-altering symptoms of this condition often accompany cognitive disorders of dementia.[20–23] Our research group has found that the presence of depression increases the risk of dementia by 16%. However, we have also noted factors that condition this relationship, such as age or the presence of other diseases, for example, type II diabetes.[24]

Both dementia and depression present biological mechanisms that link them, such as vascular disease, atrophy of the hippocampus, a larger deposit of β-amyloid plaques, and inflammatory alterations.[25,26] In this sense, according to the latest studies, and as we have explained throughout this section, the inflammatory process is an important key effector in both processes.[27,28]

This common point between depression and dementia is a promising research focus with clear clinical applicability for addressing both conditions.

## Depression and inflammation

Although the main approach to depression is based on the historically accepted "monoamine depletion hypothesis,"[29,30] this hypothesis is not sufficient to explain the depressive disorder; especially in the last 20 years,

several studies are pointing to the involvement of the inflammatory process in the disorder. This fact would justify the serotonergic, noradrenergic and dopaminergic dysfunction[31,32] inherent to depression; thus, we can speak of an "inflammatory hypothesis". Authors such as Liu et al.[28] link depression to the inflammatory process through increased levels of pro-inflammatory cytokines such as TNF-α and IL-6, decreased circulating levels of IL-1β and IL-8 in blood and cerebrospinal fluid,[33] and increased corticotropin-releasing hormone levels; the latter results in an increase in the activity of the hypothalamic–pituitary–adrenal (HPA) axis, which in turn introduces stress into the process.

Chronic stress induces the weakening of BBB (described in animal experiments) and the consequent passage of circulating pro-inflammatory mediators.[34] Therefore, authors such as Dudek et al.[34] describe how stress-induced alteration of BBB permeability is linked to the inflammation of endothelium and involvement of tight junctions.

Furthermore, as noted above, increased IL-6 and C-reactive protein (CRP) levels could predict the development of depressive symptoms.[35,36] Both molecules are predictive, indicating that inflammation precedes depression, but are also associated with cognitive symptoms of depression.[37]

Therefore, the passage of peripheral myeloid cells into the brain in depressive processes would constitute an important clue supporting the existence of a central inflammatory response in depression that would be mainly driven by peripheral inflammatory events.[38]

The verification of this inflammatory response in depression suggests the possible existence of other causal biological pathways/processes in depressive processes[39] and opens the door to the improvement of the response of current antidepressant therapies since, as reported by authors such as Miller and Raison,[31] 30–50% of depressed people do not respond to commonly prescribed antidepressant treatments and only 30% of patients remit.

## Dementia and inflammation

In recent years, the inflammatory process has become important in the neurodegenerative pathology of Alzheimer's disease (AD). Inflammation can "conduct" the pathogenesis of AD once the pathological process has begun.[40,41] Even the studies conducted by Lee et al.[42] highlight the ability of pro-inflammatory microglia activation to aggravate and initiate the pathological process. At present, AD is considered to be a tauopathy initiated by β-amyloid peptide accompanied by neuroinflammation, thus connecting the 3 pathophysiological and anatomopathological events typical of AD.[42–45]

In elderly population, age affects the microglial function and is associated with an alteration in amyloid metabolism, aggravated by sustained exposure to pro-inflammatory cytokines, such as TNF-α, and the whole process can inhibit microglial function.[46]

In this regard, the disruption of BBB by inflammatory mediators during the progression of AD has been described. In the BBB, the neurovascular unit (NVU) is responsible for neurovascular coupling, i.e., the interaction of neuronal (neurons and glia) and vascular tissues (endothelial cells, pericytes and adventitial cells).[14] Several authors show how this coupling is impaired in AD,[47] suggesting the important role of NVU in the progression of cognitive impairment. Other situations in which this coupling is also altered, and which are also related to AD, are hypertension[48] and ischemic stroke[49] (postmortem studies emphasize the important role of vascular pathology in a significant percentage of AD patients).[50]

In this way, aging appears to be an aggravating factor in the development of neurodegenerative diseases such as AD. In addition, and based on the studies reviewed, aging also contributes to an increase in vulnerability to certain conditions such as depression,[51,52] through sustained activation of pro-inflammatory signals (Fig. 1).

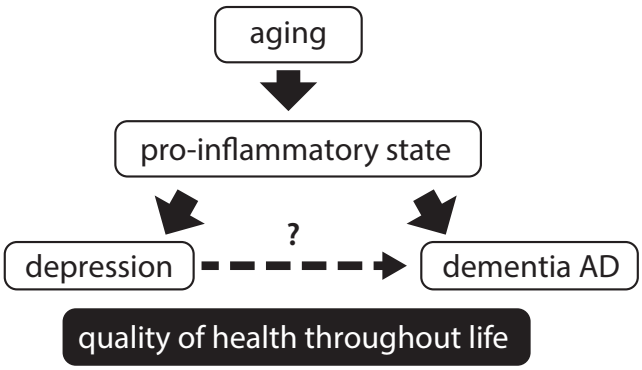


Fig. 1. Scheme linking aging, depression and dementia

AD – Alzheimer's disease.

Given this knowledge, it is necessary to develop new research lines in order to establish the link between depression and dementia; and, based on what is known, to establish strategies of modulation of pro-inflammatory states that could modify the prevalence of neurodegenerative diseases such as dementia.

### ORCID iDs

Maria del Pilar Carrera-González https://orcid.org/0000-0001-6575-8240
Vanesa Cantón-Habas https://orcid.org/0000-0002-3928-0092
Manuel Rich-Ruiz https://orcid.org/0000-0003-3317-267X

### References

1. Chowdhary N, Barbui C, Anstey KJ, et al. Reducing the risk of cognitive decline and dementia: WHO recommendations. *Front Neurol*. 2021;12:765584. doi:10.3389/fneur.2021.765584
2. Hoyer S. The young-adult and normally aged brain – its blood flow and oxidative metabolism: A review. Part I. *Arch Gerontol Geriatr*. 1982;1(2):101–116. doi:10.1016/0167-4943(82)90010-3
3. Pomatto LCD, Davies KJA. Adaptive homeostasis and the free radical theory of ageing. *Free Radic Biol Med*. 2018;124:420–430. doi:10.1016/j.freeradbiomed.2018.06.016

4. Lee S, Wu Y, Shi XQ, Zhang J. Characteristics of spinal microglia in aged and obese mice: Potential contributions to impaired sensory behavior. *Immun Ageing*. 2015;12:22. doi:10.1186/s12979-015-0049-5
5. Schutze S, Ribes S, Kaufmann A, et al. Higher mortality and impaired elimination of bacteria in aged mice after intracerebral infection with *E. coli* are associated with an age-related decline of microglia and macrophage functions. *Oncotarget*. 2014;5(24):12573–12592. doi:10.18632/oncotarget.2709
6. Babcock AA, Ilkjaer L, Clausen BH, et al. Cytokine-producing microglia have an altered beta-amyloid load in aged APP/PS1 Tg mice. *Brain Behav Immun*. 2015;48:86–101. doi:10.1016/j.bbi.2015.03.006
7. Lourbopoulos A, Erturk A, Hellal F. Microglia in action: How aging and injury can change the brain's guardians. *Front Cell Neurosci*. 2015;9:54. doi:10.3389/fncel.2015.00054
8. Henry CJ, Huang Y, Wynne AM, Godbout JP. Peripheral lipopolysaccharide (LPS) challenge promotes microglial hyperactivity in aged mice that is associated with exaggerated induction of both pro-inflammatory IL-1beta and anti-inflammatory IL-10 cytokines. *Brain Behav Immun*. 2009;23(3):309–317. doi:10.1016/j.bbi.2008.09.002
9. Norden DM, Godbout JP. Review. Microglia of the aged brain: Primed to be activated and resistant to regulation. *Neuropathol Appl Neurobiol*. 2013;39(1):19–34. doi:10.1111/j.1365-2990.2012.01306.x
10. Chung HY, Cesari M, Anton S, et al. Molecular inflammation: Underpinnings of aging and age-related diseases. *Ageing Res Rev*. 2009;8(1):18–30. doi:10.1016/j.arr.2008.07.002
11. Schuitemaker A, van der Doef TF, Boellaard R, et al. Microglial activation in healthy aging. *Neurobiol Aging*. 2012;33(6):1067–1072. doi:10.1016/j.neurobiolaging.2010.09.016
12. DiSabato DJ, Quan N, Godbout JP. Neuroinflammation: The devil is in the details. *J Neurochem*. 2016;139(Suppl 2):136–153. doi:10.1111/jnc.13607
13. Salminen A, Ojala J, Kaarniranta K, Haapasalo A, Hiltunen M, Soininen H. Astrocytes in the aging brain express characteristics of senescence-associated secretory phenotype. *Eur J Neurosci*. 2011;34(1):3–11. doi:10.1111/j.1460-9568.2011.07738.x
14. Zhao Z, Nelson AR, Betsholtz C, Zlokovic BV. Establishment and dysfunction of the blood–brain barrier. *Cell*. 2015;163(5):1064–1078. doi:10.1016/j.cell.2015.10.067
15. Huang WJ, Zhang X, Chen WW. Role of oxidative stress in Alzheimer's disease. *Biomed Rep*. 2016;4(5):519–522. doi:10.3892/br.2016.630
16. Sasaki N, Fukatsu R, Tsuzuki K, et al. Advanced glycation end products in Alzheimer's disease and other neurodegenerative diseases. *Am J Pathol*. 1998;153(4):1149–1155. doi:10.1016/S0002-9440(10)65659-3
17. Swardfager W, Lanctot K, Rothenburg L, Wong A, Cappell J, Herrmann N. A meta-analysis of cytokines in Alzheimer's disease. *Biol Psychiatry*. 2010;68(10):930–941. doi:10.1016/j.biopsych.2010.06.012
18. Nehra G, Bauer B, Hartz AMS. Blood–brain barrier leakage in Alzheimer's disease: From discovery to clinical relevance. *Pharmacol Ther*. 2022;234:108119. doi:10.1016/j.pharmthera.2022.108119
19. Tanaka M, Vecsei L. Editorial of Special Issue "Crosstalk between depression, anxiety, and dementia: Comorbidity in behavioral neurology and neuropsychiatry". *Biomedicines*. 2021;9(5):517. doi:10.3390/biomedicines9050517
20. Gatchel JR, Rabin JS, Buckley RF, et al. Longitudinal association of depression symptoms with cognition and cortical amyloid among community-dwelling older adults. *JAMA Netw Open*. 2019;2(8):e198964. doi:10.1001/jamanetworkopen.2019.8964
21. Battaglia S. Neurobiological advances of learned fear in humans. *Adv Clin Exp Med*. 2022;31(3):217–221. doi:10.17219/acem/146756
22. Torok N, Tanaka M, Vecsei L. Searching for peripheral biomarkers in neurodegenerative diseases: The tryptophan–kynurenine metabolic pathway. *Int J Mol Sci*. 2020;21(24):9338. doi:10.3390/ijms21249338
23. Battaglia S, Harrison BJ, Fullana MA. Does the human ventromedial prefrontal cortex support fear learning, fear extinction or both? A commentary on subregional contributions. *Mol Psychiatry*. 2022;27(2):784–786. doi:10.1038/s41380-021-01326-4
24. Canton-Habas V, Rich-Ruiz M, Romero-Saldana M, Carrera-Gonzalez MDP. Depression as a risk factor for dementia and Alzheimer's disease. *Biomedicines*. 2020;8(11):457. doi:10.3390/biomedicines8110457
25. Sacuiu S, Insel PS, Mueller S, et al. Chronic depressive symptomatology in mild cognitive impairment is associated with frontal atrophy rate which hastens conversion to Alzheimer dementia. *Am J Geriatr Psychiatry*. 2016;24(2):126–135. doi:10.1016/j.jagp.2015.03.006
26. Steffens DC. Late-life depression and the prodromes of dementia. *JAMA Psychiatry*. 2017;74(7):673–674. doi:10.1001/jamapsychiatry.2017.0658
27. Finneran DJ, Nash KR. Neuroinflammation and fractalkine signaling in Alzheimer's disease. *J Neuroinflamm*. 2019;16(1):30. doi:10.1186/s12974-019-1412-9
28. Liu CH, Zhang GZ, Li B, et al. Role of inflammation in depression relapse. *J Neuroinflamm*. 2019;16(1):90. doi:10.1186/s12974-019-1475-7
29. Massart R, Mongeau R, Lanfumey L. Beyond the monoaminergic hypothesis: Neuroplasticity and epigenetic changes in a transgenic mouse model of depression. *Philos Trans R Soc Lond B Biol Sci*. 2012;367(1601):2485–2494. doi:10.1098/rstb.2012.0212
30. Rosenblat JD, Cha DS, Mansur RB, McIntyre RS. Inflamed moods: A review of the interactions between inflammation and mood disorders. *Prog Neuropsychopharmacol Biol Psychiatry*. 2014;53:23–34. doi:10.1016/j.pnpbp.2014.01.013
31. Miller AH, Raison CL. The role of inflammation in depression: From evolutionary imperative to modern treatment target. *Nat Rev Immunol*. 2016;16(1):22–34. doi:10.1038/nri.2015.5
32. Song C, Wang H. Cytokines mediated inflammation and decreased neurogenesis in animal models of depression. *Prog Neuropsychopharmacol Biol Psychiatry*. 2011;35(3):760–768. doi:10.1016/j.pnpbp.2010.06.020
33. Kiecolt-Glaser JK, Derry HM, Fagundes CP. Inflammation: Depression fans the flames and feasts on the heat. *Am J Psychiatry*. 2015;172(11):1075–1091. doi:10.1176/appi.ajp.2015.15020152
34. Dudek KA, Dion-Albert L, Lebel M, et al. Molecular adaptations of the blood–brain barrier promote stress resilience vs. depression. *Proc Natl Acad Sci U S A*. 2020;117(6):3326–3336. doi:10.1073/pnas.1914655117
35. Jokela M, Virtanen M, Batty GD, Kivimaki M. Inflammation and specific symptoms of depression. *JAMA Psychiatry*. 2016;73(1):87–88. doi:10.1001/jamapsychiatry.2015.1977
36. Smith KJ, Au B, Ollis L, Schmitz N. The association between C-reactive protein, interleukin-6 and depression among older adults in the community: A systematic review and meta-analysis. *Exp Gerontol*. 2018;102:109–132. doi:10.1016/j.exger.2017.12.005
37. Gimeno D, Kivimaki M, Brunner EJ, et al. Associations of C-reactive protein and interleukin-6 with cognitive symptoms of depression: 12-year follow-up of the Whitehall II study. *Psychol Med*. 2009;39(3):413–423. doi:10.1017/S0033291708003723
38. Krugel U, Fischer J, Radicke S, Sack U, Himmerich H. Antidepressant effects of TNF-alpha blockade in an animal model of depression. *J Psychiatr Res*. 2013;47(5):611–616. doi:10.1016/j.jpsychires.2013.01.007
39. Carvalho LA, Torre JP, Papadopoulos AS, et al. Lack of clinical therapeutic benefit of antidepressants is associated overall activation of the inflammatory system. *J Affect Disord*. 2013;148(1):136–140. doi:10.1016/j.jad.2012.10.036
40. Metcalfe MJ, Figueiredo-Pereira ME. Relationship between tau pathology and neuroinflammation in Alzheimer's disease. *Mt Sinai J Med*. 2010;77(1):50–58. doi:10.1002/msj.20163
41. Shabab T, Khanabdali R, Moghadamtousi SZ, Kadir HA, Mohan G. Neuroinflammation pathways: A general review. *Int J Neurosci*. 2017;127(7):624–633. doi:10.1080/00207454.2016.1212854
42. Lee DC, Rizer J, Selenica ML, et al. LPS-induced inflammation exacerbates phospho-tau pathology in rTg4510 mice. *J Neuroinflamm*. 2010;7:56. doi:10.1186/1742-2094-7-56
43. Herber DL, Mercer M, Roth LM, et al. Microglial activation is required for Abeta clearance after intracranial injection of lipopolysaccharide in APP transgenic mice. *J Neuroimmune Pharmacol*. 2007;2(2):222–231. doi:10.1007/s11481-007-9069-z
44. Shaftel SS, Kyrkanides S, Olschowka JA, Miller JN, Johnson RE, O'Banion MK. Sustained hippocampal IL-1 beta overexpression mediates chronic neuroinflammation and ameliorates Alzheimer plaque pathology. *J Clin Invest*. 2007;117(6):1595–1604. doi:10.1172/JCI31450
45. Lee S, Varvel NH, Konerth ME, et al. CX3CR1 deficiency alters microglial activation and reduces beta-amyloid deposition in two Alzheimer's disease mouse models. *Am J Pathol*. 2010;177(5):2549–2562. doi:10.2353/ajpath.2010.100265
46. Hickman SE, Allison EK, El Khoury J. Microglial dysfunction and defective beta-amyloid clearance pathways in aging Alzheimer's disease mice. *J Neurosci*. 2008;28(33):8354–8360. doi:10.1523/JNEUROSCI.0616-08.2008

47. Viticchi G, Falsetti L, Vernieri F, et al. Apolipoprotein E genotype and cerebrovascular alterations can influence conversion to dementia in patients with mild cognitive impairment. *J Alzheimers Dis*. 2014;41(2):401–410. doi:10.3233/JAD-132480
48. Presa JL, Saravia F, Bagi Z, Filosa JA. Vasculo-neuronal coupling and neurovascular coupling at the neurovascular unit: Impact of hypertension. *Front Physiol*. 2020;11:584135. doi:10.3389/fphys.2020.584135
49. Silvestrini M, Vernieri F, Pasqualetti P, et al. Impaired cerebral vasoreactivity and risk of stroke in patients with asymptomatic carotid artery stenosis. *JAMA*. 2000;283(16):2122–2127. doi:10.1001/jama.283.16.2122
50. Falsetti L, Viticchi G, Zaccone V, et al. Shared molecular mechanisms among Alzheimer's disease, neurovascular unit dysfunction and vascular risk factors: A narrative review. *Biomedicines*. 2022;10(2):439. doi:10.3390/biomedicines10020439
51. Sibille E. Molecular aging of the brain, neuroplasticity, and vulnerability to depression and other brain-related disorders. *Dialogues Clin Neurosci*. 2013;15(1):53–65. doi:10.31887/DCNS.2013.15.1/esibille
52. Bartsch T, Wulff P. The hippocampus in aging and disease: From plasticity to vulnerability. *Neuroscience*. 2015;309:1–16. doi:10.1016/j.neuroscience.2015.07.084

# Efficacy and safety of sacubitril/valsartan in an outpatient setting: A single-center real-world retrospective study in HFrEF patients with focus on possible predictors of clinical outcome

Elisabeth J. Fröb[B–D,F], Jürgen R. Sindermann[E,F], Holger Reinecke[E,F], Izabela Tuleta[A,C–F]

Department of Cardiology I – Coronary and Peripheral Vascular Disease, Heart Failure, University Hospital Münster, Germany

A – research concept and design; B – collection and/or assembly of data; C – data analysis and interpretation;
D – writing the article; E – critical revision of the article; F – final approval of the article

Advances in Clinical and Experimental Medicine, ISSN 1899–5276 (print), ISSN 2451–2680 (online) *Adv Clin Exp Med*. 2022;31(5):475–487

**Address for correspondence**
Izabela Tuleta
E-mail: izat@gmx.de

**Funding sources**
None declared

**Conflict of interest**
None declared

**Acknowledgements**
We would like to thank Dr. René Schmidt, Institute of Biostatistics and Clinical Research, University Hospital Münster, Germany, for his great support in the statistical data analyses.

Received on August 11, 2021
Reviewed on October 5, 2021
Accepted on January 10, 2022

Published online on January 29, 2022

**Cite as**
Fröb EJ, Sindermann JR, Reinecke H, Tuleta I. Efficacy and safety of sacubitril/valsartan in an outpatient setting: A single-center real-world retrospective study in HFrEF patients with focus on possible predictors of clinical outcome. *Adv Clin Exp Med*. 2022;31(5):475–487. doi:10.17219/acem/145664

**DOI**
10.17219/acem/145664



## Abstract

**Background.** Currently, data on sacubitril/valsartan therapy from the real-world settings are scarce and the predictors of a good clinical responsiveness to this drug are unknown.

**Objectives.** To assess efficacy and safety profile of sacubitril/valsartan and to identify predictors for a better clinical outcome.

**Materials and methods.** Clinical, laboratory and echocardiographic data of 95 chronic heart failure (CHF) patients with reduced ejection fraction (HFrEF) were retrospectively analyzed. A good efficacy of sacubitril/valsartan was defined as the fulfilment of at least 2 of the following criteria: improvement of left ventricular ejection fraction (LVEF) or functional status, and reduction of N-terminal pro-brain natriuretic peptide (NT-proBNP) levels or hospitalization rates.

**Results.** Under sacubitril/valsartan, major improvements were observed in LVEF, the New York Heart Association (NYHA) class, NT-proBNP levels, and hospitalization rates. Patients with a good efficacy of sacubitril/valsartan were characterized by initially worse LVEF (median (interquartile range (IQR)): 29.0% (23.0–33.0%) compared to 32.0% (28.5–38.0%) with more frequent nonischemic etiology (65.4% compared to 41.9%) and hospitalizations for CHF/month (0.016 (0.004–0.057) compared to 0.000 (0.000–0.012)), lower cholesterol (42.3% compared to 65.1%), higher C-reactive protein (CRP) levels at baseline (0.5 mg/L (0.5–1.0 mg/L) compared to 0.5 mg/L (0.5–0.5 mg/L)), and a shorter timespan between CHF diagnosis and the start of sacubitril/valsartan treatment (66.0 (11.0–127.0) compared to 111 (73.0–211.0) months) ($p < 0.05$ each). In a multivariate Cox analysis, only the last 2 parameters were shown to be independent predictors of good clinical responsiveness to sacubitril/valsartan (hazard ratio (HR) = 1.263, 95% confidence interval (95% CI) = [1.048; 1.521]; HR = 0.992, 95% CI = [0.987; 0.997], $p < 0.05$, respectively).

**Conclusions.** Sacubitril/valsartan improved LVEF, NYHA class, NT-proBNP levels, and hospitalization rates, mostly without relevant side effects. The independent predictors of a good clinical efficacy were higher CRP levels at baseline and a shorter delay between CHF diagnosis and the initialization of sacubitril/valsartan therapy.

**Key words:** CRP, sacubitril/valsartan, NYHA class, chronic heart failure with reduced left ventricular ejection fraction, hospitalization rates

# Background

Sacubitril/valsartan has been proven to be effective in the therapy of patients with chronic heart failure with reduced ejection fraction (HFrEF).[1] A post hoc analysis of the PARADIGM-HF study showed that the patients with HFrEF benefited equally in terms of the study endpoint, composed of cardiovascular (CV) death or hospitalization for heart failure (HF), regardless of baseline left ventricular ejection fraction (LVEF).[2] Moreover, benefits of sacubitril/valsartan over enalapril were consistent across subgroups of patients with different HF etiologies, although patients with nonischemic cardiomyopathy (NICM) were younger, more frequently female and had higher N-terminal pro-brain natriuretic peptide (NT-proBNP) levels in comparison with ischemic cardiomyopathy (ICM) patients.[2] Furthermore, the presence of diabetes,[2] hospitalizations prior treatment[2] and the background pharmacological, interventional or device therapy did not have any relevant influence on the primary endpoint of the PARADIGM-HF study.[2,3] Also, the LVEF improvement, as a single endpoint in other study, did not differ between patients with different HF etiologies and comorbidities such as diabetes, arterial hypertension and atrial fibrillation. There was only a trend toward LVEF improvement in patients treated with medium/high doses of sacubitril/valsartan compared to the patients treated with the low ones.[4] Other authors reported that the LVEF improvement of at least 5% was more frequent in patients with lower LV dilation.[5] Therefore, no relevant specific parameters were identified up to date which would be connected to a significantly better responsiveness to sacubitril/valsartan therapy.

# Objectives

The aim of our present study was to prove efficacy and safety of sacubitril/valsartan therapy in an outpatient real-world setting with an emphasis on potential predictors of a good clinical outcome under this medication.

# Materials and methods

## Study population, inclusion/exclusion criteria and data source

All procedures performed in this study involving human participants were in accordance with the ethical standards set by the institutional research committee and with the 1964 Declaration of Helsinki and its later amendments. The local Ethics Committee of the Medical Faculty of the University of Münster, Germany, approved the study design.

All patients treated in our outpatient chronic heart failure (CHF) center between January 2018 and June 2019 were retrospectively screened for the therapy with sacubitril/valsartan (Fig. 1). Within this period, patients undergoing the sacubitril/valsartan therapy completed their last follow-up visit. The baseline visit before the initiation of sacubitril/valsartan treatment took place either within the abovementioned timeframe or before it, depending on the duration of the sacubitril/valsartan therapy (the earliest timepoint of sacubitril/valsartan prescription: mid-2016). Data collected within 3 months before the prescription of sacubitril/valsartan were considered baseline data. The inclusion criteria were as follows: age ≥18 years; clinical stability, defined as a status demanding no relevant changes in medication; and/or hospitalization in the last 3 months before baseline and follow-up. Patients who did not meet the inclusion criteria and for whom we were unable to collect all clinical, instrumental and laboratory data were excluded from the study. The decision to prescribe the sacubitril/valsartan therapy in patients enrolled was based on the European Society of Cardiology (ESC) guidelines, which recommend sacubitril/valsartan therapy in CHF patients with LVEF ≤ 40% who are still symptomatic despite adequate CHF therapy.[6]

Data sources included medical records from our clinic, patient information supplied by other healthcare providers such as primary care physicians and cardiologists, and the patient records from previous hospital admissions.

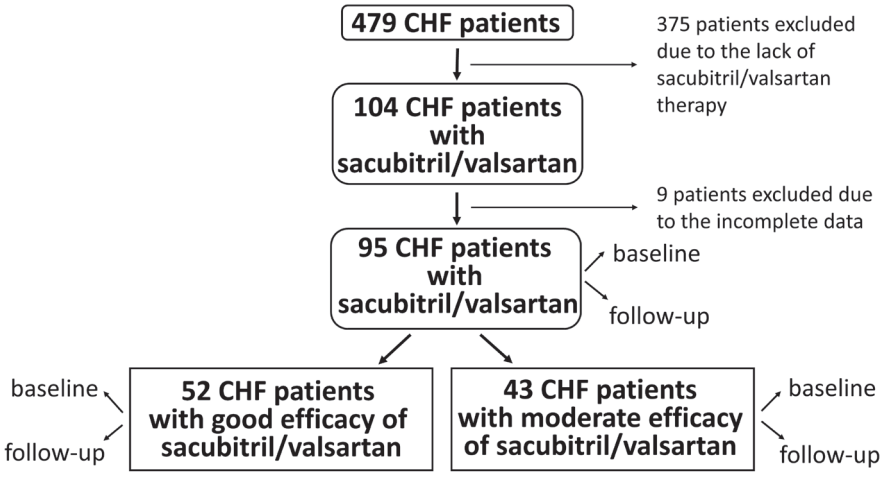


**Fig. 1.** Flowchart of the study design

CHF – chronic heart failure.

## Patient cohorts and analyzed variables

Patient characteristics based on clinical, laboratory and instrumental results were compared before the initialization of sacubitril/valsartan therapy and during this therapy, at the last available follow-up within the data collection period (Table 1).

Clinical parameters included age, gender, body mass index (BMI), etiology of cardiomyopathy, observation period (timespan from the initial diagnosis to the start of sacubitril/valsartan treatment and the duration of sacubitril/valsartan therapy), dyspnea in daily activities according to the New York Heart Association (NYHA) classification, presence of cardiovascular risk factors, comorbidities, medication, and cardiac electronical devices. Instrumental diagnostics consisted of blood pressure and heart rate measurements, electrocardiogram (ECG), echocardiography, and laboratory analyses.

## Endpoints and definitions

To examine whether patients notably benefited from the sacubitril/valsartan treatment, a score consisting of an improved LVEF of at least 5%,[2,3] decreased hospitalization rates for CHF (number of all hospitalizations divided by the observation period in months), better physical capacity (defined as an improvement in stair climbing of at least half a floor before stopping for dyspnea), and reduced NT-proBNP blood levels (reduction by at least 50%)[7] was used. Each attribute had a value of 1 point and if the total count amounted to at least 2 points, such case was assigned to a good efficacy group. Patients who did not fulfil these criteria constituted a group of a moderate efficacy. The abovementioned clinical, laboratory and instrumental findings were compared between both groups (Table 2).

Furthermore, side effects attributed to sacubitril/valsartan treatment were also evaluated (Table 3). When evaluating side effects, hypotension was defined as being clinically relevant if it caused orthostatic dizziness, affected everyday life and/or resulted in the reduction of HF medication. Anemia de novo was assessed under sacubitril/valsartan treatment according to the World Health Organization (WHO) definition (hemoglobin concentration <12 g/dL for women and <13 g/dL for men).[8] The deterioration in kidney function and the acute kidney injury (AKI) were diagnosed based on the Kidney Disease: Improving Global Outcome (KDIGO) criteria and defined as a reduction in glomerular filtration rate (GFR), resulting in a decrease in the classification of chronic kidney disease by at least 1 stage (deterioration in kidney function), and as an increase in serum creatinine of ≥0.3 mg/dL within 48 h, or ≥50% within 7 days, or urine output of <0.5 mL/kg/h for >6 h (AKI).[9,10]

## Statistical analyses

The comparisons of qualitative dichotomous or polytomous variables between the same set of patients at baseline and at follow-up were conducted by means of the McNemar and marginal homogeneity tests, respectively (Table 1). For the calculations of potential differences between numerical parameters in patients prior to and under sacubitril/valsartan therapy, the Wilcoxon signed-rank test was

**Table 1.** Baseline characteristics and course of clinical, instrumental and laboratory findings under sacubitril/valsartan therapy

| Parameter | Baseline (prior to sacubitril/valsartan) n = 95 | Follow-up (under sacubitril/valsartan) n = 95 | Test value | p-value |
|---|---|---|---|---|
| Age [years], median (IQR) | 57.0 (50.0–69.0) | 59.0 (52.0–70.0) | –7.716 | <0.001* |
| Male gender, n (%) | 71 (74.7) | – | – | – |
| BMI [kg/m$^2$], median (IQR) | 27.8 (25.0–31.8) | 28.7 (25.4–32.0) | –2.296 | 0.022* |
| Time from diagnosis to sacubitril/valsartan start [months], median (IQR) | 92.5 (25.0–147.8) | – | – | – |
| Time from sacubitril/valsartan start to follow-up start [months], median (IQR) | – | 17.0 (10.0–26.3) | – | – |
| NICM, n (%) | 53 (55.8) | – | – | – |
| LVEF (%), median (IQR) | 30.5 (25.0–35.0) | 35.0 (30.0–43.3) | –5.330 | <0.001* |
| LVEF improvement ≥5%, n (%) | – | 48 (50.5) | – | – |
| LVEF improvement ≥5%, median (IQR) | – | 12.0 (9.0–21.0) | – | – |
| NYHA class<br>– NYHA I, n (%)<br>– NYHA II, n (%)<br>– NYHA III, n (%)<br>– NYHA IV, n (%) | <br>7 (7.4)<br>21 (22.1)<br>62 (65.3)<br>5 (5.3) | <br>20 (21.1)<br>30 (31.6)<br>44 (46.3)<br>1 (1.1) | 5.164<br>–<br>–<br>–<br>– | <0.001*<br>–<br>–<br>–<br>– |
| Functional improvement (≥half a floor), n (%) | – | 50 (52.6) | – | – |
| NT-proBNP [pg/mL], median (IQR) | 843.0 (404.0–2591.0) | 660.5 (231.5–2162.8) | –2.572 | 0.01* |

Table 1. Baseline characteristics and course of clinical, instrumental and laboratory findings under sacubitril/valsartan therapy – cont.

| Parameter | Baseline (prior to sacubitril/valsartan) n = 95 | Follow-up (under sacubitril/valsartan) n = 95 | Test value | p-value |
|---|---|---|---|---|
| NT-proBNP improvement ≥50%, n (%) | – | 27 (28.4) | – | – |
| Hospitalizations for CHF per month, median (IQR) | 0.009 (0.000–0.027) | 0.000 (0.000–0.000) | –3.499 | <0.001* |
| Improvement in hospitalizations for CHF per month, n (%) | – | 51 (53.7) | – | – |
| **Medical history at baseline** | | | | |
| Arterial hypertension, n (%) | 63 (66.3) | – | – | – |
| Diabetes mellitus, n (%) | 28 (29.5) | – | – | – |
| Dyslipidemia, n (%) | 50 (52.6) | – | – | – |
| Smokers<br>– current smokers, n (%)<br>– previous smokers, n (%) | <br>14 (14.7)<br>46 (48.4) | <br>–<br>– | <br>–<br>– | <br>–<br>– |
| Familiar history of cardiovascular disease, n (%) | 41 (43.2) | – | – | – |
| Chronic kidney disease (eGFR ≤ 60 mL/min/1.73 m$^2$), n (%) | 36 (37.9) | – | – | – |
| PAD, n (%) | 20 (21.1) | – | – | – |
| CAD, n (%)<br>– number of vessels, median (IQR)<br>– number of MI, median (IQR) | 45 (47.4)<br>0.0 (0.0–1.0)<br>0.0 (0.0–2.0) | –<br>–<br>– | –<br>–<br>– | –<br>–<br>– |
| CABG, n (%) | 13 (13.7) | – | – | – |
| Stroke, n (%) | 19 (20.0) | – | – | – |
| Hyperuricemia, n (%) | 19 (20.0) | – | – | – |
| Obstructive lung diseases<br>– COPD, n (%)<br>– asthma, n (%) | <br>11 (11.6)<br>7 (7.4) | <br>–<br>– | <br>–<br>– | <br>–<br>– |
| OSAS, n (%) | 21 (22.1) | – | – | – |
| **Medication** | | | | |
| BB, n (%) | 93 (97.9) | 95 (100.0) | – | – |
| BB (% of target dose), median (IQR) | 0.5 (0.4–1.0) | 0.5 (0.5–1.0) | –0.609 | 0.543 |
| ACEI or ARB, n (%) | 93 (97.9) | 0 (0.0) | – | – |
| ACEI or ARB (% of target dose), median (IQR) | 0.75 (0.5–1.0) | 0.00 | – | – |
| Sacubitril/valsartan, n (%) | 0 (0.0) | 95 (100.0) | – | – |
| Sacubitril/valsartan (% of target dose), median (IQR) | 0.00 | 0.65 ±0.30 | – | – |
| MRA, n (%) | 80 (84.2) | 80 (84.2) | – | – |
| MRA (% of target dose), median (IQR) | 1.0 (1.0–1.0) | 1.0 (1.0–1.0) | –0.154 | 0.878 |
| Diuretics, n (%) | 79 (83.2) | 77 (81.1) | 23.765 | 0.791 |
| Diuretics (% of target dose), median (IQR) | 0.5 (1.0–2.0) | 0.5 (1.0–2.0) | –0.665 | 0.506 |
| Amiodarone, n (%) | 14 (14.7) | 14 (14.7) | – | – |
| Oral anticoagulation, n (%) | 43 (45.3) | 43 (45.3) | – | – |
| **BP and heart rate** | | | | |
| Systolic BP [mm Hg], median (IQR) | 117.5 (108.5–125.0) | 110.0 (100.0–125.0) | –2.255 | 0.024* |
| Diastolic BP [mm Hg], median (IQR) | 75.0 (70.0–80.0) | 70.0 (68.5–80.0) | –0.502 | 0.616 |
| Mean arterial pressure [mm Hg], median (IQR) | 87.0 (82.3–93.3) | 85.7 (76.7–93.3) | –1.290 | 0.197 |
| Heart rate [bpm], median (IQR) | 70.0 (60.0–76.0) | 64.0 (58.0–74.0) | –2.803 | 0.005* |
| **ECG/electronic cardiac device** | | | | |
| Atrial fibrillation (paroxysmal or permanent), n (%) | 41 (43.2) | 41 (43.2) | – | – |
| VA per month, median (IQR) | 0.000 (0.000–0.004) | 0.000 (0.000–0.000) | –0.206 | 0.837 |
| Carrier of ICD, n (%)<br>– for primary prophylaxis<br>– for secondary prophylaxis | 53 (55.8)<br>42 (44.2)<br>11 (11.6) | 65 (68.4)<br>53 (55.8)<br>12 (12.6) | –2.840 | 0.005* |
| Left bundle branch block, n (%) | 35 (36.8) | 35 (36.8) | – | – |

**Table 1.** Baseline characteristics and course of clinical, instrumental and laboratory findings under sacubitril/valsartan therapy – cont.

| Parameter | Baseline (prior to sacubitril/valsartan) n = 95 | Follow-up (under sacubitril/valsartan) n = 95 | Test value | p-value |
|---|---|---|---|---|
| Carrier of CRT (as ICD upgrade or primary CRT-D implantation), n (%) | 19 (20.0) | 29 (30.5) | 54.052 | 0.002* |
| Carrier of PM, n (%) | 5 (5.3) | 5 (5.3) | – | – |
| **Echocardiography** | | | | |
| Moderate or severe mitral valve regurgitation, n (%) | 18 (18.9) | 14 (14.7) | 15.598 | 0.454 |
| Moderate or severe tricuspid valve regurgitation, n (%) | 6 (6.3) | 9 (9.5) | 4.251 | 0.549 |
| Moderate or severe aortic valve regurgitation, n (%) | 2 (2.1) | 2 (2.1) | – | – |
| LV enlargement, n (%) | mild: 14 (14.7)<br>moderate: 20 (21.1)<br>severe: 43 (45.3) | mild: 10 (10.5)<br>moderate: 24 (25.3)<br>severe: 33 (34.7) | –1.286 | 0.198 |
| LA enlargement, n (%) | mild: 20 (21.1)<br>moderate: 20 (21.1)<br>severe: 27 (28.4) | mild: 10 (10.5)<br>moderate: 21 (22.1)<br>severe: 20 (21.1) | –3.178 | 0.001* |
| RV enlargement, n (%) | mild: 3 (3.2)<br>moderate: 10 (10.5)<br>severe: 3 (3.2) | mild: 4 (4.2)<br>moderate: 6 (6.3)<br>severe: 0 (0.0) | –1.325 | 0.185 |
| RA enlargement, n (%) | mild: 11 (11.6)<br>moderate: 13 (13.7)<br>severe: 9 (9.5) | mild: 5 (5.3)<br>moderate: 6 (6.3)<br>severe: 8 (8.4) | –2.968 | 0.003* |
| **Laboratory values** | | | | |
| Creatinine [mg/dL], median (IQR) | 1.2 (1.0–1.4) | 1.3 (1.0–1.6) | –3.767 | <0.001* |
| Urea [mg/dL], median (IQR) | 20.0 (15.0–26.0) | 18.0 (14.0–27.0) | –0.623 | 0.533 |
| GFR [mL/min], median (IQR) | 66.0 (51.0–80.8) | 60.0 (43.0–76.0) | –4.150 | <0.001* |
| Uric acid [mg/dL], median (IQR) | 6.8 (5.7–8.3) | 6.6 (5.2–7.7) | –1.087 | 0.277 |
| Hemoglobin [g/dL], median (IQR) | 14.4 (12.9–15.1) | 13.7 (12.6–14.8) | –1.923 | 0.054 |
| Aspartate transaminase [U/L], median (IQR) | 30.0 (24.0–36.5) | 27.0 (24.0–32.0) | –2.554 | 0.011* |
| Potassium [mmol/L], median (IQR) | 4.4 (4.2–4.8) | 4.5 (4.2–4.8) | –1.300 | 0.194 |
| CK [U/L], median (IQR) | 105.0 (79.5–156.0) | 108.5 (74.0–128.0) | –1.415 | 0.157 |
| CRP [mg/dL], median (IQR) | 0.5 (0.5–0.8) | 0.5 (0.5–0.6) | –1.376 | 0.169 |

ACEI – angiotensin-converting enzyme inhibitor; ARB – angiotensin II receptor blocker; BB – beta blocker; BMI – body mass index; BP – blood pressure; CABG – coronary artery bypass graft; CAD – coronary artery disease; CHF – chronic heart failure; COPD – chronic obstructive pulmonary disease; CRP – C-reactive protein; CK – creatinine kinase; CRT(-D) – cardiac resynchronization therapy (-implantable cardioverter defibrillator); ECG – electrocardiogram; (e)GFR – (estimated) glomerular filtration rate; HCT – hydrochlorothiazide; ICD – implantable cardioverter defibrillator; LA – left atrium; LV – left ventricle; LVEF – left ventricular ejection fraction; MI – myocardial infarction; MRA – mineralocorticoid receptor antagonist; NICM – nonischemic cardiomyopathy; NYHA – level of cardiopulmonal fitness according to the New York Heart Association; NT-proBNP – N-terminal pro-brain natriuretic peptide; OSAS – obstructive sleep apnea syndrome; PAD – peripheral artery disease; PM – pacemaker; RA – right atrium; RV – right ventricle; VA – ventricular arrhythmias. Data are presented as median (interquartile range (IQR)) (Wilcoxon signed-rank test) or n (%) (McNemar test for dichotomous variables and marginal homogeneity tests for polytomous variables). * – statistically significant value of $p < 0.05$. Target dose calculation (for most important drugs; others calculated as equivalent doses): ramipril 10 mg = 1.0; enalapril 20 mg = 1.0; candesartan 32 mg = 1.0; valsartan 320 mg = 1.0; irbesartan 300 mg = 1.0; sacubitril/valsartan 2 × 97/103 mg = 1.0; hydrochlorothiazide 25 mg = 1.0; bisoprolol 10 mg = 1.0; metoprolol 190 mg = 1.0; carvedilol 50 mg = 1.0; spironolacton 25 mg = 1.0; eplerenon 25 mg = 1.0; torasemid 10 mg = 1.0; hydrochlorothiazide 25 mg = 1.0; xipamid 20 mg = 1.0; furosemid 40 mg = 1.0.

used (Table 1). In order to compare measures between patients with a good and moderate sacubitril/valsartan efficacy, the Mann–Whitney U test for continuous variables (Table 2) and the $\chi^2$ test for categorical data (Table 2,3) were applied. Quantitative values were expressed as a median (interquartile range (IQR)), and categorical measures were presented as a number of events (n) and their percentage in the total number of patients (%). Univariate (Table 4) and multivariate (Table 5) Cox regression analyses were performed for the identification of possible predictors of a good efficacy of sacubitril/valsartan therapy. The proportional hazards (PH) assumption based on the scaled Schoenfeld residuals showed a random pattern against time. No adjustment for multiple testing was performed since the analyses were regarded as explorative. Local, unadjusted p-values <0.05 were considered statistically significant. Statistical analysis was conducted using IBM SPSS Statistics v. 26 software (IBM Corp., Armonk, USA).

**Table 2.** Characteristics of patients with a good and moderate efficacy under sacubitril/valsartan

| Parameters | Good efficacy of sacubitril/valsartan n = 52 | Moderate efficacy of sacubitril/valsartan n = 43 | Test value | p-value |
|---|---|---|---|---|
| Mean age [years], median (IQR) | prior s/v: 57.5 (50.0–69.8)<br>under s/v: 59.0 (50.5–71.5) | prior s/v: 57.0 (50.0–63.0)<br>under s/v: 58.0 (52.0–66.0) | –0.714<br>–0.752 | prior s/v: 0.575<br>under s/v: 0.452 |
| BMI [kg/m$^2$], median (IQR) | prior s/v: 27.4 (24.2–33.3)<br>under s/v: 28.6 (25.1–34.3) | prior s/v: 28.4 (25.3–30.6)<br>under s/v: 28.7 (25.4–30.8) | –0.082<br>–0.572 | prior s/v: 0.934<br>under s/v: 0.567 |
| Male gender, n (%) | 38 (73.1) | 33 (76.7) | 0.168 | 0.682 |
| Time from diagnosis to sacubitril/valsartan therapy start (months), median (IQR) | 66.0 (11.0–127.0) | 111.0 (73.0–211.0) | –2.672 | 0.008* |
| Time from sacubitril/valsartan therapy start to follow-up visit (months), median (IQR) | 18.0 (8.0–27.0) | 17.0 (10.0–23.0) | –0.300 | 0.764 |
| NICM, n (%) | 34 (65.4) | 18 (41.9) | 5.257 | 0.022* |
| LVEF (%), median (IQR) | prior s/v: 29.0 (23.0–33.0)<br>under s/v: 38.0 (32.0–45.0) | prior s/v: 32.0 (28.5–38.0)<br>under s/v: 30.0 (25.0–39.0) | –2.768<br>–3.625 | prior s/v: 0.006*<br>under s/v: <0.001* |
| NYHA class, n (%) | prior s/v: NYHA I: 5 (9.6)<br>NYHA II: 10 (19.2)<br>NYHA III: 34 (65.4)<br>NYHA IV: 3 (5.8)<br>under s/v: NYHA I: 17 (32.7)<br>NYHA II: 18 (34.6)<br>NYHA III: 17 (32.7)<br>NYHA IV: 0 (0.0) | prior s/v: NYHA I: 2 (4.6)<br>NYHA II: 11 (25.6)<br>NYHA III: 28 (65.1)<br>NYHA IV: 2 (4.7)<br>under s/v: NYHA I: 3 (7.0)<br>NYHA II: 13 (30.2)<br>NYHA III: 26 (60.5)<br>NYHA IV: 1 (2.3) | 1.273<br>12.752 | prior s/v: 0.736<br>under s/v: 0.005* |
| NT-proBNP [pg/mL], median (IQR) | prior s/v: 975.0 (470–3086.0)<br>under s/v: 471.0 (208.5–1089.3) | prior s/v: 783.5 (263.8–2190.0)<br>under s/v: 835.0 (341.0–2628.8) | –1.229<br>–1.772 | prior s/v: 0.219<br>under s/v: 0.076 |
| Hospitalizations for CHF per month, median (IQR) | prior s/v: 0.016 (0.004–0.057)<br>under s/v: 0.000 (0.000–0.000) | prior s/v: 0.000 (0.000–0.012)<br>under s/v: 0.000 (0.000–0.033) | –3.882<br>–3.047 | prior s/v: <0.001*<br>under s/v: 0.002* |
| **Medical history at baseline** | | | | |
| Arterial hypertension, n (%) | 35 (67.3) | 28 (65.1) | 0.051 | 0.822 |
| Diabetes mellitus, n (%) | 12 (23.1) | 16 (37.2) | 2.261 | 0.133 |
| Dyslipidemia, n (%) | 22 (42.3) | 28 (65.1) | 4.911 | 0.027* |
| Smokers<br>– current smokers, n (%)<br>– previous smokers, n (%) | <br>8 (15.4)<br>25 (48.1) | <br>6 (14.0)<br>21 (48.8) | 0.038<br>–<br>– | 0.981<br>–<br>– |
| Familiar history of cardiovascular disease, n (%) | 22 (42.3) | 19 (44.2) | 0.034 | 0.854 |
| Chronic kidney disease (eGFR ≤ 60 mL/min/1.73 m$^2$), n (%) | 19 (36.5) | 17 (39.5) | 0.090 | 0.764 |
| PAD, n (%) | 11 (21.2) | 9 (20.9) | 0.108 | 0.948 |
| CAD, n (%)<br>– number of vessels, median (IQR)<br>– number of MI, median (IQR)<br>– CABG, n (%) | 19 (36.5)<br>0.00 (0.00–2.00)<br>0.00 (0.00–0.75)<br>5 (9.6) | 26 (60.5)<br>1.00 (0.00–2.00)<br>0.00 (0.00–1.00)<br>8 (18.6) | 5.405<br>–1.529<br>–1.923<br>1.610 | 0.020*<br>0.126<br>0.055<br>0.204 |
| Stroke, n (%) | 9 (17.3) | 10 (23.3) | 1.064 | 0.588 |
| Hyperuricemia, n (%) | 10 (19.2) | 9 (20.9) | 0.042 | 0.837 |
| Obstructive lung diseases<br>– COPD, n (%)<br>– asthma, n (%) | <br>6 (11.5)<br>4 (7.7) | <br>5 (11.6)<br>3 (7.0) | 0.906<br>–<br>– | 0.924<br>–<br>– |
| OSAS, n (%) | 14 (26.9) | 7 (16.3) | 1.549 | 0.213 |
| **Medication** | | | | |
| BB, n (%) | prior s/v: 51 (98.1)<br>under s/v: 52 (100.0) | prior s/v: 42 (97.7)<br>under s/v: 43 (100.0) | 0.019<br>– | prior s/v: 0.892<br>– |
| BB (% of target dose), median (IQR) | prior s/v: 0.5 (0.3–1.0)<br>under s/v: 0.5 (0.4–1.0) | prior s/v: 0.5 (0.5–1.0)<br>under s/v: 0.5 (0.5–1.0) | –0.412<br>–0.265 | prior s/v: 0.681<br>under s/v: 0.791 |
| ACEI or ARB, n (%) | prior s/v: 51 (98.1) | prior s/v: 42 (97.7) | 0.816 | prior s/v: 0.366 |
| ACEI or ARB (% of target dose), median (IQR) | prior s/v: 0.5 (0.5–1.0) | prior s/v: 0.8 (0.5–1.0) | –0.899 | prior s/v: 0.369 |
| Sacubitril/valsartan, n (%) | under s/v: 52 (100) | under s/v: 43 (100) | – | – |

**Table 2.** Characteristics of patients with a good and moderate efficacy under sacubitril/valsartan – cont.

| Parameters | Good efficacy of sacubitril/valsartan n = 52 | Moderate efficacy of sacubitril/valsartan n = 43 | Test value | p-value |
|---|---|---|---|---|
| Sacubitril/valsartan (% of target dose), median (IQR) | under s/v: 0.5 (0.5–1.0) | under s/v: 0.5 (0.3–1.0) | –0.165 | under s/v: 0.869 |
| Mineralocorticoid receptor antagonists, n (%) | prior s/v: 44 (84.6)<br>under s/v: 44 (84.6) | prior s/v: 36 (83.7)<br>under s/v: 36 (83.7) | 0.014<br>0.014 | prior s/v: 0.905<br>under s/v: 0.905 |
| Mineralocorticoid receptor antagonists (% of target dose), median (IQR) | prior s/v: 1.0 (1.0–1.0)<br>under s/v: 1.0 (1.0–1.0) | prior s/v: 1.0 (1.0–2.0)<br>under s/v: 1.0 (1.0–1.0) | –1.543<br>–0.150 | prior s/v: 0.123<br>under s/v: 0.881 |
| Diuretics, n (%) | prior s/v: 43 (82.7)<br>under s/v: 40 (76.9) | prior s/v: 36 (83.7)<br>under s/v: 37 (86.0) | 0.018<br>1.276 | prior s/v: 0.894<br>under s/v: 0.259 |
| Diuretics (% of target dose), median (IQR) | prior s/v: 1.0 (0.5–2.0)<br>under s/v: 1.0 (0.5–2.0) | prior s/v: 1.0 (1.0–2.0)<br>under s/v: 1.0 (0.5–2.0) | –0.066<br>–0.249 | prior s/v: 0.948<br>under s/v: 0.804 |
| Amiodarone, n (%) | prior/under s/v: 6 (11.5) | prior/under s/v: 8 (18.6) | 0.935 | 0.333 |
| Oral anticoagulation, n (%) | prior/under s/v: 23 (44.2) | prior/under s/v: 20 (46.5) | 0.049 | 0.824 |
| BP and heart rate | | | | |
| Systolic BP [mm Hg], median (IQR) | prior s/v: 120 (108.0–125.0)<br>under s/v: 116.0 (104.0–130.0) | prior s/v: 115.0 (107.5–122.5)<br>under s/v: 110.0 (96.3–118.5) | –0.642<br>–2.415 | prior s/v: 0.521<br>under s/v: 0.016* |
| Diastolic BP [mm Hg], median (IQR) | prior s/v: 75.0 (70.0–80.0)<br>under s/v: 76.0 (70.0–80.0) | prior s/v: 75.0 (69.0–80.0)<br>under s/v: 70.0 (65.0–80.0) | –0.060<br>–1.688 | prior s/v: 0.952<br>under s/v: 0.091 |
| Mean arterial pressure, median (IQR) | prior s/v: 87.3 (82.0–95.0)<br>under s/v: 90.0 (79.0–96.7) | prior s/v: 86.7 (82.3–93.3)<br>under s/v: 83.3 (76.7–90.0) | –0.335<br>–2.205 | prior s/v: 0.737<br>under s/v: 0.027* |
| Heart rate [bpm], median (IQR) | prior s/v: 70.0 (60.5–79.5)<br>under s/v: 63.0 (58.0–72.0) | prior s/v: 68.0 (60.0–75.0)<br>under s/v: 65.0 (57.0–75.0) | –0.591<br>–1.063 | prior s/v: 0.554<br>under s/v: 0.288 |
| ECG/electronic cardiac device | | | | |
| Atrial fibrillation (paroxysmal or permanent), n (%) | prior/under s/v: 22 (42.3) | prior/under s/v: 19 (44.2) | 0.034 | prior/under s/v: 0.854 |
| VA per month, median (IQR) | prior s/v: 0.000 (0.000–0.000)<br>under s/v: 0.000 (0.000–0.000) | prior s/v: 0.000 (0.000–0.007)<br>under s/v: 0.000 (0.000–0.000) | –0.847<br>–0.376 | prior s/v: 0.397<br>under s/v: 0.707 |
| Carrier of ICD, n (%) | prior s/v: 26 (50.0)<br>under s/v: 33 (63.5) | prior s/v: 26 (60.5)<br>under s/v: 30 (69.8) | 1.040<br>0.419 | prior s/v: 0.308<br>under s/v: 0.517 |
| Left bundle branch block, n (%) | prior/under s/v: 22 (42.3) | prior/under s/v: 13 (30.2) | 2.662 | prior/under s/v: 0.264 |
| Carrier of CRT (as ICD-upgrade or primarily CRT-D implantation), n (%) | prior s/v: 7 (13.5)<br>under s/v: 12 (23.1) | prior s/v: 12 (27.9)<br>under s/v: 17 (39.5) | 3.070<br>3.006 | prior s/v: 0.080<br>under s/v: 0.083 |
| Carrier of PM, n (%) | prior/under s/v: 2 (3.8) | prior/under s/v: 3 (7.0) | 0.463 | prior/under s/v: 0.496 |
| Echocardiography | | | | |
| Moderate to severe mitral valve regurgitation, n (%) | prior s/v: 7 (13.5)<br>under s/v: 5 (9.6) | prior s/v: 11 (25.6)<br>under s/v: 9 (20.9) | 2.251<br>2.398 | prior s/v: 0.134<br>under s/v: 0.121 |
| Moderate to severe tricuspid valve regurgitation, n (%) | prior s/v: 3 (5.8)<br>under s/v: 3 (5.8) | prior s/v: 3 (7.0)<br>under s/v: 6 (14.0) | 0.058<br>1.838 | prior s/v: 0.810<br>under s/v: 0.175 |
| Moderate to severe aortic valve regurgitation, n (%) | prior s/v: 1 (1.9)<br>under s/v: 2 (3.8) | prior s/v: 1 (2.3)<br>under s/v: 0 (0.0) | 0.019<br>1.689 | prior s/v: 0.892<br>under s/v: 0.194 |
| LV volume increase, n (%) | prior s/v:<br>mild: 9 (17.3)<br>moderate: 12 (23.1)<br>severe: 21 (40.4)<br>under s/v:<br>mild: 5 (9.6)<br>moderate: 11 (21.2)<br>severe: 18 (34.6) | prior s/v:<br>mild: 5 (11.6)<br>moderate: 8 (18.6)<br>severe: 22 (51.2)<br>under s/v:<br>mild: 6 (14.0)<br>moderate: 13 (30.2)<br>severe: 17 (39.5) | 1.348<br>4.312 | prior s/v: 0.718<br>under s/v: 0.230 |
| LA volume increase, n (%) | prior s/v:<br>mild: 12 (23.1)<br>moderate: 10 (19.2)<br>severe: 14 (26.9)<br>under s/v:<br>mild: 5 (9.6)<br>moderate: 10 (19.2)<br>severe: 7 (13.5) | prior s/v:<br>mild: 8 (18.6)<br>moderate: 12 (27.9)<br>severe: 13 (30.2)<br>under s/v:<br>mild: 6 (14.0)<br>moderate: 10 (23.3)<br>severe: 13 (30.2) | 1.565<br>6.919 | prior s/v: 0.667<br>under s/v: 0.075 |

Table 2. Characteristics of patients with a good and moderate efficacy under sacubitril/valsartan – cont.

| Parameters | Good efficacy of sacubitril/valsartan n = 52 | Moderate efficacy of sacubitril/valsartan n = 43 | Test value | p-value |
|---|---|---|---|---|
| RV volume increase, n (%) | prior s/v:<br>mild: 3 (5.8)<br>moderate: 5 (9.6)<br>severe: 3 (5.8)<br>under s/v:<br>mild: 2 (3.8)<br>moderate: 1 (1.9)<br>severe: 0 (0.0) | prior s/v:<br>mild: 0 (0.0)<br>moderate: 5 (11.6)<br>severe: 0 (0.0)<br>under s/v:<br>mild: 2 (4.7)<br>moderate: 5 (11.6)<br>severe: 0 (0.0) | 5.309<br>3.837 | prior s/v: 0.151<br>under s/v: 0.147 |
| RA volume increase, n (%) | prior s/v:<br>mild: 6 (11.5)<br>moderate: 7 (13.5)<br>severe: 5 (9.6)<br>under s/v:<br>mild: 5 (9.6)<br>moderate: 2 (3.8)<br>severe: 3 (5.8) | prior s/v:<br>mild: 6 (14.0)<br>moderate: 7 (16.3)<br>severe: 5 (11.6)<br>under s/v:<br>mild: 1 (2.3)<br>moderate: 4 (9.3)<br>severe: 5 (11.6) | 0.525<br>4.097 | prior s/v: 0.913<br>under s/v: 0.251 |
| Laboratory values | | | | |
| Creatinine [mg/dL], median (IQR) | prior s/v: 1.1 (0.9–1.4)<br>under s/v: 1.3 (1.0–1.5) | prior s/v: 1.2 (1.0–1.4)<br>under s/v: 1.3 (1.1–1.6) | –1.303<br>–1.078 | prior s/v: 0.193<br>under s/v: 0.281 |
| Urea [mg/dL], median (IQR) | prior s/v: 20.0 (14.0–29.5)<br>under s/v: 17.0 (14.0–27.8) | prior s/v: 20.0 (18.0–25.8)<br>under s/v: 20.5 (15.8–26.3) | –0.036<br>–1.081 | prior s/v: 0.971<br>under s/v: 0.280 |
| GFR [mL/min], median (IQR) | prior s/v: 67.0 (51.0–87.0)<br>under s/v: 60.0 (43.3–76.0) | prior s/v: 62.0 (51.0–76.0)<br>under s/v: 59.0 (42.0–73.0) | –0.837<br>–0.666 | prior s/v: 0.402<br>under s/v: 0.505 |
| Uric acid [mg/dL], median (IQR) | prior s/v: 7.0 (5.7–9.0)<br>under s/v: 6.1 (5.1–7.5) | prior s/v: 6.7 (5.7–7.8)<br>under s/v: 6.8 (5.4–7.7) | –0.908<br>–0.780 | prior s/v: 0.364<br>under s/v: 0.436 |
| Hemoglobin [g/dL], median (IQR) | prior s/v: 14.1 (12.7–15.1)<br>under s/v: 13.7 (12.7–14.7) | prior s/v: 14.4 (13.1–15.3)<br>under s/v: 13.7 (12.4–15.1) | –0.582<br>–0.259 | prior s/v: 0.560<br>under s/v: 0.796 |
| Aspartate transaminase [U/L], median (IQR) | prior s/v: 30.0 (21.0–38.0)<br>under s/v: 26.0 (24.0–31.0) | prior s/v: 30.0 (25.0–36.0)<br>under s/v: 28.0 (23.0–33.0) | –0.343<br>–0.498 | prior s/v: 0.731<br>under s/v: 0.619 |
| Potassium [mmol/L], median (IQR) | prior s/v: 4.5 (4.2–4.8)<br>under s/v: 4.5 (4.3–4.7) | prior s/v: 4.4 (4.2–4.6)<br>under s/v: 4.5 (4.2–4.9) | –0.368<br>–0.203 | prior s/v: 0.713<br>under s/v: 0.839 |
| CK [U/L], median (IQR) | prior s/v: 102.5 (80.8–142.5)<br>under s/v: 106.0 (73.0–131.0) | prior s/v: 108.0 (72.2–186.0)<br>under s/v: 111.0 (74.0–128.0) | –0.810<br>–0.383 | prior s/v: 0.418<br>under s/v: 0.701 |
| CRP [mg/L], median (IQR) | prior s/v: 0.5 (0.5–1.0)<br>under s/v: 0.5 (0.5–0.6) | prior s/v: 0.5 (0.5–0.5)<br>under s/v: 0.5 (0.5–0.6) | –1.977<br>–0.386 | prior s/v: 0.048*<br>under s/v: 0.700 |

ACEI – angiotensin-converting enzyme inhibitors; ARB – angiotensin-II-receptor blockers; BB – beta blocker; BMI – body mass index; BP – blood pressure; CABG – coronary artery bypass graft; CAD – coronary artery disease; CHF – chronic heart failure; COPD – chronic obstructive pulmonary disease; CRP – C-reactive protein; CK – creatinine kinase; CRT-D – cardiac resynchronization therapy (-implantable cardioverter defibrillator); ECG – electrocardiogram; (e)GFR – (estimated) glomerular filtration rate; ICD – implantable cardioverter defibrillator; LA – left atrium; LV – left ventricle; LVEF – left ventricular ejection fraction; MI – myocardial infarction; MRA – mineralocorticoid receptor antagonist; NICM – nonischemic cardiomyopathy; NT-proBNP – N-terminal pro-brain natriuretic peptide; NYHA – level of cardiopulmonal fitness according to New York Heart Association; OSAS – obstructive sleep apnoea syndrome; PAD – peripheral artery disease; PM – pacemaker; RA – right atrium; RV – right ventricle; s/v – sacubitril/valsartan; VA – ventricular arrhythmias. Data are presented as median (interquartile range (IQR)) (Mann–Whitney U test) or n (%) ($\chi^2$ test). * – statistically significant value of $p < 0.05$. Target dose calculation (for most important drugs; others calculated as equivalent doses): ramipril 10 mg = 1.0; enalapril 20 mg = 1.0; candesartan 32 mg = 1.0; valsartan 320 mg = 1.0; irbesartan 300 mg = 1.0; 2 × sacubitril/valsartan 97/103 mg = 1,0; hydrochlorothiazide 25 mg = 1.0; bisoprolol 10 mg = 1.0; metoprolol 190 mg = 1.0; carvedilol 50 mg = 1.0; spironolacton 25 mg = 1.0; eplerenon 25 mg = 1.0; torasemid 10 mg = 1.0; hydrochlorothiazide 25 mg = 1.0; xipamid 10 mg = 0.5; furosemid 40 mg = 1.0.

# Results

## Patient characteristics before and after the initiation of sacubitril/valsartan therapy

Out of the total number of 479 CHF patients, 104 patients were under sacubitril/valsartan treatment (Fig. 1). After the exclusion of patients with missing data, 95 patients were enrolled in our study. Within the period of data collection, no patient on sacubitril/valsartan therapy died. The median duration of sacubitril/valsartan therapy amounted to 17.0 (IQR: 10.0–26.3) months. Until then, the sacubitril/valsartan treatment was intermittently paused for a short period due to the side effects and thereafter prescribed again in 7 patients. In 3 cases, sacubitril/valsartan treatment had to be permanently withdrawn because of the drug intolerance and the data collection

**Table 3.** Side effects under sacubitril/valsartan therapy

| Clinical symptom | Total number of patients, n = 95 | Good efficacy of sacubitril/valsartan, n = 52 | Moderate efficacy of sacubitril/valsartan, n = 43 | Test value | p-value |
|---|---|---|---|---|---|
| Hypotension, n (%) | 48 (50.5) (thereof without clinical relevance: 13 (13.7)) | 28 (53.8) (thereof without clinical relevance: 5 (9.6)) | 20 (46.5) (thereof without clinical relevance: 7 (16.3)) | 0.236 | 0.627 |
| Orthostatic dizziness, n (%) | 35 (36.8) (thereof without clinical relevance: 15 (15.8)) | 21 (40.4) (thereof without clinical relevance: 9 (17.3)) | 14 (32.6) (thereof without clinical relevance: 6 (14.0)) | 0.620 | 0.431 |
| Kidney functional deterioration, n (%) | 29 (30.5) (thereof with AKI: 4 (4.2)) | 19 (36.5) (thereof with AKI: 1 (1.9)) | 10 (23.3) (thereof with AKI: 3 (7.0)) | 1.958 | 0.162 |
| Anemia de novo, n (%) | 8 (8.4) | 3 (5.8) | 5 (11.6) | 1.048 | 0.306 |
| Hyperkalemia, n (%) | 7 (7.4) | 1 (1.9) | 6 (14.0) | 4.991 | 0.025* |
| Indefinite dizziness, n (%) | 4 (4.2) | 1 (1.9) | 3 (7.0) | 1.490 | 0.222 |
| Headache, n (%) | 2 (2.1) | 2 (3.8) | 0 (0.0) | 1.689 | 0.194 |
| Diarrhea, n (%) | 2 (2.1) | 2 (3.8) | 0 (0.0) | 1.689 | 0.194 |
| Cough, n (%) | 1 (1.1) | 1 (1.9) | 0 (0.0) | 0.836 | 0.361 |
| Angioedema, n (%) | 0 (0.0) | 0 (0.0) | 0 (0.0) | – | – |

AKI – acute kidney injury according to Kidney Disease: Improving Global Outcome (KDIGO) criteria. Data are presented as n (%) ($\chi^2$ test). * – statistically significant value of $p < 0.05$.

**Table 4.** Univariate Cox regression analysis predicting good clinical efficacy of sacubitril/valsartan

| Parameters | Probability of a good sacubitril/valsartan efficacy | p-value |
|---|---|---|
| LVEF prior to sacubitril/valsartan | HR = 0.982, 95% CI = [0.948; 1.018] | 0.318 |
| NICM | HR = 2.523, 95% CI = [1.371; 4.644] | 0.003* |
| Hospitalizations for CHF per month prior to sacubitril/valsartan | HR = 1.632, 95% CI = [0.944; 2.818] | 0.079 |
| Dyslipidemia | HR = 1.872, 95% CI = [1.062; 3.302] | 0.030* |
| CRP levels prior to sacubitril/valsartan therapy | HR = 1.289, 95% CI = [1.080; 1.539] | 0.005* |
| Time from diagnosis to sacubitril/valsartan start | HR = 0.993, 95% CI = [0.989; 0.997] | <0.001* |

CHF – chronic heart failure; CRP – C-reactive protein; LVEF – left ventricular ejection fraction; NICM – nonischemic cardiomyopathy. Data are presented as hazard ratio (HR) with 95% confidence interval (95% CI) and p-values (univariate Cox regression analysis). * – statistically significant value of $p < 0.05$.

**Table 5.** Multivariate Cox regression analysis predicting a good clinical efficacy of sacubitril/valsartan; the final model

| Parameters | Probability of a good sacubitril/valsartan efficacy | p-value |
|---|---|---|
| LVEF prior to sacubitril/valsartan | – | N/S: 0.928 |
| NICM | – | N/S: 0.267 |
| Hospitalizations for CHF per month prior to sacubitril/valsartan | – | N/S: 0.467 |
| Dyslipidemia | – | N/S: 0.434 |
| CRP levels prior to sacubitril/valsartan therapy | HR = 1.263, 95% CI = [1.048; 1.521] | 0.014* |
| Time from diagnosis to sacubitril/valsartan start | HR = 0.992, 95% CI = [0.987; 0.997] | <0.001* |

CHF – chronic heart failure; CRP – C-reactive protein; LVEF – left ventricular ejection fraction; NICM – nonischemic cardiomyopathy. Data are presented as hazard ratio (HR) with 95% confidence interval (95% CI) and p-values for selected variables. For non-selected variables (N/S), p-values of score test are displayed (multivariate Cox regression analysis). * – statistically significant value of $p < 0.05$.

was stopped at this timepoint. Baseline characteristics of all patients enrolled in the study are listed in Table 1. The patients were 57.0 (50.0–69.0) years old, mostly male, with a high prevalence of cardiovascular risk factors and presenting both ischemic and nonischemic etiologies of CHF. Almost all patients received optimal CHF drug therapy. The median time between the HF diagnosis and the initiation of the sacubitril/valsartan therapy was 92.5 (25.0–147.8) months. In 5 patients in the good efficacy group and in 3 patients in the moderate efficacy group, sacubitril/valsartan was prescribed within 1 month after the diagnosis of HF (de novo HF caused by either myocarditis, acute coronary ischemia or unclear nonischemic cardiomyopathy). Under sacubitril/valsartan therapy, the following parameters significantly improved: LVEF, NYHA class, NT-proBNP levels, the hospitalization rates, and the left (LA) and right (RA) atrial volumes, whereas the left ventricular (LV) and right ventricular (RV) volumes

demonstrated a decreasing trend. The heart rate was relevantly slower at a follow-up. Aspartate transaminase blood concentrations significantly decreased, probably as a reflection of a better cardiac function. In contrast, kidney function defined as changes in serum creatinine and GFR relevantly declined.

### Characteristics of patients with a good and moderate efficacy of sacubitril/valsartan therapy, and possible predictors of outcome

When comparing patients with a good to moderate sacubitril/valsartan efficacy at baseline, the first group was characterized by relevantly worse LVEF of a predominantly nonischemic etiology, higher hospitalization rates for CHF, shorter period between CHF diagnosis and the initiation of sacubitril/valsartan therapy, and lower cholesterol and higher C-reactive protein (CRP) blood levels (Table 2). The good efficacy group showed by definition significantly higher LVEF, lower NYHA classes, reduced hospitalization rates for CHF, and a strong trend toward decreasing NT-proBNP levels at a follow-up.

### Univariate and multivariate Cox regression analyses of good efficacy

The parameters which significantly differed between the groups with a good and moderate efficacy at baseline, such as LVEF, NICM, hospitalizations for CHF, dyslipidemia, CRP levels, and the time from diagnosis to the initiation of sacubitril/valsartan treatment, were included in the univariate Cox regression analysis (Table 4). The multivariate Cox regression analysis found only 2 parameters to be independently associated with a good efficacy (Table 5): higher CRP levels prior to sacubitril/valsartan therapy (hazard ratio (HR) = 1.263, confidence interval (95% CI) = [1.048; 1.521], p = 0.014), and a shorter time between CHF diagnosis and the initialization of sacubitril/valsartan treatment (HR = 0.992, 95% CI = [0.987; 0.997], p < 0.001).

### Side effects

The most common side effects of sacubitril/valsartan treatment in our study were well-known adverse effects of this medication, such as arterial hypotension, worsening of kidney function followed by (less frequent) anemia, hyperkalemia, non-orthostatic dizziness, gastrointestinal disorders, headache, and cough (Table 3). Clinically relevant angioedema was not detected in any case. Interestingly, comparing the side effects in patients with a good to moderate efficacy, hyperkalemia was significantly more common in patients benefiting less from valsartan/sacubitril. In contrast, a tendency toward a more deteriorated kidney function (but not AKI), as defined in "Endpoints and definitions" section, was found in the good efficacy group.

## Discussion

Our present study is a real-world research on sacubitril/valsartan therapy, identifying the parameters of a good clinical outcome under this treatment. In comparison with the patient population from the PARADIGM-HF study,[1] patients in our trial were in average younger, more frequently in NYHA class III than II, had more comorbidities, presented more often NICM as a CHF etiology, and were more frequently treated with mineralocorticoid antagonists and the implantable cardioverter-defibrillator (ICD)/cardiac resynchronization therapy (CRT) (Table 1).

In line with other studies, sacubitril/valsartan improved cardiac function with reversal of cardiac remodeling and positively influenced functional status, NT-proBNP levels and hospitalization rates.[1,2,11] The overall tolerance of sacubitril/valsartan was good, without major adverse effects, and did not differ between patients with a good and moderate efficacy, except for more frequent hyperkalemia in the moderate efficacy group (Table 3), which could be an effect of a slightly worse kidney function resulting from more reduced LVEF, with a consequent hypotension and/or more frequently present cardiovascular risk factors for generalized atherosclerosis in this group. Anemia was not pronounced in both groups at baseline and there was no significant decrease in hemoglobin (Hb) levels under sacubitril/valsartan therapy in either of the groups. This is an important information, as it is known that anemia increases hospitalization and mortality rates in CHF patients.[12] However, this does not allow to draw any conclusions about the iron status in patients enrolled in this study, since anemia is mostly driven by the upregulation of neurohumoral and inflammatory cytokines and a concomitant renal disease in CHF patients, and not by iron deficiency.[12] Iron deficiency itself is an independent risk factor of poor outcomes in CHF patients with reduced LVEF, regardless of Hb levels.[13] So far, there are no data supporting relevant adverse effects of sacubitril/valsartan on iron metabolism.

In total, 52 out of 95 patients (54.7%) reached the clinical endpoint of a good efficacy of sacubitril/valsartan, defined as an improvement of at least 2 parameters out of 4, including LVEF, NT-proBNP, NYHA class, and hospitalization rates. The decision to take into consideration at least 2 of the abovementioned parameters to judge the clinical efficacy under sacubitril/valsartan therapy was due to the fact that single non-mortality-related endpoints may be less reliable in adequately reflecting a good clinical responsiveness to therapy than composite endpoints. Indeed, it is known that NYHA class change alone may not properly assess a good clinical effectiveness of the CHF treatment, as CHF patients may not accurately report on their symptoms or may complain only few or even no symptoms due to the avoidance of physical activity.[14] Furthermore, the addition of LVEF with NT-proBNP and hospitalization frequency under sacubitril/valsartan therapy to our clinical endpoint, makes such an endpoint also relevant

for the survival estimation, as both reduced LVEF and increased hospitalization rates enhance mortality.[1,15]

Patients in a good efficacy group had significantly lower LVEF, more NICM, more frequent hospitalization rates for CHF, less dyslipidemia, higher CRP levels at baseline, and a shorter time between CHF diagnosis and the start of sacubitril/valsartan therapy. Additionally, they were characterized by a tendency toward less frequent diabetes (Table 2).

A multivariate Cox regression analysis evaluating relevant parameters significantly different at baseline between the groups, demonstrated that only 2 factors, higher blood CRP levels at baseline and a shorter time between the diagnosis of CHF and the start of sacubitril/valsartan therapy, were independent predictors of clinical success under this therapy.

Sacubitril/valsartan, as a composite drug of sacubitril and valsartan, was shown to exert, besides a positive influence on cardiac structure and function, also beneficial extracardiac impact such as metabolic effects with HbA1c level reductions, suggesting potential pleiotropic effects of this medication.[2] Valsartan was demonstrated to lower inflammatory levels and microalbuminuria in patients with metabolic syndrome,[16] and had protective effects against smoking-induced LV systolic dysfunction by attenuating oxidative stress, cardiomyocyte apoptosis and inflammation.[17] Similarly, the combination of a low dose of fluvastatin and valsartan was proven to act anti-inflammatory and antioxidative in apparently healthy middle-aged men[18] and in patients with type II diabetes.[19] Moreover, the coadministration of captopril and valsartan reduced inflammation levels in patients after the interventional therapy for acute myocardial infarction.[20] Studies on sacubitril/valsartan revealed that sacubitril/valsartan ameliorated atherosclerosis and inflammation in apoE–/– mice, as compared with valsartan alone.[21] Sacubitril/valsartan improved renal function by reducing the oxidative stress, inflammation and fibrosis beyond the effects of therapy with valsartan alone.[22] Furthermore, sacubitril/valsartan prevented cardiac rupture after myocardial infarction, due to the inhibition of inflammation and degradation response of macrophages.[23]

Thus, better effects of sacubitril/valsartan on clinical outcome in patients with higher inflammatory levels prior to sacubitril/valsartan therapy in our study could suggest that sacubitril/valsartan acts in this patient subpopulation even more effectively, as it may additionally unfold its further property, namely the anti-inflammatory one. Indeed, higher inflammation levels in the good efficacy group were decreased under sacubitril/valsartan therapy, and reached the levels comparable to those in the moderate efficacy group at the last follow-up in our study (Table 2). Since the inflammation is associated with left ventricular dysfunction[24,25] and higher mortality,[26] the attenuation of this process could explain better results of sacubitril/valsartan treatment in patients with enhanced inflammation before the start of sacubitril/valsartan therapy.

The second parameter which positively influenced the responsiveness to sacubitril/valsartan therapy in our study was a shorter time between the CHF diagnosis and the start of sacubitril/valsartan treatment. It may be assumed that this finding could be associated with the fact that early after CHF diagnosis, the magnitude of heart structure and function deterioration is not so high and the pathological changes are still at least partly reversible, compared to those in advanced CHF. In line with this assumption, sacubitril/valsartan seemed to be less effective in NYHA class III and IV patients for the primary endpoint of the PARADIGM-HF study, but not for death from cardiovascular causes.[2] However, because of the underrepresentation of NYHA class III and IV in the PARADIGM-HF study, these results should be proven in further trials. Similarly, the improvement of LVEF was associated with lower LV dilation prior to sacubitril/valsartan treatment,[5] indicating that sacubitril/valsartan therapy should be initiated earlier, when the cardiac remodeling is not advanced yet.[5] This result could also have another explanation connected to the findings stating that in acute HF with elevated BNP and NT-proBNP levels, neprilysin catalytic activity is inhibited.[27] Analogically, in advanced CHF with high BNP and NT-proBNP blood concentrations, the neprilysin catalytic activity could be suppressed, thus potentially affecting the actions of sacubitril/valsartan. In contrast, risk scores such as the Meta-Analysis Global Group in Chronic Heart Failure (MAGGIC) score with independent predictors of all-cause mortality, cardiovascular mortality and hospitalizations for CHF including baseline characteristics, comorbidities and concurrent medication, as well as the Eplerenone in Mild Patients Hospitalization and Survival Study in Heart Failure (EMPHASIS-HF) risk score with 10 independent risk factors showed that the subgroups of patients with different quartiles benefited from sacubitril/valsartan over enalapril, and the greatest absolute benefit was detected in patients with the highest risk, defined, among others, by a more advanced, long-lasting HF.[28] However, in the high-risk patient groups, the levels of inflammation could have been higher than in the other ones, so that the anti-inflammatory effect of sacubitril/valsartan could possibly outweigh the attenuated effectiveness, due to a longer persistence of HF before the start of sacubitril/valsartan therapy.

Another aspect of our finding is that the inclusion criteria for sacubitril/valsartan should not exclude patients who do not perfectly match the inclusion criteria of the PARADIGM-HF study, or due to the concerns about potential side effects. Also, hasty withdrawal or significant reduction of sacubitril/valsartan dose only because of minor, clinically not significant adverse effects should be avoided. Another important issue are patients in NYHA class I with low NT-proBNP levels who were not enrolled in the PARADIGM-HF study. Since NYHA class or NT-proBNP levels do not reliably predict the clinical benefit of sacubitril/valsartan treatment, withholding this therapy from those patients could possibly put them at risk of disease

progression. Therefore, further investigations on this issue are urgently needed, since the current European Guidelines still recommend sacubitril/valsartan treatment in patients with a persistence of symptomatic CHF who had to previously undergo angiotensin-converting enzyme inhibitor (ACEI)/angiotensin receptor blocker (ARB) therapy.[7]

## Limitations

Our study has some limitations, primarily arising from its retrospective design and the associated bias. Additionally, the study's meaningfulness could potentially be affected by a relatively small sample size and the limited follow-up time. Furthermore, NYHA class reported by patients was not verified using functional tests. Also, as a single-center experience in an outpatient setting in Germany, the results might represent local practice and cannot be uncritically extrapolated to more advanced CHF stages demanding hospitalizations. Moreover, a control group treated with standard HF medication is lacking since, after the approval of sacubitril/valsartan, all patients fulfilling the indication criteria for sacubitril/valsartan in our outpatient section were gradually switched to this drug. Also, the target dose of sacubitril/valsartan was not reached in many cases because of already occurring side effects or preventive actions aimed at avoiding possible adverse effects under higher medication doses. However, according to the PARADIGM-HF study, lower sacubitril/valsartan doses are still effective and more beneficial in terms of outcome than the comparable ACEI/ARB doses. Another limitation of our study is the documentation of LV performance through the assessment of LVEF, without the calculation of strain in a speckle tracking analysis. Although the strain measurement could be useful to better estimate the magnitude of LV dysfunction, such analysis was not routinely performed in our patient collective, as it may be of a higher importance in population with apparently preserved LV function to detect early changes in LV.[29] Moreover, the vast majority of patients who fulfilled the criterion of the LVEF improvement of at least 5%, had an increase in LVEF relevantly higher than 5% (median (IQR): 12% (9–21%)), so that the potential errors in the LVEF estimation over the course of time resulting from the inaccuracy of the method seem to be limited.

Nevertheless, despite all the above limitations, our findings present real-world data which confirm the safety and efficacy of this quite new drug, with an emphasis on potential factors predicting the best clinical results.

# Conclusions

In conclusion, our present study found worse LVEF, increased hospitalization rates for CHF, less frequent hyperlipidemia and increased CRP at baseline together with more predominant NICM and a shorter time between CHF diagnosis and the start of sacubitril/valsartan therapy to be associated with a good clinical response and outcome under sacubitril/valsartan therapy, defined as an improvement of at least 2 of the following parameters: LVEF, NT-proBNP, NYHA class, or the hospitalization rates. However, only increased CRP blood levels at baseline and a shorter time from the CHF diagnosis to the initiation of sacubitril/valsartan therapy turned out to be independently associated with a good clinical response to sacubitril/valsartan treatment in a multivariate Cox regression analysis. Thus, this study may contribute to optimized patient selection and help to predict clinical prognosis of patients undergoing sacubitril/valsartan therapy. However, further prospective studies with a larger number of patients are required to definitely prove these findings.


## ORCID iDs

Elisabeth J. Fröb https://orcid.org/0000-0002-4269-558X
Jürgen R. Sindermann https://orcid.org/0000-0002-1370-0060
Holger Reinecke https://orcid.org/0000-0002-4515-1609
Izabela Tuleta https://orcid.org/0000-0002-8482-591X


## References


1. McMurray JJ, Packer M, Desai AS, et al. PARADIGM-HF Investigators and Committees. Angiotensin-neprilysin inhibition versus enalapril in heart failure. *N Engl J Med*. 2014;371(11):993–1004. doi:10.1056/NEJMoa1409077
2. Almufleh A, Marbach J, Chih S, et al. Ejection fraction improvement and reverse remodeling achieved with sacubitril/valsartan in heart failure with reduced ejection fraction patients. *Am J Cardiovasc Dis*. 2017;7(6):108–113. PMID:29348971.
3. Bayard G, Da Costa A, Pierrard R, Roméyer-Bouchard C, Guichard JB, Isaaz K. Impact of sacubitril/valsartan on echo parameters in heart failure patients with reduced ejection fraction: A prospective evaluation. *Int J Cardiol Heart Vasc*. 2019;25:100418. doi:10.1016/j.ijcha.2019.100418
4. Sauer AJ, Cole R, Jensen BC, et al. Practical guidance on the use of sacubitril/valsartan for heart failure. *Heart Fail Rev*. 2019;24(2):167–176. doi:10.1007/s10741-018-9757-1
5. Lin AH, Chin JC, Sicignano NM, Evans AM. Repeat hospitalizations predict mortality in patients with heart failure. *Mil Med*. 2017;182(9):e1932–e1937. doi:10.7205/MILMED-D-17-00017
6. Ponikowski P, Voors AA, Anker SD, et al. ESC Scientific Document Group. 2016 ESC Guidelines for the diagnosis and treatment of acute and chronic heart failure: The Task Force for the diagnosis and treatment of acute and chronic heart failure of the European Society of Cardiology (ESC). Developed with the special contribution of the Heart Failure Association (HFA) of the ESC. *Eur Heart J*. 2016;37(27):2129–2200. doi:10.1093/eurheartj/ehw128
7. Zile MR, Claggett BL, Prescott MF, et al. Prognostic implications of changes in N-terminal pro-B-type natriuretic peptide in patients with heart failure. *J Am Coll Cardiol*. 2016;68(22):2425–2436. doi:10.1016/j.jacc.2016.09.931
8. Blanc B, Finch CA, Hallberg L, Lawkowicz W, Layrisse M, Mollin DL. Nutritional anaemias: Report of a WHO Scientific Group. *WHO Tech Rep Ser*. 1968;405:1–40. PMID:4975372.
9. Levey AS, Eckardt KU, Tsukamoto Y, et al. Definition and classification of chronic kidney disease. A position statement from Kidney Disease: Improving Global Outcomes (KDIGO). *Kidney Int*. 2005;67(6):2089–2100. doi:10.1111/j.1523-1755.2005.00365.x
10. Khwaja A. KDIGO clinical practice guidelines for acute kidney injury. *Nephron Clin Pract*. 2012;120(4):c179–c184. doi:10.1159/000339789
11. Januzzi JL Jr, Prescott MF, Butler J, et al. PROVE-HF Investigators. Association of change in N-terminal pro-B-type natriuretic peptide following initiation of sacubitril-valsartan treatment with cardiac structure and function in patients with heart failure with reduced ejection fraction. *JAMA*. 2019;322(11):1085–1095. doi:10.1001/jama.2019.12821

12. Anand IS, Gupta P. Anemia and iron deficiency in heart failure: Current concepts and emerging therapies. *Circulation*. 2018;138(1):80–98. doi:10.1161/CIRCULATIONAHA.118.030099
13. Fitzsimons S, Yeo TJ, Ling LH, et al. Impact of change in iron status over time on clinical outcomes in heart failure according to ejection fraction phenotype. *ESC Heart Fail*. 2021;8(6):4572–4583. doi:10.1002/ehf2.13617.
14. Yandrapalli S, Andries G, Biswas M, Khera S. Profile of sacubitril/valsartan in the treatment of heart failure: Patient selection and perspectives. *Vasc Health Risk Manag*. 2017;13:369–382. doi:10.2147/VHRM.S114784
15. Smith KR, Hsu CC, Berei TJ, et al. PARADIGM-HF trial: Secondary analyses address unanswered questions. *Pharmacotherapy*. 2018;38(2):284–298. doi:10.1002/phar.2075
16. Shishido T, Konta T, Nishiyama S, et al. Suppressive effects of valsartan on microalbuminuria and CRP in patients with metabolic syndrome (Val-Mets). *Clin Exp Hypertens*. 2011;33(2):117–123. doi:10.3109/10641963.2010.531837
17. Zhou X, Li C, Xu W, Chen J. Protective effects of valsartan against cigarette smoke-induced left ventricular systolic dysfunction in rats. *Int J Cardiol*. 2013;167(3):677–680. doi:10.1016/j.ijcard.2012.03.068
18. Janić M, Lunder M, Prezelj M, Šabovič M. A combination of low-dose fluvastatin and valsartan decreases inflammation and oxidative stress in apparently healthy middle-aged males. *J Cardiopulm Rehabil Prev*. 2014;34(3):208–212. doi:10.1097/HCR.0000000000000027
19. Lunder M, Janić M, Savić V, Janež A, Kanc K, Šabovič M. Very low-dose fluvastatin-valsartan combination decreases parameters of inflammation and oxidative stress in patients with type 1 diabetes mellitus. *Diabetes Res Clin Pract*. 2017;127:181–186. doi:10.1016/j.diabres.2017.03.019
20. Gong X, Zhou R, Li Q. Effects of captopril and valsartan on ventricular remodeling and inflammatory cytokines after interventional therapy for AMI. *Exp Ther Med*. 2018;16(4):3579–3583. doi:10.3892/etm.2018.6626
21. Zhang H, Liu G, Zhou W, Zhang W, Wang K, Zhang J. Neprilysin inhibitor-angiotensin II receptor blocker combination therapy (sacubitril/valsartan) suppresses atherosclerotic plaque formation and inhibits inflammation in apolipoprotein E-deficient mice. *Sci Rep*. 2019;9(1):6509. doi:10.1038/s41598-019-42994-1
22. Jing W, Vaziri ND, Nunes A, et al. LCZ696 (sacubitril/valsartan) ameliorates oxidative stress, inflammation, fibrosis and improves renal function beyond angiotensin receptor blockade in CKD. *Am J Transl Res*. 2017;9(12):5473–5484. PMID:29312499.
23. Ishii M, Kaikita K, Sato K, et al. Cardioprotective effects of LCZ696 (sacubitril/valsartan) after experimental acute myocardial infarction. *JACC Basic Transl Sci*. 2017;2(6):655–668. doi:10.1016/j.jacbts.2017.08.001
24. Hasper D, Hummel M, Kleber FX, Reindl I, Volk HD. Systemic inflammation in patients with heart failure. *Eur Heart J*. 1998;19(5):761–765. doi:10.1053/euhj.1997.0858
25. Torre-Amione G, Kapadia S, Benedict C, Oral H, Young JB, Mann DL. Proinflammatory cytokine levels in patients with depressed left ventricular ejection fraction: A report from the studies of left ventricular dysfunction (SOLVD). *J Am Coll Cardiol*. 1996;27(5):1201–1206. doi:10.1016/0735-1097(95)00589-7
26. Pellicori P, Zhang J, Cuthbert J, et al. High-sensitivity C-reactive protein in chronic heart failure: Patient characteristics, phenotypes, and mode of death. *Cardiovasc Res*. 2020;116(1):91–100. doi:10.1093/cvr/cvz198
27. Vodovar N, Séronde MF, Laribi S, et al. GREAT Network. Elevated plasma B-type natriuretic peptide concentrations directly inhibit circulating neprilysin activity in heart failure. *JACC Heart Fail*. 2015;3(8):629–636. doi:10.1016/j.jchf.2015.03.011
28. Simpson J, Jhund PS, Silva Cardoso J, et al. PARADIGM-HF Investigators and Committees. Comparing LCZ696 with enalapril according to baseline risk using the MAGGIC and EMPHASIS-HF risk scores: An analysis of mortality and morbidity in PARADIGM-HF. *J Am Coll Cardiol*. 2015;66(19):2059–2071. doi:10.1016/j.jacc.2015.08.878
29. Smiseth OA, Torp H, Opdahl A, Haugaa KH, Urheim S. Myocardial strain imaging: How useful is it in clinical decision making? *Eur Heart J*. 2016;37(15):1196–1207. doi:10.1093/eurheartj/ehv529

# Association between systemic inflammatory response syndrome and hematoma expansion in intracerebral hemorrhage

*Yu Zhu[A–F], *Zhikai Xie[A–F], Jie Shen[B,C], Lihui Zhou[B,C], Zongchi Liu[B,C], Di Ye[B,C], Fan Wu[B,C], Sohaib Hasan Abdullah Ezzi[B,C], Zahraa Sh Hmood[B,C], Renya Zhan[A,E,F]

Department of Neurosurgery, The First Affiliated Hospital, Zhejiang University School of Medicine, Hangzhou, China

A – research concept and design; B – collection and/or assembly of data; C – data analysis and interpretation; D – writing the article; E – critical revision of the article; F – final approval of the article

Advances in Clinical and Experimental Medicine, ISSN 1899–5276 (print), ISSN 2451–2680 (online) *Adv Clin Exp Med*. 2022;31(5):489–498

**Address for correspondence**
Renya Zhan
E-mail: 1196057@zju.edu.cn

**Funding sources**
This study was supported by National Natural Science Foundation of China (grant No. 81701208), Key Research & Development Plan of Zhejiang Province (grant No. 2019C03034) and Medicine & Health Technology Plan of Zhejiang Province (grants No. 2019KY395 and 201234160).

**Conflict of interest**
None declared

*Yu Zhu and Zhikai Xie contributed equally to this manuscript.

Received on June 1, 2021
Reviewed on October 26, 2021
Accepted on January 14, 2022

Published online on February 11, 2022

## Abstract

**Background.** Hematoma expansion (HE) is a relatively common complication after intracerebral hemorrhage.

**Objectives.** To explore the association between systemic inflammatory response syndrome (SIRS) and HE in patients with intracerebral hemorrhage (ICH).

**Materials and methods.** From June 2013 to October 2020, the sociodemographic data and clinical data of 780 ICH patients were collected. The logistic regression analysis with odd ratios (ORs) and 95% confidence intervals (95% CIs) was performed to analyze the risk factors for HE in patients with ICH.

**Results.** Hematoma expansion occurred in 151 (19.36%) patients with ICH. Significant differences were presented between SIRS and HE (OR = 2.549, 95% CI: [1.497; 4.342], p = 0.0006). After adjusting the covariates, a further analysis showed that the respiratory rate >20 beats/min (OR = 3.436, 95% CI: [1.981; 5.960], $p < 0.0001$), white blood cell (WBC) $> 12\times10^9$/L or WBC $\leq 4\times10^9$/L (OR = 2.489, 95% CI: [1.494; 4.149], p = 0.0005) increased the risk for HE in ICH patients. Our study also found that the significant differences between HE and non-HE patients in proportion of patients with history of diabetes mellitus, basal ganglia hemorrhage, hypothalamus hemorrhage and fasting blood glucose (all $p < 0.05$) (OR = 2.076, 95% CI: [1.274; 3.381], p = 0.0034), basal ganglia hemorrhage (OR = 2.512, 95% CI: [1.496; 4.218], p = 0.0005), hypothalamus hemorrhage (OR = 2.121, 95% CI: [1.007; 4.466], p = 0.0479), high C-reactive protein (CRP) (OR = 1.013, 95% CI: [1.002; 1.024], p = 0.0184), and hyperglycemia (OR = 1.099, 95% CI: [1.026; 1.178], p = 0.0074) were associated with an increased risk of HE in ICH patients.

**Conclusions.** The SIRS is closely associated with the risk of HE. Respiratory rate >20 beats/min and WBC count >12($10^9$/L) or ≤4($10^9$/L) increased the risk for HE in ICH patients. These findings can help to achieve the early prevention of HE and improve the prognosis of ICH patients.

**Key words:** risk factors, C-reactive protein, SIRS, intracerebral hemorrhage, hematoma expansion

**Cite as**
Zhu Y, Xie Z, Shen J, et al. Association between systemic inflammatory response syndrome and hematoma expansion in intracerebral hemorrhage. *Adv Clin Exp Med*. 2022;31(5):489–498. doi:10.17219/acem/145852

**DOI**
10.17219/acem/145852

# Background

Hematoma expansion (HE), which is defined as an increase in hematoma volume by >33% or an absolute increase in hematoma volume by >12.5 mL, is a relatively common complication after intracerebral hemorrhage (ICH).[1] Several studies demonstrated that HE was closely related to the neurologic deterioration,[2] poor neurologic functional outcome and ICH mortality.[3] Acute HE is an important factor leading to the deterioration of the clinical condition of stroke patients. Research has shown that HE occurred in ICH patients and was a major influence factor for early deterioration and poor clinical prognosis.[3,4]

A prior study found that the mortality rate of ICH patients in the HE group was 53.6%, while in the non-HE group the mortality rate was 6.3%.[5] The HE has been proven to be an independent predictive factor of 30-day mortality and poor prognosis.[6] Numerous studies focused on the risk factors for HE in ICH.[7] Several laboratory indicators have been identified as risk factors for HE, such as basal ganglia hemorrhage was associated with HE,[7] early peripheral blood neutrophilia was an imaging marker of secondary damage to cerebral hematoma and a risk factor for poor prognosis of ICH,[2,7] the increase in the level of pro-inflammatory cytokine C-reactive protein (CRP) was a general risk factor for HE,[8] and so on. To our knowledge, there were rare reports on the association between systemic inflammatory response syndrome (SIRS) and HE. The SIRS was defined by the presence of 2 or more of the following factors: body temperature <36°C or >38°C, respiratory rate >20 breaths per min, heart rate >90 beats per min, or white blood cell (WBC) count $<4 \times 10^9$/L or $>12 \times 10^9$/L in the absence of infection.[9] Furthermore, SIRS is an immune-related aseptic inflammatory response, which is common in various critically ill patients.[10] The SIRS is common in patients with vascular disease.[11] It was also found that SIRS was observed in 14% of ICH patients on admission and was related to the severity of stroke, infection and prognosis.[12] However, the association between SIRS and HE in ICH patients remains undetermined.

# Objectives

To recognize the risk factors for HE in ICH patients is of great importance for the early prevention of HE. In this study, we assessed and retrospectively analyzed the general data, imaging data and laboratory indicators of patients with ICH, with the aim of identifying the association between SIRS and HE.

# Materials and methods

## Patients

This was a retrospective study. The sociodemographic and clinical data of 780 patients with ICH, who were diagnosed using baseline computed tomography (CT) scan within 6 h after the symptoms onset at The First Affiliated Hospital, Zhejiang University School of Medicine, Hangzhou, China, between June 2013 and October 2020, were collected. Patients aged ≥18 years were included in this study. Exclusion criteria: 1) patients with a secondary cause of their ICH such as potential aneurysm, vascular malformations, neoplasms, head injury, venous infarction, and hemorrhagic transformation of an ischemic stroke; 2) patients with the history of acute infection or fever 1 month before ICH; 3) patients with cardiovascular and cerebrovascular diseases or surgical trauma within 3 months before ICH; 4) patients with severe hepatic and renal dysfunction, and coagulation impediment; 5) patients with incomplete or missing information. All patients voluntarily participated in the study and an informed consent was obtained from every patient or their next of kin prior to the collection of data. The study was approved by the Institutional Review Board of The First Affiliated Hospital, Zhejiang University School of Medicine, Hangzhou, China (approval No. 201310-3).

## Data collection

We collected sociodemographic and clinical data for patients with ICH on admission, including age, gender, smoking history (patients who smoked more than 100 cigarettes in their whole life), drinking history (patients who had at least 12 drinks (12 ounces of beer, a 5 ounce glass of wine or 1.5 ounces of liquor) of any type of alcoholic beverage in any given year of their life), underlying diseases conditions and SIRS data (body temperature, heart rate, respiratory rate, and WBC count). The underlying diseases included hypertension, diabetes, hemorrhagic stroke, and ischemic stroke.

All patients underwent Glasgow Coma Scale (GCS) and Graeb score[13] assessment and blood pressure measurement. The Graeb score is based on the left, the right, the 3rd and the 4th lateral ventricle score, and the possible total score is 12 points.[13] The score of 0 points indicates no intraventricular hemorrhage, from 1 to 4 points indicates mild intraventricular hemorrhage, from 5 to 8 points indicates moderate intraventricular hemorrhage, and from 9 to 12 points indicates severe intraventricular hemorrhage. Also, all patients underwent head CT examination for midline shift within 3 h of symptoms onset. After that, we collected 5 mL of venous blood from patients for blood routine, liver and kidney function, coagulation function and myocardial enzyme spectrum examination, and performed fasting blood glucose (FBG) test the next day.

All patients underwent cranial CT scan again 24 h from the symptoms onset to identify hematoma features: hematoma volume (ABC/2 method), midline shift and ICH location. The ICH volumes of the CT scans were calculated using the ABC/2 formula. The HE was defined as an increase in hematoma volume by >33% or an absolute increase in hematoma volume by >12.5 mL. The GCS and Graeb score were used to measure the severity of ICH.

The laboratory indicators were as follows: international normalized ratio (INR), platelet (PLT), hemoglobin (Hb), neutrophil/lymphocyte ratio (NLR), platelet/lymphocyte ratio (PLR), body temperature, heart rate, WBC, neutrophils and lymphocytes (LC) count, and CRP.

## Statistical analyses

The statistical analysis was conducted using IBM SPSS v. 20.0 statistical software (IBM Corp., Armonk, USA). All statistical tests were two-tailed. The data were tested using Kolmogorov–Smirnov test for normality (Table 1). The non-normal data were described using median and quartiles (M (Q1, Q3)) and the comparison between groups was performed with the Mann–Whitney U test. The numeric data were compared using $\chi^2$ test and presented as n (%). The value of $p < 0.05$ was considered statistically significant. The logistic regression was used to analyze the possible risk factors of HE in ICH patients. The variables with significant differences in univariate analysis were included in the multivariable logistic regression for adjustment, and stepwise logistic regression was performed with significance level for entry (SLENTRY) = 0.05, and significance level for entry (SLSTAY) = 0.05 for entering and removing risk factors, respectively. The presence of collinearity (having less than 2 variance inflation factors in Table 2,3), goodness-of-fit and $R^2$ measure on the influencing factors of the multivariable logistic model were calculated.

# Results

## Baseline characteristics of patients

Seven hundred and eighty ICH patients were involved in the study (498 males and 282 females), with the median age of 63 years. There were 240 cases (30.77%) of smoking, 209 cases (26.79%) of drinking, 42 cases (5.38%) with history of hemorrhagic stroke, 57 cases (7.31%) with history of ischemic stroke, 552 cases (70.77%) with the history of hypertension, and 104 cases (13.33%) with the history of diabetes mellitus. Among 780 ICH patients, 151 patients (19.36%) experienced HE (HE group) and 629 patients (80.64%) did not experience HE (non-HE group).

## Univariate analysis for HE in ICH patients

The results of univariate analysis for HE in ICH patients were listed in Table 4, and the distribution of studied variables is demonstrated in Fig. 1A and Fig. 1B. The values in the HE group were significantly higher than those in the non-HE group in proportion of patients with history of diabetes mellitus ($\chi^2 = 6.919$, $p = 0.0085$), midline shift >0.5 cm ($\chi^2 = 8.708$, $p = 0.0032$), basal ganglia hemorrhage ($\chi^2 = 9.000$, $p = 0.0111$), body temperature >38 or <36°C ($\chi^2 = 6.249$, $p = 0.0124$), WBC count >12 or $<4\times10^9$/L ($\chi^2 = 7.039$, $p = 0.0080$), and fasting blood

**Table 1.** Test of normal distribution within compared groups

| Variables | Non-HE group | | HE group | |
|---|---|---|---|---|
| | Statistics | p-value | Statistics | p-value |
| Age [years] | 0.038 | 0.0300 | 0.106 | <0.0100 |
| Hematoma volume [mL] | 0.182 | <0.0100 | 0.199 | <0.0100 |
| SBP [mm Hg] | 0.049 | <0.0100 | 0.087 | <0.0100 |
| DBP [mm Hg] | 0.055 | <0.0100 | 0.060 | >0.1500 |
| GCS score | 0.199 | <0.0100 | 0.198 | <0.0100 |
| INR | 0.459 | <0.0100 | 0.425 | <0.0100 |
| PLT [$10^9$/L] | 0.060 | <0.0100 | 0.067 | 0.0910 |
| Hb [mg/L] | 0.091 | <0.0100 | 0.092 | <0.0100 |
| Neutrophils count [$10^9$/L] | 0.078 | <0.0100 | 0.164 | <0.0100 |
| LC count [$10^9$/L] | 0.122 | <0.0100 | 0.137 | <0.0100 |
| NLR [%] | 0.146 | <0.0100 | 0.251 | <0.0100 |
| PLR [%] | 0.130 | <0.0100 | 0.220 | <0.0100 |
| CRP [mg/L] | 0.372 | <0.0100 | 0.319 | <0.0100 |
| FBG [mmol/L] | 0.136 | <0.0100 | 0.142 | <0.0100 |

HE – hematoma expansion; SBP – systolic blood pressure; DBP – diastolic blood pressure; GCS – Glasgow Coma Score; INR – international normalized ratio; PLT – platelet; Hb – hemoglobin; LC – lymphocytes; NLR – neutrophil/lymphocyte ratio; PLR – platelet/lymphocyte ratio; CRP – C-reactive protein; FBG – fasting blood glucose.

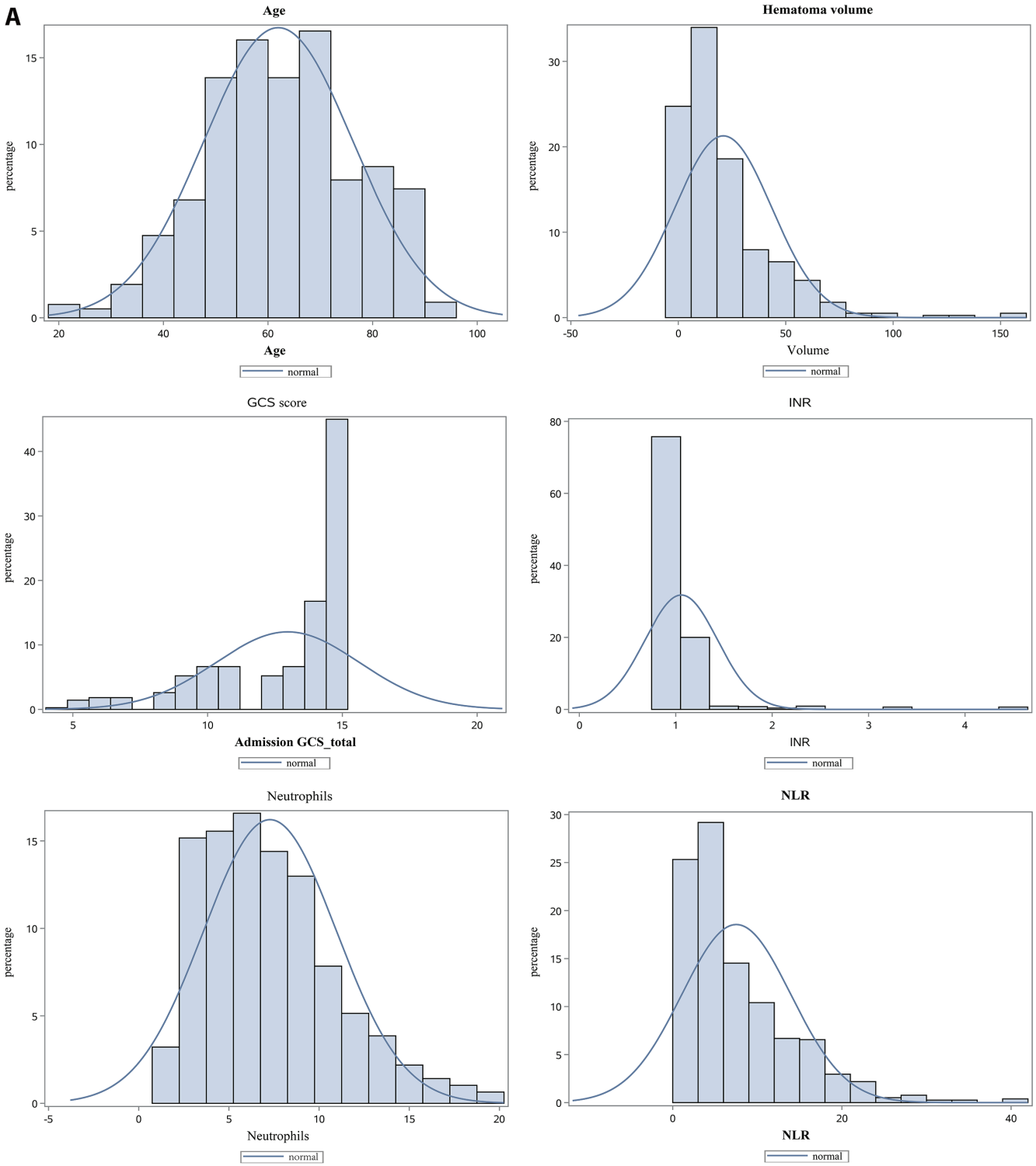


Fig. 1A. Distribution of the studied variables

GCS – Glasgow Coma Score; INR – international normalized ratio; NLR – neutrophil/lymphocyte ratio.

glucose (Z = 2.831, p = 0.0046). Meanwhile, the values in the HE group were significantly lower than those in the non-HE group in proportion of patients smoking ($\chi^2$ = 5.065, p = 0.0244), neutrophils count (Z = –4.403, p < 0.0001), respiratory rate >20 breaths/min ($\chi^2$ = 39.959, p < 0.0001), PLT (Z = –1.930, p = 0.0536), NLR (Z = –3.377, p = 0.0007), and PLR (Z = –2.488, p = 0.0128).

## Multivariate logistic regression analysis for HE in ICH patients

According to the results of univariate analysis, the history of diabetes, smoking history, midline shift, ICH location, SIRS (body temperature, heart rate, respiratory rate, WBC count), INR, PLT, neutrophils count, NLR,

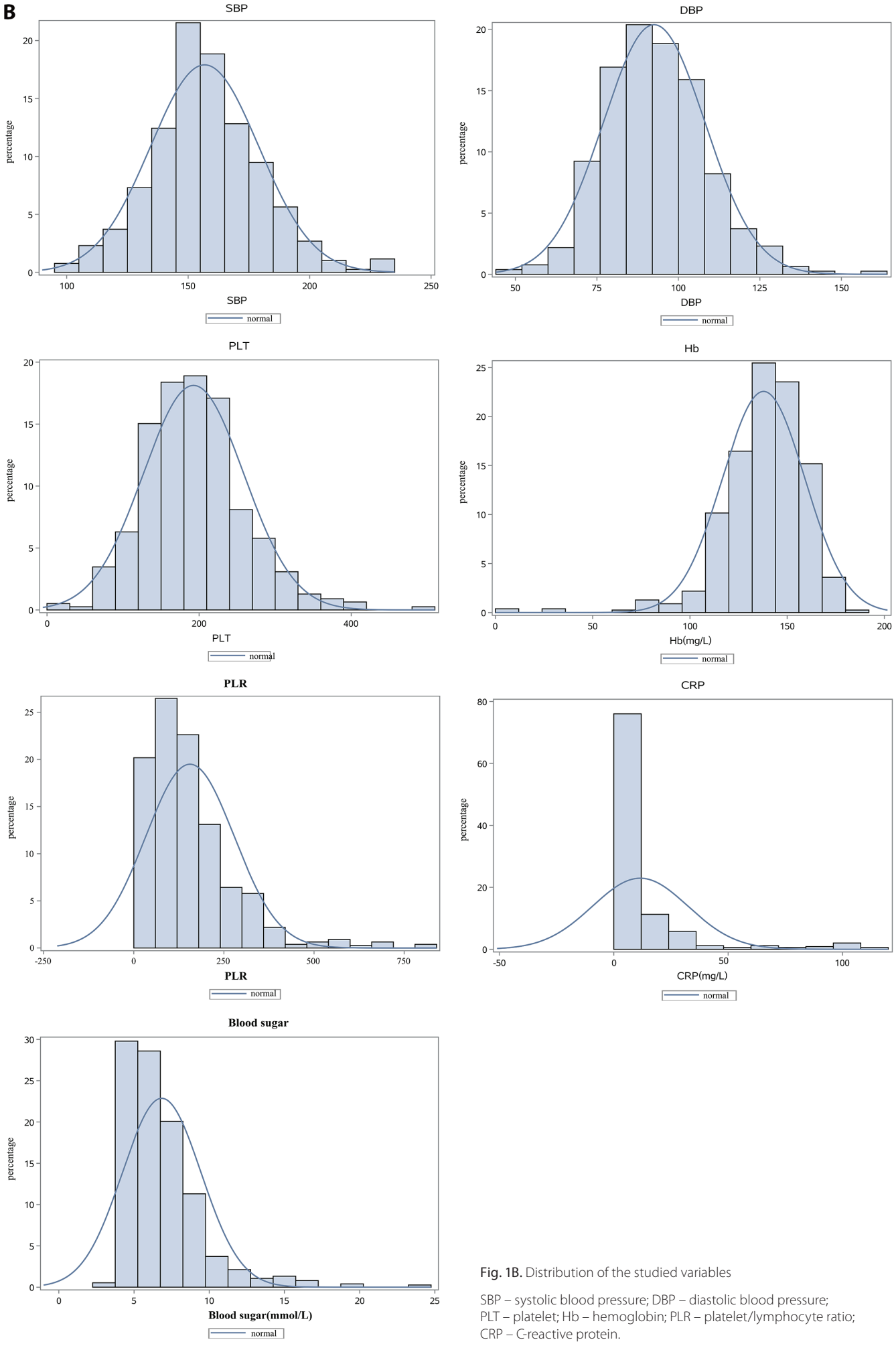


**Fig. 1B.** Distribution of the studied variables

SBP – systolic blood pressure; DBP – diastolic blood pressure; PLT – platelet; Hb – hemoglobin; PLR – platelet/lymphocyte ratio; CRP – C-reactive protein.

**Table 2.** The influencing factors' colinearity of multivariable logistic regression for HE in ICH patients

| Variables | TOL | VIF |
|---|---|---|
| Midline shift [cm] | 0.924 | 1.082 |
| ICH location: basal ganglia | 0.930 | 1.076 |
| ICH location: hypothalamus | 0.933 | 1.072 |
| SIRS | 0.863 | 1.159 |
| Neutrophils [$10^9$/L] | 0.855 | 1.170 |
| CRP [mg/L] | 0.961 | 1.041 |
| FBG [mmol/L] | 0.947 | 1.056 |

HE – hematoma expansion; SIRS – systemic inflammatory response syndrome; ICH – intracerebral hemorrhage; CRP – C-reactive protein; FBG – fasting blood glucose; TOL – tolerance; VIF – variance inflation factor.

**Table 3.** The influencing factors' colinearity of multivariable logistic regression for SIRS in ICH patients

| Variables | TOL | VIF |
|---|---|---|
| Midline shift [cm] | 0.899 | 1.112 |
| ICH location: basal ganglia | 0.917 | 1.091 |
| ICH location: hypothalamus | 0.920 | 1.087 |
| Body temperature (>38°C or <36°C) | 0.876 | 1.142 |
| Respiratory rate (>20 breaths/min) | 0.927 | 1.078 |
| WBC (>12 × $10^9$/L or <4 × $10^9$/L) | 0.960 | 1.042 |
| Heart rate (>90 beats/min) | 0.699 | 1.430 |
| Neutrophils [$10^9$/L] | 0.680 | 1.472 |
| CRP [mg/L] | 0.926 | 1.080 |
| FBG [mmol/L] | 0.937 | 1.067 |

SIRS – systemic inflammatory response syndrome; ICH – intracerebral hemorrhage; WBC – white blood cell; CRP – C-reactive protein; FBG – fasting blood glucose; TOL – tolerance; VIF – variance inflation factor.

**Table 4.** Baseline characteristics of HE and non-HE groups

| Variables | df | Non-HE group (n = 629) | HE group (n = 151) | Statistics | p-value |
|---|---|---|---|---|---|
| Age, years, M ($Q_1$, $Q_3$) | 1 | 63.00 (53.00, 71.00) | 61.00 (51.00, 75.00) | Z = –0.488 | 0.6257[a] |
| Gender, n (%)<br>Male<br>Female | 1 | 405 (64.4)<br>224 (35.6) | 93 (61.6)<br>58 (38.4) | $\chi^2$ = 0.413 | 0.5204[b] |
| Smoke history, n (%)<br>No<br>Yes | 1 | 424 (67.4)<br>205 (32.6) | 116 (76.8)<br>35 (23.2) | $\chi^2$ = 5.065 | 0.0244[b] |
| Drinking history, n (%)<br>No<br>Yes | 1 | 458 (72.8)<br>171 (27.2) | 113 (74.8)<br>38 (25.2) | $\chi^2$ = 0.253 | 0.6147[b] |
| Medical history, n (%) | | | | | |
| Hemorrhagic stroke, n (%)<br>No<br>Yes | 1 | 598 (95.1)<br>31 (4.9) | 140 (92.7)<br>11 (7.3) | $\chi^2$ = 1.327 | 0.2493[b] |
| Ischemic stroke, n (%)<br>No<br>Yes | 1 | 587 (93.3)<br>42 (6.7) | 136 (90.1)<br>15 (9.9) | $\chi^2$ = 1.906 | 0.1674[b] |
| Hypertension, n (%)<br>No<br>Yes | 1 | 184 (29.3)<br>445 (70.7) | 44 (29.1)<br>107 (70.9) | $\chi^2$ = 0.001 | 0.9780[b] |
| Diabetes mellitus, n (%)<br>No<br>Yes | 1 | 555 (88.2)<br>74 (11.8) | 121 (80.1)<br>30 (19.9) | $\chi^2$ = 6.919 | 0.0085[b] |
| Hematoma volume [mL], M ($Q_1$, $Q_3$) | 1 | 12.86 (6.14, 28.17) | 12.00 (5.21, 29.00) | Z = 0.019 | 0.9849[a] |
| Midline shift [cm], n (%)<br>≤0.5<br>>0.5 | 1 | 517 (82.2)<br>112 (17.8) | 108 (71.5)<br>43 (28.5) | $\chi^2$ = 8.708 | 0.0032[b] |
| ICH location, n (%)<br>Basal ganglia<br>Hypothalamus<br>Other brain parts | 2 | 336 (53.4)<br>215 (34.2)<br>78 (12.4) | 101 (66.9)<br>36 (23.8)<br>14 (9.3) | $\chi^2$ = 9.000 | 0.0111[b] |
| SBP [mm Hg], M ($Q_1$, $Q_3$) | 1 | 155.00 (145.00, 170.00) | 156.00 (137.00, 170.00) | Z = –0.662 | 0.5080[a] |

PLR, CRP, and FBG values were included in the multivariate logistics regression analysis, and the final regression model included midline shift, ICH location, respiratory rate, WBC and neutrophils count, CRP and FBG. The results of logistic regression analysis (Table 5) revealed that the risk of HE in ICH patients with midline shift >0.5 cm was 2.076 times higher than in ICH patients with midline shift ≤0.5 cm (odds ratio (OR) = 2.076, 95% confidence interval (95% CI): [1.274; 3.381], p = 0.0034). The risk of HE in ICH patients with basal ganglia hemorrhage and

**Table 4.** Baseline characteristics of HE and non-HE groups – cont.

| Variables | df | Non-HE group (n = 629) | HE group (n = 151) | Statistics | p-value |
|---|---|---|---|---|---|
| DBP [mm Hg], M ($Q_1$, $Q_3$) | 1 | 92.00 (82.00, 102.00) | 90.00 (78.00, 102.00) | Z = –0.485 | 0.6278[a] |
| SIRS, n (%)<br>No<br>Yes | 1 | 535 (85.1)<br>94 (14.9) | 108 (71.5)<br>43 (28.5) | $\chi^2$ = 15.401 | <0.0001[b] |
| Body temperature [°C], n (%)<br>36–38<br>>38 or <36 | 1 | 566 (90.0)<br>63 (10.0) | 125 (82.8)<br>26 (17.2) | $\chi^2$ = 6.249 | 0.0124[b] |
| Heart rate [beats/min], n (%)<br>≤90<br>>90 | 1 | 132 (21.0)<br>497 (79.0) | 31 (20.5)<br>120 (79.5) | $\chi^2$ = 0.015 | 0.9015[b] |
| Respiratory rate [breaths/min], n (%)<br>≤20<br>>20 | 1 | 63 (10.0)<br>566 (90.0) | 45 (29.8)<br>106 (70.2) | $\chi^2$ = 39.959 | <0.0001[b] |
| WBC count [$10^9$/L], n (%)<br>4–12<br>>12 or <4 | 1 | 475 (75.5)<br>154 (24.48) | 98 (64.9)<br>53 (35.1) | $\chi^2$ = 7.039 | 0.0080[b] |
| Graeb score, n (%)<br>No intraventricular hemorrhage<br>Mild intraventricular hemorrhage<br>Moderate intraventricular hemorrhage<br>Severe intraventricular hemorrhage | 3 | 448 (71.2)<br>98 (15.6)<br>64 (10.2)<br>19 (3.0) | 108 (72.0)<br>23 (15.3)<br>13 (8.7)<br>6 (4.0) | $\chi^2$ = 0.645 | 0.886[b] |
| GCS score, M ($Q_1$, $Q_3$) | 1 | 12.00 (9.00, 14.00) | 13.00 (11.00, 14.00) | Z = 1.507 | 0.1317[a] |
| INR, M ($Q_1$, $Q_3$) | 1 | 0.99 (0.95, 1.04) | 0.98 (0.95, 1.02) | Z = –0.333 | 0.7388[a] |
| PLT [$10^9$/L], M ($Q_1$, $Q_3$) | 1 | 187.00 (150.00, 235.00) | 184.00 (136.00, 215.00) | Z = –1.930 | 0.0536[a] |
| Hb [mg/L], M ($Q_1$, $Q_3$) | 1 | 140.00 (127.00, 154.00) | 140.00 (126.00, 150.00) | Z = –0.237 | 0.8129[a] |
| Neutrophils count [$10^9$/L], M ($Q_1$, $Q_3$) | 1 | 7.20 (4.80, 9.60) | 5.40 (3.40, 8.90) | Z = –4.403 | <0.0001[a] |
| LC count [$10^9$/L], M ($Q_1$, $Q_3$) | 1 | 1.20 (0.81, 1.70) | 1.27 (0.80, 1.91) | Z = 1.146 | 0.2518[a] |
| NLR (%), M ($Q_1$, $Q_3$) | 1 | 5.64 (3.12, 10.33) | 3.53 (1.69, 11.88) | Z = –3.377 | 0.0007[a] |
| PLR (%), M ($Q_1$, $Q_3$) | 1 | 136.54 (81.00, 206.80) | 98.57 (62.59, 207.35) | Z = –2.488 | 0.0128[a] |
| CRP [mg/L], M ($Q_1$, $Q_3$) | 1 | 0.00 (0.00, 2.30) | 1.00 (0.00, 8.60) | Z = 4.270 | <0.0001[a] |
| FBG [mmol/L], M ($Q_1$, $Q_3$) | 1 | 5.90 (4.93, 7.50) | 7.02 (5.13, 8.31) | Z = 2.831 | 0.0046[a] |

[a] – derived from Mann–Whitney U test; [b] – derived from $\chi^2$ test; M – median; HE – hematoma expansion; df – degrees of freedom; ICH – intracerebral hemorrhage; SBP – systolic blood pressure; DBP – diastolic blood pressure; SIRS – systemic inflammatory response syndrome; WBC – white blood cell; LC – lymphocytes; GCS – Glasgow Coma Score; INR – international normalized ratio; PLT – platelet; Hb – hemoglobin; NLR – neutrophil/lymphocyte ratio; PLR – platelet/lymphocyte ratio; CRP – C-reactive protein; FBG – fasting blood glucose.

hypothalamus hemorrhage was respectively 2.512 and 2.121 times higher than in those with bleeding occurring in other parts of brain (OR = 2.512, 95% CI: [1.496; 4.218], p = 0.0005; OR = 2.121, 95% CI: [1.007; 4.466], p = 0.0479). The association between SIRS patients and the risk of HE was significant (OR = 2.549, 95% CI: [1.497; 4.342], p = 0.0006). The HE risk in patients decreased by 15.5% for every 1×$10^9$/L increase in neutrophils count (OR = 0.845, 95% CI: [0.792; 0.902], p < 0.0001), increased by 1.3% for every 1 mg/L increase in CRP (OR = 1.013, 95% CI: [1.002; 1.024], p = 0.0184), and increased by 9.9% for every 1 mmol/L increase in FBG (OR = 1.099, 95% CI: [1.026; 1.178], p = 0.0074). The value of goodness-of-fit was 7.704, p = 0.463 and $R^2$ was 0.136 in the multivariable logistic regression model.

After adjusting midline shift, ICH location, neutrophils count, CRP and FBG, the further analysis demonstrated that the risk of HE in ICH patients with respiratory rate >20 breaths/min was 3.436 higher than in patients with respiratory rate ≤20 breaths/min (OR = 3.436, 95% CI: [1.981; 5.690], p < 0.0001). The risk of HE in ICH patients with WBC count >12($10^9$/L) or ≤4($10^9$/L) is 2.489 times higher than in those with WBC count 4–12 ($10^9$/L) (OR = 2.489, 95% CI: [1.494; 4.149], p = 0.0005) (Table 6). The value of goodness-of-fit was 10.953, p = 0.204 and $R^2$ was 0.179.

## Discussion

Intracerebral hemorrhage is associated with poor prognosis and high mortality. Its morbidity in China is far higher than in Europe or in the USA.[14] Hematoma expansion is a leading cause of poor prognosis and neurological deterioration in patients with ICH, as well as an important therapeutic goal of ICH.[15] In this study, the results showed that SIRS was significantly associated with the risk of HE. The logistic regression analysis was performed to analyze

**Table 5.** Multivariate logistic regression analysis for HE in ICH patients

| Variables | df | β | SE | Wald | p-value | OR (95% CI) |
|---|---|---|---|---|---|---|
| Constant | – | –2.218 | 0.365 | 36.966 | <0.0001 | – |
| Midline shift [cm] | 1 | | | | – | |
| ≤0.5 | | | – | | | Ref |
| >0.5 | – | 0.730 | 0.249 | 8.601 | 0.0034 | 2.076 [1.274; 3.381] |
| ICH location | 2 | | | | – | |
| Other brain parts | | | – | | | Ref |
| Basal ganglia | – | 0.921 | 0.264 | 12.126 | 0.0005 | 2.512 [1.496; 4.218] |
| Hypothalamus | – | 0.752 | 0.380 | 3.912 | 0.0479 | 2.121 [1.007; 4.466] |
| SIRS | 1 | 0.936 | 0.272 | 11.863 | 0.0006 | 2.549 [1.497; 4.342] |
| Neutrophils count [$10^9$/L] | 1 | –0.168 | 0.033 | 25.411 | <0.0001 | 0.845 [0.792; 0.902] |
| CRP [mg/L] | 1 | 0.013 | 0.006 | 5.555 | 0.0184 | 1.013 [1.002; 1.024] |
| FBG [mmol/L] | 1 | 0.095 | 0.035 | 7.185 | 0.0074 | 1.099 [1.026; 1.178] |

HE – hematoma expansion; df – degrees of freedom; SE – standard error; SIRS – systemic inflammatory response syndrome; ICH – intracerebral hemorrhage; CRP – C-reactive protein; FBG – fasting blood glucose; OR – odds ratio; 95% CI – 95% confidence interval.

**Table 6.** Multivariate logistic regression analysis for SIRS in ICH patients

| Variables | df | β | SE | Wald | p-value | OR (95% CI) |
|---|---|---|---|---|---|---|
| Body temperature (>38°C or <36°C) | 1 | 0.259 | 0.337 | 0.591 | 0.4422 | 1.295 [0.669; 2.507] |
| Respiratory rate (>20 breaths/min) | 1 | 1.234 | 0.281 | 19.287 | <0.0001 | 3.436 [1.981; 5.960] |
| WBC count (>12 × $10^9$/L or <4 × $10^9$/L) | 1 | 0.912 | 0.261 | 12.249 | 0.0005 | 2.489 [1.494; 4.149] |
| Heart rate (>90 beats/min) | 1 | –0.326 | 0.287 | 1.289 | 0.2563 | 0.722 [0.411; 1.267] |

SIRS – systemic inflammatory response syndrome; ICH – intracerebral hemorrhage; df – degrees of freedom; SE – standard error; WBC – white blood cell; OR – odds ratio; 95% CI – 95% confidence interval. The model with adjustment of midline shift, ICH location, neutrophils, C-reactive protein (CRP) and fasting blood glucose (FBG).

the risk factors for HE and the results indicated that midline shift >0.5 cm, basal ganglia hemorrhage, hypothalamus hemorrhage, respiratory rate >20 breaths/min, WBC count >12($10^9$/L) or ≤4($10^9$/L), high CRP, and hyperglycemia were the risk factors for HE in patients with ICH.

Inflammation, which is the main pathological feature of ICH and the leading factor of HE, plays a key role in the development of hemorrhage-induced brain injury and perihematomal edema.[16] A number of studies have shown that inflammatory markers such as interleukin 6 (IL-6), neutrophils count and CRP were significantly associated with a short-term poor prognosis of ICH.[8,17,18] The neutrophils, as the biomarkers of the severity of systemic inflammation, generally promote the production of chemokines, cytokines, reactive oxygen species (ROS), and extracellular proteases in the brain.[19] In addition, the inflammatory response after ICH does not only occur in a given part of the brain, but also causes systemic inflammation: the neutrophils promote the rapid recruitment of peripheral cytokines and chemokines within a few hours of the onset.[20,21] Interestingly, our study indicated that the HE risk in patients with ICH decreased by 15.5% for every 1×$10^9$/L increase in neutrophils count. This may be attributed to the small sample size, whereas well-designed and larger sample studies for verification are still required.

Multiple researches reported that higher WBC count is associated with more serious ICH in the case of decreased consciousness, increased baseline hematoma volume and existing intraventricular hemorrhage.[22,23] Morotti et al.[24] conducted a retrospective analysis to investigate the relationship between WBC count and HE using multivariate logistic regression. The results showed that a higher WBC count was associated with a lower risk of HE. Subsequently, the inflammation was not only a nonspecific stress-related response, but was also beneficial to ICH patients in improving the coagulation response and limiting HE. Conversely, our study found that WBC count >12($10^9$/L) or ≤4($10^9$/L) was associated with an increased risk of HE in patients with ICH. This may have occured due to the different admission year of the selected patients.[24] The medical equipment and conditions of patients admitted early may not be as good as they are now, which means that our research is more accurate and convincing.

Little research was available on the association between respiratory rate and HE in ICH patients. Previous studies showed that acute respiratory distress syndrome (ARDS) normally occurred in 20% of patients with ICH.[25,26] The ARDS is a type of acute respiratory failure with severe hypoxemia and extremely difficult breathing as typical symptoms, and is associated with a high morbidity

and mortality burden.[27] Our study further investigated the relationship between the respiratory rate and HE using multivariate logistic regression analysis. The results demonstrated that the respiratory rate >20 breaths/min was related to the increased risk of HE in patients with ICH.

To our knowledge, there were few studies investigating the association of SIRS with HE after ICH. A retrospective study of ICH patients at New York University (NYU) Langone Medical Center Manhattan Campus (New York, USA) found that SIRS was associated with HE within the first 24 h of the onset of symptoms,[28] which was consistent with our findings. The SIRS is an immune-related aseptic inflammatory response common in various critically ill patients.[10] The possible mechanisms of SIRS include: a pro-inflammatory response of inflammatory cytokines; an increased release of toxic substances such as excitatory amino acids, nitric oxide and free radicals; and an increased production of thrombin, which induces glial in neuronal apoptosis of cells.[11,29,30] Previous studies focused on the association between SIRS and the outcomes after ICH. Boehme et al.[12] found that patients with SIRS were at an increased risk of poor prognosis, but SIRS was not an independent predictor of poor functional outcomes after ICH. Melmed et al. suggested that the relationship between SIRS and poor clinical outcome was mediated by HE.[28] An another study conducted by Hagen et al.[11] explored the associations of SIRS with long-term functional outcome and contributing factors after ICH, the results of which showed independent associations of SIRS with larger hematoma volumes. The present study investigated the relationship between the risk of HE in ICH patients and body temperature, heart rate, respiratory rate, and WBC count. The findings suggested that respiratory rate >20 breaths/min and WBC count >12($10^9$/L) or ≤4($10^9$/L) were related to an increased risk of HE in patients with ICH.

## Limitations

The strength of our study was a large sample size, which made the results more powerful and convincing. Unfortunately, it was a retrospective study and some clinical data were missing, such as the information on the use of antiplatelet drugs and anticoagulant drugs before the admission.

# Conclusions

We have established that in patients with ICH, SIRS was positively associated to the risk of HE, especially regarding the indicators of respiratory rate and WBC count, which may help indentify the ICH patients. This finding may achieve the early prevention of HE in ICH patients and open targeted therapeutic regimens for improving the prognosis of patients with ICH.

## ORCID iDs

Yu Zhu https://orcid.org/0000-0001-8360-4368
Zhikai Xie https://orcid.org/0000-0002-8927-1565
Jie Shen https://orcid.org/0000-0002-6367-3814
Lihui Zhou https://orcid.org/0000-0002-4639-264X
Zongchi Liu https://orcid.org/0000-0002-2384-2919
Di Ye https://orcid.org/0000-0001-5643-3487
Fan Wu https://orcid.org/0000-0002-6671-5282
Sohaib Hasan Abdullah Ezzi https://orcid.org/0000-0002-6080-6239
Zahraa Sh Hmood https://orcid.org/0000-0002-3791-3925
Renya Zhan https://orcid.org/0000-0002-0619-6257

## References

1. Li Q, Huang YJ, Zhang G, et al. Intraventricular hemorrhage and early hematoma expansion in patients with intracerebral hemorrhage. *Sci Rep*. 2015;5:11357. doi:10.1038/srep11357
2. Lattannzi S, Brigo F, Trinka E, Cagnetti C, Di Napoli M, Silvestrini M. Neutrophil-to-lymphocyte ratio in acute cerebral hemorrhage: A system review. *Transl Stroke Res*. 2019;10(2):137–145. doi:10.1007/s12975-018-0649-4
3. O'Carroll CB, Brown BL, Freeman WD. Intracerebral hemorrhage: A common yet disproportionately deadly stroke subtype. *Mayo Clin Proc*. 2021;96(6):1639–1654. doi:10.1016/j.mayocp.2020.10.034
4. Altintas O, Duruyen H, Baran G, et al. The relationship of hematoma growth to red blood cell distribution width in patients with hypertensive intracerebral hemorrhage. *Turk Neurosurg*. 2017;27(3):368–373. doi:10.5137/1019-5149.JTN.16136-15.1
5. Elkhatib T, Shehta N, Bessar AA. Hematoma expansion predictors: Laboratory and radiological risk factors in patients with acute intracerebral hemorrhage. A prospective observational study. *J Stroke Cerebrovasc Dis*. 2019;28(9):2177–2186. doi:10.1016/j.jstrokecerebrovasdis.2019.04.038
6. Demchuk AM, Dowlatshahi D, Rodriguez-Luna D, et al. Prediction of haematoma growth and outcome in patients with intracerebral haemorrhage using the CT-angiography spot sign (PREDICT): A prospective observational study. *Lancet Neurol*. 2012;11(4):307–314. doi:10.1016/S1474-4422(12)70038-8
7. Li Z, You M, Long C, et al. Hematoma expansion in intracerebral hemorrhage: An update on prediction and treatment. *Front Neurol*. 2020;11:702. doi:10.3389/fneur.2020.00702
8. Löppönen P, Qian C, Tetri S, et al. Predictive value of C-reactive protein for the outcome after primary intracerebral hemorrhage. *J Neurosurg*. 2014;121(6):1374–1379. doi:10.3171/2014.7.JNS132678
9. Huang WC, Chou RH, Chang CC, et al. Systemic inflammatory response syndrome is an independent predictor of one-year mortality in patients with acute myocardial infarction. *Acta Cardiol Sin*. 2017;33(5):477–485. doi:10.6515/acs20170603a
10. Chalmers S, Khawaja A, Wieruszewski PM, Gajic O, Odeyemi Y. Diagnosis and treatment of acute pulmonary inflammation in critically ill patients: The role of inflammatory biomarkers. *World J Crit Care Med*. 2019;8(5):59–71. doi:10.5492/wjccm.v8.i5.59
11. Hagen M, Sembill JA, Sprugel MI, et al. Systemic inflammatory response syndrome and long-term outcome after intracerebral hemorrhage. *Neurol Neuroimmunol Neuroinflamm*. 2019;6(5):e588. doi:10.1212/NXI.0000000000000588
12. Boehme AK, Comeau ME, Langefeld CD, et al. Systemic inflammatory response syndrome, infection, and outcome in intracerebral hemorrhage. *Neurol Neuroimmunol Neuroinflamm*. 2017;5(2):e428. doi:10.1212/NXI.0000000000000428
13. Graeb D, Robertson W, Lapointe J, Nugent RA, Harrison PB. Computed tomographic diagnosis of intraventricular hemorrhage: Etiology and prognosis. *Radiology*. 1982;143(1):91–96. doi:10.1148/radiology.143.1.6977795
14. Ji N, Lu JJ, Zhao YL, Wang S, Zhao JZ. Imaging and clinical prognostic indicators for early hematoma enlargement after spontaneous intracerebral hemorrhage. *Neurol Res*. 2009;31(4):362–366. doi:10.1179/174313209X444035
15. Yogendrakumar V, Ramsay T, Menon B, Qureshi AI, Saver JL, Dowlatshahi D. Hematoma expansion shift analysis to assess acute intracerebral hemorrhage treatments. *Neurology*. 2021;97(8):e755–e764. doi:10.1212/wnl.0000000000012393

16. Loan JJ, Kirby C, Emelianova K, et al. Secondary injury and inflammation after intracerebral haemorrhage: A systematic review and meta-analysis of molecular markers in patient brain tissue. *J Neurol Neurosurg Psychiatry*. 2022;93(2):126–132. doi:10.1136/jnnp-2021-327098
17. Lattanzi S, Cagnetti C, Provinciali L, Silvestrini M. Neutrophil-to-lymphocyte ratio predicts the outcome of acute intracerebral hemorrhage. *Stroke*. 2016;47(6):1654–1657. doi:10.1161/STROKEAHA.116.013627
18. Fonseca S, Costa F, Seabra M, et al. Systemic inflammation status at admission affects the outcome of intracerebral hemorrhage by increasing perihematomal edema but not the hematoma growth. *Acta Neurol Belg*. 2021;121(3):649–659. doi:10.1007/s13760-019-01269-2
19. Katsuki H, Hijioka M. Intracerebral hemorrhage as an axonal tract injury disorder with inflammatory reactions. *Biol Pharm Bull*. 2017; 40(5):564–568. doi:10.1248/bpb.b16-01013
20. Askenase M, Sansing L. Stages of the inflammatory response in pathology and tissue repair after intracerebral hemorrhage. *Semin Neurol*. 2016;36(3):288–297. doi:10.1055/s-0036-1582132
21. Dickens AM, Tovar-Y-Romo LB, Yoo SW, et al. Astrocyte-shed extracellular vesicles regulate the peripheral leukocyte response to inflammatory brain lesions. *Sci Signal*. 2017;10(473):eaai7696. doi:10.1126/scisignal.aai7696
22. Behrouz R, Hafeez S, Miller CM. Admission leukocytosis in intracerebral hemorrhage: Associated factors and prognostic implications. *Neurocrit Care*. 2015;23(3):370–373. doi:10.1007/s12028-015-0128-7
23. Wang Y, Zhang G. New silent cerebral infarction in patients with acute non-cerebral amyloid angiopathy intracerebral hemorrhage as a predictor of recurrent cerebrovascular events. *Med Sci Monit*. 2019;25:418–426. doi:10.12659/msm.914423
24. Morotti A, Phuah CL, Anderson CD, et al. Leukocyte count and intracerebral hemorrhage expansion. *Stroke*. 2016;47(6):1473–1478. doi:10.1161/STROKEAHA.116.013176
25. Lang C, Dettinger J, Berchtold-Herz M, et al. Intracerebral hemorrhage in COVID-19 patients with pulmonary failure: A propensity score-matched registry study. *Neurocrit Care*. 2021;34(3):739–747. doi:10.1007/s12028-021-01202-7
26. Kitamura Y, Nomura M, Shima H, et al. Acute lung injury associated with systemic inflammatory response syndrome following subarachnoid hemorrhage: A survey by the Shonan Neurosurgical Association. *Neurol Med Chir (Tokyo)*. 2010;50(6):456–460. doi:10.2176/nmc.50.456
27. Confalonieri M, Salton F, Fabiano F. Acute respiratory distress syndrome. *Eur Respir Rev*. 2017;26(144):160116. doi:10.1183/16000617.0116-2016
28. Melmed KR, Carroll E, Lord AS, et al. Systemic inflammatory response syndrome is associated with hematoma expansion in intracerebral hemorrhage. *J Stroke Cerebrovasc Dis*. 2021;30(8):105870. doi:10.1016/j.jstrokecerebrovasdis.2021.105870
29. Stelmasiak M, Słotwiński R. Infection-induced innate antimicrobial response disorders: From signaling pathways and their modulation to selected biomarkers. *Cent Eur J Immunol*. 2020;45(1):104–116. doi:10.5114/ceji.2020.94712
30. Saand A, Yu F, Chen J, Chou SHY. Systemic inflammation in hemorrhagic strokes: A novel neurological sign and therapeutic target? *J Cereb Blood Flow Metab*. 2019;39(6):959–988. doi:10.1177/0271678x19841443

# Comparative assessment of pharmacokinetic parameters between HS016, an adalimumab biosimilar, and adalimumab (Humira®) in healthy subjects and ankylosing spondylitis patients: Population pharmacokinetic modeling

Xiaofeng Zeng[1,A,D–F], Jing Zhang[2,A,E,F], Jicheng Yu[2,C,D,F], Xiaojie Wu[2,B,D,F], Yuancheng Chen[2,C,D,F], Jufang Wu[2,B,D,F], Xiaoli Yang[2,B,D,F], Jingjing Wang[2,C,D,F], Guoying Cao[2,A,E,F]

[1] Department of Rheumatology, Peking Union Medical College Hospital, Peking Union Medical College and Chinese Academy of Medical Sciences, National Clinical Research Center for Immunologic Diseases, Ministry of Science & Technology, Key Laboratory of Rheumatology and Clinical Immunology, Ministry of Education, Beijing, China
[2] Phase I Clinical Trial Center, Huashan Hospital, Fudan University, Shanghai, China

A – research concept and design; B – collection and/or assembly of data; C – data analysis and interpretation; D – writing the article; E – critical revision of the article; F – final approval of the article

Advances in Clinical and Experimental Medicine, ISSN 1899–5276 (print), ISSN 2451–2680 (online) *Adv Clin Exp Med*. 2022;31(5):499–509

**Address for correspondence**
Guoying Cao
E-mail: 13651900963@163.com

**Funding sources**
None declared

**Conflict of interest**
None declared

Received on August 24, 2021
Reviewed on December 30, 2021
Accepted on January 19, 2022

Published online on February 11, 2022

## Abstract

**Background.** The HS016 is an adalimumab biosimilar related to the immunoglobulin G1 (IgG1) antibody, with a similar amino acid sequence.

**Objectives.** To quantify the differences in the pharmacokinetic (PK) parameters of HS016 and adalimumab in healthy individuals and patients with ankylosing spondylitis (AS).

**Materials and methods.** The PK data for HS016 and adalimumab were obtained in a randomized, double-blind, phase 1 clinical study in Chinese healthy subjects after a single-dose subcutaneous administration (136 healthy subjects), and in a randomized, double-blind, phase 3 trial of AS patients who received subcutaneous injection of HS016 or adalimumab once every 2 weeks for 24 weeks (366 AS patients).

**Results.** The time course of HS016 and adalimumab was characterized by a one-compartment model with first-order absorption and elimination kinetics. Age, body weight, creatinine clearance (CLcr) and anti-drug antibody were covariates for the apparent clearance (CL/F); body weight and subject type were significant covariates for the apparent volume of distribution (V/F). The V/F and CL/F were estimated at 11.3 L and 0.0102 L/h. The ratios of the geometric least square (LS) means (HS016 compared to the adalimumab treatment group after multiple doses) in healthy subjects were 97.14 (87.70, 107.59) for the concentration-time curve from time zero to the last measurable concentration ($AUC_{0-t}$) and 99.14 (90.03, 109.16) for the maximum serum drug concentration within a steady-state dosing interval ($C_{max,ss}$); the ratios (90% confidence interval (90% CI)) in AS patients were 97.03 [84.10; 111.96] for the AUC within the steady-state dose intervals ($AUC_{0-tau}$) and 99.62 [88.09; 112.68] for $C_{max,ss}$.

**Conclusions.** The systemic exposure of HS016 was similar to that of adalimumab in healthy subjects and AS patients, demonstrating PK similarity.

**Key words:** HS016, adalimumab, population pharmacokinetics, biosimilar, patients with ankylosing spondylitis

**Acknowledgements**
The authors would like to acknowledge Zhejiang Hisun Pharmaceutical Co., Ltd. for their support of this article. Other institutions that participated in the study are as follows: Huashan Hospital, Peking Union Medical College Hospital, The First Affiliated Hospital of Xi'an Jiaotong University, Changhai Hospital, West China Hospital, The First Affiliated Hospital of Anhui Medical University, The First Affiliated Hospital of Kunming Medical University, Qilu Hospital of Shandong University, Zhongshan Hospital, The Second Affiliated Hospital of Zhejiang University School of Medicine, Xiangya Hospital, Beijing Hospital, The First Affiliated Hospital of Shanxi Medical University, The Second Xiangya Hospital of Central South University, The First Affiliated Hospital of Harbin Medical University, Peking University Third Hospital, Tongji Medical College of Huazhong University of Science and Technology, Guangdong Second Provincial General Hospital, The Third Hospital of Hebei Medical University, Zhuzhou Central Hospital, Shanghai Guanghua Hospital of Integrated Traditional Chinese and Western Medicine, China-Japan Friendship Hospital, Union Hospital-Tongji Medical College of Huazhong University of Science and Technology, The Second Affiliated Hospital of Guangzhou Medical University, Jiangsu Province Hospital, Peking University First Hospital, Tianjian Medical University General Hospital, and The Second Affiliated Hospital of Shanxi Medical University.

**Cite as**
Zeng X, Zhang J, Yu J, et al. Comparative assessment of pharmacokinetic parameters between HS016, an adalimumab biosimilar, and adalimumab (Humira®) in healthy subjects and ankylosing spondylitis patients: Population pharmacokinetic modeling. *Adv Clin Exp Med*. 2022;31(5):499–509. doi:10.17219/acem/145947

**DOI**
10.17219/acem/145947

# Background

Humira® (adalimumab) is a human monoclonal immunoglobulin G1 (IgG1) antibody that targets tumor necrosis factor alpha (TNF-α). It has profoundly improved the therapy of inflammatory disease and has been approved in the treatment of ankylosing spondylitis (AS) and numerous other conditions, including rheumatoid arthritis and Crohn's disease.[1] Ankylosing spondylitis is considered to be one of the most common members of the spondyloarthritis (SpA) group of arthritic diseases,[2] with a prevalence in China of approx. 0.22%,[3] a rate comparable to that in Asian countries and Caucasians.[4] The access of patients to therapy with, e.g., adalimumab for the treatment of chronic inflammatory disorders is often limited due to the economic burden.[5] The introduction of biosimilars will lower the treatment costs for the much needed treatment.[5] To obtain the marketing approval for a biosimilar drug, an assessment must be made of the risk/benefit ratio based on the equivalence studies and regulated clinical trials in accordance with the requirements of the regulatory authorities.[6–8]

The HS016 is an adalimumab biosimilar developed by Zhejiang Hisun Pharmaceutical Co., Ltd. (Taizhou, China). In order to be approved for market, the biosimilarity between HS016 and the reference drug must be demonstrated. Thus, a pharmacokinetic (PK) study with HS016 and adalimumab as the reference drug was conducted in healthy volunteers,[9] and a phase 3 study aimed at evaluating a range of PK parameters and any safety issues was conducted in AS patients.[10]

Limited data can be used to accurately calculate PK parameters using population modeling, in contrast to the non-compartmental method. In addition, the inter-product and inter-individual variability (IIV) allows for the quantification and indentification of covariate factors, using the population method that may have an influence on the availability of the test drug.[11] The PK similarity analyses using nonlinear mixed-effects models have already been performed for some other biosimilars.[12,13] Therefore, in the present study, the similarities in PK parameters between HS016 and adalimumab, both in healthy subjects and AS patients, were also assessed by a comparison of the predicted time-dependent drug serum concentrations, evaluated with a PK population model that used data from the 2 abovementioned clinical studies.

# Objectives

The aim of this study was to incorporate data from previous studies in patients with AS and healthy male volunteers, with the aim of creating a PK population model of HS016 and adalimumab, and describing the PK similarity between HS016 and adalimumab, in order to understand the PK characteristics of these 2 drugs in a large Chinese population.

# Materials and methods

## Subjects

There were 2 studies included in this analysis. A brief description of the study designs is provided below and in Table 1.

First research (HS016-I), a phase 1 single-dose study, compared the HS016 with adalimumab in healthy Chinese men.

The second research (HS016-III) was a phase 3 multiple-dose study that compared HS016 with adalimumab in Chinese patients with AS. Patients were stratified according to their age (<40 years and ≥40 years) and C-reactive protein (CRP) concentration (<28.0 mg/L and ≥28.0 mg/L). The age range was 18–65 years and patients were diagnosed with AS according to the 1984 modified New York criteria.[14]

The ethics committees of participating hospitals approved the study protocols. The study was carried out in accordance with the Declaration of Helsinki. The informed consent was provided by all study participants before they underwent any procedures.

**Table 1.** Overview of clinical trials

| Study No. | Population | Dosing | PK sampling | ADA sampling |
|---|---|---|---|---|
| HS016-I (phase I) | Chinese healthy men, n = 136 (68 for HS016 and 68 for Humira®) | single-dose subcutaneous injection of 40 mg (strength: 40 mg/0.8 mL) | predose, 6, 12, 24, 48, 72, 96, 120, 144, 168, 192, 216, 336, 504, 672, 840, 1008, 1344, and 1680 h postdose | screening period, predose, 336, 1008 and 1680 h postdose |
| HS016-III (phase III) | patients with ankylosing spondylitis, n = 366 (235 for HS016 and 131 for Humira®) | multiple-dose subcutaneous injection of 40 mg once every 2 weeks (strength: 40 mg/0.8 mL) | predose of 1st dose (day 1), day 15 (week 2), day 29 (week 4), day 43 (week 6), day 64 (week 8), day 71 (week 10) (occasion 1); predose of day 85 (week 12), 6, 10, 24, 72, 120, 168, 216, 264 h postdose (occasion 2); predose of day 99 (week 14), day 113 (week 16), day 127 (week 18), day 141 (week 20), day 155 (week 22), day 169 (week 24) (occasion 3); within 4 weeks of last dose for early withdrawal subjects | screening period, day 15 (week 2), day 29 (week 4), day 64 (week 8), day 99 (week 12), day 127 (week 18), and day 169 (week 24); within 4 weeks of last dose for early withdrawal subjects |

PK – pharmacokinetic; ADA – anti-drug antibody.

## Sampling and bioanalytical methods

Samples of blood were collected from the subjects in order to determine the range of PK parameters and for the anti-drug antibody (ADA) analysis. The sampling data are described in Table 1.

A validated quantitative enzyme-linked immunosorbent immunoassay (ELISA) was employed to measure HS016 and adalimumab concentrations in human serum collected from healthy subjects and patients in the HS016-I and HS016-III studies. The lower limit of quantitation (LLOQ) for both drugs was 15.625 ng/mL. The validation showed that the results fell within standard accepted criteria.

Bridging electrochemiluminescence (Meso Scale Discovery, Rockville, USA) was used to detect anti-HS016 and adalimumab antibodies.

## Population pharmacokinetic analysis

### Software

NONMEM v. 7.3.0 software (ICON, Dublin, Ireland) was used to conduct population analyses of PK parameters and simulations,[15] together with PsN tool kit (v. 4.6.2) (a process embedded in NONMEM instead of an independent software)[16] and R v. 3.6.1 for Windows (R Foundation for Statistical Computing, Vienna, Austria). The NONMEM datasets were constructed using SAS v. 9.4 (SAS Institute, Cary, USA).

### PK structural model

The PK parameters of adalimumab have been widely reported and based on published data,[17–19] and a one-compartment model was used to evaluate the elimination rate of adalimumab in patients with hidradenitis suppurativa, rheumatoid arthritis (RA) and Crohn's disease. Also, only 1 declining phase of the logarithmic serum concentration time course of adalimumab and its biosimilar was observed in healthy subjects.[20] Therefore, this model was tested, which was fitted to the available data, and was parameterized according to the absorption rate constant (KA), the apparent volume of distribution (V/F) and the apparent clearance (CL/F) (ADVAN2, TRANS2), by employing a first order conditional estimation method that utilized an interaction (FOCE-I) fitting subroutine.

### Statistical model

The IIV and the inter-occasion variability (IOV) of PK parameters of adalimumab and HS016 were determined using the exponential error model (eq. 1):

$$P_{i,k} = P_{tv} \times \exp(\eta^{P_i} + IOV^{P_k}) \quad (1)$$

where $P_{i,k}$ is the individual PK value for the $i^{th}$ individual and $k^{th}$ occasion; $P_{tv}$ is the population estimate; and $\eta^{P_i}$ and $IOV^{P_k}$ were assumed to have normally distributed inter-individual and inter-occasion random variables, with zero mean and variance of $\omega_P^2$ and $\pi_P^2$. Three occasions were defined: one for the time before the intended week 12, one for the time between the intended week 12 and week 14, and the other one for the time after the intended week 14.

The residual variability was determined using a combined additive and proportional model (eq. 2):

$$C_{ij} = \hat{C}_{ij}(1 + \varepsilon_{P_{ij}}) + \varepsilon_{a_{ij}} \quad (2)$$

where $C_{ij}$ is the $j^{th}$ observed drug concentration of an individual i; $\hat{C}_{ij}$ is the $j^{th}$ model predicted concentration for an individual i; and $\varepsilon_{P_{ij}}$ and $\varepsilon_{a_{ij}}$ are the proportional and additive residual random errors for an individual i and a measurement j, presumed to have independent and identical normal distributions: $\varepsilon \sim$ NID: Normally and Independently Distributed $(0, \sigma^2)$.

### Covariate analysis

The following covariates were tested: age, sex, baseline body weight (BW) in kg, baseline body mass index (BMI) and surface area of the body, subject type (healthy subjects compared to AS patients), treatment (adalimumab compared to HS016), drinking or smoking habit, presence of ADA (a subject with at least 1 ADA-positive sample relative to baseline at any time after the initiation of treatment), baseline serum albumin, baseline alanine aminotransferase (ALT), baseline alkaline phosphatase (ALP), baseline aspartate aminotransferase (AST), baseline CRP, baseline erythrocyte sedimentation rate, baseline total bilirubin, baseline serum creatinine, baseline creatinine clearance (CLcr), and the presence of concomitant medication (salazosulfapyridine, celecoxib, diclofenac, meloxicam, and methotrexate).

After the completion of the structural model establishment, empirical Bayes estimates for inter-individual random effects could be determined. For the hierarchical models, changes in the minimum value of the objective function (OFV) were analyzed using a $\chi^2$ test in order to determine whether the data were statistically significant. The most significant covariate factor was retained in the model once for each iteration, and then the forward addition was repeated. Covariates were included if the OFV decrease was >3.84 ($\chi^2$, $p < 0.05$). All influential covariates were retained in the model and then a full covariate model was computed. The final model was established using the backward elimination method. After each iteration, a single covariate was deleted from the full covariate model to consider if it was necessary. If the OFV model increased by >6.63 ($\chi^2$, $p < 0.01$) after removing 1 covariate, that covariate was considered significantly influential.

The covariates that were continuous, were incorporated using a power function centered around the value of the median, thus (eq. 3):

$$P_{tv} = P_{pop} \times \left(\frac{Cov}{Covariate_{median}}\right)^{\theta cov} \quad (3)$$

where $P_{tv}$ is the typical value of the parameter with covariate value Cov; $P_{pop}$ is the typical value of the PK parameter P; and $\theta_{cov}$ is the estimated exponent parameter of the continuous covariate.

Categorical variables were modeled as follows (eq. 4):

$$P_{tv} = P_{pop} \times (\theta_{cov})^{FLAG} \quad (4)$$

where $P_{tv}$ is the typical value of the parameter with covariate value cov; $P_{pop}$ is the typical value of the PK parameter P; $\theta_{cov}$ is the estimated fraction parameter of the categorical covariate; and FLAG is either covariate value, appropriately.

### Evaluation of the model

Three techniques were used to evaluate the interim and final models: (1) the examination of goodness-of-fit (GOF) diagnostic plots; (2) the visual predictive check; and (3) the bootstrap. A visual predictive check (VPC) was used to assess the predictability of the PK model; 1000 simulated duplicates of PK datasets were generated using model parameter estimates. Simulation predictions at 90% were compared to the actual data by superimposing it on various percentile intervals of simulated data (5%, 50% and 95%).

To assess the robustness of the PK population final model, 1000 bootstrap duplicates were built by random sampling of the original data. The parameters were estimated for each bootstrap duplicate and employed to determine the median and 95% confidence intervals (95% CIs). The median and 95% CIs for the bootstrap PK parameters were calculated as the 50$^{th}$ percentile, with a range of 2.5$^{th}$ to 97.5$^{th}$ of results from each duplicate. Subsequently, a comparison was made between the parameters derived from the original data and the model-derived bootstrap parameters.

## Pharmacokinetic similarity assessment

The main PK endpoints were: the concentration-time curve (AUC) from time zero to area ($AUC_{0-t}$); zero time to infinity ($AUC_{0-\infty}$); the maximum serum drug concentration ($C_{max}$) after a single-dose in healthy men and AS patients; the AUC within the steady-state dose intervals ($AUC_{0-tau}$); and the maximum serum drug concentration within a steady-state dosing interval ($C_{max, ss}$) after multiple doses in AS patients. These values were calculated using the specific PK parameters of the 2 drugs estimated using the model.

To assess the similarity of PK parameters between HS016 and adalimumab, a statistical evaluation based on the average equivalence was employed. The simulated PK parameters ($C_{max}$, $AUC_{0-t}$ and $AUC_{0-\infty}$; $C_{max, ss}$ and $AUC_{0-tau}$) between subjects treated with HS016 and adalimumab were analyzed using the analysis of variance (ANOVA) with the natural log-transformed values of all PK parameters as dependent variables. The differences in natural log-transformed least square (LS) means between the treatments (HS016 and adalimumab) and associated 90% CIs were estimated. The back transformation revealed the ratio of the geometric LS means and related 90% CIs to the original parameters. The equivalence of PK between HS016 (test product) and adalimumab (reference product) were concluded when the 90% CIs of the ratios of the geometric means were entirely contained within 80% to 125%.[7,8]

# Results

## Subjects

A total of 8659 HS016 and adalimumab serum concentrations from 502 subjects were included in the analyses, including 2352 concentrations from 136 healthy subjects (1165 concentrations from 68 subjects for HS016, 1187 concentrations from 68 subjects for adalimumab) and 6307 concentrations from 366 AS patients (4023 concentrations from 235 patients for HS016 and 2284 concentrations from 131 patients for adalimumab). The demographics of participants included in the PK population analysis at baseline, stratified according to the study and treatment method, are presented in Table 2. All of the covariates exhibited similar distributions for the 2 treatments in each study.

**Table 2.** Summary of baseline demographics of the participants included in the pharmacokinetic (PK) population analysis stratified according to the study and treatment

| Study No. | HS016-I (healthy subjects) | | | HS016-III (patients) | | | All | | |
|---|---|---|---|---|---|---|---|---|---|
| Patient characteristics | HS016 (n = 68, 13.55%) | Humira® (n = 68, 13.55%) | all (n = 136, 27.09%) | HS016 (n = 235, 46.81%) | Humira® (n = 131, 26.10%) | all (n = 366, 72.91%) | HS016 (n = 303, 60.36%) | Humira® (n = 199, 39.64%) | all (n = 502, 100.00%) |
| Age [years] | 26.0 (18–36) | 25.0 (18–37) | 25.0 (18–37) | 30.0 (19–63) | 30.0 (18–58) | 30.0 (18–63) | 29.0 (18–63) | 28.0 (18–58) | 29.0 (18–63) |
| Weight [kg] | 62.70 (53–70) | 62.65 (50.6–70) | 62.70 (50.6–70) | 65.00 (50–85) | 65.00 (51–85) | 65.00 (50–85) | 64.70 (50–85) | 64.00 (50.6–85) | 64.15 (50–85) |
| BMI [kg/m$^2$] | 22.10 (20–25) | 21.40 (20–24.6) | 21.90 (20–25) | 23.56 (18.07–27.89) | 23.12 (20.05–27.98) | 23.54 (18.07–27.98) | 23.00 (18.07–27.89) | 22.28 (20–27.98) | 22.67 (18.07–27.98) |
| Body surface area [m$^2$] | 1.71 (1.54–1.88) | 1.72 (1.49–1.88) | 1.71 (1.49–1.88) | 1.75 (1.4–2.1) | 1.76 (1.49–2.07) | 1.75 (1.4–2.1) | 1.73 (1.4–2.1) | 1.75 (1.49–2.07) | 1.74 (1.4–2.1) |

**Table 2.** Summary of baseline demographics of the participants included in the pharmacokinetic (PK) population analysis stratified according to the study and treatment – cont.

| Study No. | HS016-I (healthy subjects) | | | HS016-III (patients) | | | All | | |
|---|---|---|---|---|---|---|---|---|---|
| Baseline serum albumin [g/L] | 49.00 (43–53) | 49.00 (44–53) | 49.00 (43–53) | 45.80 (35–54.6) | 45.00 (33–53.2) | 45.40 (33–54.6) | 46.90 (35–54.6) | 47.00 (33–53.2) | 47.00 (33–54.6) |
| Baseline alkaline phosphatase [IU/L] | 68.50 (47–117) | 76.50 (38–114) | 73.00 (38–117) | 94.00 (35–208.8) | 96.60 (33–238) | 94.95 (33–238) | 87.00 (35–208.8) | 88.00 (33–238) | 87.00 (33–238) |
| Baseline alanine aminotransferase [IU/L] | 18.00 (9–49) | 15.00 (7–39) | 17.00 (7–49) | 16.50 (6–82) | 16.00 (5–69) | 16.05 (5–82) | 17.00 (6–82) | 16.00 (5–69) | 16.60 (5–82) |
| Baseline aspartate aminotransferase [IU/L] | 17.00 (12–38) | 16.50 (12–25) | 17.00 (12–38) | 18.00 (9–42) | 17.70 (10–62) | 18.00 (9–62) | 18.00 (9–42) | 17.00 (10–62) | 17.40 (9–62) |
| Baseline CRP [mg/L] | 1.64 (1.555–4.07) | 1.58 (1.555–1.69) | 1.58 (1.555–4.07) | 12.70 (0.1–135.38) | 14.80 (0.1–140) | 13.70 (0.1–140) | 7.40 (0.1–135.38) | 4.01 (0.1–140) | 6.76 (0.1–140) |
| Baseline erythrocyte sedimentation rate [mm/h] | 2.00 (1.69–13) | 2.00 (2–11) | 2.00 (1.69–13) | 22.00 (1–121) | 27.00 (2–99) | 24.00 (1–121) | 16.00 (1–121) | 14.00 (2–99) | 15.50 (1–121) |
| Baseline total bilirubin [µmol/L] | 10.75 (5.5–22.8) | 11.35 (3.5–21.5) | 10.95 (3.5–22.8) | 8.50 (3.6–23.4) | 8.50 (2.9–20.2) | 8.50 (2.9–23.4) | 8.90 (3.6–23.4) | 9.50 (2.9–21.5) | 9.30 (2.9–23.4) |
| Baseline serum creatinine [µmol/L] | 76.00 (55–100) | 73.00 (53–93) | 74.00 (53–100) | 65.00 (32–119) | 66.00 (39.1–97) | 65.00 (32–119) | 67.00 (32–119) | 69.00 (39.1–97) | 68.00 (32–119) |
| Baseline creatinine clearance | 117.47 (87.07–165.9) | 118.98 (89.39–188.19) | 118.36 (87.07–188.19) | 134.19 (67.31–222) | 127.21 (82.18–222.65) | 132.39 (67.31–222.65) | 129.09 (67.31–222) | 124.54 (82.18–222.65) | 126.89 (67.31–222.65) |
| Sex, n (%) | | | | | | | | | |
| Female | 0 (0.00) | 0 (0.00) | 0 (0.00) | 30 (12.77) | 14 (10.69) | 44 (12.02) | 30 (9.90) | 14 (7.04) | 44 (8.76) |
| Male | 68 (100.00) | 68 (100.00) | 136 (100.00) | 205 (87.23) | 117 (89.31) | 322 (87.98) | 273 (90.10) | 185 (92.96) | 458 (91.24) |
| Smoking history, n (%) | | | | | | | | | |
| Absent | 45 (66.18) | 47 (69.12) | 92 (67.65) | 167 (71.06) | 90 (68.70) | 257 (70.22) | 212 (69.97) | 137 (68.84) | 349 (69.52) |
| Present | 23 (33.82) | 21 (30.88) | 44 (32.35) | 68 (28.94) | 41 (31.30) | 109 (29.78) | 91 (30.03) | 62 (31.16) | 153 (30.48) |
| Drinking history, n (%) | | | | | | | | | |
| Absent | 68 (100.00) | 65 (95.59) | 133 (97.79) | 226 (96.17) | 122 (93.13) | 348 (95.08) | 294 (97.03) | 187 (93.97) | 481 (95.82) |
| Present | 0 (0.00) | 3 (4.41) | 3 (2.21) | 9 (3.83) | 9 (6.87) | 18 (4.92) | 9 (2.97) | 12 (6.03) | 21 (4.18) |
| ADA, n (%) | | | | | | | | | |
| Negative | 14 (20.59) | 5 (7.35) | 19 (13.97) | 50 (21.28) | 22 (16.79) | 72 (19.67) | 64 (21.12) | 27 (13.57) | 91 (18.13) |
| Positive | 54 (79.41) | 63 (92.65) | 117 (86.03) | 185 (78.72) | 109 (83.21) | 294 (80.33) | 239 (78.88) | 172 (86.43) | 411 (81.87) |
| Concomitant salazosulfapyridine, n (%) | | | | | | | | | |
| Absent | 68 (100.00) | 68 (100.00) | 136 (100.00) | 164 (69.79) | 85 (64.89) | 249 (68.03) | 232 (76.57) | 153 (76.88) | 385 (76.69) |
| Present | 0 (0.00) | 0 (0.00) | 0 (0.00) | 71 (30.21) | 46 (35.11) | 117 (31.97) | 71 (23.43) | 46 (23.12) | 117 (23.31) |
| Concomitant celecoxib, n (%) | | | | | | | | | |
| Absent | 68 (100.00) | 68 (100.00) | 136 (100.00) | 181 (77.02) | 100 (76.34) | 281 (76.78) | 249 (82.18) | 168 (84.42) | 417 (83.07) |
| Present | 0 (0.00) | 0 (0.00) | 0 (0.00) | 54 (22.98) | 31 (23.66) | 85 (23.22) | 54 (17.82) | 31 (15.58) | 85 (16.93) |
| Concomitant diclofenac, n (%) | | | | | | | | | |
| Absent | 68 (100.00) | 68 (100.00) | 136 (100.00) | 189 (80.43) | 97 (74.05) | 286 (78.14) | 257 (84.82) | 165 (82.91) | 422 (84.06) |
| Present | 0 (0.00) | 0 (0.00) | 0 (0.00) | 46 (19.57) | 34 (25.95) | 80 (21.86) | 46 (15.18) | 34 (17.09) | 80 (15.94) |
| Concomitant meloxicam, n (%) | | | | | | | | | |
| Absent | 68 (100.00) | 68 (100.00) | 136 (100.00) | 207 (88.09) | 120 (91.60) | 327 (89.34) | 275 (90.76) | 188 (94.47) | 463 (92.23) |
| Present | 0 (0.00) | 0 (0.00) | 0 (0.00) | 28 (11.91) | 11 (8.40) | 39 (10.66) | 28 (9.24) | 11 (5.53) | 39 (7.77) |
| Concomitant methotrexate, n (%) | | | | | | | | | |
| Absent | 68 (100.00) | 68 (100.00) | 136 (100.00) | 230 (97.87) | 124 (94.66) | 354 (96.72) | 298 (98.35) | 192 (96.48) | 490 (97.61) |
| Present | 0 (0.00) | 0 (0.00) | 0 (0.00) | 5 (2.13) | 7 (5.34) | 12 (3.28) | 5 (1.65) | 7 (3.52) | 12 (2.39) |

All continuous values are reported as median (min–max), while categories are reported in absolute numbers and percentages.
ADA – anti-drug antibody; BMI – body mass index; CRP – C-reactive protein.

## Serum concentrations

Figure 1 shows the mean serum concentrations of HS016 and adalimumab in the phase 1 study, following the administration of single 40 mg subcutaneous doses. Figure 2 shows the results from the phase 3 study of the mean serum HS016 and adalimumab concentrations at week 12, after the administration of 40 mg subcutaneous doses once every 2 weeks. After single and multiple doses, the PK profiles of HS016 and adalimumab were virtually identical. Only 1 declining phase of the logarithmic serum concentration time courses of adalimumab and its biosimilar HS016 were analyzed.

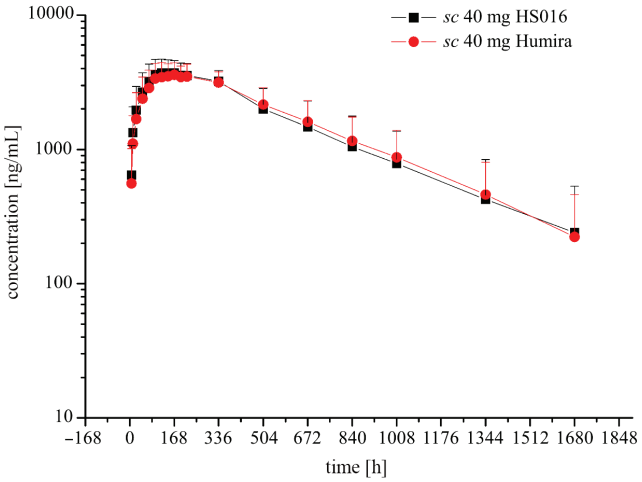


Fig. 1. Compared serum concentrations of HS016 and adalimumab over the study period in healthy participants after a single-dose (phase 1 study)

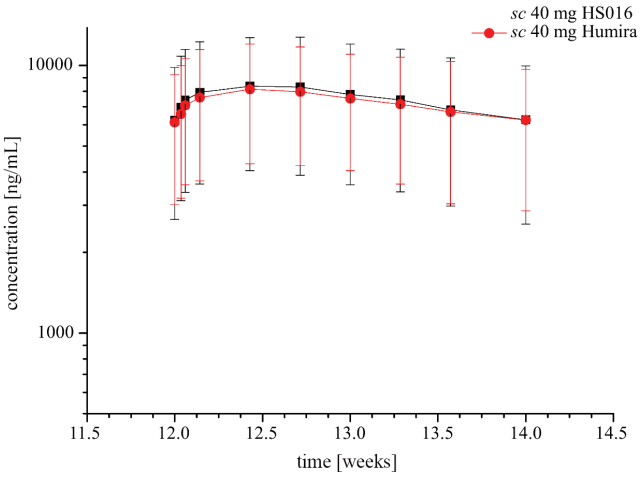


Fig. 2. Compared mean serum concentrations of HS016 and adalimumab over the study period in ankylosing spondylitis (AS) patients at week 12 after 40 mg treatments (phase 3 study)

## PK population modeling

The time courses of HS016 and adalimumab serum concentrations in healthy subjects and AS patients achieved the best fit when a one-compartment model was employed after the subcutaneous administration. The treatment (DRUG) was not identified as the significant covariate and BW, age, CLcr, and the presence of ADA were shown to be significant covariates for CL/F, BW and subject type as covariates for V/F, and the subject type as a statistically significant covariate for KA. An exponential term was used for IIV and IOV. A combined error model best explained the residual error.

The final population PK model was as follows (eq. 5–7):

$$\mathrm{CL/F_{i,k}} = \begin{array}{l}\theta_{\mathrm{CL/F_{pop}}} \times (\theta_{\mathrm{ADA}})^{1-\mathrm{ADA}} \times \left(\frac{\mathrm{AGE}}{29}\right)^{\theta_{\mathrm{AGE}}} \times \left(\frac{\mathrm{BW}}{64.15}\right)^{\theta_{\mathrm{BW}}} \\ \times \left(\frac{\mathrm{CLcr}}{126.88}\right)^{\theta_{\mathrm{CLcr}}} \times \exp\left(\eta^{\mathrm{CL/F,i}} + \mathrm{IOV}^{\mathrm{CL/F,i}}\right)\end{array} \quad (5)$$

$$\mathrm{V/F_i} = \theta_{\mathrm{V/F_{pop}}} \times \left(\frac{\mathrm{BW}}{64.15}\right)^{\theta_{\mathrm{BW}}} \times \left(\theta_{\mathrm{TYPE}}\right)^{1-\mathrm{TYPE}} \times \exp\left(\eta^{\mathrm{V/F,i}}\right) \quad (6)$$

$$\mathrm{KA_i} = \theta_{KA_{\mathrm{pop}}} \times (\theta_{\mathrm{TYPE}})^{1-\mathrm{TYPE}} \times \exp(\eta^{\mathrm{KA,i}}) \quad (7)$$

where θ represents the fixed-effect parameters, CL/F is clearance corrected for bioavailability, AGE is age, and i and k are the predicted value of $k^{th}$ plasma concentration of the $i^{th}$ patient. The AGE, BW and CLcr were continuous covariates, while categorical covariates included ADA (where ADA describes absent = 0 and present = 1) and TYPE (where healthy subjects = 0 and AS patients = 1). The η and IOV represent the IIV and IOV, respectively.

The estimated parameters derived from the final model and its validation are given in Table 3.

## Evaluation of the model

The GOF plots of the PK population final model are displayed in Fig. 3. The plots exhibited good correlations between an individual prediction and the observation with lines of identity and trend line overlaid, and the individual predictions fitting the identity line well. This finding has proven the excellent predictive power of the model. The conditional weighted residual error had no misspecification of residuals related to population predictions (PRED) and time, was mostly distributed within ±5 and was well distributed along the zero-line relative to PRED.

The VPC was used to determine the predictive accuracy of the final model (Fig. 4). A total of 1000 simulated duplicates of the PK dataset were produced from the estimates derived from the final model. The model described the observed data well, and $50^{th}$ percentiles of measured drug concentrations generally fell within the prediction of 90% CI, suggesting that the model produced a good description of the PK parameters of HS016 and adalimumab.

A total of 993 out of 1000 bootstrap duplicates successfully converged and the estimated PK parameter values based on the original data were found to be in a good agreement with the median values of PK parameters estimated using bootstrap duplicates (Table 3).

**Table 3.** Parameter estimates of the final population pharmacokinetic (PK) model for HS016 and adalimumab and bootstrap results

| Parameter | Estimate | SE | RSE (%) | Bootstrap estimate | Bootstrap 95% CI |
|---|---|---|---|---|---|
| Fixed-effect parameters | | | | | |
| $\theta_{CL/Fpop}$ [L/h] | 0.0179 | 0.000534 | 3.0 | 0.0179 | (0.0169; 0.0190) |
| $\theta_{V/Fpop}$ [L] | 11.3 | 0.241 | 2.1 | 11.3 | (10.8; 11.8) |
| $\theta_{KApop}$ [1/h] | 0.0298 | 0.00189 | 6.3 | 0.0297 | (0.0262; 0.0336) |
| $\theta_{ADA}^{CL/F}$ | –0.431 | 0.0277 | –6.4 | –0.429 | (–0.481; –0.377) |
| $\theta_{AGE}^{CL/F}$ | 0.410 | 0.118 | 28.8 | 0.414 | (0.182; 0.638) |
| $\theta_{BW}^{CL/F}$ | 0.824 | 0.254 | 30.8 | 0.830 | (0.292; 1.30) |
| $\theta_{CLcr}^{CL/F}$ | 0.600 | 0.162 | 27.0 | 0.587 | (0.270; 0.940) |
| $\theta_{TYPE}^{KA}$ | –0.474 | 0.0458 | –9.7 | –0.474 | (–0.558; –0.363) |
| $\theta_{BW}^{V/F}$ | 1.16 | 0.164 | 14.1 | 1.17 | (0.828; 1.50) |
| $\theta_{TYPE}^{V/F}$ | –0.299 | 0.0228 | –7.6 | –0.298 | (–0.342; –0.255) |
| Inter-individual variability (IIV) | | | | | |
| $\eta_{CL/F}$ (CV%) | 0.271 (52.06) | 0.0301 | 11.1 (Shr = 11%) | 0.266 | (0.211; 0.328) |
| $\eta_{V/F}$ (CV%) | 0.0902 (30.03) | 0.0163 | 18.1 (Shr = 19%) | 0.0877 | (0.0573; 0.123) |
| $\eta_{KA}$ (CV%) | 0.662 (81.36) | 0.0721 | 10.9 (Shr = 20%) | 0.659 | (0.529; 0.821) |
| Inter-occasion variability (IOV) | | | | | |
| $IOV_1^{CL/F}$ | 0.0921 | – | – | 0.0911 | (0.0665; 0.127) |
| $IOV_2^{CL/F}$ | 0.0921 | – | – | 0.0911 | (0.0665; 0.127) |
| $IOV_3^{CL/F}$ | 0.0921 | – | – | 0.0911 | (0.0665; 0.127) |
| Residual variability | | | | | |
| $\varepsilon_1$ | 0.110 | 0.00731 | 6.6 | 0.109 | (0.0957; 0.124) |
| $\varepsilon_2$ | 344 | 27.1 | 7.9 | 342 | (290; 398) |

CV – coefficient of variation; SQRT – square root; ADA – anti-drug antibody; AGE – age; BW – body weight; CLcr – creatinine clearance; CL/F – apparent clearance; 95% CI – 95% confidence interval; $\varepsilon_1$ – proportional error; $\varepsilon_2$ – additive error; η – constant of inter-individual variability (variance); IOV – inter-occasion variability (variance); KA – absorption rate constant; pop – population; RSE – relative standard error; SE – standard error; Shr – shrinkage; θ – typic value; TYPE – subject type (healthy subject and patients); V/F – apparent volume of distribution. The IOV for CL/F was included in the final model, corresponding to the 3 occasions: one for the time before the intended week 12 ($IOV_1^{CL/F}$), one for the time between intended week 12 and week 14 ($IOV_2^{CL/F}$) and the other one for the time after the intended week 14 ($IOV_3^{CL/F}$).

**Table 4.** Statistical analysis of pharmacokinetic (PK) primary endpoints after single- and multiple-dose administration in healthy subjects

| Dosing period | Parameter [unit] | Treatment | n | Geometric of LS means | Ratio of geometric LS means (%) | 90% CI (%) |
|---|---|---|---|---|---|---|
| Single-dose | $C_{max}$ [µg/mL] | HS016<br>Humira® | 68<br>68 | 3.77<br>3.59 | 105.11 | [98.14; 112.58] |
| | $AUC_{0-t}$ [µg×h/mL] | HS016<br>Humira® | 68<br>68 | 2358.77<br>2413.96 | 97.71 | [89.26; 106.97] |
| | $AUC_{0-\infty}$ [µg×h/mL] | HS016<br>Humira® | 68<br>68 | 2507.74<br>2581.63 | 97.14 | [87.60; 107.71] |
| Multiple doses | $C_{max, ss}$ [µg/mL] | HS016<br>Humira® | 68<br>68 | 8.56<br>8.63 | 99.14 | [90.03; 109.16] |
| | $AUC_{0-tau}$ [µg×h/mL] | HS016<br>Humira® | 68<br>68 | 2502.85<br>2576.66 | 97.14 | [87.70; 107.59] |

90% CI – 90% confidence interval; LS – least squares; n – number of subjects; $C_{max, ss}$ – maximum serum drug concentration within a steady-state dosing interval; AUC – concentration-time curve.

## Pharmacokinetic assessment

The analyses of the main PK endpoints after single- and multiple-dose administrations by subject were evaluated to determine the PK similarity (Table 4,5).

In healthy subjects, the ratios of the geometric LS means (the HS016 group compared to the adalimumab treatment group after a single-dose) were 90% CIs: 97.71 [89.26; 106.97] for $AUC_{0-t}$, 97.14 [87.60; 107.71] for $AUC_{0-\infty}$ and 105.11 [98.14; 112.58] for $C_{max}$. Virtually identical results were found when the PK parameters of HS016 and adalimumab at steady state (after multiple doses) were determined; the corresponding values were 97.14 [87.70; 107.59] for $AUC_{0-tau}$ and 99.14 [90.03; 109.16] for $C_{max, ss}$.

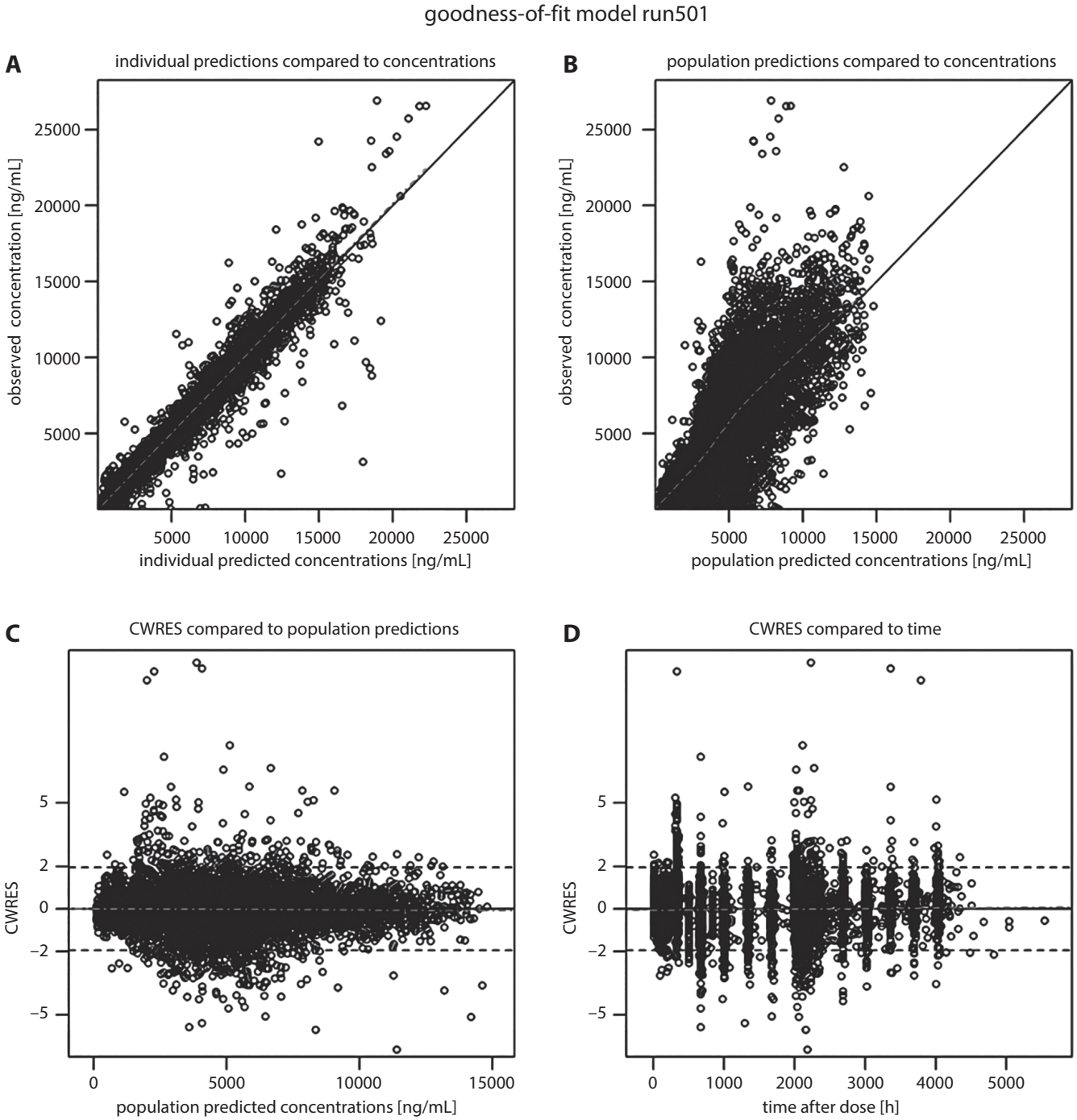


Fig. 3. Diagnostic plots showing the fit to the model. A. Plot of individual predicted compared to measured concentrations; B. Plot of population predictions (PRED) compared to measured concentrations. Improvements from B to A show that the model can adequately predict individually observed concentrations; C. PRED compared to conditional weighted residual errors; D. Time after dose compared to conditional weighted residuals (CWRES) for the population model, where the residuals were distributed randomly around the unity line

The limits for the abovementioned CIs of the ratios were within the 80–125% interval.

In AS patients, the ratios of the geometric LS means (the HS016 group compared to the adalimumab therapy group after a single-dose) were 90% CIs: 98.10 [86.24; 111.59] for $AUC_{0-t}$, 97.08 [83.84; 112.41] for $AUC_{0-\infty}$ and 105.59 [98.12; 113.63] for $C_{max}$. The corresponding values for the PK of HS016 and adalimumab at steady state were 97.03 [84.10; 111.96] for $AUC_{0-tau}$ and 99.62 [88.09; 112.68] for $C_{max,ss}$. The limits for the abovementioned CIs of the ratios were within the 80–125% interval.

## Discussion

The study investigated the PK parameters of the adalimumab biosimilar HS016 in a large number of Chinese AS patients, the serum concentrations and treatment cycles,

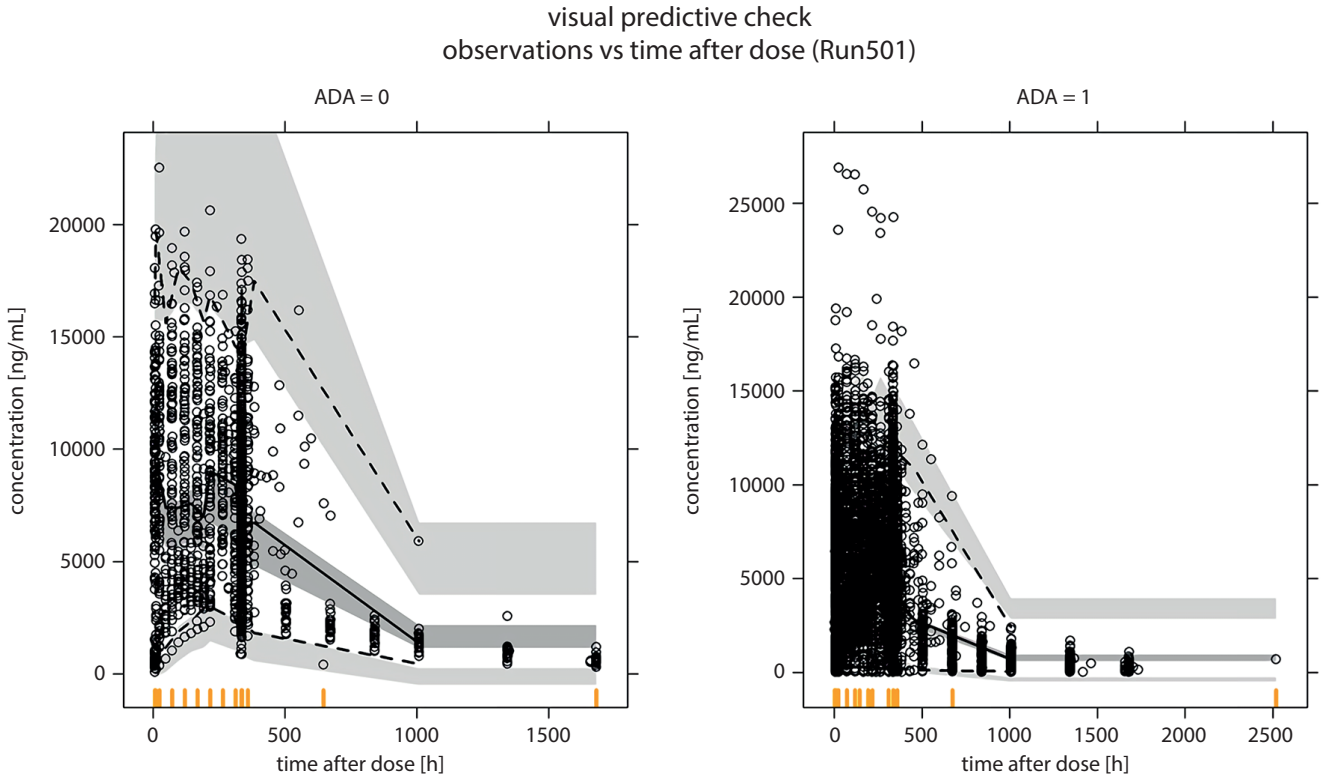


**Fig. 4.** Visual predictive checks for the final pharmacokinetic (PK) population model. Circles indicate the measured data, solid lines the median of the predicted concentrations, dotted lines the 95$^{th}$ and 5$^{th}$ percentile of the observed data from up to down. The band indicates the 90% prediction interval (90% CI). Anti-drug antibody (ADA) = 0 represents the absence of ADA, ADA = 1 represents the presence of ADA

**Table 5.** Statistical analysis of pharmacokinetic (PK) primary endpoints after single- and multiple-dose administration in ankylosing spondylitis (AS) patients

| Dosing period | Parameter (unit) | Treatment | n | Geometric of LS means | Ratio of geometric LS means (%) | 90% CI (%) |
|---|---|---|---|---|---|---|
| Single-dose | $C_{max}$ [µg/mL] | HS016<br>Humira® | 235<br>131 | 2.92<br>2.77 | 105.59 | [98.12; 113.63] |
| | $AUC_{0-t}$ [µg×h/mL] | HS016<br>Humira® | 235<br>131 | 1926.39<br>1963.69 | 98.10 | [86.24; 111.59] |
| | $AUC_{0-\infty}$ [µg×h/mL] | HS016<br>Humira® | 235<br>131 | 2250.48<br>2318.14 | 97.08 | [83.84; 112.41] |
| Multiple doses | $C_{max, ss}$ [µg/mL] | HS016<br>Humira® | 235<br>131 | 7.83<br>7.86 | 99.62 | [88.09; 112.68] |
| | $AUC_{0-tau}$ [µg×h/mL] | HS016<br>Humira® | 235<br>131 | 2203.06<br>2270.42 | 97.03 | [84.10; 111.96] |

90% CI – 90% confidence interval; LS – least squares; n – number of subjects; $C_{max, ss}$ – maximum serum drug concentration within a steady-state dosing interval; AUC – concentration-time curve.

in order to introduce PK methods that measured the drugs characteristics accurately. A total of 8659 HS016 and adalimumab serum concentrations from 502 subjects were included in the analyses, including 2352 from 136 healthy individuals and 6307 from 366 AS patients (4023 from 235 patients for HS016 and 2284 from 131 patients for adalimumab).

As a part of the biosimilarity assessment, we sought to detect possible differences between the PK parameters of the test and reference drugs. In the target patient population, full intensive sampling of concentration-time curves for all included patients was sometimes not available. However, the implementation of a non-compartmental method needs a powerful sample profile to evaluate the AUC using the trapezoidal method. In our study, the sample size required to detect the PK biosimilarity was decreased along with the exclusion of patients with sparse sampling. The PK similarity analysis using nonlinear mixed-effects models have already been performed for other biosimilars,[12,13] and a PK population approach has been previously used to assess adalimumab actions in patients with other indications.[17–19]

The PK population model developed to compare HS016 and adalimumab permitted us to employ insubstantial sampling and facilitated the quantitation of any potential

changes in the PK parameters of the 2 treatment regimens. We demonstrated that the time course of HS016 was well-characterized by the developed model. In the present study, adalimumab and its biosimilar PK parameters were assessed in healthy subjects and AS patients after a single dose or multiple doses at steady-state concentrations, in accordance with the Food and Drug Administration (FDA) bioequivalence guidelines.[8] Simultaneously, the large sample size increased our ability to detect any differences between the 2 investigated drugs.

The abovementioned one-compartment population PK model best described adalimumab and HS016 PK in healthy males and AS patients after one-dose or multiple-dosage regimens. The population estimates for CL/F (the absence of ADA) and V/F were 0.01 L/h and 11.3 L for AS patients, and they were comparable to patients with hidradenitis suppurativa (0.0278 L/h and 13.5 L), RA (0.013 L/h and 10.8 L) and Crohn's disease (0.014 L/h and 7.8 L).[17–19]

The factors that had a significant effect on PK parameters for adalimumab in the model were BW, age, CLcr, presence of ADA on CL/F, BW, and subject type on V/F and KA. The covariate analysis revealed that CL/F increased in a patient who became ADA-positive for both HS016 and adalimumab. For both drugs, CL/F also increased with increasing BW, age and CLcr. Age, BW and the presence of ADA have also been previously reported to be significant factors for adalimumab.[18,19] In our study, the treatment (adalimumab compared to HS016) was not an important covariate, indicating that the PK parameters of both drugs were similar.

The ratios of the geometric LS means (HS016 compared to adalimumab) met the expectations for the statistical equivalence of AUC and $C_{max}$ after a single-dose, and at steady state. Thus, systemic exposure (AUC and $C_{max}$) and the linked variability calculated using a PK population model revealed that the PK parameters of HS016 and adalimumab were similar. The geometric LS means of AUC and $C_{max}$ were also comparable to the results reported by the literature in healthy subjects.[20]

It is noteworthy that because of the complex nature of the PK population model, a number of limitations may restrict its validity. There may exist a potential bias in the simulated data that makes the predicted data different from the measured data. For example, the population model underpredicted PK profiles of HS016 and adalimumab, as shown by VPC (Fig. 4). We compared the results with those obtained using traditional non-compartmental analysis in the phase 1 study (results not shown), the PK bioequivalence results from non-compartmental analysis and the model-based approach and showed their similarity, thereby demonstrating that our model-based approach can be used for the equivalence testing.

In addition, we have also explored the relationship between the exposure (AUC and $C_{max}$) of HS016 or adalimumab at steady state and pharmacodynamic (PD) parameters (maximum decrease changes from baseline of CRP and erythrocyte sedimentation rate). It showed that the correlation between the PK and PD parameters was not different ($p > 0.05$), and that the trends were consistent between HS016 and adalimumab.

## Limitations

The study has several limitations. All patient data came exclusively from Chinese participants and the trials had strict inclusion and exclusion criteria, which might not reflect real-world clinical conditions.

# Conclusions

Systemic exposure ($C_{max}$, AUC parameters) of HS016 and associated variability were similar to adalimumab in healthy male subjects and AS patients. The 90% CIs for all parameters fell within a range of 80–125% predefined bioequivalence interval.


### ORCID iDs

Xiaofeng Zeng https://orcid.org/0000-0001-9484-8093
Jing Zhang https://orcid.org/0000-0003-1017-7304
Jicheng Yu https://orcid.org/0000-0002-2381-2365
Xiaojie Wu https://orcid.org/0000-0002-0081-6507
Yuancheng Chen https://orcid.org/0000-0002-5731-9114
Jufang Wu https://orcid.org/0000-0001-8619-0690
Xiaoli Yang https://orcid.org/0000-0002-6774-7956
Jingjing Wang https://orcid.org/0000-0002-6107-0235
Guoying Cao https://orcid.org/0000-0002-8321-6637


### References


1. Food and Drug Administration (FDA). Adalimumab indications and usage. https://www.accessdata.fda.gov/drugsatfda_docs/label/2018/125057s408lbl.pdf. Accessed March 20, 2020.
2. Ng SC, Liao Z, Yu DTT, Chan ESY, Zhao L, Gu J. Epidemiology of spondyloarthritis in the People's Republic of China: Review of the literature and commentary. *Semin Arthritis Rheum*. 2007;37(1):39–47. doi:10.1016/j.semarthrit.2007.01.003
3. Xiang YJ, Dai SM. Prevalence of rheumatic diseases and disability in China. *Rheumatol Int*. 2008;29(5):481–490. doi:10.1007/s00296-008-0809-z
4. Dean LE, Jones GT, MacDonald AG, Downham C, Sturrock RD, Macfarlane GJ. Global prevalence of ankylosing spondylitis. *Rheumatology (Oxford)*. 2014;53(4):650–657. doi:10.1093/rheumatology/ket387
5. Yoo DH. The rise of biosimilars: Potential benefits and drawbacks in rheumatoid arthritis. *Expert Rev Clin Immunol*. 2014;10(8):981–983. doi:10.1586/1744666X.2014.932690
6. de Mora F. Biosimilar: What it is not. *Br J Clin Pharmacol*. 2015;80(5):949–956. doi:10.1111/bcp.12656
7. European Medicines Agency (EMA). Guideline on similar biological medicinal products containing biotechnology derived proteins as active substance: Non-clinical and clinical issues. https://www.ema.europa.eu/en/documents/scientific-guideline/guideline-similar-biological-medicinal-products-containing-biotechnology-derived-proteins-active_en-2.pdf. Accessed March 20, 2020.
8. Food and Drug Administration (FDA). Guidance for industry. Clinical pharmacology data to support a demonstration of biosimilarity to a reference product. http://www.fda.gov/downloads/drugs/guidancecomplianceregulatoryinformation/guidances/ucm397017.pdf. Accessed March 20, 2020.
9. Cao G, Yu J, Wu J, et al. A Randomized, double-blind, parallel-group, phase 1 clinical trial comparing the pharmacokinetic, safety, and immunogenicity of the biosimilar HS016 and the originator adalimumab in Chinese healthy male subjects. *Clin Pharmacol Drug Dev*. 2021;10(3):317–325. doi:10.1002/cpdd.816

10. Su J, Li M, He L, et al. Comparison of the efficacy and safety of adalimumab (Humira) and the adalimumab biosimilar candidate (HS016) in Chinese patients with active ankylosing spondylitis: A multicenter, randomized, double-blind, parallel, phase III clinical trial. *BioDrugs*. 2020;34(3):381–393. doi:10.1007/s40259-020-00408-z
11. Food and Drug Administration (FDA). Guidance for industry. Population pharmacokinetics. https://www.fda.gov/media/128793/download. Accessed March 20, 2020.
12. Dubois A, Gsteiger S, Balser S, et al. Pharmacokinetic similarity of biologics: Analysis using nonlinear mixed-effects modeling. *Clin Pharmacol Ther*. 2012;91(2):234–242. doi:10.1038/clpt.2011.216
13. Candelaria M, Gonzalez D, Fernández Gómez FJ, et al. Comparative assessment of pharmacokinetics, and pharmacodynamics between RTXM83™, a rituximab biosimilar, and rituximab in diffuse large B-cell lymphoma patients: A population PK model approach. *Cancer Chemother Pharmacol*. 2018;81(3):515–527. doi:10.1007/s00280-018-3524-9
14. Linden SVD, Valkenburg HA, Cats A. Evaluation of diagnostic criteria for ankylosing spondylitis. *Arthritis Rheum*. 1984;27(4):361–368. doi:10.1002/art.1780270401
15. Beal SL, Boeckmann AJ, Bauer RJ, eds. *NONMEM Users Guides (1989–2013)*. Ellicott City, USA: Icon Development Solutions; 2013.
16. Lindbom L, Pihlgren P, Jonsson N. PsN-Toolkit: A collection of computer intensive statistical methods for non-linear mixed effect modeling using NONMEM. *Comput Methods Programs Biomed*. 2005;79(3):241–257. doi:10.1016/j.cmpb.2005.04.005
17. Nader A, Beck D, Noertersheuser P, Williams D, Mostafa N. Population pharmacokinetics and immunogenicity of adalimumab in adult patients with moderate-to-severe hidradenitis suppurativa. *Clin Pharmacokinet*. 2017;56(9):1091–1102. doi:10.1007/s40262-016-0502-4
18. Ternant D, Ducourau E, Fuzibet P, et al. Pharmacokinetics and concentration–effect relationship of adalimumab in rheumatoid arthritis. *Br J Clin Pharmacol*. 2015;79(2):286–297. doi:10.1111/bcp.12509
19. Vande Casteele N, Baert F, Bian S, et al. Subcutaneous absorption contributes to observed interindividual variability in adalimumab serum concentrations in Crohn's disease: A prospective multicentre study. *J Crohns Colitis*. 2019;13(10):1248–1256. doi:10.1093/ecco-jcc/jjz050
20. Hillson J, Mant T, Rosano M, et al. Pharmacokinetic equivalence, comparable safety, and immunogenicity of an adalimumab biosimilar product (M923) to Humira in healthy subjects. *Pharmacol Res Perspect*. 2018;6(1):e00380. doi:10.1002/prp2.380

# High intraoperative pulse pressure is a risk factor for postoperative acute kidney injury in a cohort of abdominal surgery patients: An exploratory study

Zbigniew Putowski[A–F], Łukasz Krzych[A–F], Szymon Czajka[A–F]

Department of Anaesthesiology and Intensive Care, Medical University of Silesia, Katowice, Poland

A – research concept and design; B – collection and/or assembly of data; C – data analysis and interpretation; D – writing the article; E – critical revision of the article; F – final approval of the article

Advances in Clinical and Experimental Medicine, ISSN 1899–5276 (print), ISSN 2451–2680 (online) *Adv Clin Exp Med*. 2022;31(5):511–517

**Address for correspondence**
Zbigniew Putowski
E-mail: putowski.zbigniew@gmail.com

**Funding sources**
None declared

**Conflict of interest**
None declared

Received on September 13, 2021
Reviewed on December 12, 2021
Accepted on January 19, 2022

Published online on February 15, 2022

## Abstract

**Background.** Both intraoperative hypotension and hypertension have been reported to increase the occurrence of acute kidney injury (AKI). However, the impact of the intraoperative pulse pressure (PP) on the latter complications remains relatively unknown.

**Objectives.** To explore whether high intraoperative PP values are associated with postoperative AKI.

**Materials and methods.** The data for this study come from a prospective cohort study in which patients who underwent abdominal surgery between October 1, 2018 and July 15, 2019 in university hospital in Katowice, Poland were included in the analysis. Pre- and intraoperative data, including blood pressure measurements, were acquired from medical charts. Several PP thresholds were applied: >50, >55, >60, >65, >70, >75, >80, >85, and >90 mm Hg. Additionally, by analyzing the maximal PP during the procedures, the cutoff point for the occurrence of outcomes was estimated. Postoperative AKI was considered as the outcome of the study. Univariable and multivariable analyses were performed to assess PP relationship with AKI.

**Results.** Four hundred and ninety-four patients were included in the analysis. The AKI was present in 32 (6.5%) cases. The receiver operating characteristic (ROC) curve analysis estimated a cutoff point of >84 mm Hg of maximal PP to be associated with the outcome. The PP values above 80 mm Hg and onward were successfully included in the multivariable statistical models. A model in which PP > 90 mm Hg (odds ratio (OR) = 4.03; 95% confidence interval (95% CI): [1.53; 10.62]) was included, had the best predicting value in predicting hypoperfusion injury (area under the receiver operating characteristics (AUROC) = 0.88). Apart from PP, intraoperative hypotension, presence of chronic arterial hypertension, chronic kidney disease, and procedure duration were independently associated with AKI.

**Conclusions.** High intraoperative PP may be associated with the occurrence of postoperative AKI. However, the effect of high PP should be confirmed in other noncardiac populations to prove the generalizability of our results.

**Key words:** acute kidney injury, hemodynamic monitoring, general surgery, pulse pressure

**Cite as**
Putowski Z, Krzych Ł, Czajka S. High intraoperative pulse pressure is a risk factor for postoperative acute kidney injury in a cohort of abdominal surgery patients: An exploratory study. *Adv Clin Exp Med*. 2022;31(5):511–517. doi:10.17219/acem/145946

**DOI**
10.17219/acem/145946

## Background

Hypoperfusion-related organ injury is a fairly frequent perioperative complication.[1–4] Intraoperative hypotension (IOH) has been linked with postoperative myocardial injury (MI), acute kidney injury (AKI) and stroke.[1–3] Perioperative Quality Initiative (POQI) consensus statement on intraoperative blood pressure underlines that mean arterial pressure (MAP) below 60–70 mm Hg and systolic blood pressure (SBP) below 100 mm Hg are associated with hypoperfusion-related organ injury and death.[4] However, hypertensive events during surgery may also worsen the prognosis, as intraoperative episodes of SBP above 160 mm Hg have been correlated with the risk of myocardial injury and infarction.[4] Lastly, diastolic blood pressure (DBP) below 50 mm Hg is also reported to be harmful.[5]

Although ambulatory pulse pressure (PP) is considered one of the best predictors of cardiovascular risk, it has been poorly investigated in the perioperative period.[6] The association between high preoperative PP values and the relationship with postoperative complications (mainly myocardial infarction, AKI and stroke) has been explored mostly in cardiosurgical patient populations. The POQI has called for further research on the matter in noncardiac surgery.[7]

## Objectives

In an exploratory fashion, we sought to verify whether elevated intraoperative PP values are associated with postoperative AKI in the abdominal surgery population.

## Materials and methods

The data used in this study come from a prospective cohort study previously published by our team.[8] We screened 576 consecutive patients who underwent abdominal surgery between October 1, 2018 and July 15, 2019, in a University Hospital in Katowice, Poland. Procedures of organ procurement (n = 11), reoperations (n = 24), procedures performed in local anesthesia or monitored anesthesia supervision (n = 33), procedures classified as immediate according to the National Confidential Enquiry into Patient Outcome and Death (NCEPOD) Classification of Intervention[9] (n = 14), and patients with proven cardiac valve defects (n = 14) were excluded from the study (Fig. 1). Demographic and medical data were recorded, including sex, age, weight, height, and comorbidities and their pharmacological treatment, according to the International Classification of Diseases (ICD-10) criteria.[10] Body mass index (BMI) and Charlson comorbidity index (CCI) were subsequently calculated. Type and duration of anesthesia, as well as type, duration and urgency of surgery were recorded. Perioperative risk was assessed based on an individual patient's risk, according to the American Society of Anesthesiologists (ASA) physical status (PS) classification,[11] and procedural risk, according to the European Society of Cardiology and European Society of Anaesthesiology recommendations.[12] Primary arterial hypertension was diagnosed based on medical records.

The SBP and DBP were measured on a nondominant arm using an automated noninvasive oscillometric BP monitoring device (Dräger Infinity Gamma XL; Dräger, Lübeck, Germany) with a cuff of appropriate size, depending on a patient's arm circumference, and recorded in 5-minute intervals during anesthesia, from the first preinduction measurement until the last measurement during recovery from anesthesia in the operating theater. The MAP values were automatically calculated. Pulse pressure was calculated as the difference between SBP and DBP. The need for norepinephrine (NE) use and its doses, together with intraoperative fluid balance, were analyzed.

Taking into consideration other studies on clinical consequences of abnormal PP, and the fact that PP revolves usually around values of 40 mm Hg, we distinguished following absolute PP thresholds: >50, >55, >60, >65, >70, >75, >80, >85, and >90 mm Hg.[5,13–15] Additionally, by analyzing

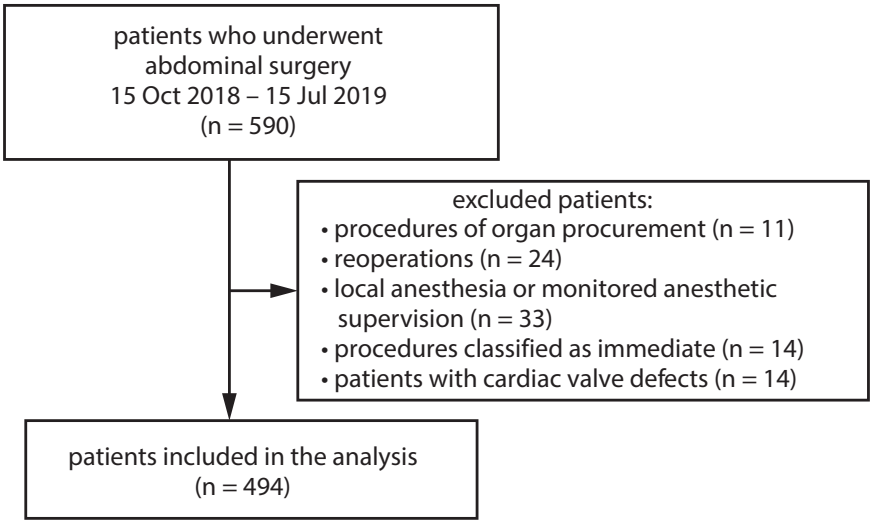


Fig. 1. Flow diagram for the patient selection process

the maximal PP during the procedure, the best cutoff point associated with the occurrence of AKI was estimated. We used maximal PP (presented as the median of all maximal PPs recorded among all the patients) and not an average or a median, due to a number of reasons. Firstly, the average value is much more confounded by extreme values of the distribution of numbers. Secondly, choosing maximal PP over average or median PP is better suited for finding a cutoff point for PP that is associated with postoperative AKI. In this study, we explored the role of high PP values; therefore, we naturally sought higher values and tried to find thresholds that would be easily identifiable by a clinician. In contrast, the average or the median value reflects rather a global trend in values and does not bring any specific information.

Moreover, we analyzed the occurrence of high systolic (defined as SBP > 160 mm Hg[16]), low diastolic (defined as DBP < 50 mm Hg[17]) and low mean arterial pressure (defined as MAP < 60 mm Hg[18]). We excluded pre-induction measurements in order to assess only those BP values that occurred during anesthesia.

In the postoperative period, the incidents of AKI were recorded and defined as a serum creatinine increase ≥0.3 mg/dL within 48 h or an increase in serum creatinine by ≥1.5 times baseline, which is known or presumed to have occurred within the prior 7 days.[19] This outcome was considered as the endpoint. In addition, incidents of AKI were classified as stages based on Kidney Disease Improving Global Outcomes (KDIGO) guidelines.[20]

STrengthening the Reporting of OBservational studies in Epidemiology (STROBE) statement was applied for appropriate reporting.[21]

Statistical analysis was performed using MedCalc statistical software v. 18.1 (MedCalc Software Ltd., Ostend, Belgium). Continuous variables were expressed as median and interquartile range (IQR). Qualitative variables were expressed as absolute values and/or percentages. Between-group differences for quantitative variables were assessed using the Mann–Whitney U test. Their distribution was verified with the Shapiro–Wilk test. The $\chi^2$ tests were applied for qualitative variables. The correlation was assessed using Spearman's rank correlation coefficient. The receiver operating characteristic (ROC) curve analysis was implemented to assess the relationship between AKI and maximal PP. In order to control the potential confounding factors, we used multivariable logistic regression with all variables that achieved p-value <0.1 in the univariable analysis. The Hosmer–Lemeshow test was performed to assess the goodness-of-fit of multivariable logistic regressions. If applicable, odds ratios (ORs) and area under the receiver operating characteristics (AUROC) with 95% confidence intervals (95% CIs) were calculated. All tests were two-tailed. A value of $p < 0.05$ was considered statistically significant.

## Results

A total number of patients included in the analysis was 494, out of which 239 (46%) were male. The median age of participants was 65 years (IQR 46–68). Older age, higher ASA-PS class and higher CCI were found to be significant preoperative risk factors for the occurrence of AKI. Detailed preoperative population characteristics are presented in Table 1, whereas intraoperative population characteristics are presented in Table 2. The primary outcome (AKI) was diagnosed in 32 (6.7%) patients. According to KDIGO criteria, 24 patients (75%) suffered from stage 1 AKI, 5 patients (15.6%) from stage 2 AKI and 3 patients (9.4%) from stage 3 AKI.[19] Pre-induction PP was not associated with the outcome (Table 1).

**Table 1.** Preoperative population characteristics

| Variable | AKI (–) (n = 462) | AKI (+) (n = 32) | p-value | df/test-value |
|---|---|---|---|---|
| Age [years] | 61 (44–68) | 67 (62–73) | 0.0002 | U-value = 5010 |
| Male (n) | 213 (46.1) | 17 (53.1) | 0.4738 | df = 1 |
| BMI [kg/m$^2$] | 25.6 (22.5–29.0) | 27.4 (22.6–30.7) | 0.2318 | U-value = 6426 |
| Arterial hypertension | 197 (42.6) | 26 (81.2) | <0.0001 | df = 1 |
| Chronic kidney disease (n) | 8 (1.7) | 5 (15.6) | <0.0001 | df = 1 |
| Pre-induction SBP [mm Hg] | 140 (125–155) | 142.5 (132.5–155) | 0.1985 | U-value = 6308 |
| Pre-induction MAP [mm Hg] | 101.7 (92–110) | 101.5 (95–113) | 0.5473 | U-value = 6297 |
| Pre-induction PP [mm Hg] | 56 (48–66) | 59 (50–75) | 0.2595 | U-value = 6439 |
| ASA-PS I/II | 279 (60.4) | 10 (31.2) | 0.0012 | df = 1 |
| ASA-PS III/IV/V | 183 (39.6) | 22 (68.7) | 0.0012 | df = 1 |
| CCI [pts] | 3 (1–5) | 5 (3–7) | 0.0001 | U-value = 4434 |
| Premedication | 278 (60.2) | 22 (62.5) | 0.7949 | df = 1 |

AKI – acute kidney injury; PP – pulse pressure; ASA-PS – American Society of Anesthesiologists physical class; BMI – body mass index; SBP – systolic blood pressure; MAP – mean arterial pressure; CCI – Charlson comorbidity index; df – degrees of freedom. Age, BMI, pre-induction SBP, pre-induction MAP, pre-induction PP, and CCI were analyzed using Mann–Whitney test, whereas sex, arterial hypertension, chronic kidney disease, ASA-PS, and premedication were tested with $\chi^2$ test.

**Table 2.** Intraoperative population characteristics

| Variable | AKI (–) (n = 462) | AKI (+) (n = 32) | p-value | df/test-value |
|---|---|---|---|---|
| General + epidural anesthesia (n) | 23 (6.5) | 9 (28.1) | <0.0001 | df = 1 |
| Procedure risk I (n)* | 43 (9.3) | 1 (3.1) | 0.2356 | df = 1 |
| Procedure risk II (n)* | 308 (66.7) | 17 (53.1) | 0.1188 | df = 1 |
| Procedure risk III (n)* | 111 (24.0) | 14 (43.7) | 0.0132 | df = 1 |
| Oncological procedure (n) | 216 (46.8) | 22 (68.7) | 0.0161 | df = 1 |
| Catecholamine use (n) | 194 (42) | 26 (81.2) | <0.0001 | df = 1 |
| Catecholamine dose [μg/kg/min] | 0.06 (0.042–0.091) | 0.073 (0.061–0.108) | 0.1166 | U-value = 1636 |
| Procedure duration [min] | 220.0 (120.0–330.0) | 392.5 (255.0–557.0) | <0.0001 | U-value = 3297 |
| Fluid dose [mL/kg/h] | 6.79 (5.16–8.80) | 6.64 (4.71–8.59) | 0.5337 | U-value = 6906 |
| Mean arterial pressure [mm Hg] | 83.33 (78.33–88.33) | 85.17 (78.33–89.67) | 0.5765 | U-value = 6956 |
| Minimal pulse pressure during anesthesia [mm Hg] | 30 (25–35) | 25 (20–32) | 0.0419 | U-value = 5816 |
| Median pulse pressure during anesthesia [mm Hg] | 45.0 (40–51.2) | 50 (45–60) | 0.0028 | U-value = 5058 |
| Maximal pulse pressure during anesthesia [mm Hg] | 65 (56–75) | 82.5 (66–93.5) | <0.0001 | U-value = 4018 |
| MAP < 60 mm Hg during anesthesia (n) | 106 (22.9) | 14 (43.7) | 0.0080 | df = 1 |
| SBP > 160 mm Hg during anesthesia (n) | 98 (21.2) | 10 (31.2) | 0.1844 | df = 1 |
| DBP < 50 mm Hg during anesthesia (n) | 133 (28.8) | 15 (46.9) | 0.0309 | df = 1 |

AKI – acute kidney injury; df – degrees of freedom; MAP – mean arterial pressure; SBP – systolic blood pressure; DBP – diastolic blood pressure; * according to European Society of Cardiology and European Society of Anaesthesiology recommendations.[11] General + epidural anesthesia, procedure risks, oncological procedures, catecholamine use, MAP < 60 mm Hg, SBP > 160 mm Hg, and DBP < 50 mm Hg were tested with $\chi^2$ test, whereas catecholamine dose, procedure duration, fluid dose, MAP, and minimal, maximal and median pulse pressure during anesthesia were tested using Mann–Whitney test.

**Table 3.** Correlation between pulse pressure and systolic blood pressure, diastolic blood pressure and mean arterial pressure

| Variable | Median pulse pressure AKI (–) (n = 462) | Median pulse pressure AKI (+) (n = 32) |
|---|---|---|
| Median systolic blood pressure | R = 0.649; p < 0.01 | R = 0.604; p < 0.01 |
| Median diastolic blood pressure | R = –0.214; p < 0.01 | R = –0.623; p < 0.01 |
| Pre-induction pulse pressure | R = 0.446; p < 0.01 | R = 0.447; p < 0.01 |

AKI – acute kidney injury. The values are Spearman's rank correlation coefficients.

In patients who developed AKI, PP more negatively correlated with DBP than in patients without AKI (Table 3).

Maximal PP registered over the course of the procedure was associated with the outcome (AUROC = 0.728; p < 0.001), with a cutoff point >84 mm Hg (Fig. 2).

In univariable analyses, all PP thresholds, except for >50 mm Hg, were statistically significant predictors of AKI (Fig. 3). In multivariable logistic regressions, PP values >80, >84, >85, and >90 mm Hg were included in the final statistical models. It was discovered that PP > 90 mm Hg predicted AKI with the highest accuracy, even after the adjustment for various confounding factors, including intraoperative hypertension (Table 4). Low DBP (<50 mm Hg) and high SBP (>160 mm Hg) were not significant in the multivariable models.

## Discussion

The main finding of our exploratory study is that increasing intraoperative values of PP were associated with the occurrence of postoperative AKI. This association persisted after adjusting for confounding factors (most importantly: high SBP and low DBP). We found a cutoff point of >84 mm Hg of maximal PP to be associated with AKI. In regards to the predetermined thresholds, PP above 80 mm Hg and onward was linked to AKI. Pulse pressure above 90 mm Hg, out of all PP thresholds applied, appeared to be the best predictor of postoperative AKI.

To our knowledge, this is the first study investigating the role of intraoperative PP in abdominal surgery in such a complex manner. It is known that increased ambulatory

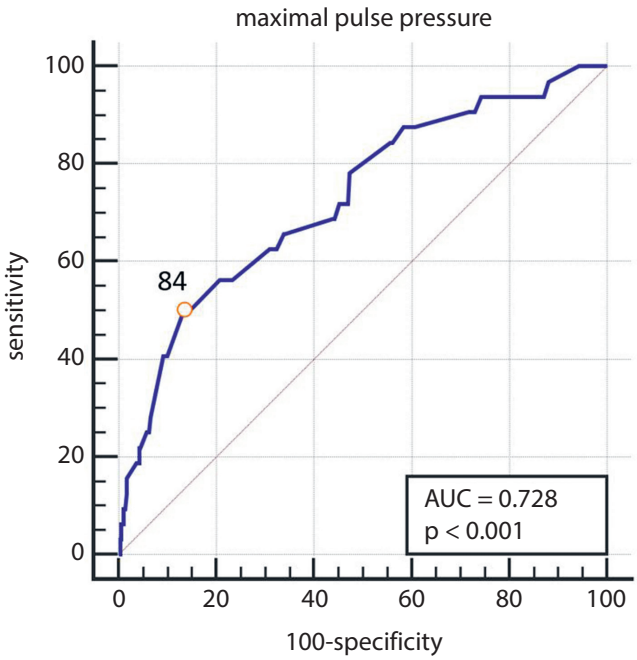


Fig. 2. The receiver operating characteristic (ROC) curve analysis of maximal pulse pressure (PP) values registered over the course of procedure

AUC – area under the curve.

PP is strongly associated with cardiovascular events, not only in the general population but also in cardiac surgery setting, irrespective of the presence of chronic arterial hypertension.[6,22,23] Pulse pressure stands as a proxy for general vascular health and reflects cardiovascular risk better than isolated measurements of either SBP or DBP.[24] Generally, a value of PP is determined by stroke volume, left ventricle contractility and arterial compliance. Interestingly, pre-induction PP values (a reflection of baseline PP) alone were not significantly related to the outcome. In studies by Abbott et al. and Mitrev et al., it was found that increasing values of ambulatory and pre-induction PP were significantly related to the increased occurrence of postoperative MI and AKI.[5,25] It must be remembered, however, that those studies were performed among cardiac surgery patients with pre-existing cardiac morbidities, and the effect of preoperative PP might have been more significant than in the noncardiac setting. The fact that in our cohort pre-induction PP was not associated with AKI, gave us more space to explore the impact of intraoperative values. Nevertheless, intraoperative PP positively correlated with the pre-induction values. The negative correlation between PP and DBP was especially interesting, since it was 2 times stronger in patients with the compromised outcome. Lowered DBP is known to decrease coronary perfusion and could be associated with the development of hypoperfusion-induced organ injury.[16,26,27] However, after taking into account low DBP (<50 mm Hg) in multivariate analyses, PP thresholds remained significant and low DBP was not included in the models.

We discovered that patients who experienced AKI exhibited higher values of PP, and the ORs varied, depending on the threshold applied. Contrary to our hypothesis, Ahuja et al., in a large cohort of 23,000 patients, found that PP below 35 mm Hg was linked to postoperative MI and AKI.[17] Indeed, in our cohort, the AKI group experienced lower minimal PP compared to the non-AKI group (median 25 mm Hg compared to 30 mm Hg). Low PP is thought to predict cardiovascular events in patients with impaired cardiac function: decreased contractility of left ventricle causes SBP to achieve lower values and negatively impact the value of PP. It must be remembered that Ahuja et al. explored only the lowest values of PP and called for further research regarding high intraoperative PP.[17]

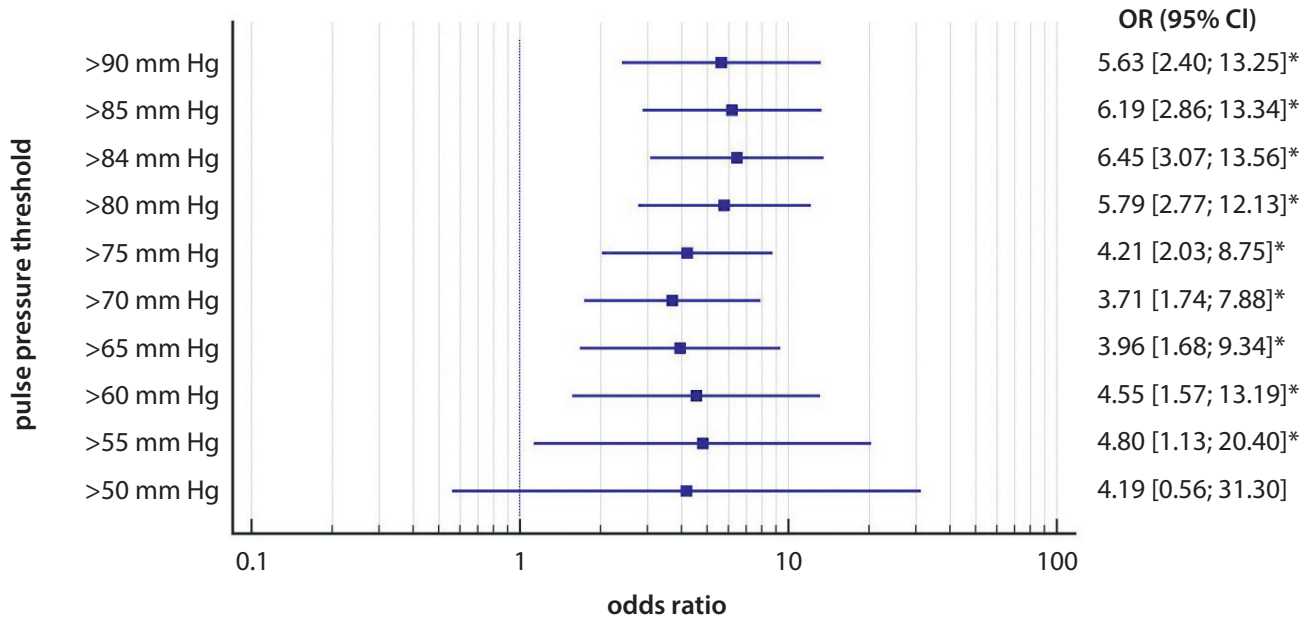


Fig. 3. Pulse pressure thresholds and their relationship with acute kidney injury. The box represents odds ratio (OR) whereas the whiskers represent confidence intervals (CIs). The asterisk represents statistically significant values

**Table 4.** Multivariate logistic regression models in predicting the occurrence of acute kidney injury (AKI)

| Variable* | Model | | | |
|---|---|---|---|---|
| | PP > 80 mm Hg (1/0) | PP > 84 mm Hg (1/0) | PP > 85 mm Hg (1/0) | PP > 90 mm Hg (1/0) |
| Pulse pressure | OR = 2.61<br>95% CI: [1.13; 6.05]<br>β = 0.96<br>p = 0.0245 | OR = 3.13<br>95% CI: [1.35–7.22]<br>β = 1.14<br>p = 0.0011 | OR = 3.17<br>95% CI: [1.33–7.54]<br>β = 1.15<br>p = 0.0090 | OR = 4.03<br>95% CI: [1.53–10.62]<br>β = 1.39<br>p = 0.0048 |
| Chronic arterial hypertension (1/0) | OR = 3.13<br>95% CI: [1.17–8.35]<br>β = 1.14<br>p = 0.0226 | OR = 3.07<br>95% CI: [1.29–7.06]<br>β = 1.12<br>p = 0.0079 | OR = 3.20<br>95% CI: [1.21–8.46]<br>β = 1.16<br>p = 0.0192 | OR = 4.20<br>95% CI: [1.56–11.35]<br>β = 1.43<br>p = 0.0046 |
| Procedure duration (per 1 min) | OR = 1.006<br>95% CI: [1.003–1.008]<br>β = 0.0062<br>p < 0.0001 | OR = 1.006<br>95% CI: [1.003–1.009]<br>β = 0.0063<br>p < 0.0001 | OR = 1.007<br>95% CI: [1.003–1.009]<br>β = 0.0066<br>p < 0.0001 | OR = 1.007<br>95% CI: [1.003–1.009]<br>β = 0.0066<br>p < 0.0001 |
| Chronic kidney disease (1/0) | OR = 6.72<br>95% CI: [1.71–26.45]<br>β = 1.90<br>p < 0.0001 | OR = 6.59<br>95% CI: [1.66–26.17]<br>β = 1.88<br>p < 0.0001 | OR = 5.93<br>95% CI: [1.47–23.84]<br>β = 1.78<br>p < 0.0001 | OR = 6.14<br>95% CI: [1.54–24.53]<br>β = 1.81<br>p < 0.0001 |
| Intraoperative hypotension (MAP < 60 mm Hg) (1/0) | not included | not included | not included | OR = 2.54<br>95% CI: [1.07–6.04]<br>β = 0.93<br>p = 0.0102 |
| AUROC | 0.861;<br>(0.828–0.891);<br>p < 0.0001 | 0.866;<br>(0.83–0.89);<br>p < 0.0001 | 0.862;<br>(0.83–0.89);<br>p < 0.0001 | 0.880;<br>(0.85–0.91);<br>p < 0.0001 |
| Hosmer–Lemeshow test | $\chi^2 = 3.49$;<br>p = 0.8995 | $\chi^2 = 7.71$;<br>p = 0.4621 | $\chi^2 = 4.68$;<br>p = 0.7887 | $\chi^2 = 3.87$;<br>p = 0.8768 |

PP – pulse pressure; MAP – mean arterial pressure; AUROC – area under the receiver operating characteristics; OR – odds ratio; 95% CI – 95% confidence interval; β – coefficient; p – p-value. * Variables that failed to be significant in the multivariable models were as follows: PP > 50 mm Hg, PP > 55 mm Hg, PP > 60 mm Hg, PP > 65 mm Hg, PP > 70 mm Hg, PP > 75 mm Hg, age, American Society of Anesthesiologists (ASA) III/IV/V, Charlson comorbidity index (CCI), adjunction of regional anesthesia, procedure risk (III), oncological procedure, catecholamine use, systolic blood pressure (SBP) >160 mm Hg, diastolic blood pressure (DBP) <50 mm Hg, SBP (per 1 mm Hg).

High PP could influence systemic circulation in numerous ways. First, kidneys have a high resting blood flow. With the increase of PP, perfusion of this organ becomes more pulsatile and it is thought to damage endothelium and smooth muscle and induce shear stress, which can cause plaque to rupture and form thrombosis.[28–30] Additionally, high PP can decrease flow-mediated vasodilation.[31] What is also worth mentioning is that increased PP causes aortic lumen to decrease, which results in ventricular-aortic decoupling, characterized by cardiac output that is too great to be accommodated by aortic lumen (leading to the impaired cardiac output with preserved systolic function).[5,32]

## Limitations

The abovementioned findings should be analyzed with caution due to possible confounding factors. First, the vast majority of patients had their BP measured with the oscillometric method. Due to an imperfect algorithmic method of distinguishing SBP and DBP, such patients have a higher risk of discrepancy between the registered and real BP. The discrepancy, especially in SBP, is more often expressed in patients with stiffer arteries and higher PPs.[33] In a study by Kayrak et al., oscillometric measurements led to the underestimation of PP in a group of patients with isolated systolic hypertension (but not in subjects with mixed hypertension).[34] Secondly, the true association between high intraoperative PP and AKI is, to a certain extent, determined by the preoperative PP values. Despite the fact that pre-induction PP was not significantly related to the outcome in our analysis, it is possible that intraoperative PP is only a reflection of the overall cardiovascular condition and does not impair organ perfusion in a short-term period (such as the duration of surgical procedure). Thirdly, pre-induction BP value was defined as baseline MAP. It is possible that such measurement does not represent the true baseline, as it could be influenced by stress or premedication. Additionally, the BP measurements were recorded in 5-minute intervals, and therefore, a risk of underrecognition of PP changes exists. Finally, our analysis was restricted to a limited population of abdominal patients, which reduces the generalizability of our results into all noncardiac surgery settings.

# Conclusions

High intraoperative PP may be associated with AKI in patients undergoing abdominal surgery. However, the effect of high PP should be confirmed in other noncardiac populations to prove the generalizability of our results.

## ORCID iDs

Zbigniew Putowski https://orcid.org/0000-0002-1740-4322
Łukasz Krzych https://orcid.org/0000-0002-5252-8398
Szymon Czajka https://orcid.org/0000-0001-8942-6371

## References

1. Salmasi V, Maheshwari K, Yang D, et al. Relationship between intraoperative hypotension, defined by either reduction from baseline or absolute thresholds, and acute kidney and myocardial injury after noncardiac surgery: A retrospective cohort analysis. *Anesthesiology*. 2017;126(1):47–65. doi:10.1097/ALN.0000000000001432
2. Bijker JB, Persoon S, Peelen LM, et al. Intraoperative hypotension and perioperative ischemic stroke after general surgery: A nested case-control study. *Anesthesiology*. 2012;116(3):658–664. doi:10.1097/ALN.0b013e3182472320
3. Wesselink EM, Kappen TH, Torn HM, Slooter AJC, van Klei WA. Intraoperative hypotension and the risk of postoperative adverse outcomes: A systematic review. *Br J Anaesth*. 2018;121(4):706–721. doi:10.1016/j.bja.2018.04.036
4. McEvoy MD, Gupta R, Koepke EJ, et al. Perioperative quality initiative consensus statement on postoperative blood pressure, risk and outcomes for elective surgery. *Br J Anaesth*. 2019;122:575–86. doi:10.1016/j.bja.2019.01.019
5. Abbott TEF, Pearse RM, Archbold RA, et al. Association between preoperative pulse pressure and perioperative myocardial injury: An international observational cohort study of patients undergoing non-cardiac surgery. *Br J Anaesth*. 2017;119(1):78–86. doi:10.1093/bja/aex165
6. Cheng S, Xanthakis V, Sullivan LM, Vasan RS. Blood pressure tracking over the adult life course patterns and correlates in the Framingham heart study. 2012;60(6):1393–1399. doi:10.1161/HYPERTENSIONAHA.112.201780
7. Sessler DI, Bloomstone JA, Aronson S, et al. Perioperative quality initiative consensus statement on intraoperative blood pressure, risk and outcomes for elective surgery. *Br J Anaesth*. 2019;122(5):563–574. doi:10.1016/j.bja.2019.01.013
8. Czajka S, Putowski Z, Krzych ŁJ. Intraoperative hypotension and its organ-related consequences in hypertensive subjects undergoing abdominal surgery: A cohort study. *Blood Press*. 2021;30(6):1–11. doi:10.1080/08037051.2021.1947777
9. National Confidential Enquiry Into Patient Outcome and Death. https://www.ncepod.org.uk/classification.html. Accessed January 11, 2021.
10. World Health Organization. ICD-10: International statistical classification of diseases and related health problems. 10th revision, 2004. Spanish version, 1st edition published by PAHO as: https://apps.who.int/iris/handle/10665/42980.
11. Doyle DJ, Goyal A, Bansal P, Garmon EH. *American Society of Anesthesiologists Classification (ASA Class)*. Treasure Island, USA: StatPearls Publishing; 2020. PMID:28722969.
12. Kristensen SD, Knuuti J, Saraste A, et al. 2014 ESC/ESA guidelines on non-cardiac surgery: Cardiovascular assessment and management. *Eur Heart J*. 2014;35(35):2383–2431. doi:10.1093/eurheartj/ehu282
13. Homan TD, Bordes S, Cichowski E. *Physiology, Pulse Pressure*. Treasure Island, USA: StatPearls Publishing; 2021. PMID:29494015.
14. Fontes ML, Aronson S, Mathew JP, et al. Pulse pressure and risk of adverse outcome in coronary bypass surgery. *Anesth Analg*. 2008;107(4):1122–1129. doi:10.1213/ane.0b013e31816ba404
15. Blacher J, Evans A, Arveiler D, et al. Residual cardiovascular risk in treated hypertension and hyperlipidaemia: The PRIME study. *J Hum Hypertens*. 2010;24(1):19–26. doi:10.1038/jhh.2009.34
16. Abbott TEF, Pearse RM, Archbold RA, et al. A prospective international multicentre cohort study of intraoperative heart rate and systolic blood pressure and myocardial injury after noncardiac surgery: Results of the VISION study. *Anesth Analg*. 2018;126(6):1936–1945. doi:10.1213/ANE.0000000000002560
17. Ahuja S, Mascha EJ, Yang D, et al. Associations of intraoperative radial arterial systolic, diastolic, mean, and pulse pressures with myocardial and acute kidney injury after noncardiac surgery: A retrospective cohort analysis. *Anesthesiology*. 2020;132(2):291–306. doi:10.1097/ALN.0000000000003048
18. Sun LY, Wijeysundera DN, Tait GA, Beattie WS. Association of intraoperative hypotension with acute kidney injury after elective noncardiac surgery. *Anesthesiology*. 2015;123(3):515–523. doi:10.1097/ALN.0000000000000765
19. Kellum JA, Lameire N; KDIGO AKI Guideline Work Group. Diagnosis, evaluation, and management of acute kidney injury: A KDIGO summary (Part 1). *Crit Care*. 2013;17(1):204. doi:10.1186/cc11454
20. Kellum JA, Lameire N, Aspelin P, et al. Kidney disease: Improving global outcomes (KDIGO) acute kidney injury work group. KDIGO clinical practice guideline for acute kidney injury. *Kidney Int Suppl*. 2012;2(1):1–138. https://kdigo.org/wp-content/uploads/2016/10/KDIGO-2012-AKI-Guideline-English.pdf
21. von Elm E, Altman DG, Egger M, et al.; STROBE Initiative. The Strengthening the Reporting of Observational Studies in Epidemiology (STROBE) Statement: Guidelines for reporting observational studies. *Int J Surg*. 2014;12(12):1495–1499. doi:10.1016/j.ijsu.2014.07.013
22. Mancusi C, Losi MA, Izzo R, et al. Higher pulse pressure and risk for cardiovascular events in patients with essential hypertension: The Campania Salute Network. *Eur J Prev Cardiol*. 2018;25(3):235–243. doi:10.1177/2047487317747498
23. Howell SJ, Sear YM, Yeates D, Goldacre M, Sear JW, Foex P. Hypertension, admission blood pressure and perioperative cardiovascular risk. *Anaesthesia*. 1996;51(11):1000–1004. doi:10.1111/j.1365-2044.1996.tb14990.x
24. Haider AW, Larson MG, Franklin SS, Levy D; Framingham Heart Study. Systolic blood pressure, diastolic blood pressure, and pulse pressure as predictors of risk for congestive heart failure in the Framingham Heart Study. *Ann Intern Med*. 2003;138(1):10–16. doi:10.7326/0003-4819-138-1-200301070-00006
25. Mitrev L, Speich KG, Ng S, et al. Elevated pulse pressure in anesthetized subjects before cardiopulmonary bypass is associated strongly with postoperative acute kidney injury stage. *J Cardiothorac Vasc Anesth*. 2019;33(6):1620–1626. doi:10.1053/j.jvca.2019.01.019
26. Assmann G, Cullen P, Evers T, Petzinna D, Schulte H. Importance of arterial pulse pressure as a predictor of coronary heart disease risk in PROCAM. *Eur Heart J*. 2005;26(20):2120–2126. doi:10.1093/eurheartj/ehi467
27. Sato R, Luthe SK, Nasu M. Blood pressure and acute kidney injury. *Crit Care*. 2017;21(1):28. doi:10.1186/s13054-017-1611-7
28. O'Rourke MF, Safar ME. Relationship between aortic stiffening and microvascular disease in brain and kidney: Cause and logic of therapy. *Hypertension*. 2005;46(1):200–204. doi:10.1161/01.HYP.0000168052.00426.65
29. Lyon RT, Runyon-Hass A, Davis HR, Glagov S, Zarins CK. Protection from atherosclerotic lesion formation by reduction of artery wall motion. *J Vasc Surg*. 1987;5(1):59–67. PMID:3795393.
30. Traub O, Berk BC. Laminar shear stress: Mechanisms by which endothelial cells transduce an atheroprotective force. *Arterioscler Thromb Vasc Biol*. 1998;18(5):677–685. doi:10.1161/01.atv.18.5.677
31. Ceravolo R, Maio R, Pujia A, et al. Pulse pressure and endothelial dysfunction in never-treated hypertensive patients. *J Am Coll Cardiol*. 2003;41(10):1753–1758. doi:10.1016/s0735-1097(03)00295-x
32. Mitchell GF, Lacourcière Y, Ouellet JP, et al. Determinants of elevated pulse pressure in middle-aged and older subjects with uncomplicated systolic hypertension: The role of proximal aortic diameter and the aortic pressure-flow relationship. *Circulation*. 2003;108(13):1592–1598. doi:10.1161/01.CIR.0000093435.04334.1F
33. Stergiou, G, Lourida P, Tzamouranis D, Baibas NM. Unreliable oscillometric blood pressure measurement: Prevalence, repeatability and characteristics of the phenomenon. *J Hum Hypertens*. 2009;23(12):794–800. doi:10.1038/jhh.2009.20
34. Kayrak M, Ulgen MS, Yazici M, et al. A comparison of blood pressure and pulse pressure values obtained by oscillometric and central measurements in hypertensive patients. *Blood Press*. 2010;19(2):98–103. doi:10.3109/08037050903516318

# Are in clinical practice measurements of concentrations and the calculation of mycophenolate mofetil pharmacokinetic parameters needed for optimizing therapy in patients with renal diseases or kidney transplantation?

Magdalena Hurkacz[1,A,C–F], Hanna Augustyniak-Bartosik[2,A,B,E,F], Joanna Pondel[2,A,B], Krystyna Głowacka[1,B], Magdalena Krajewska[2,A,E,F]

[1] Department of Clinical Pharmacology, Wroclaw Medical University, Poland
[2] Department and Clinic of Nephrology and Transplantation Medicine, Wroclaw Medical University, Poland

A – research concept and design; B – collection and/or assembly of data; C – data analysis and interpretation;
D – writing the article; E – critical revision of the article; F – final approval of the article

Advances in Clinical and Experimental Medicine, ISSN 1899–5276 (print), ISSN 2451–2680 (online) *Adv Clin Exp Med*. 2022;31(5):519–527

**Address for correspondence**
Magdalena Hurkacz
E-mail: magdalena.hurkacz@umed.wroc.pl

**Funding sources**
None declared

**Conflict of interest**
None declared

Received on June 30, 2021
Reviewed on November 16, 2021
Accepted on January 25, 2022

Published online on February 23, 2022

**Cite as**
Hurkacz M, Augustyniak-Bartosik H, Pondel J, Głowacka K, Krajewska M. Are in clinical practice measurements of concentrations and the calculation of mycophenolate mofetil pharmacokinetic parameters needed for optimizing therapy in patients with renal diseases or kidney transplantation? *Adv Clin Exp Med*. 2022;31(5):519–527. doi:10.17219/acem/146122

**DOI**
10.17219/acem/146122



## Abstract

**Background.** Modern pharmacotherapy requires an individual approach to patients, taking into account changes in pharmacokinetics in pathological states and between-subject variability. This procedure is of particular importance in immunosuppressive drug therapy. In recent years, the attention has been paid to the usefulness of calculating the kinetic parameters of the drug in the optimization of the immunosuppressive treatment.

**Objectives.** To assess the possibility of using mycophenolic acid (MPA) concentration measurements in order to optimize pharmacotherapy in patients with kidney diseases or after kidney transplantation.

**Materials and methods.** The study included 103 patients with renal diseases (group 1) and after kidney transplantation (group 2), treated at the Department of Nephrology and Transplantation Medicine at the University Clinical Hospital, Wrocław, Poland. The concentrations of MPA were measured using Enzyme Multiplied Immunoassay Technique (EMIT®) method. A total of 193 pharmacokinetic profiles were performed.

**Results.** The median of initial ($C_0$) concentration for all patients was 2.09 mg/L, in group 1 – 2.06 mg/L and in group 2 – 2.11 mg/L. The median concentration at 30 min after drug administration ($C_{30}$) was 11.72 mg/L in the whole study group, in group 1 – 11.52 mg/L and in group 2 – 12.72 mg/L. The median concentration at 120 min after the drug administration ($C_{120}$) was 4.73 mg/L, 4.45 mg/L and 5.57 mg/L, respectively. The median area under the curve from $C_0$ to $C_{120}$ $(AUC)_{0–120}$ was 15.77 h × mg/L for the entire study group, in group 1 – 15.46 h × mg/L and in group 2 – 16.78 h × mg/L. Using the Spearman's rank correlation coefficient for both groups, statistically significant ($p < 0.05$) correlations were found between 1) $C_0$ and $C_{30}$, 2) $C_0$ and $C_{120}$, 3) $C_0$ and $AUC_{0–120}$, 4) $C_0$ and the daily dose, 5) $C_{30}$ and $AUC_{0–120}$, and 6) $C_{30}$ and the morning dose. There were also statistically significant correlations between $C_{120}$ and $AUC_{0–120}$. Moreover, in group 1, a statistically significant correlation ($p < 0.05$) was found between 1) $C_{120}$ and the daily dose, 2) $C_{120}$ and albumin, 3) $C_{120}$ and $C_{30}$, and 4) $C_{120}$ and $AUC_{0–120}$. In the group 2, a statistically significant correlation was found between $C_{120}$ and the morning dose.

**Conclusions.** Measurements of MPA concentrations are useful for optimizing immunosuppression in patients requiring an individualized treatment.

**Key words:** transplantation, renal disease, mycophenolate mofetil, therapeutic drug monitoring, pharmacokinetics

# Background

Therapeutic drug monitoring (TDM), based on the measurement of the concentration of drugs in body fluids and adapting the dosing regimen to the therapeutic range, is currently a well-established procedure that significantly supports physicians in daily clinical practice. This procedure is of particular importance for drugs with high between-subject variability and low therapeutic index. The idea of TDM is based more on a close relationship between the concentration of a drug in the body (usually measured in the blood) and the clinical effect, than on the relationship between the dose and that effect. The therapeutic range of drugs is determined with the use of population-based retrospective investigations and pharmacokinetic modeling.[1] This method was introduced into clinical practice in the mid-1970s and is not only still widely used in clinical trials and in optimizing pharmacotherapy in hospitals, but it has also been improved with modern analytical techniques. In 1960, Buchthal et al. indicated a relationship between the plasma concentration of phenytoin in patients treated for epilepsy and the number of seizures in those patients.[2] It was one of the first publications pointing to the possibilities of optimizing the treatment using mathematical calculations. In the 1980s and 1990s, TDM was of interest for researchers, pharmacologists and medical practitioners. Currently, clinical medicine elucidates considerable benefits from these observations. However, it should be pointed out that, despite the development of numerous dosage regimens, there is still room for the improvement.

Meanwhile, the rapid development of transplantology and therapy of autoimmune diseases in recent years is strongly linked to the introduction of treatment regimens, based on the new generation of immunosuppressive drugs. The balance between the effectiveness of treatment and the frequency and severity of adverse reactions to drugs appears to be the issue in this area. In the late 20$^{th}$ century, expert communities consisting of physicians, pharmacologists and analytical chemists developed international pharmacotherapy guidelines aimed at patient care optimization.[3] The guidelines are periodically updated based on the results of meta-analyses, clinical observations and pharmacokinetic/pharmacodynamic (PK/PD) modeling. One of the groups of medicinal products for which various regimens were developed includes immunosuppressive drugs – calcineurin inhibitors (cyclosporine A (CSA), tacrolimus (TAC)), antiproliferative drugs (mycophenolate mofetil (MMF), mycophenolic acid sodium salt (EC-MPS), azathioprine (AZA)), mammalian target of rapamycin (mTOR) inhibitors (sirolimus (rapamycin), everolimus), and glucocortecosteroids (GCS). This is in line with evidence-based medicine (EBM) principles.

According to the report by the Scientific Registry of Transplant Recipients (SRTR), in 2018, 60% of transplant recipients followed a treatment regimen based on MMF+TAC+GCS, 30% of them followed a treatment regimen based on TAC+MMF, with the remaining transplant recipients following other treatment regimens. It can be said that MMF is one of the most commonly used immunosuppressive drugs in transplantation, but it is also an important element in the treatment of autoimmune diseases, which often lack registration for this drug despite its fairly widespread use.[4,5]

Compared to other medicinal products, MMF is related to lower rates of acute rejection of the transplanted organ, and reduced severity and a lower number of adverse reactions. Even though MMF was introduced over 20 years ago and initially, the doses recommended by the manufacturer were followed, clinical observations demonstrate the need for individualizing the dosage based on the concentration monitoring and PK/PD modeling, especially for organ transplant recipients.[6,7] The results of numerous studies indicate that the measurement of a single concentration (e.g., before the administration of the next steady-state drug dose) is not sufficient to predict properly the effectiveness of treatment.[5–8] Both previous observational works and the consensus recommendations point to the necessity of applying limited sampling strategies (LSSs) in order to calculate the area under the curve (AUC) in comparison to time curve, which increases predictive accuracy. Still, a uniform model is yet to be established.[8]

The generally accepted parameter that most closely reflects the pharmacokinetic processes of MMF in the body is $AUC_{0-12h}$, which is calculated based on steady-state concentrations.[9] However, it should be mentioned that the calculation of AUC should be based on many measurement timepoints, which is associated with high costs of the study. With this in mind, LSSs are more applicable to clinical practice.[9,10]

# Objectives

The study aimed to assess the possibility of using mycophenolic acid (MPA) pharmacokinetic parameters calculated on the basis of concentration measurements in the abbreviated sampling profile, to optimize pharmacotherapy in a group of patients with various renal diseases or after kidney transplantation.

# Materials and methods

## Patients and study design

Initially, 164 patients were included in the study. The inclusion criteria were: the use of pharmacotherapy according to the guidelines for MMF at a fixed dose for at least 1 month, a stable status of the underlying disease and patient's informed consent to participate in the study. Ultimately, 103 people were included in the study from the Department of Nephrology and Transplantation Medicine

Table 1. Characteristics of patients

| Parameter | Patients groups | | | | | |
|---|---|---|---|---|---|---|
| | whole study groups (n = 103) | | glomerulonephritis patients (group 1) (n = 64) | | kidney transplant recipients (group 2) (n = 39) | |
| Kinetic profiles | 193 | | 150 | | 43 | |
| Women | 48 | | 30 | | 18 | |
| Men | 55 | | 34 | | 21 | |
| Statistical parameters | mean (±SD) | CV [%] | mean (±SD) | CV [%] | mean (±SD) | CV [%] |
| Age [years] | 42.83 ±18.4 | 34.24 | 42.3 ±13.94 | 32.98 | 44.88 ±16.89 | 37.85 |
| BW [kg] | 72.94 ±14.7 | 25.27 | 73.3 ±17.33 | 23.66 | 71.6 ±32.69 | 31.94 |
| BMI [kg/m$^2$] | 25.9 ±5.8 | 22.42 | 25.95 ±5.32 | 20.50 | 25.6 ±8.09 | 31.94 |
| GFR [mL/min/1.73 m$^2$] | 61.82 ±27.88 | 45.10 | 65.08 ±29.11 | 44.73 | 50.59 ±19.58 | 38.72 |
| Duration of therapy [months] | 36.7 ±101.4 | 275.9 | 20.00 ±15.94 | 79.67 | 95.13 ±204.00 | 214.45 |
| Protein serum [g/L] | 6.02 ±0.83 | 13.75 | 9.91 ±0.81 | 13.83 | 6.49 ±0.70 | 50.82 |
| Albumin serum [g/L] | 3.99 ±2.91 | 73.05 | 3.98 ±3.23 | 81.20 | 4.04 ±0.45 | 11.04 |
| RBC [$10^{12}$/L] | 4.54 ±0.89 | 19.76 | 4.55 ±0.91 | 19.82 | 4.45 ±0.88 | 19.81 |
| HGB [g/dL] | 13.12 ±2.40 | 18.31 | 13.18 ±2.45 | 18.59 | 12.88 ±2.24 | 17.40 |
| WBC [$10^9$/L] | 6.65 ±6.26 | 94.15 | 6.54 ±6.89 | 105.36 | 7.08 ±2.29 | 32.33 |
| PLT [$10^9$/L] | 247.36 ±86.85 | 35.11 | 268.29 ±84.85 | 31.63 | 206.21 ±79.97 | 38.78 |
| CRP [mg/L] | 6.61 ±14.43 | 218.22 | 7.63 ±13.04 | 170.88 | 7.13 ±18.85 | 264.54 |
| MMF daily dose [mg] | 1217.84 ±453.67 | 37.25 | 1222 ±423.14 | 34.60 | 1200 ±550.8 | 45.86 |
| MMF morning dose [mg] | 612.26 ±231.13 | 37.75 | 612.24 ±219.32 | 35.83 | 612.32 ±270.54 | 44.18 |

BW – body weight; BMI – body mass index; GFR – glomerular filtration rate; RBC – red blood cells; HGB – hemoglobin; WBC – white blood cells; PLT – platelets; CRP – C-reactive protein; CV – coefficient of variation; MMF – mycophenolate mofetil; SD – standard deviation.

at the University Clinical Hospital, Wrocław, Poland. A total of 193 separate pharmacokinetic profiles of the drug were determined. Patients were divided into 2 groups: group 1 consisted of individuals with chronic renal diseases requiring immunosuppressive treatment (n = 64), while group 2 included individuals after a renal transplant (n = 39). In group 1, the patients had PK profiles performed during the follow-up visit at the nephrology clinic (42 patients had 2–8 PK profiles performed at intervals of at least several weeks, most often after changing MMF dosage or for clinical monitoring; only 22 patients had PK parameters determined once), while in the group of people after kidney transplantation, only 4 patients had PK tests performed several times (2–3) and 35 patients had PK profiles performed once. Material for pharmacokinetic and biochemical analyses was collected between October 2013 and December 2017. The approval of the Bioethics Committee of the Medical University of Wroclaw (No. KB/174/2013 and KB-317/2015) was obtained and each patient signed informed consent to participate in the study. All procedures were followed in accordance with the ethical standards of the responsible committee on human experimentation and with the Helsinki Declaration of 1975, as revised in 2008.

The characteristics of the study group are shown in Table 1.

In addition to the underlying disease, patients also suffered from other medical conditions. The following comorbidities were diagnosed in the patients included in the study: hypertension was observed in 57.7% of patients, diabetes mellitus – in 11.8%, thyroid dysfunction – in 91%, and frequent urinary tract infections – in 94%. In addition, the disorders of the gastrointestinal tract were observed.

## Treatment

The patients in the study group were receiving immunosuppressive treatment for the underlying diseases, based on MMF and/or GCS and calcineurin inhibitors. To prevent the adverse effect of the interaction between MMF and CSA, consisting in reducing the bioavailability of MMF, patients treated with CSA were administered a higher dose of MMF, in accordance with current treatment protocols for transplant patients. Treatment regimens applied in the groups are presented in Table 2.

In addition, the patients were receiving medication specific to the treatment of comorbidities; on average, a single patient received 6 different preparations, including MMF.

The mean morning dose of MMF was 612.26 ±231.13 mg (median: 500 mg). The mean daily dose was 1217 ±453.67 mg/day (median: 1000 mg). There was no statistically significant difference in MMF dosage between groups 1 and 2 (p = 0.98; Mann–Whitney U test). The duration of MMF immunosuppressive therapy averaged 36.74 ±101.4 months (median:

Table 2. Immunosuppressive treatment in the entire study group and by subgroups

| Immunosuppressive treatment regimens | Whole study group (n = 103) [%] | Percentage of patients in group 1 (n = 64) [%] | Percentage of patients in group 2 (n = 39) [%] |
|---|---|---|---|
| MMF+GCS | 40.8 | 65.6 | 0 |
| MMF in monotherapy | 11.6 | 18.7 | 0 |
| MMF+GCS+TAC | 29.1 | 3.1 | 71.8 |
| MMF+GCS+CSA | 12.6 | 9.4 | 17.9 |
| MMF+CSA | 2.9 | 3.1 | 2.6 |
| MMF+TAC | 1.9 | 0 | 5.1 |
| MMF+SIR | 1 | 0 | 2.6 |

MMF – mykophenolate mofetil; GCS – glucocorticosteroids; TAC – tacrolimus; CSA – cyclosporine A; SIR – sirolimus.

20 months) in the entire study group, 20.01 ±15.94 months in the renal disease group (median: 18.7 months), and 95 ±204 months in the kidney transplant group (median: 60 months). The duration of therapy was statistically significantly longer in the kidney transplant group compared to the patients with renal disease ($p < 0.001$; Mann–Whitney U test).

## Analytical methods

Concentrations of MPA, an active form of MMF, were measured in the Laboratory of Therapeutic Drug Monitoring of the Department of Clinical Pharmacology, Wroclaw Medical University, Poland, using the commercial immunoassay method – Enzyme Multiplied Immunoassay Technique (EMIT®) on a Siemens Viva-E Chemistry Analyzer (Siemens Healthcare Diagnostics Inc., Newark, USA). The Emit® 2000 Mycophenolic Acid Assay (Siemens Healthcare Diagnostics Inc.) was used. The analytical range of the test was 0.1–15 µg/mL. The material was plasma collected in accordance with a predetermined protocol. The samples for the study were collected just before the next morning dose of the drug ($C_0$), 30 min after the drug administration ($C_{30}$) and 2 h after the drug administration ($C_{120}$). The sampling profile was established based on the literature describing sampling methods in relation to MMF[11] and after previous own studies, consisting in controlling the selection of timepoints in 5 randomly selected patients who had more measurements at additional timepoints ($C_{15}$, $C_{45}$ and $C_{90}$). In addition, 3 selected measuring points were used for the analysis of the practical, economic and ethical reasons. The patients were usually treated in a hospital outpatient clinic and the long waiting time for collecting the material for the study would be burdensome for them. Other biochemical tests and anthropometric measurements were performed during routine monitoring of therapy in the Transplantation and Nephrology Outpatient Clinic and in the Diagnostic Laboratory of the Mikulicz-Radecki University Clinical Hospital, Wrocław, Poland. Pharmacokinetic calculations were performed using Kinetica v. 5.0 (Thermo Fisher Scientific, Waltham, USA) and Phoenix computer software (Phoenix Software International, El Segundo, USA); statistical calculations were performed using STATISTICA v. 13.1 software (StatSoft Inc., Tulsa, USA).

Pharmacokinetics of MPA in the study subjects was characterized by determining the parameters of $C_0$, $C_{30}$, $C_{120}$, and area under the curve (AUC) to 120 min after the dose ($AUC_{0-120}$).

## Statistical analyses

Statistical tests consisted of the calculation of basic statistics. The mean, median, minimum and maximum values, standard deviation (SD) and coefficient of variation (CV), 1st quartile (Q1), 3rd quartile (Q3), and interquartile range (IQR) were evaluated. In order to check the distribution of the examined variables and to test their compliance with the normal distribution, basic descriptive statistics were calculated, and Shapiro–Wilk distribution normality tests were performed. In patients who had more than one MPA concentration profile, the intervals between consecutive tests were at least 4 months; therefore, statistical calculations for unrelated samples were used for these patients. Correlations between quantitative variables were analyzed using the Spearman's rank correlation coefficient due to the nonparametric nature of the variables, with a value of $p < 0.05$ considered significant.

# Results

The mean value of the initial ($C_0$) concentration for the entire study group was 2.79 mg/L (median: 2.09), in group 1 it was 2.77 mg/L (median: 2.06) and in group 2 it was 2.90 mg/L (median: 2.11). The concentration at 30 min after the administration of the drug ($C_{30}$) averaged 15.23 mg/L (median: 11.72), in group 1 it was 14.89 mg/L (median: 11.52) and in group 2 it was 16.41 mg/L (median: 12.72). The mean $C_{120}$ was 5.66 mg/L (median: 4.73) in the whole group, while in group 1 and group 2 it was 5.19 mg/L (median: 4.45) and 7.38 mg/L (median: 5.57), respectively. The mean $AUC_{0-120}$ was 18.62 h × mg/L (median: 15.77) for the entire study group, 18.34 h × mg/L

**Table 3.** Detailed values of pharmacokinetic parameters and statistical analyses in the studied group of patients, divided into groups of patients with renal diseases and kidney transplant recipients

| Parameter | Patients/profiles | | | | | | | | | | | |
|---|---|---|---|---|---|---|---|---|---|---|---|---|
| | whole study group (n = 103/193) | | | | glomerulonephritis patients (group 1) (n = 64/150) | | | | kidney transplant recipients (group 2) (n = 39/43) | | | |
| | median | Q1 | Q3 | IQR | median | Q1 | Q3 | IQR | median | Q1 | Q3 | IQR |
| $C_0$ [mg/L] | 2.09 | 1.3 | 3.5 | 2.5 | 2.06 | 1.3 | 3.7 | 2.4 | 2.11 | 1.4 | 3.8 | 2.4 |
| $C_{30}$ [mg/L] | 11.72 | 6.7 | 20.5 | 13.6 | 11.52 | 7.0 | 21.0 | 13.9 | 12.72 | 4.5 | 20.3 | 15.8 |
| $C_{120}$ [mg/L] | 4.73 | 2.8 | 7.5 | 4.3 | 4.45 | 2.7 | 6.7 | 4.0 | 5.57 | 4.2 | 9.2 | 5.0 |
| $AUC_{0–120}$ [mg × h/L] | 15.77 | 10.1 | 26.1 | 15.4 | 15.46 | 10.1 | 25.4 | 15.0 | 16.78 | 10.2 | 29.4 | 19.2 |

Q1 – 1st quartile; Q3 – 3rd quartile; IQR – interquartile range; AUC – area under the curve.

(median: 15.46) and 19.63 h × mg/L (median: 16.78) for group 1 and group 2, respectively.

The comparison between pharmacokinetic parameters calculated in the groups of patients treated with combined therapy of MMF with CSA and those treated with MMF without CSA showed no significant difference between these groups (Mann–Whitney U test; $p > 0.05$). Detailed values of pharmacokinetic parameters and statistical analyses are presented in Table 3.

The MPA concentrations measured at designated timepoints observed in groups 1 and 2 are shown in Fig. 1.

The statistical analysis of correlations between individual variables of pharmacokinetic parameters and in relation to variables characterizing a patient's clinical condition was then performed.

All of the correlations below were tested using the Spearman's rank correlation coefficient.

## Patients with renal disease – group 1

In group 1, there was no statistically significant correlation ($p > 0.05$) between morning dose and $C_0$ ($r = 0.129$; $p < 0.2$), and between morning dose and $C_{120}$ ($r = 0.08$; $p < 0.4$). There was also no statistically significant correlation between daily dose and $C_{30}$ ($r = 0.14$; $p < 0.09$). However, a weak positive correlation was found between morning dose values and $C_{30}$ ($r = 0$; $p < 0.013$) and $AUC_{0–120}$ ($r = 0.2204$; $p < 0.008$), and between daily dose values and $C_0$ ($r = 0.1853$; $p < 0.026$) and $C_{120}$ ($r = 0.1951$; $p < 0.02$). There were statistically significant positive correlations of moderate strength between $C_0$ and $C_{30}$ ($r = 0.3692$; $p < 0.001$); $C_0$ and $C_{120}$ ($r = 0.5308$; $p < 0.001$); $C_{30}$ and $C_{120}$ ($r = 0.3066$; $p < 0.001$), and strong positive correlations between concentrations at each measurement point and $AUC_{0–120}$ ($r = 0.4985$; $p < 0.001$; $r = 0.8997$; $p < 0.001$; and $r = 0.5709$; $p < 0.001$, respectively). There was a weak but significant correlation between albumin levels and $C_{30}$ ($r = 0.2195$; $p < 0.011$), as well as between albumin and $AUC_{0–120}$ ($r = 0.1937$; $p < 0.024$). In contrast, no correlation was found between the aforementioned parameters and total protein levels ($p > 0.05$). Weak but statistically significant negative correlations of glomerular filtration rate (GFR) with $C_0$ ($r = –0.3851$; $p < 0.001$) and $C_{120}$ ($r = –0.4256$; $p < 0.001$) were found.

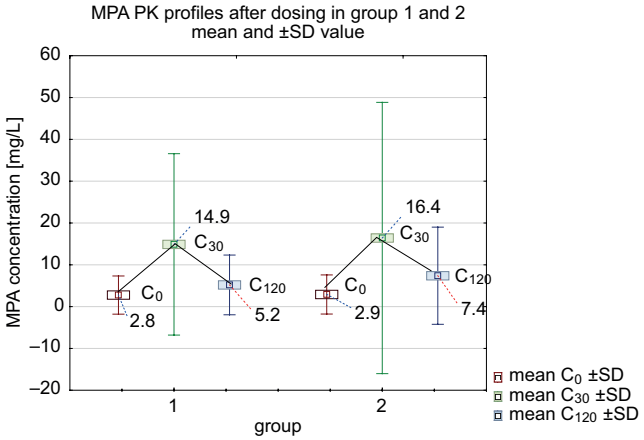


**Fig. 1.** Plasma concentrations of mycophenolic acid (MPA, mg/L) measured at designated timepoints observed in the entire study population (mean ± standard deviation (SD))

PK – pharmacokinetic.

## Kidney transplant recipients – group 2

Similarly, group 2 showed no statistically significant correlation ($p > 0.05$; Spearman's rank correlation coefficient) between the morning dose and $C_0$ ($r = 0.2$; $p < 0.054$). In contrast, it was found that there is a statistically significant moderately strong positive correlation of morning dose values with $C_{30}$ ($r = 0.5044$; $p < 0.001$), $C_{120}$ ($r = 0.4318$; $p < 0.005$) and $AUC_{0–120}$ ($r = 0.6065$; $p < 0.001$), and of the daily dose values with $C_0$ ($r = 0.25$; $p < 0.02$), $C_{30}$ ($r = 0.5128$; $p < 0.001$), $C_{120}$ ($r = 0.4721$; $p < 0.002$), and $AUC_{0–120}$ ($r = 0.6418$; $p < 0.001$). There were statistically significant positive correlations of moderate strength between $C_0$ and $C_{30}$ ($r = 0.3879$; $p < 0.012$), as well as between $C_0$ and $C_{120}$ ($r = 0.4516$; $p < 0.003$), and $C_0$ and albumin level ($r = 0.3686$; $p < 0.038$).). There was a strong positive correlation of $C_0$, $C_{30}$ and $C_{120}$ with $AUC_{0–120}$ ($r = 0.5319$; $p < 0.001$, $r = 0.9017$; $p < 0.001$, and $r = 0.4938$; $p < 0.001$, respectively). There was no statistically significant correlation between albumin and total protein levels or GFR and any of the calculated pharmacokinetic parameters ($p > 0.05$; Spearman's rank correlation coefficient).

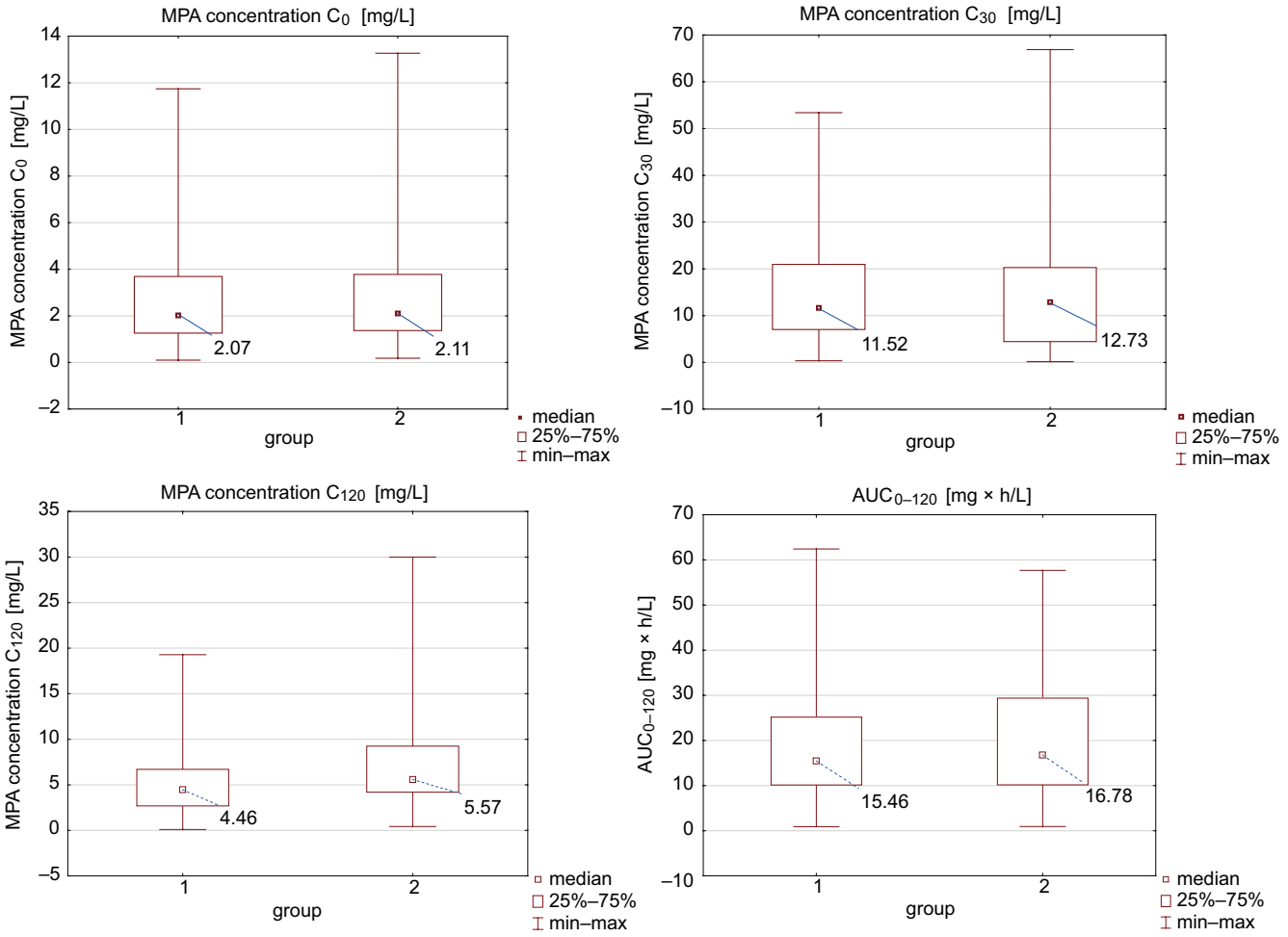


Fig. 2. Selected pharmacokinetic parameters of mycophenolic acid (MPA) in groups 1 and 2; box-whisker plots

AUC – area under the curve.

## Efficacy and tolerability

The efficacy and safety of MMF pharmacotherapy were assessed based on the biochemical parameters and clinical symptoms. In the group of kidney transplant patients, the criterion of effectiveness is the lack of graft rejection. In this group (group 2), none of the patients had acute or chronic rejection. In the group of people with various renal diseases (group 1), the criteria of effectiveness are disease remission or no clinical deterioration, the assessment based mainly on estimated GFR (eGFR), serum albumin level and the presence or absence of proteinuria.

In group 2, no signs of rejection were observed, regardless of MPA concentration and $AUC_{0-120}$. In group 1, no significant signs of clinical deterioration were found, although there was a relationship between $AUC_{0-120}$ and the level of albumin and total protein, which may indicate a significant influence of the drug on the course of the disease.

The pharmacological toxicity of MMF includes mainly the risk of opportunistic infections (bacterial, fungal, viral), neoplasm (lymphoma), bone marrow aplasia and digestive disorders, that are the clinical criteria of the safety of immunotherapy.

The selected pharmacokinetic parameters of MPA in groups 1 and 2 are shown in Fig. 2.

## Discussion

The calculation of pharmacokinetic parameters of many drug substances is an important part of modern pharmacotherapy. A recent interest in pharmacometrics has contributed to an improved efficacy and safety of treatment. There are heated discussions on the possibility of developing an ideal pharmacokinetic and/or pharmacodynamic model for the initial phase of chronic treatment that would increase a patient's chances of optimal therapy. The influence of clinical factors other than those directly related to the drug, such as a patient's age, biomarker values, dietary habits, and genetic background, are also noteworthy.[8,12] The use of immunosuppressive drugs is a good example of how PK/PD modeling can be used to define the treatment profile. Unfortunately, the high

Table 4. Results of the Shapiro–Wilk test for the assessment of the normality of the distribution of selected variables

| Parameter | Patients groups | | | | | |
|---|---|---|---|---|---|---|
| | whole study group | | glomerulonephritis patients (group 1) | | kidney transplant recipients (group 2) | |
| | W-value | p-value | W-value | p-value | W-value | p-value |
| $C_0$ [mg/L] | 0.8350 | <0.0001 | 0.8445 | <0.0001 | 0.8013 | <0.0001 |
| $C_{30}$ [mg/L] | 0.8547 | <0.0001 | 0.8999 | <0.0001 | 0.8123 | <0.0001 |
| $C_{120}$ [mg/L] | 0.8468 | <0.0001 | 0.9043 | <0.0001 | 0.8455 | <0.0001 |
| $AUC_{0–120}$ [mg × h/L] | 0.9232 | <0.0001 | 0.8947 | <0.0001 | 0.9389 | <0.001 |
| GRF | 0.9454 | <0.0001 | 0.9455 | <0.0001 | 0.9653 | 0.021 |
| Morning dose | 0.8335 | <0.0001 | 0.7551 | <0.0001 | 0.8758 | <0.0001 |
| Daily dose | 0.9171 | <0.0001 | 0.9009 | <0.0001 | 0.8947 | <0.0001 |
| Duration of therapy | 0.9168 | <0.0001 | 0.9168 | <0.0001 | 0.3811 | <0.0001 |

AUC – area under the curve; GFR – glomerular filtration rate.

interindividual variability and the dynamic changes in the health status of patients mean that there is still no clear consensus on the management of immunotherapy, especially in patients after vascular organ transplantation. The PK/PD modeling after kidney transplantation and in immune-mediated kidney diseases is a challenge for modern pharmacokinetics. The TDM is currently the gold standard in immunosuppression, but it does have some limitations due to the poor availability of analytical methods, the need for multiple sampling of the patient, the cost of the assay, and the insufficient knowledge of medical staff on interpreting the obtained results.

The present study measured MPA concentrations at 3 timepoints after MMF dosing, and calculated selected pharmacokinetic parameters of this drug in the group of subjects with renal disease and after kidney transplantation. The reported data showed that there was no statistically significant relationship between baseline concentration ($C_0$) and the morning dose, but there were statistically significant correlations between this concentration and the daily dose of MMF. These observations indicate that there are many individual factors that affect the absorption and distribution of the drug in the body, and that the use of the TDM method is one of the options for optimizing treatment.

In April 2021, the latest consensus report on MMF therapy from the International Association of Therapeutic Drug Monitoring and Clinical Toxicology was published.[7] According to this document, it is advisable to monitor MMF therapy due to the nonlinearity of the pharmacokinetics of the drug, as the drug is highly bound to plasma proteins, mainly albumin (97–99%).[13] The mean elimination half-life of MPA is 8–16 h; it is excreted through active tubular excretion in the form of the metabolite MPA glucuronide (MPAG) in the urine. The binding of MPA to albumin is reduced in diseases with significantly impaired renal function.[14]

The present observation showed a weak but significant correlation between albumin level and $C_{30}$, and also between albumin level and $AUC_{0–120}$ in the renal disease group, but no such correlation was found in kidney transplant patients. Weak but statistically significant negative correlations of GFR with $C_0$ and $C_{120}$ were found. However, both albumin levels and GFRs in both study groups showed no signs of severe renal failure, and there was a considerable interindividual variability in the obtained results.

In both observed groups, a statistically significant correlation of $AUC_{0–120}$ with the morning and daily doses was demonstrated, which indicates the usefulness of calculations of this parameter for optimal immunotherapy, especially in patients with multiple comorbidities, even despite the shortened sampling time.

According to various observations with MPA concentration measurements, the concentration value at single timepoints is not a reliable predictor. It is recommended to calculate the AUC and adjust dosing regimens based on this parameter.[8] It seems that the main reason for the necessity of the individualized therapy is the incidence of adverse effects. On the other hand, dose mismatch may cause symptoms of chronic graft rejection.[15,16]

The recommended range of AUC values, most commonly determined between 0 h and 12 h after drug administration ($AUC_{0–12h}$) is 30–45 mg × h/L in patients with autoimmune diseases and 43.98–50.5 mg × h/L in kidney transplant patients.[17–19]

There is a rapid absorption phase for MMF and, after 0.5–1 h, its maximum concentration is observed in the blood. Several publications have evaluated the usefulness of the LSS method for estimating AUC or establishing a dosing regimen. It was shown that it is possible to estimate drug concentrations based on multiple linear regression; however, the accuracy of this method depends on the number of timepoints. For MMF, the LSS based on 2 or 3 timepoints was sufficient for an acceptable predictive value; however, for EC-MPS, a higher number of measurements (4–8 timepoints) was required, and also the last measurement, performed 4–9 h after drug administration, was necessary. This may be explained by a higher interindividual variability, depending on hepatic circulation and a time-varying stage of absorption.[20–22]

In the present study, all patients received MMF, which ensured the homogeneity of assay results and total drug exposure calculations. In most publications, 3 timepoints for concentration measurements were usually used, namely 20 min, 1 h and 3 h after the drug administration. In one of the cited studies, the last timepoint was 2 h after the drug administration.[23,24]

This confirms the advisability of using in this study a material collection limited to 2 h. According to the consensus, it would be more accurate to use Bayesian estimation, although this may be difficult in clinical practice, due to the need for appropriate computational tools and knowledge in this area.

In the present study, MPA concentration and PK parameters were measured at 3 timepoints limited to 2 h. The results of the calculations presented in this study show significant correlations of $AUC_{0-120}$ with $C_{30}$ and $C_{120}$, which is consistent with the calculations of other authors.[25–28] Moreover, statistically significant relationships between the concentration values measured at individual timepoints ($C_0$, $C_{120}$) and $AUC_{0-120}$ were also demonstrated in both groups of patients and of $C_0$, $C_{30}$ and $C_{120}$ with $AUC_{0-120}$ in group 1, which indicates the possibility of using these parameters for pharmacokinetic and drug dosing calculations. In line with the recommendations of the previously cited consensus, it is possible to calculate basic PK parameters for the correct prediction of drug exposure in different groups of patients, but this requires validation and determination of other parameters not included in this study, such as biomarkers. The role of pharmacogenetic studies of MPA metabolism in assessing the efficacy and safety of MPA immunosuppression is also emphasized.

Based on the measurements of MPA concentrations and the authors' observations, it can be concluded that the use of the TDM procedure is indicated to optimize the immunosuppressive treatment of MMF and reduce the severity of complications. Determining the best sampling profile and PK calculations requires further studies on a larger group of patients, taking into account genetic conditions or the use of a mathematical pharmacokinetic model, which would reduce the need for multiple samples for testing and the cost of measurements. Currently, based on the presented results and the literature, it can be concluded that the best predictive parameter is multiple blood sampling at short intervals and the calculation of AUC. The $AUC_{0-12h}$ is often proposed in the literature, but it is difficult to carry out in an outpatient setting, mainly due to the long time of sample collection and the high cost. A biochemical parameter that is important in the interpretation of pharmacokinetic results is the albumin level, which should be analyzed in subsequent studies with respect to the clinical observation of drug effects, e.g., by analyzing a recognized quality of life scale, immunosuppressive effects and incidence of adverse effects.

## Limitations

One limitation of the present study was the inability to compare the pharmacokinetic parameters used in this project with the pharmacokinetic profiles for 12-hour follow-up in a larger group of patients, in order to confirm the obtained results.

# Conclusions

The measurements of MPA concentrations and the calculation of its pharmacokinetic parameters are useful in optimizing immunosuppression in groups of patients, requiring an individualized treatment due to individual differences and multidrug therapy, which is often the cause of drug interactions.


### ORCID iDs

Magdalena Elżbieta Hurkacz https://orcid.org/0000-0003-0846-3168
Hanna Augustyniak-Bartosik https://orcid.org/0000-0003-3969-396X
Joanna Pondel https://orcid.org/0000-0001-7055-9940
Krystyna Głowacka https://orcid.org/0000-0002-9748-2813
Magdalena Krajewska https://orcid.org/0000-0002-2632-2409


### References


1. Kang JS, Lee MH. Overview of therapeutic drug monitoring. *Korean J Int Med*. 2009;24(1):1–10. doi:10.3904/kjim.2009.24.1.1
2. Buchthal F, Svensmark O, Schiller PJ. Clinical and electroencephalographic correlations with serum levels of diphenylhydantoin. *Arch Neurol*. 1960;2(6):624–630. doi:10.1001/archneur.1960.03840120030004
3. Le Meur Y, Borrows R, Pescovitz MD, et al. Therapeutic drug monitoring of mycophenolates in kidney transplantation: Report of The Transplantation Society consensus meeting. *Transplant Rev* (Orlando). 2011; 25:58–64. doi:10.1016/j.trre.2011.01.002
4. Hart A, Smith JM, Skeans MA, et al. OPTN/SRTR 2018 annual data report: Kidney. *Am J Transpl*. 2020;20(Suppl s1):20–130. doi:10.1111/ajt.15672
5. Bolanos-Meade J, Reshef R, Fraser R, et al. Three prophylaxis regimens (tacrolimus, mycophenolate mofetil, and cyclophosphamide; tacrolimus, methotrexate, and bortezomib; or tacrolimus, methotrexate, and maraviroc) versus tacrolimus and methotrexate for prevention of graft-versus-host disease with haemopoietic cell transplantation with reduced intensity conditioning: A randomised phase 2 trial with a non-randomised contemporaneous control group (BMT CTN 1203). *Lancet Haematol*. 2019;6(3):e132–e143. doi:10.1016/S2352-3026(18)30221-7
6. van Gelder T. Therapeutic drug monitoring for mycophenolic acid is value for (little) money. *Clin Pharmacol Ther*. 2011;90(2):203–204. doi:10.1038/clpt.2011.96
7. van Gelder T, Berden JH, Berger SP. To TDM or not to TDM in lupus nephritis patients treated with MMF? *Nephrol Dial Transpl*. 2015;30(4): 560–564. doi:10.1093/ndt/gfu184
8. Bergan S, Brunet M, Hesselink DA, et al. Personalized therapy for mycophenolate: Consensus report by the international association of therapeutic drug monitoring and clinical toxicology. *Ther Drug Monit*. 2021;43(2):150–200. doi:10.1097/FTD.0000000000000871
9. Tett S, Saint-Marcoux F, Staatz C, et al. Mycophenolate, clinical pharmacokinetics, formulations, and methods for assessing drug exposure. *Transplant Rev (Orlando)*. 2011;25(2):47–57. doi:10.1016/j.trre.2010.06.001
10. Saint-Marcoux F, Vandierdonck S, Premaud A, Debord J, Rousseau A, Marquet P. Large scale analysis of routine dose adjustments of mycophenolate mofetil based on global exposure in renal transplant patients. *Ther Drug Monit*. 2011;33(3):285–294. doi:10.1097/FTD.0b013e31821633a6

11. Filler G, Mai J. Limited sampling strategy for mycophenolic acid area under the curve. *Ther Drug Monit*. 2000;22(2):169–173. doi:10.1097/00007691-200004000-00005
12. Takuathung MN, Sakuludomkan W, Koonrungsesomboon N. The impact of genetic polymorphisms on the pharmacokinetics and pharmacodynamics of mycophenolic acid: Systematic review and meta-analysis. *Clin Pharmacokin*. 2021;60(10):1291–1302. doi:10.1007/s40262-021-01037-7
13. de Winter BC, Mathot RA, Sombogaard F, Vulto AG, van Gelder T. Nonlinear relationship between mycophenolate mofetil dose and mycophenolic acid exposure: Implications for therapeutic drug monitoring. *Clin J Am Soc Nephrol*. 2011;6(3):656–663. doi:10.2215/CJN.05440610
14. Meier-Kriesche HU, Shaw LM, Korecka M, Kaplan B. Pharmacokinetics of mycophenolic acid in renal insufficiency. *Ther Drug Monit*. 2000;22(1):27–30. doi:10.1097/00007691-200002000-00005
15. Vanhove T, Kuypers D, Claes KJ, et al. Reasons for dose reduction of mycophenolate mofetil during the first year after renal transplantation and its impact on graft outcome. *Transpl Int*. 2013;26(8):813–821. doi:10.1111/tri.12133
16. Filler G, Todorova EK, Bax K, Alvarez-Elias AC, Huang SHS, Kobrzynski MC. Minimum mycophenolic acid levels are associated with donor-specific antibody formation. *Pediatr Transpl*. 2016;20(1):34–38. doi:10.1111/petr.12637
17. Abd Rahman A, Tett S, Abdul Gafor H, McWhinney BC, Staatz CE. Development of improved dosing regimens for mycophenolate mofetil based on population pharmacokinetic analyses in adults with lupus nephritis. *Eur J Drug Metab Pharmacokinet*. 2017;42(6):993–1004. doi:10.1007/s13318-017-0420-3
18. Zang J, Luo YG, Zhu ZF, Feng GW, Sun Z, Zhang XJ. Pharmacokinetic comparison of two mycophenolate mofetil formulation in kidney transplant recipients. *Ther Drug Monit*. 2018;40(5):649–654. doi:10.1097/FTD.0000000000000545
19. Graff J, Scheuermann EH, Brandhorst G, Oellerich M, Gossmann J. Pharmacokinetic analysis of mycophenolate mofetil and enteric-coated mycophenolate sodium in calcineurin inhibitor-free renal transplant recipients. *Ther Drug Monit*. 2016;38(3):388–392. doi:10.1097/FTD.0000000000000281
20. Sommerer C, Müller-Krebs S, Schaier M, et al. Pharmacokinetic and pharmacodynamic analysis of enteric-coated mycophenolate sodium: Limited sampling strategies and clinical outcome in renal transplant patients. *Br J Clin Pharmacol*. 2010;69(4):346–357. doi:10.1111/j.1365-2125.2009.03612.x
21. Pawinski T, Luszczynska P, Durlik M, et al. Development and validation of limited sampling strategies for the estimation of mycophenolic acid area under the curve in adult kidney and liver transplant recipients receiving concomitant enteric-coated mycophenolate sodium and tacrolimus. *Ther Drug Monit*. 2013;35(6):760–769. doi:10.1097/FTD.0b013e31829b88f5
22. de Winter BC, van Gelder T, Mathot RA, et al. Limited sampling strategies drawn within 3 hours postdose poorly predict mycophenolic acid area-under-the-curve after enteric-coated mycophenolate sodium. *Ther Drug Monit*. 2009;31(5):585–591. doi:10.1097/ftd.0b013e3181b8679a
23. Marquet P, Saint-Marcoux F, Premaud A, et al. Performance of the new mycophenolate assay based on IMPDH enzymatic activity for pharmacokinetic investigations and setup of Bayesian estimators in different populations of allograft recipients. *Ther Drug Monit*. 2009;31(4):443–450. doi:10.1097/FTD.0b013e3181a8f0ae
24. Lampón N, Tutor-Crespo M, Romero R, Tutor JC. Diagnostic efficiency of truncated area under the curve from 0 to 2 h (AUC0-2) of mycophenolic acid in kidney transplant recipients receiving mycophenolate mofetil and concomitant tacrolimus. *Clin Chem Lab Med*. 2011;49(7):1167–1170. doi:10.1515/CCLM.2011.191
25. Pourafshar N, Karimi A, Wen X, et al. The utility of trough mycophenolic acid levels for the management of lupus nephritis. *Nephrol Dial Transplant*. 2019;34(1):83–89. doi:10.1093/ndt/gfy026
26. Knight SR, Morris PJ. Does the evidence support the use of mycophenolate mofetil therapeutic drug monitoring in clinical practice? A systematic review. *Transplantation*. 2008;85(12):1675–1685. doi:10.1097/TP.0b013e3181744199
27. Kaczmarek I, Bigdeli AK, Vogeser M, et al. Defining algorithms of efficient therapeutic drug monitoring of mycophenolate mofetil in heart transplant recipients. *Ther Drug Monit*. 2008;30(4):419–427. doi:10.1097/FTD.0b013e31817d7064
28. Van Gelder T, Shaw LM. The rationale for and limitations of therapeutic drug monitoring for mycophenolate mofetil in transplantation. *Transplantation*. 2005;80(2 Suppl):S244–S253. doi:10.1097/01.tp.0000186380.61251.fc

# Dandelion root extracts abolish MAPK pathways to ameliorate experimental mouse ulcerative colitis

*Anfu Zhou[1,B–D,F], *Shuqing Zhang[2,B,C,F], Chengliang Yang[3,B,F], Nansheng Liao[4,C,F], Yan Zhang[5,A,C–F]

[1] Department of Gastroenterology, The First Affiliated Hospital of Hainan Medical University, Haikou, China
[2] Department of Clinical Laboratory, The Second People's Hospital of Nantong, China
[3] Department of Gastroenterology, Chifeng College Affiliated Hospital, China
[4] Department of General Surgery, The First People's Hospital of Taizhou, China
[5] Department of Gastroenterology, The First People's Hospital of Taizhou, China

A – research concept and design; B – collection and/or assembly of data; C – data analysis and interpretation;
D – writing the article; E – critical revision of the article; F – final approval of the article

Advances in Clinical and Experimental Medicine, ISSN 1899–5276 (print), ISSN 2451–2680 (online) *Adv Clin Exp Med*. 2022;31(5):529–538

**Address for correspondence**
Yan Zhang
E-mail: Zhangyan_FPHospi@163.com

**Funding sources**
None declared

**Conflict of interest**
None declared

*Anfu Zhou and Shuqing Zhang contributed equally to this work.

Received on September 9, 2021
Reviewed on December 6, 2021
Accepted on January 29, 2022

Published online on February 17, 2022

## Abstract

**Background.** Dextran sodium sulfate (DSS)-triggered ulcerative colitis (UC) model in animals provides a valuable platform to preclinically evaluate the outcome of drug candidates for UC. Dandelion root extracts (DRE) have a therapeutic effect on UC. However, the protective mechanism of DRE against UC remains unknown.

**Objectives.** To discover the targeting pathway involved in DRE-induced protection against UC.

**Materials and methods.** The UC model was developed in C57BL/6 mice by oral administration of DSS. Following DSS exposure, sulfasalazine (SASP), low dose of DRE (DRE-L), moderate dose of DRE (DRE-M), high dose of DRE (DRE-H), and DRE-H plus mitogen-activated protein kinases (MAPK) agonist (DRE-H+MA) were administered to the mice. Colon Mucosal Damage Index (CMDI) and histopathological analysis were used to evaluate the colonic mucosal damage. The cytokine levels were detected using commercial enzyme-linked immunosorbent assay (ELISA) kits. The MAPK pathway activation was determined with western blotting.

**Results.** We found that DRE-H attenuated DSS-triggered colonic mucosal damage. The DSS-induced inflammatory responses and oxidative stress in the bloodstream and colon tissues were dramatically inhibited by DRE-H administration. Also, this plant impaired DSS-provoked phosphorylation levels of extracellular signal-regulated kinases (ERK), c-Jun N-terminal kinases (JNK), p38 mitogen-activated protein kinases (p38), p65, and IκB. More importantly, MAPK agonist, BIM-23A760, removed the protective effect of DRE-H on the bloodstream and colon tissues.

**Conclusions.** The DRE-H is capable of relieving DSS-induced UC, and its mechanism links to the MAPK pathways.

**Key words:** mouse, MAPK, ulcerative colitis, dextran sodium sulfate, dandelion root extracts

**Cite as**
Zhou A, Zhang S, Yang C, Liao N, Zhang Y. Dandelion root extracts abolish MAPK pathways to ameliorate experimental mouse ulcerative colitis. *Adv Clin Exp Med*. 2022;31(5):529–538. doi:10.17219/acem/146234

**DOI**
10.17219/acem/146234

# Background

Ulcerative colitis (UC) is an inflammatory bowel disease (IBD) featured with recurrent attacks, poor outcome, prolonged illness, and high potential of colorectal carcinogenesis.[1] The annual incidence of UC has been largely increasing in China, and the current clinical drugs, including anti-inflammatory and immunosuppressive compounds, have several adverse side effects such as osteoporosis, neurotoxicity and gastrointestinal intolerance[2]; in consequence, more and more studies attempt to exploit new or alternative approaches to UC.[3] Dextran sodium sulfate (DSS), one of the sulfated polysaccharides, is a standard reagent used to create an experimental UC model in animals, as most pathological symptoms during DSS application are similar to those of UC patients.[4] Therefore, the DSS-triggered UC animal model provides a valuable platform to either develop new drug targets by constant progress in understanding the etiology and pathogenesis of UC, or pre-clinically evaluate the outcomes of drug candidates for UC.

It has long been known that dandelion (*Taraxacum*, Asteraceae family), a traditional Chinese herbal medicine, together with other herbs, can treat various ailments.[5] Recent attempts have led to discoveries of anticancer, anti-inflammatory and antioxidative functions of this plant.[6–8] By stimulating multiple death signaling pathways, the dandelion root extracts increase cell apoptosis of colorectal and pancreatic cancer and leukemia.[9–11] Inhibiting PI3K/AKT pathway is a mechanism for dandelion root extracts to ameliorate lipopolysaccharide (LPS)-triggered inflammation,[12] and reducing lipid peroxidation contributes to the antioxidative activity of dandelion root extracts on the alcohol-induced liver.[13] Although the protective effect of this plant on UC has been revealed,[14] the exact mechanism is unknown. Such a broad function of dandelion root extract might be due to its active chemical constituents, including sesquiterpenes, various triterpenes, phytosterols, and phenolic compounds.[15] Among the phenolic compounds, hydroxycinnamic acid derivatives (chlorogenic, caffeic, 4-coumaric, 3-coumaric, ferulic acids) are mainly reported, whereas flavonoids and hydroxybenzoic acid derivatives have a relatively low level.[16–18] These chemical constituents likely act individually, additively or in synergy, in order to modulate different tissue-specific functions.[19] Still, the physiological functions of dandelion and its clinical utilization clues the ability of cells to respond to its bioactive components through fundamental and widespread intracellular mechanisms.

Mitogen-activated protein kinases (MAPK) harbor 3 well-known subfamily members, extracellular signal-regulated kinases (ERK), c-Jun N-terminal kinases (JNK) and p38 mitogen-activated protein kinases (p38), that perform autophosphorylation or phosphorylate their substrates to activate or deactivate downstream molecules.[20] These kinases are ubiquitous and conserved in eukaryotes, and they are essential modulators for cell pathology, cellular physiology and various diseases.[21] Recent evidence proves that MAPK signaling pathways show a crucial correlation with the pathogenesis of UC, due to the abundant release of cytokines and inflammatory mediators by their activation.[22–24] Given the clues that MAPK pathways can be utilized by dandelion or its extracts to ameliorate the inflammation in vitro and bacterial disease in animals,[25–27] we proposed that dandelion root extracts may relieve experimental UC by regulating MAPK signaling pathways.

# Objectives

In this study, we hypothesized that MAPK signaling pathways might participate in the protection against UC by dosing dandelion root extracts in experimental UC. Therefore, this study aimed to discover the interrelationship between dandelion root extracts and MAPK pathways in the DSS-triggered experimental mouse model.

# Materials and methods

## Preparation of dandelion root extracts

Premier Herbal Inc. (Toronto, Canada; lot No. 318121) provided dandelion roots for the present study. The root extract was isolated according to the published protocol.[19] Briefly, the appropriate dandelion roots were extracted by soaking in 95% ethanol at 1:10 w/v (plant material to solvent ratio) under uninterrupted stirring for 3 days, changing the solvent every 24 h. The extract was filtered, and the solvent was removed using a rotary evaporator (Vacufage plus; Eppendorf, Hamburg, Germany). The dry extract of dandelion root was frozen at –80°C for long-term storage and redissolved by the same solvent in 100 mg/mL before use. According to the published analysis on reversed-phase high-performance liquid chromatography,[19] the main chemical constituents of dandelion root extract were hydroxybenzoic acid derivatives and hydroxycinnamic acids (gallic acid, chlorogenic acid, caffeic acid, vanillic acid, syringic acid, p-coumaric acid, and ferulic acid). For the animal experiment, 100 mg/mL of dandelion roots extracts were finally diluted in sterile distilled water to the indicated concentrations for the gavage.

## Animals and experimental design

Male and female (half-and-half) specific pathogen-free (SPF) C57BL/6 mice, 6–8 weeks of age, weighing 18 ±3 g, from the same litters, were commercially obtained from Animal Center of Hainan Medical University and housed in an environmentally controlled breeding room (temperature: 20 ±2°C, humidity: 60 ±5%, 12 h/12 h dark/light cycles) in cages, and fed with sterile water and standard laboratory rodent diets. They were maintained under

internationally accepted principles for laboratory animal use. The animal protocol complied with the Animal Research: Reporting of In Vivo Experiments (ARRIVE) guidelines and was approved by the Institutional Animal Care and Use Committee of Hainan Medical University, China (approval No. DLMU2020012341).

After 3 days of acclimatization, mice were administered 2% DSS (w/v) (36–50 kDa; MP Biomedicals, Illkirch-Graffenstaden, France) in their drinking water to induce acute UC. Mice were randomly separated into 7 groups (n = 10 per group): 1) control group (mice received regular drinking water, CON group); 2) DSS-induced UC model group (mice received 2% w/v DSS in drinking water for 10 days, UC group); 3) DSS + sulfasalazine (SASP) group (100 mg/kg/day for 10 days); 4) DSS + low dose of dandelion root extracts (DRE; 0.5 mg per mouse) group (mice received 2% w/v DSS in drinking water for 10 days, together with the administration by gavage of 1 mg per mouse of DRE twice a day, DRE-L group); 5) DSS + middle dose of DRE group (1 mg per mouse, DRE-M group); 6) DSS + high dose of DRE group (2 mg per mouse, DRE-H group); and 7) DSS+DRE-H+MAPK agonist group (DRE-H+MA group). Sulfasalazine is a certain drug used to treat UC clinically.[28] The MAPK agonist, BIM-23A760,[29] was provided by IPSEN Bioscience (Cambridge, USA)[30] and injected into the tail vein (4 μg per mouse) every other day. The volume of gavage and tail vein injection was 400 μL and 100 μL, respectively. Mice were observed for 10 days and then sacrificed by $CO_2$ inhalation.[31] Serum and colon samples were collected for the subsequent analysis.

## Colon Mucosal Damage Index

Colon Mucosal Damage Index (CMDI) was evaluated according to the following criteria[32]: (1) ulcer and inflammation: 0 points – normal; 1 point – focal congestion, no ulcer; 2 points – ulcer without congestion or thickening of the intestinal wall; 3 points – one place with inflammatory ulcer; 4 points – ulcers and inflammatory sites in 2 places; 5 points – the central part of the damage along the colon extension ≥ 1 cm; 6–10 points – the injury along the length of the colon extended ≥ 2 cm; for each increase of 1 cm of damage, the score increased by 1 point; (2) the presence of adhesion: 0 points – normal; 1 point – slight adhesion; 2 points – the main adhesion.

## Histology analysis

The colon samples were collected and fixed in 4% paraformaldehyde solution overnight, and then embedded in paraffin and sliced into 4-μm sections. The paraffin sections were stained with hematoxylin for 5 min, followed by phosphate-buffered saline (PBS) washing and dying in eosin solution for 30 s.[33] The histopathological changes were observed using a light microscope (BX50; Olympus Corp., Tokyo, Japan).

## Enzyme-linked immunosorbent assay

The levels of mouse interleukin (IL)-1β (Nanjing Senbeijia Biological Technology, Nanjing, China), IL-6 (Nanjing Senbeijia Biological Technology), tumor necrosis factor alpha (TNF-α) (Nanjing Senbeijia Biological Technology), IL-10 (Nanjing Senbeijia Biological Technology), platelet-activating factor (PAF; cat No. MBS2700185; MyBioSource, San Diego, USA), prostaglandin E2 (PGE2, MyBioSource), myeloperoxidase (MPO; cat. No. EMMPO; Invitrogen, Waltham, USA), and superoxide dismutase (SOD; cat. No. EIASODC; Thermo Fisher Scientific, Waltham, USA) were assessed in the colon homogenates and serum samples, using the abovementioned commercially available kits according to the manufacturer's specifications.[34]

## Western blotting

For the immunodetection, 50 μg of total protein extracts from cytosol or nucleus in Laemmli sample buffer (Bio-Rad, Hercules, USA) were resolved on 10% or 15% sodium dodecyl-sulfate polyacrylamide gel electrophoresis (SDS-PAGE) and then transferred to nitrocellulose membranes for western blotting. The membranes were first stained with Ponceau S to confirm the transfer efficacy. After blocking with 5% skim milk dissolved in Tris-buffered saline (TBS) containing 0.05% Tween-20 (TBST) (VWR, Lutterworth, UK) for 2 h at room temperature, membranes were incubated with anti-phospho-ERK, anti-phospho-p38, anti-phospho-JNK, anti-β actin, anti-Histone H3, anti-phospho-IκBα, anti-IκBα, anti-phospho-p65-S536, or anti-p65 (ABclonal, Woburn, USA) at appropriate dilutions, followed by goat anti-rabbit secondary antibody conjugated with horseradish peroxidase (HRP). Positive band intensities were detected using a gel documentation system (Fujifilm LAS-3000 Imager, Tokyo, Japan).[35]

## Statistical analyses

Nonparametric Kruskal–Wallis test with Dunn's multiple comparison test were only used in the data shown in Fig. 1A, since it did not fit normal distribution (Gaussian).[36] One-way analysis of variance (ANOVA) with Tukey's multiple comparison test or Welch's ANOVA test with Dunnett's T3 multiple comparisons test were used in the remaining data from Fig. 2–6. The Shapiro–Wilk and Kolmogorov–Smirnov tests were performed for normal distribution. The Shapiro–Wilk test is performed based on regression and correlation, and Kolmogorov–Smirnov test is the empirical distribution function test.[37] They analyze the normality of data in a different way. Therefore, the data with a sample size greater than 4 was considered to have a normal distribution only if it passed both tests, while a normal distribution of data with a sample size less than 5 can only be evaluated by the Shapiro–Wilk test. The Bartlett's test was used for evaluating the equal variances.[38] All data

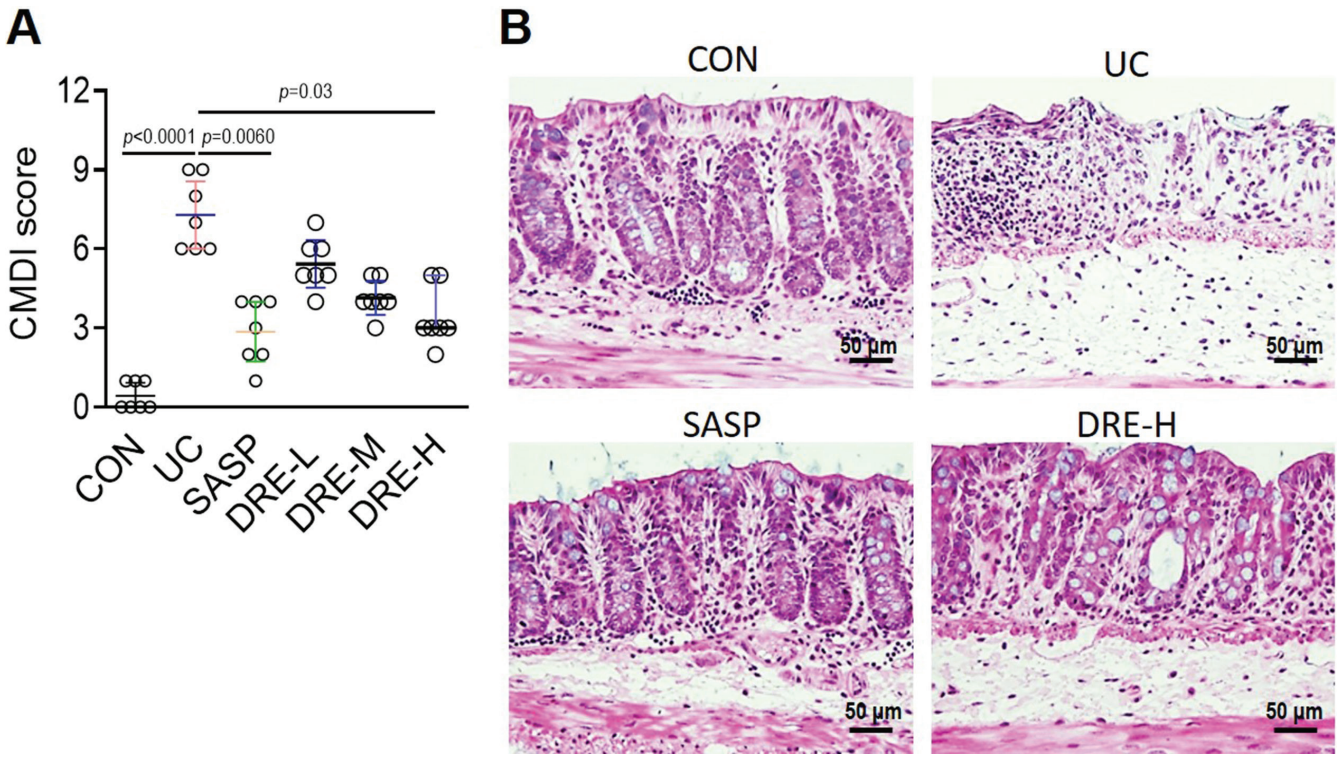


Fig. 1. Dandelion root extracts (DRE) reduced dextran sodium sulfate (DSS)-triggered colonic mucosal injury. A. Colon Mucosal Damage Index (CMDI) score was used to assess the degree of intestinal mucosal injury of mice in each group. The way to quantify the CMDI score can be found in Materials and methods section; B. Histopathological staining was used to assess the degree of intestinal mucosal damage of mice in each group. Significance differences were measured using a nonparametric Kruskal–Wallis test with Dunn's multiple comparison test (A). Data are mean ± 95% confidence interval (95% CI) (for normal distribution) or median ± interquartile range (IQR), p-value was indicated in each panel

CON – control group; UC – DSS-induced UC model group; SASP – DSS + sulfasalazine group; DRE-L – DSS + low dose of DRE group; DRE-M – DSS + middle dose of DRE group; DRE-H – DSS + high dose of DRE group.

analyses were performed using GraphPad Prism software v. 8.4.0 (GraphPad Software, San Diego, USA). A value of $p < 0.05$ was considered statistically significant.

# Results

## Dandelion root extracts ameliorate DSS-triggered colonic mucosal injury

Oral administration of DSS is a common approach to induce UC in mice.[39] As expected, the UC was successfully established in C57BL/6 mice. It was indicated by the high CMDI score and the mucosal epithelial cell degeneration and necrosis, as well as an increased number of infiltrating mucosal leukocytes in histopathological staining of the colon sections (Fig. 1A,B). Sulfasalazine, a therapeutic drug for UC,[40] and various doses of DRE were used to treat UC mice. The SASP group and the DRE-H group had significantly lower CMDI score than the UC group, while the low or middle dose of DRE (DRE-L or DRE-M) groups showed only slight but no statistically significant reduction of CMDI score compared to the UC group (Fig. 1A). Therefore, the DRE-H group was selected for the following experiments. Consistently, the mild epithelial cell degeneration and necrosis, as well as a small number of inflammatory cells were observed in colonic sections derived from SASP and DRE-H groups (Fig. 1B).

## Dandelion root extracts weaken DSS-triggered inflammatory cytokines

The effects of DRE on the DSS-induced colonic mucosal inflammation were evaluated by assessing several inflammatory markers in mouse serum and intestinal tissues. As shown in Fig. 2A–H, the proinflammatory cytokines, TNF-α, IL-6, and IL-1β, were markedly enhanced, and the anti-inflammatory cytokine, IL-10, was significantly reduced in serum and colon tissues of the UC group. More importantly, all of the abnormal changes of these inflammatory indicators induced by DSS were reversed, mainly by the oral administration of SASP or DRE-H, suggesting the anti-inflammatory action of DRE in UC mice.

## Dandelion root extracts improve DSS-triggered oxidative injury in the colon

Several factors (PAF, PGE2, MPO, and SOD) related to colonic oxidative injury were further assessed

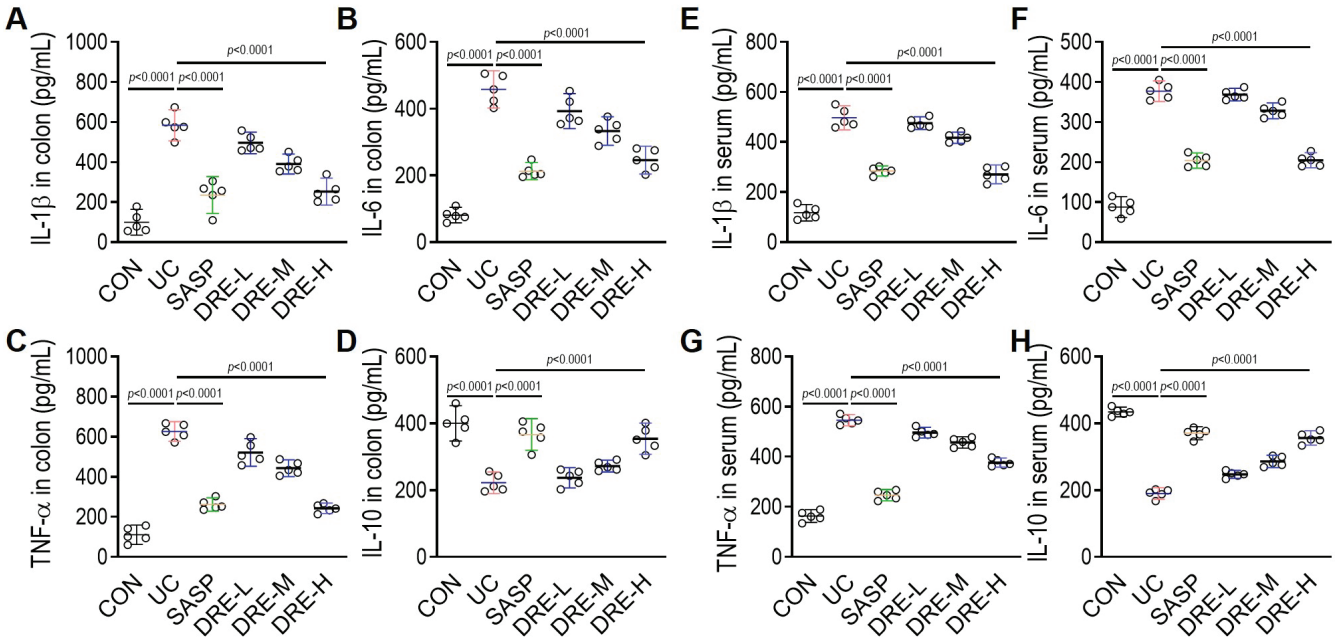


Fig. 2. Dandelion root extracts (DRE) inhibited dextran sodium sulfate (DSS)-triggered colonic mucosal inflammation. After ulcerative colitis (UC) development and drug treatment in C57BL/6J mice, enzyme-linked immunosorbent assay (ELISA) assay was utilized to detect pro- or anti-inflammatory cytokines in colon tissues (A–D) and serum samples (E–H). These cytokines include interleukin (IL)-1β (A,E), IL-6 (B,F), tumor necrosis factor alpha (TNF-α) (C,G), and IL-10 (D,H). The homogenate from tissues or serum were diluted with appropriate fold to get a measurement that fits in standard curves provided with ELISA kits, and those standard curves were used to calculate the concentration of cytokines. Significant differences were measured using one-way analysis of variance (ANOVA) with Tukey's multiple comparison test (A–H). Data are mean ± 95% confidence interval (95% CI), p-value was indicated in each panel

CON – control group; UC – DSS-induced UC model group; SASP – DSS + sulfasalazine group; DRE-L – DSS + low dose of DRE group; DRE-M – DSS + middle dose of DRE group; DRE-H – DSS + high dose of DRE group.

to determine the antioxidative effect of DRE in UC mice. The DSS substantially triggered oxidative injury, as demonstrated by the upregulation of PAF, PGE2 and MPO levels, and the downregulation of the activity of SOD in either colonic tissues or serum samples (Fig. 3A–H). Interestingly, SASP and DRE-H dramatically ameliorated oxidative stress in UC mice by increasing SOD activity and decreasing PAF, PGE2 and MPO levels. In addition, the antioxidative activity between SASP and DRE-H groups is similar.

## Dandelion root extracts impact the MAPK signaling pathways

First, it was investigated whether the action of DRE against UC is related to MAPK signaling pathways. As shown in Fig. 4, the phosphorylation level of ERK, JNK or p38 in colon tissues was strongly induced by the oral administration of DSS, and the application of DRE-H entirely blocked the DSS-induced high phosphorylation of the 3 indicators. Nuclear factor kappa B (NF-κB) is downstream of MAPK signaling pathways. The phosphorylation levels of NF-κB p65 and IκBα, 2 indicators of NF-κB activation, were obviously enhanced by the DSS treatment, but the abundances of IκBα and p65 in the cytoplasm were significantly decreased by the DSS exposure (Fig. 4A,B). The production of NF-κB p65 in nuclei was enhanced by the DSS treatment, suggesting the robust translocation of p65 into nuclei (Fig. 4A,C). Notably, the administration of DRE-H could completely reverse all the abovementioned DSS-triggered alterations (Fig. 4), revealing that DRE-H likely blocks the activation of NF-κB through the inhibition of phosphorylation levels of ERK, JNK and p38.

## Dandelion root extracts target MAPK to improve DSS-triggered UC

To investigate further whether the therapeutic effect of DRE against UC is achieved by suppressing MAPK signaling pathways, the MAPK agonist, BIM-23A760, was applied in C57BL/6 mice during DRE-H administration. Interestingly, BIM-23A760 removed anti-inflammatory and antioxidative actions of DRE-H by reinducing IL-1β, IL-6, TNF-α, PAF, PGE2, and MPO, and resuppressing the levels of IL-10 and SOD in serum and tissue samples (Fig. 5A–H). At the same time, the inhibitory effect of DRE-H on DSS-triggered activities of ERK, JNK and p38, and their downstream transcriptional factor NF-κB was omitted by this agonist (Fig. 6A–C), which seems to prove that the re-activation of MAPK pathways could block the therapeutic effect of DRE-H against UC. In other words, the inhibition of MAPK signaling pathways could be a mechanistic explanation for DRE to relieve UC in mice.

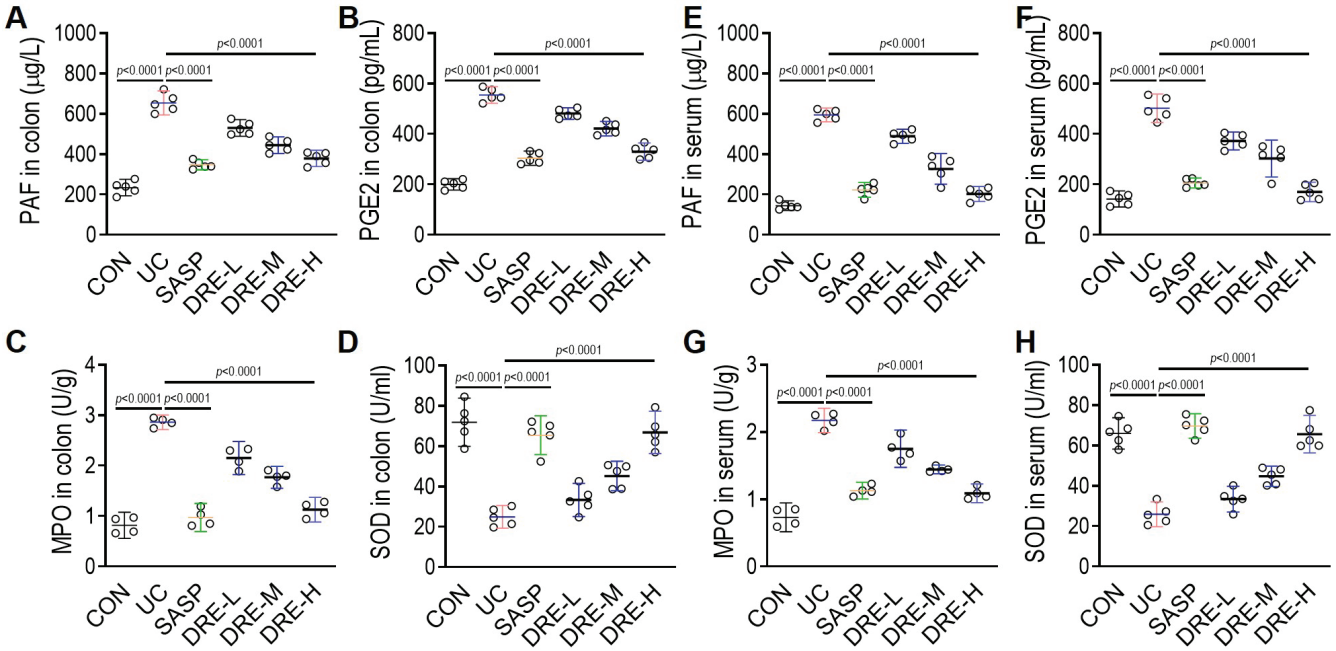


Fig. 3. Dandelion root extracts (DRE) improved dextran sodium sulfate (DSS)-triggered oxidative stress in animals. Enzyme-linked immunosorbent assay (ELISA) was utilized to detect oxidative stress-related factors in colon tissues (A–D) and serum samples (E–H). These factors include platelet-activating factor (PAF) (A,E), prostaglandin E2 (PGE2) (B and F), myeloperoxidase (MPO) (C,G), and superoxide dismutase (SOD) (D,H). Significant differences were measured using one-way analysis of variance (ANOVA) with Tukey's multiple comparison test (A–H). Data are mean ± 95% confidence interval (95% CI), p-value was indicated in each panel

CON – control group; UC – DSS-induced ulcerative colitis (UC) model group; SASP – DSS + sulfasalazine group; DRE-L – DSS + low dose of DRE group; DRE-M – DSS + middle dose of DRE group; DRE-H – DSS + high dose of DRE group.

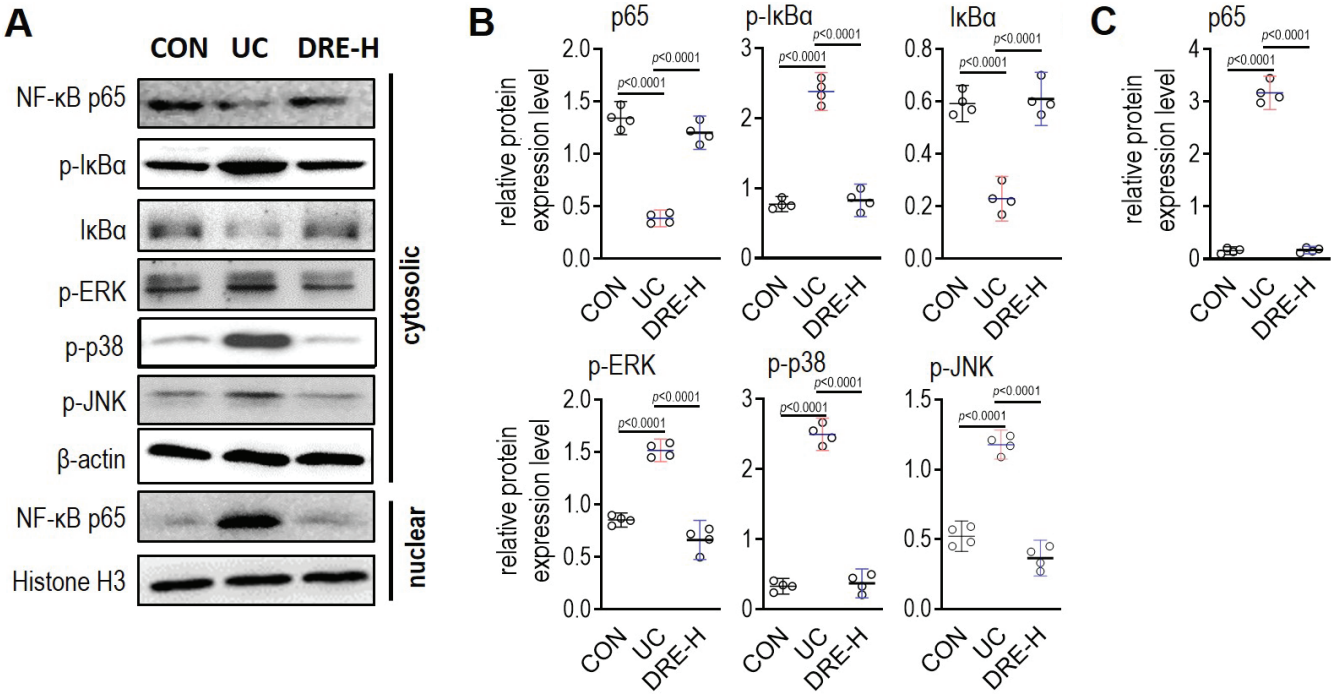


Fig. 4. Dandelion root extracts (DRE) largely normalized dextran sodium sulfate (DSS)-induced activation of nuclear factor kappa B (NF-κB) and mitogen-activated protein kinases (MAPK) signaling pathways. A. Western blotting was used to detect the production of p65 and IκBα and the phosphorylation of p65, IκBα, extracellular signal-regulated kinases (ERK), c-Jun N-terminal kinases (JNK), and p38 mitogen-activated protein kinases (p38); B. Relative expression of cytosolic proteins shown in A was quantified using ImageJ; C. Relative expression of nuclear protein, p65, shown in A was quantified using ImageJ. One-way analysis of variance (ANOVA) with Tukey's multiple comparison test (B) and Welch's ANOVA test with Dunnett's T3 multiple comparisons test (C) were used to identify significant differences. Data are mean ± 95% confidence interval (95% CI), p-value was indicated in each panel

CON – control group; UC – DSS-induced ulcerative colitis (UC) model group; DRE-H – DSS + high dose of DRE group.

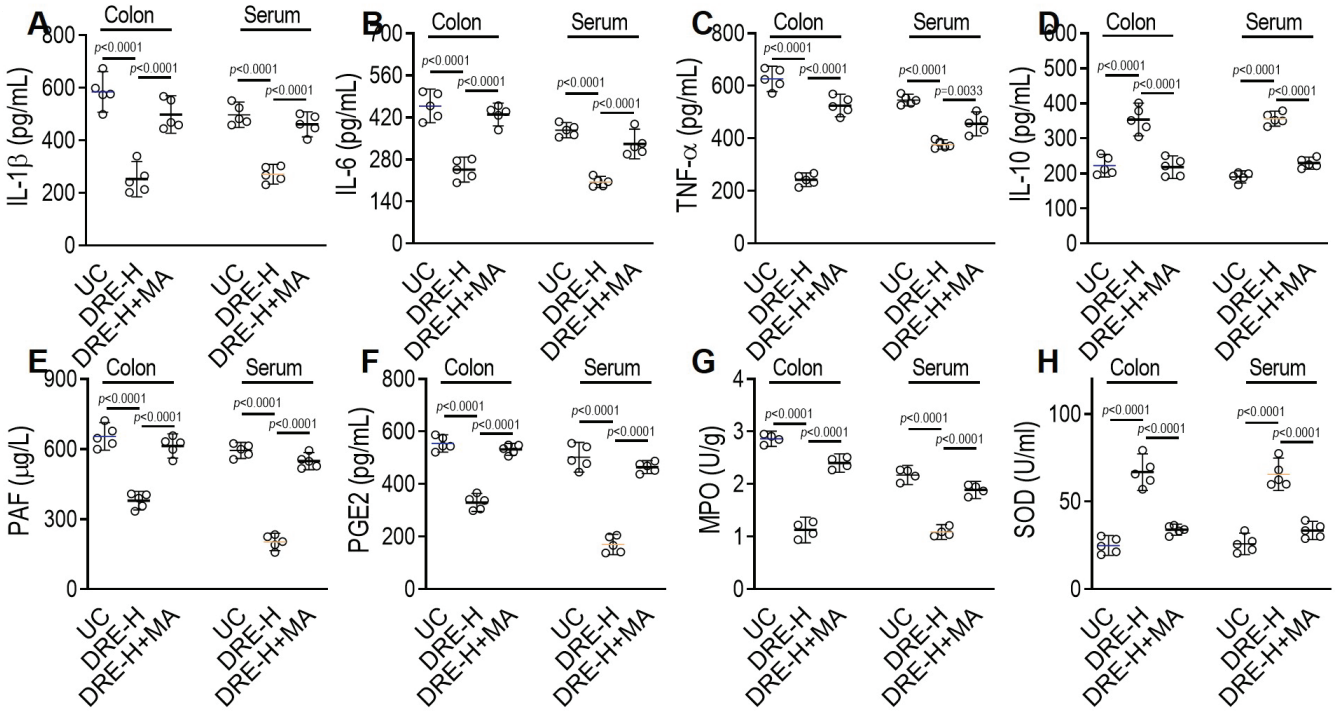


Fig. 5. Dandelion root extracts (DRE) improved dextran sodium sulfate (DSS)-induced inflammation and oxidative stress through mitogen-activated protein kinases (MAPK) signaling pathways. After treatment with DRE for ulcerative colitis (UC) in C57BL/6J mice, enzyme-linked immunosorbent assay (ELISA) assay was utilized to detect inflammatory and oxidative stress-related factors in colon tissues and serum samples. These factors include interleukin (IL)-1β (A), IL-6 (B), tumor necrosis factor alpha (TNF-α) (C), IL-10 (D), platelet-activating factor (PAF) (E), prostaglandin E2 (PGE2) (F), myeloperoxidase (MPO) (G), and superoxide dismutase (SOD) (H). The homogenate from tissues or serum were diluted with appropriate fold to get a measurement that fits in standard curves provided with ELISA kits, and those standard curves were used to calculate the concentration of cytokines. Significant differences were measured using one-way analysis of variance (ANOVA) with Tukey's multiple comparison test (A–H). Data are mean ± 95% confidence interval (95% CI), p-value was indicated in each panel

UC – DSS-induced ulcerative colitis (UC) model group; DRE-H – DSS + high dose of DRE group; DRE-H+MA – DSS+DRE-H+mitogen-activated protein kinases (MAPK) agonist group.

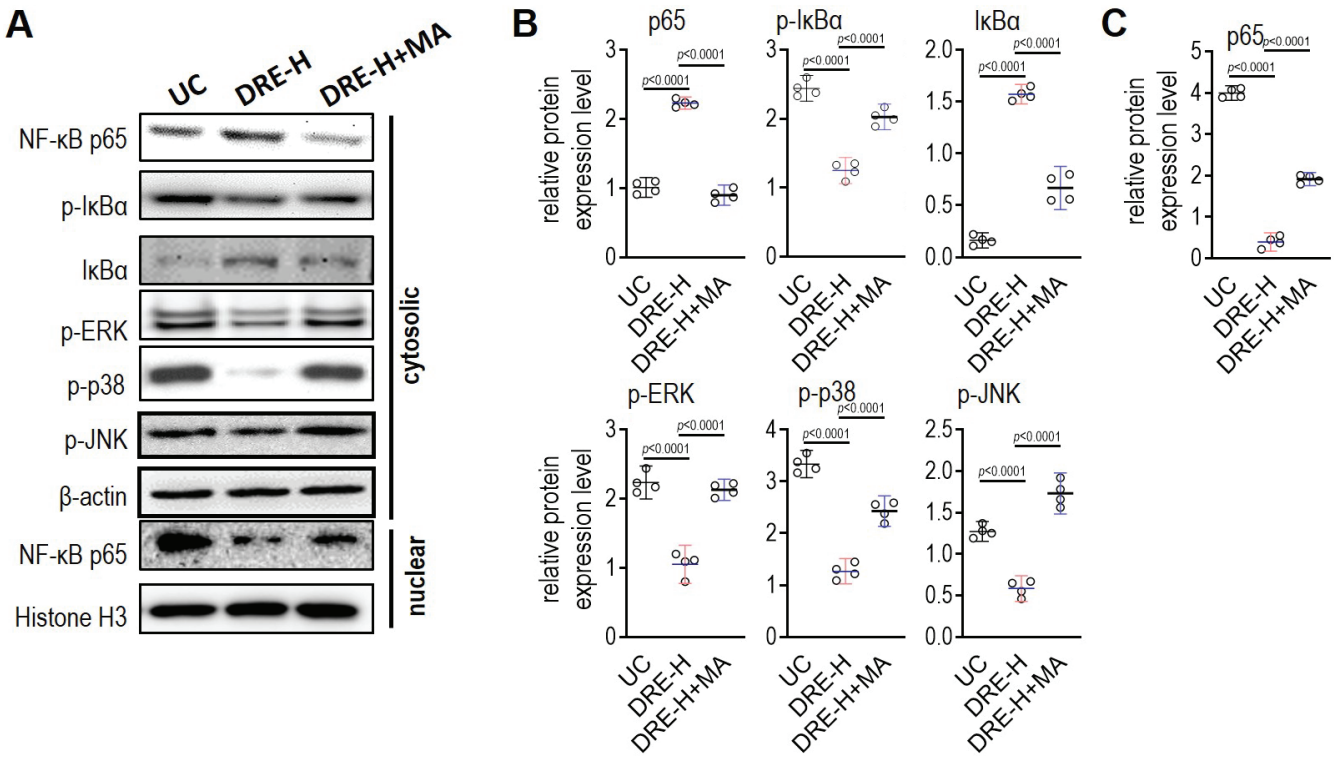


Fig. 6. Mitogen-activated protein kinases (MAPK) agonist erased the inhibitory effect of dandelion root extracts (DRE) on nuclear factor kappa B (NF-κB) and MAPK activation. A. Western blotting was performed to detect the production of p65 and IκBα and the phosphorylation of p65, IκBα, extracellular signal-regulated kinases (ERK), c-Jun N-terminal kinases (JNK), and p38 mitogen-activated protein kinases (p38); B. Relative expression of cytosolic proteins shown in A was quantified using ImageJ; C. Relative expression of nuclear protein, p65, shown in A was quantified using ImageJ. Significance differences were measured using one-way analysis of variance (ANOVA) with Tukey's multiple comparison test (B,C). Data are mean ± 95% confidence interval (95% CI), p-value was indicated in each panel

UC – DSS-induced ulcerative colitis (UC) model group; DRE-H – DSS + high dose of DRE group; DRE-H+MA – DSS+DRE-H+MAPK agonist group.

# Discussion

There seems to be a consensus that DSS acts as a toxic factor, damaging gut epithelial cells and destroying the integrity of the mucosal barrier, thereby disseminating gut bacteria or other microbes into the lamina propria.[41] This dissemination provokes immune and concomitant inflammatory responses by recruiting neutrophils and other leukocytes to the injured sites and accumulating several leukocyte-expressed proinflammatory cytokines, including IL-1β, IL-6 and TNF-α; the latter aggravate the disease further.[42] Our data consistently showed that leukocytes and their secreted cytokines were accumulated, and that MPO, the principal constituent of neutrophil cytoplasmic granules, as well as PAF, the stimulator for leukocyte adhesion, were enhanced in DSS-exposed colon tissues. In the current study, the application of DRE-H reduced the accumulation of neutrophils and other leukocytes, as demonstrated by the reduction of DSS-triggered leukocytes infiltration, proinflammatory cytokines, MPO activity, and PAF level. Moreover, the DSS-triggered increase of proinflammatory cytokines, MPO and PAF in the bloodstream were also improved by the oral administration of DRE-H. Besides its effect on proinflammatory cytokines, DRE-H also supported the anti-inflammatory cytokine, IL-10. The IL-10 is deficient in patients with UC and has been proposed as a potent anti-inflammatory therapy in this disease.[43] The mechanisms responsible for its anti-inflammatory action have been recently explored, and this anti-inflammatory action is dependent on the promotion of mitophagy that clears dysfunctional mitochondria featured by low membrane potential and a high level of reactive oxygen species (ROS).[44] Without the effective IL-10 signaling, damaged mitochondria are accumulated and result in dysregulated activation of the inflammasome and the production of IL-1β. Thus, all of the abovementioned evidence supports the protective effect of DRE-H on UC, which is in line with the previous findings.[14]

The NF-κB is an inflammation-associated signal essential for the host defense to different infections and intracellular changes of reduction-oxidation state.[45,46] Without any stimulations, NF-κB forms an inactive and stable complex with inhibitory protein IκB in the cytoplasm. Once the cells get activated by various stimuli, the inhibitory protein IκB is phosphorylated and then dissociated from NF-κB. After the translocation into the nucleus and a subsequent attachment to the κB binding sites, NF-κB triggers the expression of several downstream genes, including inflammatory mediators.[47,48] In this study, DSS treatment largely elicited the phosphorylation of NF-κB and IκB, while DRE-H diminished their phosphorylation, indicating the anti-inflammatory molecular mechanism dependent on NF-κB for DRE. Three prominent MAPK pathway members, ERK, JNK and p38, can arouse the action of NF-κB.[49] Interestingly, we found that these 3 kinases were all provoked in DSS-injured tissues and had a similar expression pattern as NF-κB, suggesting that their activation likely modulated the activation of NF-κB in circulation and colon tissues from DSS-treated animals. Given the strong ability of DRE-H to weaken the phosphorylation levels of ERK, JNK and p38, it is therefore reasonable to hypothesize that the mechanism of action of this plant seems to require the involvement of MAPK signaling pathways to inhibit NF-κB activation and ensuing inflammatory events. The MAPK agonist BIM-23A760 was simultaneously injected into animals during DRE application to examine this proposal. After the agonist usage, the effect of DRE-H on protecting animals against UC disappeared, as demonstrated by the measurement of the level of inflammatory cytokines, PAF, MPO, PGE2, and SOD, and the phosphorylated levels of NF-κB, IκB, ERK, JNK, and p38. These data support the mechanism through which DRE can inhibit UC in DSS-administrated rats by blocking MAPK signaling pathways.

## Limitations

Firstly, this study only clarified the action and involved the mechanism of total extracts of dandelion root in DSS-induced UC model. The potential bioactive compounds (hydroxybenzoic acid derivatives and hydroxycinnamic acids) need to be further exaxmined. Secondly, there might be other signaling pathways involved in the protection of DRE, which should be also investigated in future studies. Lastly, our study only validated the effect of DRE on DSS-induced UC. The function of this plant on experimental UC triggered by other drugs, including 2,4,6-trinitrobenzenesulfonic acid (TNBS), Oxazolone and acetic acid, remains unknown.

# Conclusions

The present study shows that DRE-H treatment protects mice against DSS-induced UC. This protective effect is attributed to its anti-inflammatory and antioxidative roles by inhibiting MAPK pathways and its downstream target – NF-κB. These findings do not only further support the potential application of dandelion for UC but also provide a mechanistic explanation for the protective function of dandelion against UC.

## ORCID iDs

Anfu Zhou https://orcid.org/0000-0001-9535-7069
Shuqing Zhang https://orcid.org/0000-0001-5570-5858
Chengliang Yang https://orcid.org/0000-0001-9384-1025
Nansheng Liao https://orcid.org/0000-0002-7076-8811
Yan Zhang https://orcid.org/0000-0003-1488-740X

## References

1. Itzkowitz SH, Yio X. Inflammation and cancer IV. Colorectal cancer in inflammatory bowel disease: The role of inflammation. *Am J Physiol Gastrointest Liver Physiol*. 2004;287(1):G7–G17. doi:10.1152/ajpgi.00079.2004

2. Hendrickson BA, Gokhale R, Cho JH. Clinical aspects and pathophysiology of inflammatory bowel disease. *Clin Microbiol Rev*. 2002;15(1):79–94. doi:10.1128/CMR.15.1.79-94.2002
3. Hanai H, Iida T, Takeuchi K, et al. Curcumin maintenance therapy for ulcerative colitis: Randomized, multicenter, double-blind, placebo-controlled trial. *Clin Gastroenterol Hepatol.* 2006;4(12):1502–1506. doi:10.1016/j.cgh.2006.08.008
4. Jialing L, Yangyang G, Jing Z, et al. Changes in serum inflammatory cytokine levels and intestinal flora in a self-healing dextran sodium sulfate-induced ulcerative colitis murine model. *Life Sci.* 2020;263:118587. doi:10.1016/j.lfs.2020.118587
5. Sweeney B, Vora M, Ulbricht C, Basch E. Evidence-based systematic review of dandelion (*Taraxacum officinale*) by natural standard research collaboration. *J Herb Pharmacother.* 2005;5(1):79–93. doi:10.1080/J157v05n01_09
6. Sigstedt SC, Hooten CJ, Callewaert MC, et al. Evaluation of aqueous extracts of *Taraxacum officinale* on growth and invasion of breast and prostate cancer cells. *Int J Oncol*. 2008;32(5):1085–1090. doi:10.3892/ijo.32.5.1085
7. Koo HN, Hong SH, Song BK, Kim CH, Yoo YH, Kim HM. *Taraxacum officinale* induces cytotoxicity through TNF-alpha and IL-1alpha secretion in Hep G2 cells. *Life Sci.* 2004;74(9):1149–1157. doi:10.1016/j.lfs.2003.07.030
8. Martinez M, Poirrier P, Chamy R, et al. *Taraxacum officinale* and related species: An ethnopharmacological review and its potential as a commercial medicinal plant. *J Ethnopharmacol.* 2015;169:244–262. doi:10.1016/j.jep.2015.03.067
9. Ovadje P, Ammar S, Guerrero JA, Arnason JT, Pandey S. Dandelion root extract affects colorectal cancer proliferation and survival through the activation of multiple death signalling pathways. *Oncotarget*. 2016;7(45):73080–73100. doi:10.18632/oncotarget.11485
10. Ovadje P, Chatterjee S, Griffin C, Tran C, Hamm C, Pandey S. Selective induction of apoptosis through activation of caspase-8 in human leukemia cells (Jurkat) by dandelion root extract. *Pancreas*. 2012;41(7):1039–1047. doi:10.1097/MPA.0b013e31824b22a2
11. Ovadje P, Chochkeh M, Akbari-Asl P, Hamm C, Pandey S. Selective induction of apoptosis and autophagy through treatment with dandelion root extract in human pancreatic cancer cells. *Pancreas*. 2012;41(7):1039–1047. doi:10.1097/MPA.0b013e31824b22a2
12. Ma C, Zhu L, Wang J, et al. Anti-inflammatory effects of water extract of *Taraxacum mongolicum* hand.-Mazz on lipopolysaccharide-induced inflammation in acute lung injury by suppressing PI3K/Akt/mTOR signaling pathway. *J Ethnopharmacol.* 2015;168:349–355. doi:10.1016/j.jep.2015.03.068
13. You Y, Yoo S, Yoon HG, et al. In vitro and in vivo hepatoprotective effects of the aqueous extract from *Taraxacum officinale* (dandelion) root against alcohol-induced oxidative stress. *Food Chem Toxicol*. 2010;48(6):1632–1637. doi:10.1016/j.fct.2010.03.037
14. Ding A, Wen X. Dandelion root extract protects NCM460 colonic cells and relieves experimental mouse colitis. *J Nat Med.* 2018;72(4):857–866. doi:10.1007/s11418-018-1217-7
15. Schütz K, Carle R, Schieber A. Taraxacum: A review on its phytochemical and pharmacological profile. *J Ethnopharmacol*. 2006;107(3):313–323. doi:10.1016/j.jep.2006.07.021
16. Williams CA, Goldstone F, Greenham J. Flavonoids, cinnamic acids and coumarins from the different tissues and medicinal preparations of *Taraxacum officinale*. *Phytochemistry*. 1996;42(1):121–127. doi:10.1016/0031-9422(95)00865-9
17. Ivanov IG. Polyphenols content and antioxidant activities of *Taraxacum officinale* FH Wigg (dandelion) leaves. *Int J Res Phytochem Pharmacol*. 2014;6(4):889–893. https://impactfactor.org/PDF/IJPPR/6/IJPPR,Vol6,Issue4,Article37.pdf
18. Kenny O, Smyth TJ, Hewage CM, Brunton NP. Antioxidant properties and quantitative UPLC-MS/MS analysis of phenolic compounds in dandelion (*Taraxacum officinale*) root extracts. *Free Radic Antioxid*. 2014;4(1):55–61. doi:10.5530/fra.2014.1.9
19. Gerbino A, Russo D, Colella M, et al. Dandelion root extract induces intracellular $Ca^{2+}$ increases in HEK293 cells. *Int J Mol Sci*. 2018;19(4):1112. doi:10.3390/ijms19041112
20. Soares-Silva M, Diniz FF, Gomes GN, Bahia D. The mitogen-activated protein kinase (MAPK) pathway: Role in immune evasion by trypanosomatids. *Front Microbiol*. 2016;7:183. doi:10.3389/fmicb.2016.00183
21. Peti W, Page R. Molecular basis of MAP kinase regulation. *Protein Sci*. 2013;22(12):1698–1710. doi:10.1002/pro.2374
22. Setia S, Nehru B, Sanyal SN. Upregulation of MAPK/Erk and PI3K/Akt pathways in ulcerative colitis-associated colon cancer. *Biomed Pharmacother.* 2014;68(8):1023–1029. doi:10.1016/j.biopha.2014.09.006
23. Shi L, Lin Q, Li X, et al. Alliin, a garlic organosulfur compound, ameliorates gut inflammation through MAPK-NF-κB/AP-1/STAT-1 inactivation and PPAR-γ activation. *Mol Nutr Food Res*. 2017;61(9):1601013. doi:10.1002/mnfr.201601013
24. Sroufe IA, Gardner T, Bresnahan KA, Quarnberg SM, Wiedmeier PR. Insights into the pathophysiology of ulcerative colitis: Interleukin-13 modulates STAT6 and p38 MAPK activity in the colon epithelial sodium c hannel. *J Physiol.* 2017;595(2):421–422. doi:10.1113/JP272492
25. Ge BJ, Zhao P, Li HT, et al. *Taraxacum mongolicum* protects against *Staphylococcus aureus*-infected mastitis by exerting anti-inflammatory role via TLR2-NF-κB/MAPKs pathways in mice. *J Ethnopharmacol.* 2021;268:113595. doi:10.1016/j.jep.2020.113595
26. Lai J, Peng L, Chen H, et al. Amino acid sequence identification and anti-inflammatory potency evaluation of dandelion oligopeptides in LPS-induced RAW264. 7 macrophage cells. *J Mol Struct*. 2020;1216:128280. doi:10.1016/j.molstruc.2020.128280
27. Xiong H, Cheng Y, Zhang X, Zhang X. Effects of taraxasterol on iNOS and COX-2 expression in LPS-induced RAW 264.7 macrophages. *J Ethnopharmacol.* 2014;155(1):753–757. doi:10.1016/j.jep.2014.06.023
28. González-Ramírez AE, González-Trujano ME, Hernandez-Leon A, et al. Limonene from *Agastache mexicana* essential oil produces antinociceptive effects, gastrointestinal protection and improves experimental ulcerative colitis. *J Ethnopharmacol.* 2021;280:114462. doi:10.1016/j.jep.2021.114462
29. Halem HA, Hochgeschwender U, Rih JK, et al. TBR-760, a dopamine-somatostatin compound, arrests growth of aggressive nonfunctioning pituitary adenomas in mice. *Endocrinology*. 2020;161(8):bqaa101. doi:10.1210/endocr/bqaa101
30. Gruszka A, Culler MD, Melmed S. Somatostatin analogs and chimeric somatostatin–dopamine molecules differentially regulate human growth hormone and prolactin gene expression and secretion in vitro. *Mol Cell Endocrinol.* 2012;362(1–2):104–109. doi:10.1016/j.mce.2012.05.020
31. Chen X, Shi M, Tong X, et al. Glycosylation-dependent opsonophagocytic activity of staphylococcal protein A antibodies. *Proc Natl Acad Sci U S A*. 2020;117(37):22992–23000. doi:10.1073/pnas.2003621117
32. Zhang H, Zhang ZH, Song GM, et al. Development of an XBP1 agonist, HLJ2, as a potential therapeutic agent for ulcerative colitis. *Eur J Pharm Sci*. 2017;109:56–64. doi:10.1016/j.ejps.2017.07.028
33. Dai M, Wang F, Zou Z, Xiao G, Chen H, Yang H. Metabolic regulations of a decoction of *Hedyotis diffusa* in acute liver injury of mouse models. *Chin Med.* 2017;12(1):35. doi:10.1186/s13020-017-0159-4
34. Pang R, Zhou H, Huang Y, Su Y, Chen X. Inhibition of host arginase activity against staphylococcal bloodstream infection by different metabolites. *Front Immunol.* 2020;11:1639. doi:10.3389/fimmu.2020.01639
35. Chen XH, Liu SR, Peng B, et al. Exogenous l-valine promotes phagocytosis to kill multidrug-resistant bacterial pathogens. *Front Immunol*. 2017;8:207. doi:10.3389/fimmu.2017.00207
36. Isik A, Soran A, Grasi A, Barry N, Sezgin E. Lymphedema after sentinel lymph node biopsy: Who is at risk? [published online as ahead of print on June 30, 2021]. *Lymphat Res Biol.* 2021. doi:10.1089/lrb.2020.0093
37. Yap BW, Sim CH. Comparisons of various types of normality tests. *J Stat Comput Simul*. 2011;81(12):2141–2155. doi:10.1080/00949655.2010.520163
38. Isik A, Isik N, Kurnaz E. Complete breast autoamputation: Clinical image. *Breast J.* 2020;26(11):2265–2266. doi:10.1111/tbj.14072
39. Taya S, Kakehashi A, Wongpoomchai R, Gi M, Ishii N, Wanibuchi H. Preventive effects of *Spirogyra neglecta* and a polysaccharide extract against dextran sodium sulfate induced colitis in mice. *Asian Pac J Cancer Prev*. 2016;17(4):2235–2245. doi:10.7314/apjcp.2016.17.4.2235
40. Klotz U, Maier K, Fischer C, Heinkel K. Therapeutic efficacy of sulfasalazine and its metabolites in patients with ulcerative colitis and Crohn's disease. *N Engl J Med.* 1980;303(26):1499–1502. doi:10.1056/NEJM198012253032602
41. Kitajima S, Takuma S, Morimoto M. Histological analysis of murine colitis induced by dextran sulfate sodium of different molecular weights. *Exp Anim*. 2000;49(1):9–15. doi:10.1538/expanim.49.9

42. Lu MC, Ji JA, Jiang YL, et al. An inhibitor of the Keap1-Nrf2 protein-protein interaction protects NCM460 colonic cells and alleviates experimental colitis. *Sci Rep*. 2016;6(1):26585. doi:10.1038/srep26585
43. Li MC, He SH. IL-10 and its related cytokines for treatment of inflammatory bowel disease. *World J Gastroenterol*. 2004;10(5):620–625. doi:10.3748/wjg.v10.i5.620
44. Ip WKE, Hoshi N, Shouval DS, Snapper S, Medzhitov R. Anti-inflammatory effect of IL-10 mediated by metabolic reprogramming of macrophages. *Science*. 2017;356(6337):513–519. doi:10.1126/science.aal3535
45. Liang Y, Zhou Y, Shen P. NF-kappaB and its regulation on the immune system. *Cell Mol Immunol*. 2004;1(5):343–350. PMID:1625893.
46. Ginn-Pease ME, Whisler RL. Redox signals and NF-κB activation in T cells. *Free Radic Biol Med*. 1998;25(3):346–361. doi:10.1016/s0891-5849(98)00067-7
47. Xu L, Yu Y, Sang R, Li J, Ge B, Zhang X. Protective effects of taraxasterol against ethanol-induced liver injury by regulating CYP2E1/Nrf2/HO-1 and NF-κB signaling pathways in mice. *Oxid Med Cell Longev*. 2018;2018:8284107. doi:10.1155/2018/8284107
48. Zhang ZH, Mi C, Wang KS, et al. Chelidonine inhibits TNF-α-induced inflammation by suppressing the NF-κB pathways in HCT116 cells. *Phytother Res*. 2018;32(1):65–75. doi:10.1002/ptr.5948
49. Ma L, Liu H, Xie Z, et al. Ginsenoside Rb3 protects cardiomyocytes against ischemia-reperfusion injury via the inhibition of JNK-mediated NF-κB pathway: A mouse cardiomyocyte model. *PloS One*. 2014;9(8):e103628. doi:10.1371/journal.pone.0103628

# Effect of obesity on fertility parameters in WIO mice model

Naif Alsuhaymi[A,B,D]

Department of Emergency Medical Services, College of Health Sciences in Al-Qunfudhah, Umm Al-Qura University, Makkah, Saudi Arabia

A – research concept and design; B – collection and/or assembly of data; C – data analysis and interpretation;
D – writing the article; E – critical revision of the article; F – final approval of the article

Advances in Clinical and Experimental Medicine, ISSN 1899–5276 (print), ISSN 2451–2680 (online) *Adv Clin Exp Med*. 2022;31(5):539–546

**Address for correspondence**
Naif Alsuhaymi
E-mail: nasuhaymi@uqu.edu.sa

**Funding sources**
None declared

**Conflict of interest**
None declared

**Acknowledgements**
The author would like to thank Dr. Ahmed Darwish and Dr. Abd El-Nasser Khattab from Biotechnology Research Institute, Cairo, Egypt, for their assistance in caring of the animal models during experiments at the animal house.

Received on April 13, 2021
Reviewed on October 24, 2021
Accepted on January 3, 2022

Published online on January 29, 2022

## Abstract

**Background.** Male infertility is mostly due to low sperm quality, which accounts for about 50% of the causes of infertility. The reasons for low sperm quality are still unclear. Nowadays, many drinks contain high levels of fat, and its effect on fertility is not yet known.

**Objectives.** To investigate the effect of cholesterol-containing water on male fertility.

**Materials and methods.** Forty BALB/c male mice were divided into 2 groups: the control group and the water-induced obesity (WIO) group. Body and testicular weights were recorded and analyzed statistically. Testicular tissues were examined. Serum contents of total cholesterol (TC), triglycerides (TG), low-density lipoprotein (LDL), free testosterone (FT), luteinizing hormone (LH), and follicle-stimulating hormone (FSH) were determined. Motility count and morphology of sperm were analyzed. Real-time polymerase chain reaction (RT-PCR) was performed for *SYCP3*, *VEGFA* and *WT1* genes.

**Results.** The results showed that the WIO group presented the highly significant values for mice body and testis weight, and TC, TG and LDL level in serum ($p < 0.05$), when compared to the control group. The level of FT, LH and FSH in serum was significantly decreased ($p < 0.05$) in the WIO group compared with the control group. Seminiferous tubules of testes became thin, and Sertoli cells showed mild atrophy in this group. Also, the count and motility of sperm significantly reduced while the ratio of sperm abnormalities significantly increased in the WIO group compared with the control group ($p < 0.05$). The results of RT-PCR showed that *SYCP3*, *VEGFA* and *WT1* genes were significantly downregulated ($p < 0.05$) in the WIO group compared with the control group.

**Conclusions.** This study indicated that drinks containing high levels of fat may have negative effects on male fertility due to the reduction of the sexual hormones level in serum, the expression of *SYCP3*, *VEGFA* and *WT1* genes, count and motility of sperm, as well as an increase in sperm abnormalities and pathological changes in the testicular tissues.

**Key words:** obesity, gene expression, mice, fertility

**Cite as**
Alsuhaymi N. Effect of obesity on fertility parameters in WIO mice model. *Adv Clin Exp Med*. 2022;31(5):539–546. doi:10.17219/acem/145510

**DOI**
10.17219/acem/145510

## Background

The synaptonemal complex (SC) holds homologous chromosomes during the prophase of the first meiotic division[1] and is essential for synapsis and meiotic recombination.[2] Meiotic failure, infertility and embryonic death of mice occur due to the disruption of SC formation.[3] The defective construction of SC correlates with miscarriage, infertility and Down's syndrome in humans.[4] The *SYCP3* gene is the main constituent of the SC and plays a vital role in the meiosis of spermatogenesis, as well as fertility and homologous chromosome pairing in males.[5] Vascular endothelial growth factor A (*VEGFA*) has been expressed in semen, seminal vesicles, prostate, and normal testis.[6] The *VEGFA* is vital for blood vessel development and endothelial cell migration. In addition, it regulates the spermatogonial stem cell pool and male reproductive lifespan.[7] Wilms' tumor gene (*WT1*) has been expressed in testis, kidneys and ovaries.[8] It has an important role in ovarian follicle development[9] and spermatogenesis.[10]

Previous studies indicated that obesity correlated with infertility; it has been observed that bodyweight is significantly increased in patients with male factor infertility.[11] In recent years, overweight in adults males was correlated with low semen quality.[12,13] Obesity has been associated with subfertility and was shown to be related to long waiting time to pregnancy.[14] Over the past half-century, several scientific reports had proven that the decrease in semen quality and male reproductive capacity has occurred in parallel with the increase in obesity rates,[15] indicating the need to focus on the probability of obesity as a cause of male infertility and reduction in fecundity. Testosterone deficiency may contribute to a decrease in semen quality and total sperm count in obese men.[16] The previous epidemiological studies suggested a significant negative association between high body mass index (BMI) and the semen parameters, involving semen volume,[17] and sperm concentration,[18] motility[19] and morphology.[20] Spermatogenesis is affected by altered levels of sex hormones in obese men, such as decreased free or total testosterone levels and increased estradiol levels in serum.[21] Moreover, diet-induced obesity increases the DNA fragmentation index in spermatozoa, causing clear weakening of male fertility.[22]

The previous studies demonstrated the negative effect of high-fat-diet-induced obesity on fertility, but the mechanism of how obesity can cause male subfertility was poorly characterized. In this study, we initially established water-induced obesity (WIO) model in order to determine whether obesity affects the decline of male fertility as well as serum reproductive hormone levels, sperm morphology, and/or disrupts testicular morphology and expression of some genes related to male fertility.

## Objectives

Although changes in the sexual hormones and the count, motility and quality of sperm, as well as testicular histopathology accompanied by increasing adiposity have been identified by several previous studies on high-fat diet, the effect of WIO on the sexual hormones level and count, motility and morphology of sperm, testicular histopathology and gene expression related fertility remain unknown. Also, to our knowledge, this is the first study focusing on the effect of obesity on the expression of *SYCP3*, *VEGFA* and *WT1* genes in testis.

## Materials and methods

### WIO model

To study the effect of obesity on the expression of some genes related to fertility, BALB/c mice model was developed, in which obesity was enhanced by adding 0.5 g of cholesterol and 0.1 g of ox gall to 400 mL of drinking water manipulation, in order to model the human condition. After BALB/c mice were given drinking water containing a high level of cholesterol for 70 days, the WIO model was successfully established.

### Experimental design

The experimental procedure used in this investigation was approved by the Animal Care and Use Committee of National Research Centre (Cairo, Egypt; approval No. NRCE-CBD1992020). Forty BALB/c male mice aged 2 weeks, weighing 21–25 g, were divided into 2 groups; each group included 20 mice housed in cages maintained at 22 ±2°C with 50 ±5% humidity and 12 h light/dark cycle. The control group was fed normal diet for 70 days; the WIO group was fed normal diet and 0.5 g of cholesterol with 0.1 g of ox gall in 400 mL of drinking water for 70 days. During this period, individual body weight for the 2 groups was measured every 2 weeks. At the end of experiment, all mice were sacrificed by neck vertebra luxation. The testes of each mouse were taken and weighted; one testis was stored in 10% formalin for the histopathological examination, and the second testis was stored in –80°C for the examination of gene expression.

### Measurement of lipid profile and sexual hormones

Blood samples were collected from the eyes of all mice from the control group and the WIO group at the end of the experiment, and then centrifuged at 5000 rpm for 10 min to collect serum. A specific kit (MAK045, RAB0734) bought from Sigma-Aldrich (St. Louis, USA)

was used to measure total cholesterol (TC), triglycerides (TG) and low-density lipoprotein (LDL) levels at 546 nm with a spectrophotometer (UV-240; Shimadzu, Kyoto, Japan). Free testosterone (FT), luteinizing hormone (LH) and follicle-stimulating hormone (FSH) levels were determined using competitive immunoassay technique.[23]

## Testicular histopathology

Testicular tissue samples were taken from all mice from the control group and the WIO group. The samples were fixed in 10% formalin, processed and stained with hematoxylin and eosin (H&E). Histopathological studies using light microscopy and photomicrographs were made.

## Sperm parameter

At the end of the experiment and after sacrificing the mice, the epididymides were removed from each mouse. Then, sperm was collected in Petri dish containing 1 mL of phosphate buffered saline at 37°C through cutting cauda of epididymides. Motility and count of spermatozoa were calculated using hemocytometer and a drop of a homogenate smeared on a cleaned slide. These slides were left to dry and coded, and then stained with approx. 0.05% aqueous eosin Y solution. About 1000 sperm cells were examined to detect morphological abnormalities in sperm head and tail for each mouse.

## Gene expression

Testicular tissues were homogenized using a homogenizer (Z722375, IKA 3703100; Thermo Fisher Scientific), and suspended in TRIzol® (Thermo Fisher Scientific) in order to extract total RNA for quantitative real-time polymerase chain reaction (qRT-PCR). The NanoDrop spectrophotometer (Thermo Fisher Scientific, Waltham, USA) was used to measure the quantity and quality of RNA. The cDNA synthesis was performed using COSMO cDNA synthesis kit (WF10205002; Willowfort, Birmingham, UK), according to the manufacturer's instruction. Real-time polymerase chain reaction was performed on 4 host genes (*SYCP3*, *VEGFA*, *WT1*, and *β-actin*). The primers were designed using National Center for Biotechnology Information (NCBI) primer BLAST, and checked using Oligo v. 7 (Molecular Biology Insights, Inc. (DBA Oligo, Inc.), Colorado Springs, USA). All primers were synthesized by Macrogen, Inc. (Seoul, South Korea) (Table 1). The gene expression was normalized to mice β-actin and analyzed using EvaGreen® qPCR Mix Plus (ROX) (Solis BioDyne, Tartu, Estonia) using Stratagene Mx3000P RT-PCR system (Agilent Technologies, Santa Clara, USA).

## Statistical analyses

There are 3 different types of data obtained from the experiment. Non-normal data distribution (sperm morphology) was analyzed using Mann–Whitney test. Normal data distribution had unequal variances between the groups (FT and FSH analysis, and the 1st week, 2nd week, 6th week and 8th week body weight measurement) and was analyzed using Welch's test. Normal data distribution had equal variances in the group (lipid profile, LH and the other measurements of body weight) and was analyzed using independent t-test. The normality distribution was tested using Shapiro–Wilk test (SPSS v. 18 software (SPSS Inc., Chicago, USA)). The analyses of the relative quantification by RT-PCR were performed using the $2^{-\Delta\Delta CT}$ value method. The value of $p < 0.05$ was considered statistically significant.

# Results

## Body and testicular weight

Forty mice were included in the experiment, divided into a control group (n = 20, weight: mean ± standard deviation (SD) = 23.3 ±0.51 g) and a WIO group (n = 20, 23.2 ±0.5 g), and they did not present any significant differences in body weight between the 2 groups. During the first 7 days, mice body weight non-significantly increased in the WIO group (25 ±0.3 g) compared with the control group (24.6 ±0.5 g). The difference in body weight of mice between the WIO and control became significant after 2 weeks (14 days) of drinking water provided to them, and persisted for the subsequent 70 days

Table 1. Sequence of primers

| Gene | Accession No. | Nucleotide sequence 5′–3′ | Size |
|---|---|---|---|
| *SYCP3* | NM_011517.2 | F-GACAGCGACAGCTCACCGG<br>R-GGTGGCTTCCCAGATTTCCCAGA | 90 |
| *VEGFA* | NM_001025257.3 | F-TGCTCTCTTGGGTGCACTGGAC<br>R-GACGGCAGTAGCTTCGCTGGT | 147 |
| *WT1* | NM_144783.2 | F-GGCGCTTTGAGGGGTCCGAC<br>R-AAAGTGGGCGGAGCACCGAC | 205 |
| *β-actin* | NM_007393.5 | F 5′-GGCACCACACCTTCTACAATG-3′<br>R 5′-GGGGTGTTGAAGGTCTCAAAC-3′ | 133 |

Table 2. Body and testicular weight of mice

| Weight measured | Weight time | Groups (mean ±SD) | | p-value | 95% CI of the difference | |
|---|---|---|---|---|---|---|
| | | control (n = 20) | WIO (n = 20) | | lower | upper |
| Body weight | zero time | 23.3 ±0.55 | 23.2 ±0.5 | 0.6261[t] | –0.2495 | 0.4095 |
| | 7 days | 24.62 ±0.3 | 25 ±0.58 | 0.0673[w] | –0.5811 | 0.0211 |
| | 14 days | 25.9 ±0.53 | 28.2 ±0.3 | 0.0001[w] | –2.5145 | –1.9655 |
| | 28 days | 27.7 ±0.48 | 30.1 ±0.43 | 0.0001[t] | –2.6755 | –2.0845 |
| | 42 days | 28.9 ±0.14 | 30.2 ±0.31 | 0.0001[w] | –1.4255 | –1.1145 |
| | 56 days | 27.9 ±0.62 | 31.2 ±0.29 | 0.0001[w] | –2.5405 | –1.9195 |
| | 70 days | 28.7 ±0.5 | 31.8 ±0.52 | 0.0001[t] | –3.4195 | –2.7605 |
| Testicular weight | after death | 0.1 ±0.03 | 0.12 ±0.02 | 0.0151[t] | –0.0377 | –0.0043 |

SD – standard deviation; WIO – water-induced obesity; [t] – t-test; [w] – Welch's test; 95% CI – 95% confidence interval. Values are considered highly significant at $p < 0.01$. Values are considered significant at $p < 0.05$.

($p < 0.001$). Also, testicular weight significantly increased in the WIO group (n = 20, 0.12 ±0.02) compared with the control group (n = 20, 0.1 ±0.003) (Table 2).

## Lipid profile and sexual hormones

Five replicates of serum samples were used to determine TC, TG, LDL, FT, FSH, and LH levels in each group, and each replicate was collected from 4 mice. Total cholesterol (230.2 ±5.8 mg/dL), TG (210.4 ±5.6 mg/dL) and LDL (135.8 ±2.2 mg/dL) significantly increased in the WIO group compared with the control group (125.2 ±3.9 mg/dL, 98.8 ±4.2 mg/dL and 50 ±2.7 mg/dL, respectively). Free testosterone (0.1 ±0.01 pg/dL), FSH (0.04 ±0.03 pg/dL) and LH (0.02 ±0.01 pg/dL) significantly decreased in the WIO group compared with the control group (30.8 ±1.3 pg/dL, 1 ±0.16 pg/dL, and 0.02 ±0.03 pg/dL, respectively) (Table 3).

## Sperm motility and count

Sperm motility was reduced by 50% in the WIO group compared with the control group. Sperm count of obese mice was recorded as $16 \times 10^6$/mL, while for the control group it was $40 \times 10^6$/mL.

## Sperm morphology

Sperm morphology was normal by 83.9% and abnormal by 16.1% in control group, while WIO group presented 58.6% normal morphology and 41.4% abnormal morphology. Median with 1st and 3rd quartile of normal sperm in WIO group was (585.5; 584,587.5), without hock abnormality (24.5; 24,25), small head (148; 146,150), amorphous head (76; 75,77), banana head (16; 15,17.75), triangle head (10; 9,12) and coiled tail (138; 137,140), compared with control group ((839; 834.4,844.1), (12.2; 11.3,13), (48; 46,50), (32; 31,32.6), (4; 3,5), (2; 1,3.75), and (62; 61,63), respectively)) (Table 4 and Fig. 1).

## Testicular histopathology

Testicular tissue of all mice was stained with H&E to confirm the effects of WIO on morphological changes in this tissue. The analysis of images obtained with light microscopy showed some changes that occurred in the testicular cells. The structure of the seminiferous tubules was normal and complete, with slight edema in the Leydig cells of the control group (Fig. 2A), while in the WIO group, seminiferous tubules showed mild to severe depletion of spermatozoa, spermatogonial cells showed severe sloughing, and mild atrophy of Sertoli cells has been noticed (Fig. 2B).

Table 3. Biochemical analyses of the cholesterol profile and sex hormones

| Lipid profile | Groups (mean ±SD) | | p-value | 95% CI of the difference | |
|---|---|---|---|---|---|
| | control (n = 20) | WIO (n = 20) | | lower | upper |
| Cholesterol [mg/dL] | 125.2 ±3.9 | 230.2 ±5.8 | 0.0001[t] | –112.204 | –97.798 |
| Triglycerides [mg/dL] | 98.8 ±4.2 | 210.4 ±5.6 | 0.0001[t] | –118.928 | –104.27 |
| LDL [mg/dL] | 50 ±2.7 | 135.8 ±2.2 | 0.0001[t] | –88.646 | –81.354 |
| FT [pg/mL] | 30.8 ±1.3 | 0.1 ±0.01 | 0.0001[w] | 29.339 | 32.028 |
| FSH [pg/mL] | 1 ±0.16 | 0.01 ±0.04 | 0.0001[w] | 0.823 | 1.150 |
| LH [pg/mL] | 0.9 ±0.03 | 0.01 ±0.01 | 0.0001[t] | 0.838 | 0.918 |

SD – standard deviation; LDL – low-density lipoprotein; FT – free testosterone; FSH – follicle stimulating hormone; LH – luteinizing hormone; [t] – t-test; [w] – Welch's test; 95% CI – 95% confidence interval; WIO – water-induced obesity. Values are considered highly significant at $p < 0.01$. Values are considered significant at $p < 0.05$.

Table 4. Sperm morphology analysis using Mann–Whitney test for nonparametric data

| Sperm morphology | Control (median (Q1, Q3)) | WIO (median (Q1, Q3)) | z-value | p-value |
|---|---|---|---|---|
| Normal | 839 (834.4, 844.1) | 585.5 (584, 587.5) | –5.436 | 0.0001 |
| Without hock | 12.2 (11.3, 13) | 24.5 (24, 25) | –5.436 | 0.0001 |
| Small head | 48 (46, 50) | 148 (146, 150) | –5.436 | 0.0001 |
| Amorphous head | 32 (31, 32.6) | 76 (75, 77) | –5.436 | 0.0001 |
| Banana head | 4 (3, 5) | 16 (15, 17.75) | –5.438 | 0.0001 |
| Triangle head | 2 (1, 3.75) | 10 (9, 12) | –5.441 | 0.0001 |
| Coiled tail | 62 (61, 63) | 138 (137, 140) | –5.441 | 0.0001 |

Q1 – 1st quartile; Q3 – 3rd quartile; WIO – water-induced obesity.

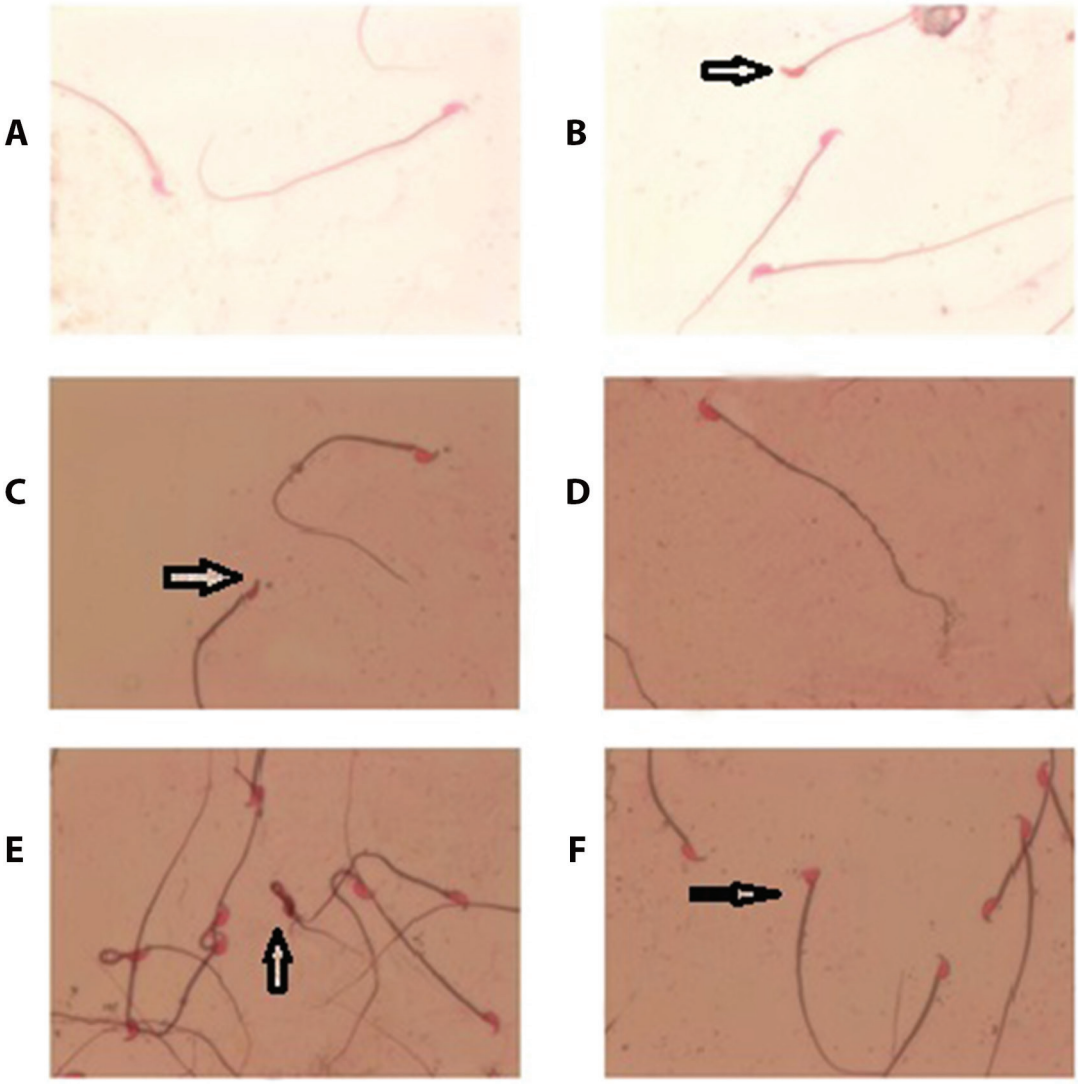


Fig. 1. Sperm morphology. A. Normal sperm; B. Banana head; C. Small head; D. Without hock; E. Coiled tail; F. Triangle head

## Gene expression

Expressions of *VEGFA* gene (0.28) and *SYCP3* gene (0.48) were highly significantly downregulated in the WIO group compared with the control group. At the same time, the expression of *WT1* gene (0.8) was significantly downregulated in the WIO group compared with the control group (Fig. 3).

## Discussion

Infertility is one of the causes of psychological problems for people and production deficiency in farm animals. Based on epidemiological data, an average of 10% of the world's population of the reproductive age suffers from infertility.[24] Fifty percent of cases of male infertility occur due to the low quality of sperm, which has become a source

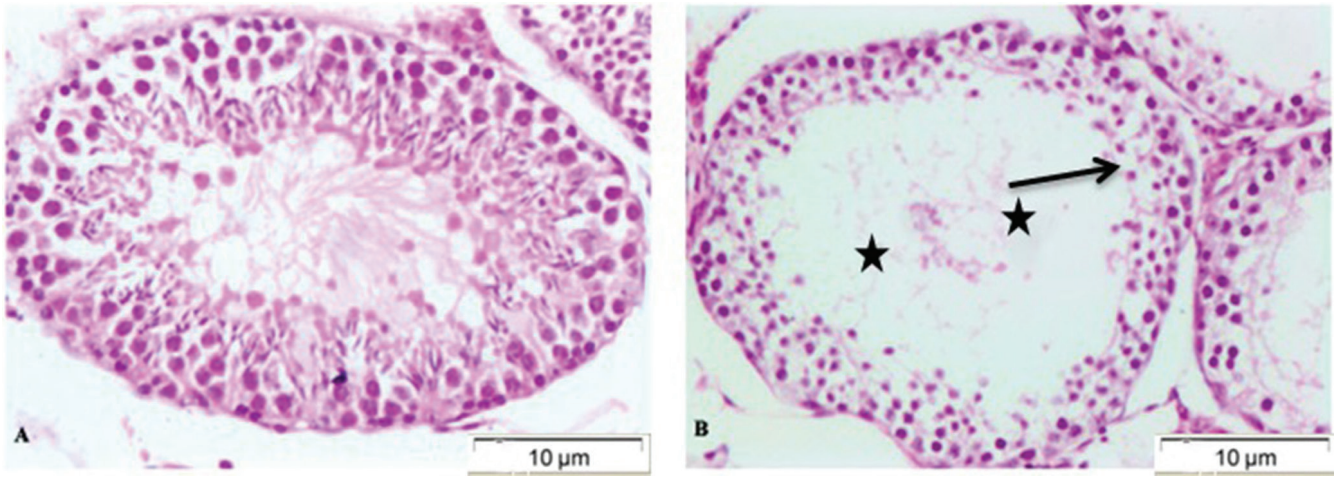


Fig. 2. Photomicrographs of hematoxylin and eosin (H&E)-stained testicular sections. A. Testis of control group; B. Testis of water-induced obesity (WIO) group. Black star indicates mild to severe depletion of spermatozoa, while black arrow shows severe sloughing

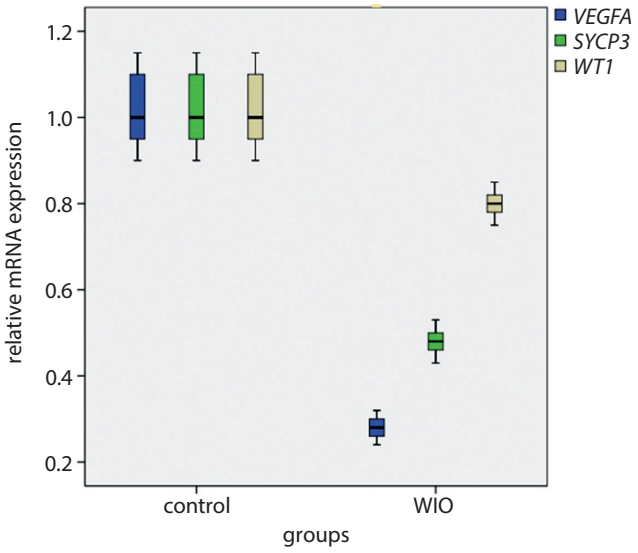


Fig. 3. Expression of *VEGFA* gene (0.28 ±0.03, p = 0.0012), *SYCP3* gene (0.48 ±0.02, p = 0.0015) and *WT1* gene (0.8 ±0.04, p = 0.0324) in the water-induced obesity (WIO) group compared with the control group. Top rectangle represents upper quartile, bottom rectangle represents lower quartile, center line represents median value, plus bar represents maximum value, and minus bar represents minimum value

of concern in the world.[25] Several studies reported the association between obesity and male infertility.[11] The high-fat diet may have a critical role in metabolic diseases, causing an increase in TC, LDL and high-density lipoprotein (HDL) levels, accompanied by a significant body weight gain. In a study by Fan et al., the increase of body weight in mice fed on a high-fat diet became significant after 3 weeks.[26] Dardmeh et al.[27] found that an increase of body weight of mice fed a high-fat diet became significant after 4 weeks. Moreover, testicular weight significantly increased in these mice compared with the control group. In the present study, the body weight of the WIO group mice significantly increased compared with the control group after 2 weeks. Also, the testicular weight showed a significant increase in the WIO group. The serum contents of TC, TG and LDL in the WIO group increased significantly in comparison with the control group. Total cholesterol, TG and LDL significantly increased in mice fed a high-fat diet.[28] In obese and hyperlipidemic mice, the level of testosterone hormone in serum was significantly decreased, and the same results were shown in humans.[29] In the present study, the TH level in serum significantly decreased in the WIO group compared with the control group. This is probably due to the harmful and degenerative effects of high cholesterol levels on the secretory ability of Leydig and Sertoli cells.[30] Also, our results showed a significant reduction of LH and FSH in WIO group compared with the control group, in agreement with the previous studies on diet-induced obese (DIO) mice model.[27] The decrease in LH and FSH levels may be correlated with the alteration of androgens to estradiol, resulting in increased serum estrogen levels.[31] The higher levels of estradiol in DIO models decrease the production and secretion of LH and FSH, causing a reduced testicular function and the testosterone production.[32] Also, it was suggested that exuberant estradiol has direct harmful effect on spermatogenesis.[32] In this study, we found that count and motile of sperm significantly decreased in the WIO group compared with the control group. In addition, the presence of abnormalities in shape of sperm head and tail in WIO group was significantly higher than in the control group, in which a significantly higher percentage of immotile sperm was recorded,[33] altering the spermatogenesis process and affecting sperm maturation.[31] The percentage of progressively and nonprogressively motile sperm significantly decreased in the high-fat diet group, which recorded the significantly higher percentage of immotile sperm.[34] Although many studies have been conducted to investigate the negative effect of obesity on fertility, sperm quality, quantity and motility, as well as its effect on sexual hormones, there is not a single study on the effect of obesity on the expression of genes associated with fertility. The *SYCP3* plays

an important role in meiosis of spermatogenesis and fertility.[5] Mice deficient in *SYCP3* fail to establish synapses, leading to meiotic disruption during male spermatogenesis.[35] The *VEGFA* regulates spermatogonial stem cell pool and male reproductive lifespan.[7] The *VEGFA* is the first selective tissue-angiogenic molecule that stimulates the existence and proliferation of the endothelial cells of testis, and may aid in the entry of hormones into the vascular system.[36] The *WT1* gene is associated with ovarian follicle development[9] and spermatogenesis.[10] In the present study, the expressions of *VEGFA*, *SYCP3* and *WT1* genes were significantly decreased in the WIO group compared with the control group. In addition, histological analysis of obese mice testis showed the leanness of the seminiferous tubules, a clear deterioration of sperm cells within the seminiferous tubules with the formation of seminal giant cells, interstitial edema, and necrosis of Leydig cells. The *VEGFA* isoforms produced by Sertoli and germ cells are needed to maintain sperm quality and normal fertility.[37] These results may help in explaining the relationship between the pathological changes in testicular tissues of obese mice and the downregulation of *VEGFA*, *SYCP3* and *WT1* genes.

## Limitations

In this study, we encountered 1 limitation. The amount of blood taken from each mouse was small, and therefore the volume of serum extracted from it would also be very small and insufficient for all biochemical analyses. Thus, the solution was to collect 4 blood samples from each group into 1 tube, providing 5 replicates for each group. Although we could not obtain results of all biochemical analyses from each animal individually, the outcome of our study is consistent with the previous studies about the effect of obesity on the level of the sexual hormones and TC, TG, LDL, and HDL in serum.

# Conclusions

Water-induced obesity led to an increase in body and testicular weight, and in the serum content of TC, TG, and LDL. In addition, it reduced the level of FT, LH and FSH in serum. Seminiferous tubules of obese mice testis became thin and showed mild to severe depletion of spermatozoa. Also, Sertoli cells showed mild atrophy. The WIO caused the downregulation in the expression of *SYCP3*, *VEGFA* and *WT1* genes associated with spermatogenesis, the abnormality in the sperm shape of either head or tail, and reduced count and motility of sperm. Therefore, this study recommends limiting the amount of drinks containing high percentage of fat.

### ORCID iDs

Naif Alsuhaymi https://orcid.org/0000-0002-6011-745X

## References

1. Syrjänen JL, Pellegrini L, Davies OR. A molecular model for the role of SYCP3 in meiotic chromosome organisation. *Elife*. 2014;3:e02963. doi:10.7554/eLife.02963
2. Cahoon CK, Hawley RS. Regulating the construction and demolition of the synaptonemal complex. *Nat Struct Mol Biol*. 2016;23(5):369–377. doi:10.1038/nsmb.3208
3. Kouznetsova A, Benavente R, Pastink A, Hoog C. Meiosis in mice without a synaptonemal complex. *PLoS One*. 2011;6(12):e28255. doi:10.1371/journal.pone.0028255
4. Bolor H, Mori T, Nishiyama S, et al. Mutations of the *SYCP3* gene in women with recurrent pregnancy loss. *Am J Hum Genet*. 2009;84(1):14–20. doi:10.1016/j.ajhg.2008.12.002
5. Syrjänen JL, Heller I, Candelli A, et al. Single-molecule observation of DNA compaction by meiotic protein SYCP3. *eLife*. 2017;6:e22582. doi:10.7554/eLife.22582.001
6. Huminiecki L, Chan HY, Lui S, et al. Vascular endothelial growth factor transgenic mice exhibit reduced male fertility and placental rejection. *Mol Hum Reprod*. 2001;7(3):255–264. doi:10.1093/molehr/7.3.255
7. Caires KC, de Avila JM, Cupp AS, McLean DJ. VEGFA family isoforms regulate spermatogonial stem cell homeostasis in vivo. *Endocrinology*. 2012;153(2):887–900. doi:10.1210/en.2011-1323
8. Genetics Home Reference. WT1 gene. https://ghr.nlm.nih.gov/gene/WT1. Accessed October 20, 2016.
9. Nathan A, Reinhardt P, Kruspe D, et al. The Wilms tumor protein Wt1 contributes to female fertility by regulating oviductal proteostasis. *Hum Mol Genet*. 2017;26(9):1694–1705. doi:10.1093/hmg/ddx075
10. Wang XN, Li ZS, Ren Y, et al. The Wilms tumor gene, *Wt1*, is critical for mouse spermatogenesis via regulation of sertoli cell polarity and is associated with non-obstructive azoospermia in humans. *PLoS Genet*. 2013;9(8):e1003645. doi:10.1371/journal.pgen.1003645
11. Magnusdottir EV, Thorsteinsson T, Thorsteinsdottir S, Heimisdottir M, Olafsdottir K. Persistent organochlorines, sedentary occupation, obesity and human male subfertility. *Hum Reprod*. 2005;20(1):208–215. doi:10.1093/humrep/deh569
12. Fejes I, Koloszár S, Závaczki Z, Daru J, Szöllösi J, Pál A. Effect of body weight on testosterone/estradiol ratio in oligozoospermic patients. *Arch Androl*. 2006;52(2):97–102. doi:10.1080/01485010500315479
13. Hammoud AO, Wilde N, Gibson M, Parks A, Carrell DT, Meikle AW. Male obesity and alteration in sperm parameters. *Fertil Steril*. 2008;90(6):2222–2225. doi:10.1016/j.fertnstert.2007.10.011
14. Ramlau-Hansen CH, Thulstrup AM, Nohr EA, Bonde JP, Sørensen TIA, Olsen J. Subfecundity in overweight and obese couples. *Hum Reprod*. 2007;22(6):1634–1637. doi:10.1093/humrep/dem035
15. Jungheim ES, Travieso JL, Carson KR, Moley KH. Obesity and reproductive function. *Obstet Gynecol Clin North Am*. 2012;39(4):479–493. doi:10.1016/j.ogc.2012.09.002
16. Giagulli VA, Kaufman JM, Vermeulen A. Pathogenesis of the decreased androgen levels in obese men. *J Clin Endocrinol Metab*. 1994;79(4):997–1000. doi:10.1210/jcem.79.4.7962311
17. Chavarro JE, Toth TL, Wright DL, Meeker JD, Hauser R. Body mass index in relation to semen quality, sperm DNA integrity, and serum reproductive hormone levels among men attending an infertility clinic. *Fertil Steril*. 2010;93(7):2222–2231. doi:10.1016/j.fertnstert.2009.01.100
18. Paasch U, Grunewald S, Kratzsch J, Glander HJ. Obesity and age affect male fertility potential. *Fertil Steril*. 2010;94(7):2898–2901. doi:10.1016/j.fertnstert.2010.06.047
19. Martini AC, Tissera A, Estofán D, et al. Overweight and seminal quality: A study of 794 patients. *Fertil Steril*. 2010;94(5):1739–1743. doi:10.1016/j.fertnstert.2009.11.017
20. Shayeb AG, Harrid K, Mathers E, Bhattacharya S. An exploration of the association between male body mass index and semen quality. *Reprod Biomed Online*. 2011;23:717–723. doi:10.1016/j.rbmo.2011.07.018
21. Liu Y, Zhao W, Gu G, et al. Palmitoyl-protein thioesterase 1 (PPT1): An obesity-induced rat testicular marker of reduced fertility. *Mol Reprod Dev*. 2014;81(1):55–65. doi:10.1002/mrd.22281
22. Kort HI, Massey JB, Elsner CW, et al. Impact of body mass index values on sperm quantity and quality. *J Androl*. 2006;27(3):450–452. doi:10.2164/jandrol.05124

23. Sharma V, Boonen J, Chauhan NS, Thakur M, De Spiegeleer B, Dixit VK. *Spilanthes acmella* ethanolic flower extract: LC-MS alkylamide profiling and its effects on sexual behavior in male rats. *Phytomedicine*. 2011;18(13):1161–1169. doi:10.1016/j.phymed.2011.06.001
24. Hull MG, Glazener CM, Kelly NJ, et al. Population study of causes, treatment, and outcome of infertility. *Br Med J (Clin Res Ed)*. 1985; 291(6510):1693–1697. doi:10.1136/bmj.291.6510.1693
25. Ljiljak D, Milaković TT, Severinski NS, Kuna KB, Radojčić A. Sperm cell in ART. In: Wu B, ed. *Advances in Embryo Transfer*. IntechOpen; 2012: 65–73. https://www.intechopen.com/chapters/32055. Accessed April 5, 2012.
26. Fan Y, Liu Y, Xue K, et al. Diet-induced obesity in male C57BL/6 mice decreases fertility as a consequence of disrupted blood-testis barrier. *PLoS One*. 2015;10(4):1–15. doi:10.1371/journal.pone.0120775
27. Dardmeh F, Alipour H, Gazerani P, Van der Horst G, Brandsborg E, Nielsen HI. *Lactobacillus rhamnosus* PB01 (DSM 14870) supplementation affects markers of sperm kinematic parameters in a diet-induced obesity mice model. *PLoS One*. 2017;12(10):e0185964. doi:10.1371/journal.pone.0185964
28. Williams LM, Campbell FM, Drew JE, et al. The development of diet-induced obesity and glucose intolerance in C57Bl/6 mice on a high-fat diet consists of distinct phases. *PLoS One*. 2014;9(8):e106159. doi:10.1371/journal.pone.0106159
29. Pauli EM, Legro RS, Demers LM, Kunselman AR, Dodson WC, Lee PA. Diminished paternity and gonadal function with increasing obesity in men. *Fertil Steril*. 2008;90(2):346–51. doi:10.1016/j.fertnstert.2007.06.046
30. Pinto-Fochi ME, Pytlowanciv EZ, Reame V, et al. A high-fat diet fed during different periods of life impairs steroidogenesis of rat Leydig cells. *Reproduction*. 2016;152(6):795–808. doi:10.1530/REP-16-0072
31. Palmer NO, Bakos HW, Fullston T, Lane M. Impact of obesity on male fertility, sperm function and molecular composition. *Spermatogenesis*. 2012;2(4):253–263. doi:10.4161/spmg.21362
32. Pavlovich CP, King P, Goldstein M, Schlegel PN. Evidence of a treatable endocrinopathy in infertile men. *J Urol*. 2001;165(3):837–841. PMID:11176482.
33. Bieniek JM, Kashanian JA, Deibert CM, et al. Influence of increasing body mass index on semen and reproductive hormonal parameters in a multi-institutional cohort of subfertile men. *Fertil Steril*. 2016;106(5):1070–1075. doi:10.1016/j.fertnstert.2016.06.041
34. Gong T, Wei QW, Mao DG, et al. Effects of daily exposure to saccharin and sucrose on testicular biologic functions in mice. *Biol Reprod*. 2016;95(6):116. doi:10.1095/biolreprod.116.140889
35. Tsutsumi M, Kogo H, Kowa-Sugiyama H, Inagaki H, Ohye T, Kurahashi H. Characterization of a novel mouse gene encoding an SYCP3-like protein that relocalizes from the XYbody to the nucleolus during prophase of male meiosis I. *Biol Reprod*. 2011;85(1):165–171. doi:10.1095/biolreprod.110.087270
36. Hoffmann P, Saoudi Y, Benharouga M, et al. Role of EG-VEGFA in human placentation: Physiological and pathological implications. *J Cell Mol Med*. 2009;13(8B):2224–2235. doi:10.1111/j.1582-4934.2008.00554.x
37. Lu N, Sargent KM, Clopton DT, et al. Loss of vascular endothelial growth factor A (VEGFA) isoforms in the testes of male mice causes subfertility, reduces sperm numbers, and alters expression of genes that regulate undifferentiated spermatogonia. *Endocrinology*. 2013; 154(12):4790–4802. doi:10.1210/en.2013-1363

# High-resolution melting PCR analysis for genotyping the gene polymorphism of *TNF-α*, *TGF-β1*, *IL-10*, and *IFN-γ* in lung transplant recipients

Hui-Jun Mu[1,A,C,D,F], Jian Zou[1,E], Ji Zhang[2,B], Hai-Ping Zhang[3,C]

[1] Center of Clinical Research, Wuxi People's Hospital of Nanjing Medical University, China
[2] Department of Lung Transplantation, Wuxi People's Hospital of Nanjing Medical University, China
[3] Department of Dermatology, Wuxi No. 2 People's Hospital of Nanjing Medical University, China

A – research concept and design; B – collection and/or assembly of data; C – data analysis and interpretation; D – writing the article; E – critical revision of the article; F – final approval of the article

Advances in Clinical and Experimental Medicine, ISSN 1899–5276 (print), ISSN 2451–2680 (online) *Adv Clin Exp Med*. 2022;31(5):547–556

**Address for correspondence**
Hai-Ping Zhang
E-mail: wxzhhp@126.com

**Funding sources**
Wuxi Administration of Science and Technology (grant No. CES00908).

**Conflict of interest**
None declared

Received on December 12, 2017
Reviewed on July 30, 2018
Accepted on January 21, 2020

Published online on January 29, 2022

**Cite as**
Mu HJ, Zou J, Zhang J, Zhang HP. High-resolution melting PCR analysis for genotyping the gene polymorphism of *TNF-α*, *TGF-β1*, *IL-10*, and *IFN-γ* in lung transplant recipients. *Adv Clin Exp Med*. 2022;31(5):547–556. doi:10.17219/acem/116757

**DOI**
10.17219/acem/116757



## Abstract

**Background.** High-resolution melting (HRM) analysis is a genotyping method which has the advantages of simple, rapid, low-cost and closed-tube operation.

**Objectives.** This study evaluated HRM analysis as an option for detecting the single nucleotide polymorphism (SNP) of cytokine, and profiled the distribution of cytokine gene polymorphism in the lung transplant recipients (LTRs).

**Materials and methods.** High-resolution melting-polymerase chain reaction (HRM-PCR) assays for genotyping tumor necrosis factor alpha (*TNF-α*) (–308 A/G), tumor growth factor beta 1 (*TGF-β1*) (+869 T/C), interleukin 10 (*IL-10*) (–592 C/A, –819 T/C, –1082 G/A), and interferon gamma (*IFN-γ*) (+874 T/A) SNPs were developed on the LightCycler® 480. The SNPs of the aforementioned cytokine genes in 322 LTRs and 266 normal controls were detected using HRM-PCR approach. To confirm the accuracy of the HRM-PCR assay, we randomly selected 100 samples from the LTRs and detected the aforementioned SNPs with sequence-specific primer-polymerase chain reaction (SSP-PCR) method, using a commercial kit.

**Results.** The data show that the HRM-PCR assay can distinguish all the cytokine SNPs, and the results of HRM-PCR analysis are in complete concordance to the genotyping results obtained using a commercial kit ($\kappa = 1.0$). Our data also show that the allele and genotype frequencies of the abovementioned cytokine are not significantly different between the LTRs and the control groups ($p > 0.05$). In addition, we found the genotypes of *TGF-β1* +869 associated with high expression phenotype were prevalent in the LTRs. On the contrary, for *TNF-α* –308, *IL-10* and *IFN-γ*, the genotypes associated with low expression phenotype were most common in the LTRs.

**Conclusions.** In this study, we described a rapid, low-cost and high-throughput HRM-PCR technology for genotyping cytokine SNPs. Our data may be utilized for future studies examining the associations of cytokine gene polymorphisms with the prognosis of the LTRs.

**Key words:** single nucleotide polymorphism, cytokine, lung transplantation, high-resolution melt analysis

# Background

Cytokines are crucial signal molecules of immune-mediated diseases and transplant complications. The individual variability in cytokine production is determined through the effect of polymorphisms within regulatory regions of cytokine genes. In general terms, we can describe high, intermediate and low cytokine producer status according to the genotype. For tumor necrosis factor alpha (*TNF-α*), at position –308 within the promoter region, A/A, A/G and T/T genotypes correlate with a high, intermediate and low *TNF-α* production, respectively.[1] Similarly, the substitutions in codon 10 (+869) and codon 25 (+915) of tumor growth factor beta 1 (*TGF-β1*) gene correlate with the protein production.[2] The codon 10 *T (Leu) and codon 25 *G (Arg) of *TGF-β1* are the high responder alleles. For interleukin 10 (*IL-10*), 3 single nucleotide polymorphisms (SNPs) at positions –1082, –819 and –592 comprise 3 haplotypes: ACC, ATA and GCC. The genotypes of ACC/ACC, ACC/ATA and ATA/ATA are classified as low, GCC/ACC and GCC/ATA as intermediate, and GCC/GCC as high *IL-10* producer genotypes.[3] Finally, at position +874 within the intron 1 of interferon gamma (*IFN-γ*) gene, the genotypes T/T, T/A and A/A are associated with high, intermediate and low expression, respectively.[4]

Studying cytokine gene polymorphism is important to understand the cause of interindividual variation in the pathogenesis, identify disease susceptibility and poor clinical outcomes, and develop novel strategies to prevent or delay the disease process. Therefore, much effort has been committed to developing rapid, accurate and cost-effective technologies for cytokine SNP analysis. Various strategies amenable to cytokine genotyping include restriction fragment length polymorphism (RFLP),[5] sequence-specific primer-polymerase chain reaction (SSP-PCR),[6] allele-specific oligonucleotide (ASO) hybridization,[7] TaqMan genotyping assay,[8] and direct DNA sequencing.[9] Each approach has certain advantages in cytokine genotyping. However, these methods are also labor-intensive, time-consuming and expensive, especially for large genetic screening. High-resolution melting-polymerase chain reaction (HRM-PCR) analysis is an emerging sequence variation scanning technology.[10] This relatively novel approach is based on the melting properties of double-stranded DNA. Sequence variations in PCR amplicon are detected using changes in melting profiles as the temperature is increased in the presence of DNA intercalating dyes. The HRM analysis is a simple, flexile, inexpensive, sensitive, and specific method. Indeed, this technique has been widely employed to screen gene variants, such as mutation detection,[11] SNP typing,[12] methylation analysis,[13] and differentiation of bacterial strains.[14] Therefore, we considered developing an HRM-PCR method for cytokine genotyping.

Lung transplantation is the only available treatment for various end-stage lung diseases. Despite recent advances in immunosuppressive therapy and human leukocyte antigen (HLA)-matching, acute or chronic graft rejection are common complications faced by the lung transplant recipients (LTRs), which occur in approx. 40% of patients during the first 6 months after allograft transplantation.[15] Studies have shown that certain cytokine polymorphisms are implicated in acute rejection or the occurrence of chronic graft failure.[16–18] It is proposed that cytokine SNPs analysis can help improve the medication design and the graft outcome after transplantation.[19] Consequently, we profiled the distribution of cytokine polymorphism in the LTRs in the Chinese population.

In addition, the genetic heterogeneity in different ethnic populations results in the diverse distribution of cytokine polymorphism.[20] Therefore, we compared the control results with those from other healthy populations and identified significant differences.

# Objectives

The aim of this study is to develop HRM technology for detecting the SNP of cytokine and to profile the distribution of cytokine gene polymorphism in LTRs.

# Materials and methods

## Study population

In the present study, 322 patients who received lung transplantation between December 2004 and June 2016 were enrolled. The LTRs consisted of 90 females and 232 males, from 14 to 80 years of age (51.42 ±14.22 years,

Table 1. Characteristics of study participants

| Characteristics | Number (n = 322) |
|---|---|
| Age [years] | 51.42 ±14.22 |
| Gender | |
| Male, n (%) | 232 (72.05) |
| Female, n (%) | 90 (27.95) |
| Diagnosis | |
| IPF, n (%) | 66 (20.50) |
| COPD, n (%) | 53 (16.46) |
| Bronchiectasis, n (%) | 26 (8.07) |
| Silicosis, n (%) | 27 (8.39) |
| Pulmonary fibrosis, n (%) | 83 (25.78) |
| Pulmonary hypertension, n (%) | 15 (4.66) |
| Interstitial pneumonia, n (%) | 10 (3.11) |
| Lymphangioleiomyomatosis, n (%) | 7 (2.17) |
| Pulmonary emphysema, n (%) | 6 (1.86) |
| Other, n (%) | 29 (9.01) |

IPF – idiopathic pulmonary fibrosis; COPD – chronic obstructive pulmonary disease.

mean ± standard deviation (SD)). All patients were of the Chinese Han nationality and received the transplantation at the Department of Pulmonary Transplantation, Wuxi People's Hospital of Nanjing Medical University, China. The characteristics of the study LTRs are displayed in Table 1. The differences in HLA molecules between the donor and the host make a crucial contribution to the alloreactivity. Recipients and donors were genotyped with SSP-PCR (HLA-ABDR kit; One Lambda, Los Angeles, USA), following the manufacturer's instructions. The patient who best matched the donor HLA was selected as recipient for the lung transplantation.

Two hundred and sixty-six individuals (137 males and 129 females, aged 56.70 ±12.80 years, mean ±SD) from the same ethnicity and without systemic diseases were enrolled into the study as a control group. The differences in sex composition and age distribution are significant ($\chi^2 = 26.31$, $p < 0.001$; $t = 4.687$, $p < 0.01$, respectively) between the LTR and the control group.

All protocols were approved by the ethics committee on clinical new technologies and scientific research of Wuxi People's Hospital of Nanjing Medical University, China, before the study began, and the protocols conformed with the ethical guidelines of the 1975 Declaration of Helsinki.

## DNA extraction

Whole blood samples were collected before the transplantation and placed in test tubes containing EDTA-$K_2$ anticoagulant. Genomic DNA was extracted using genomic DNA purification kit (Promega, Madison, USA), according to the manufacturer's instructions. Briefly, 900 µL of Cell Lysis Solution was added to 300 µL of whole blood, mixed by inversion, incubated for 10 min at room temperature, and then centrifuged at 16,000 × g for 20 s. After centrifugation, the supernatant was discarded. Then, 300 µL of Nuclei Lysis Solution was added and it was pipetted to lyse the white blood cells. Next, 100 µL of Protein Precipitation Solution was added and vortexed for 20 s, and then centrifuged at 16,000 × g for 3 min. Finally, 300 µL of supernatant was transferred to a new tube containing 300 µL of isopropanol, mixed and centrifuged at 16,000 × g for 1 min. After centrifugation, the supernatant was discarded. Then, 300 µL of 70% ethanol was added and centrifuged as described in the step above. Next, the ethanol was aspirated and the pellet was air-dried for 10 min. The DNA was rehydrated in the appropriate volume of DNA Rehydration Solution for 1 h at 65°C.

## Genotyping of *TNF-α* (–308 A/G), *TGF-β1* (+869 T/C), *IL-10* (–592 C/A, –819 T/C, and –1082 G/A), and *IFN-γ* (+874 T/A) genes with HRM-PCR assay

The HRM-PCR was performed on a LightCycler® 480 instrument (Roche, Basel, Switzerland) with 96-well trays. The primers for genotyping *TNF-α* (–308 A/G), *TGF-β1* (+869 T/C), *IL-10* (–592 C/A, –819 T/C and –1082 G/A), and *IFN-γ* (+874 T/A) genes were listed in Table 2. The PCR was performed in 20 µL volumes; the mixture included 2.5 mM $MgCl_2$, 0.5 µM of both forward and reverse primer, 200 µM of each deoxynucleoside triphosphate (dNTP), 0.5 U of Taq DNA Polymerase (Promega), 1.0 µL of EvaGreen® (Biotium, Fremont, USA), and about 75 ng of DNA. All 6 cytokine amplicons were amplified with a touchdown PCR, as follows: an initial denaturation step at 95°C for 2 min; then the initial annealing temperature of 65°C was decreased by 0.5°C each cycle for 20 cycles and held at 55°C for 10 s for the next 30 cycles. For all cycles, denaturation at 95°C for 10 s and the extension at 72°C for 15 s were performed. The HRM was conducted at the end of each reaction and it consisted of increasing the temperature from 70°C to 99°C at intervals (ramps) of 0.02°C/s. The HRM analysis was carried out with the gene-scanning module software v. 1.5 (Roche). The software employs a three-step

Table 2. Primers of *TNF-α* –308, *IL-10* –592, *IL-10* –819, *IL-10* –1082, *TGF-β1* +869, and *IFN-γ* +874, for high-resolution melting (HRM) assay

| Gene polymorphism | | Sequence | Amplicon (bp) |
|---|---|---|---|
| *TNF-α* –308 | sense | 5′-AGGCAATAGGTTTTGAGGGGCAT-3′ | 166 |
| | antisense | 5′-GGCGGGGATTTGGAAAGTT-3′ | |
| *IL-10* –592 | sense | 5′-AAAGGAGCCTGGAACACATCCTGT-3′ | 88 |
| | antisense | 5′-AGTTCCCAAGCAGCCCTTCCATTT-3′ | |
| *IL-10* –819 | sense | 5′-TTCTCAGTTGGCACTGGTGT-3′ | 101 |
| | antisense | 5′-GTGCTCACCATGACCCCTAC-3′ | |
| *IL-10* –1082 | sense | 5′ -CACACACAAATCCAAGACAACA-3′ | 97 |
| | antisense | 5′-ATGGAGGCTGGATAGGAGGT-3′ | |
| *TGF-β1* +869 | sense | 5′-GTTCGCGCTCTCGGCAGT-3′ | 95 |
| | antisense | 5′-GTAGCCACAGCAGCGGTAGCA-3′ | |
| *IFN-γ* +874 | sense | 5′-TTCAGACATTCACAATTGATTTTATTC-3′ | 102 |
| | antisense | 5′-CCCCAATGGTACAGGTTTCT-3′ | |

analysis: 1) the normalization by selecting linear regions before (100% fluorescence) and after (0% fluorescence) the melting transition; 2) the temperature shifting by moving the curves along the x-axis, facilitating grouping; and 3) the use of the auto-group function.

### Genotyping of *TNF-α* (–308 A/G), *TGF-β1* (+869 T/C), *IL-10* (–592 C/A, –819 T/C and –1082 G/A), and *IFN-γ* (+874 T/A) genes with commercial kit

The SSP-PCR is a highly sensitive and specific method of detecting sequence polymorphism, based on the sequence-specific primer with the first 3'-terminal base matching of the specific base of each allele. To confirm the accuracy of HRM-PCR analysis, we randomly selected 100 samples from the LTRs and tested the cytokine SNPs using Cytokine Genotyping Primer Pack (One Lambda), which employs the SSP-PCR method. Briefly, 19 μL of genomic DNA (50–100 ng/μL) was mixed with 140 μL of D-Mix and 5 U of Taq DNA polymerase (Promega). This DNA mixture was dispensed into 96-well trays prealiquoted with primers and amplified on an ABI 9700 thermal cycler (Applied Biosystems, Waltham, USA). Thermocycling conditions were 10 cycles of 94°C for 10 s, 65°C for 60 s, followed by 20 cycles of 94°C for 10 s, 61°C for 50 s and 72°C for 30 s. The amplified products were electrophoresed on 2% agarose gels. The reliability of SSP-PCR reaction was judged using a negative control tube and internal positive control in each tube. The typing results were interpreted using the worksheet provided with the product.

### Comparison of allele frequencies of *TNF-α* (–308 A/G), *TGF-β1* (+869 T/C), *IL-10* (–592 C/A, –819 T/C and –1082 G/A), and *IFN-γ* (+874 T/A) genes between Chinese and other national populations

The genetic heterogeneity in populations of different ethnicities may result in the diverse distribution of cytokine polymorphism. To explore the differences in the distribution of cytokine gene polymorphisms, we reviewed the available literature and compared the results from the control group with those from other healthy populations.

### Statistical analyses

Statistical analysis was carried out using the SPSS v. 15 software (SPSS Inc., Chicago, USA). Allele and genotype frequencies were calculated by direct counting. The Hardy–Weinberg equilibrium (HWE) was tested using a $\chi^2$ test with one degree of freedom to compare the observed and expected genotype frequencies. The frequency differences for the cytokine alleles and genotypes were estimated using the $\chi^2$ test or the Fisher's exact test. The agreement between the 2 methods for SNP genotyping was determined with a Kappa test. A probability value of $p < 0.05$ was considered statistically significant and all the reported p-values were two-tailed.

## Results

### Analysis of HWE for cytokine frequencies in the LTRs and control groups

The HWE testing for *TNF-α* (–308 A/G), *TGF-β1* (+869 T/C), *IL-10* (–592 C/A, –819 T/C, –1082 G/A), and *IFN-γ* (+874 T/A) genotypes revealed no significant deviation in the LTR group ($\chi^2$ test: $\chi^2 = 1.49$, $p = 0.22$; $\chi^2 = 0.20$, $p = 0.66$; $\chi^2 = 2.21$, $p = 0.14$; $\chi^2 = 2.21$, $p = 0.14$; $\chi^2 = 1.49$, $p = 0.22$; and $\chi^2 = 0.66$, $p = 0.42$, respectively) and in the control group ($\chi^2$ test: $\chi^2 = 1.85$, $p = 0.17$; $\chi^2 = 0.06$, $p = 0.81$; $\chi^2 = 3.75$, $p = 0.05$; $\chi^2 = 3.75$, $p = 0.05$; $\chi^2 = 0.88$, $p = 0.35$; and $\chi^2 = 0.98$, $p = 0.32$, respectively).

### Genotyping of *TNF-α* (–308 A/G), *TGF-β1* (+869 T/C), *IL-10* (–592 C/A, –819 T/C and –1082 G/A), and *IFN-γ* (+874 T/A) genes with HRM-PCR assay

The HRM-PCR analysis effectively distinguished the polymorphism of *TNF-α* (–308 A/G), *TGF-β1* (+869 T/C), *IL-10* (–592 C/A, –819 T/C and –1082 G/A), and *IFN-γ* (+874 T/A) genes. Figure 1 shows the curves of melting profiles of normalized data of *TNF-α* (–308 A/G), *TGF-β1* (+869 T/C), *IL-10* (–592 C/A, –819 T/C and –1082 G/A), and *IFN-γ* (+874 T/A) genes, and distinguishable inferences between the 3 genotypes are clearly observable. Using specified post-melting parameters, all the cytokine variants from the LTRs and the control were identified. To confirm the accuracy of the HRM-PCR assays, we detected the cytokine SNPs of 100 LTRs samples with the SSP-PCR method, using a commercial kit (One Lambda) (Fig. 2). When analyzing the data of these 100 specimens, we found a 100% concordance between the HRM-PCR analysis and the SSP-PCR assay for the abovementioned cytokine SNPs, with a Kappa test value of 1.0 (data not shown).

### Distribution of cytokine genotype in LTRs of different age and gender group

Because there are differences in gender and age composition between the LTRs and the control group, it may lead to differences in cytokine genotype distribution. Therefore, we analyzed the distribution of LTRs cytokine genotypes in different gender and age groups. The data show that there are no differences in genotype distribution of *TNF-α* (–308 A/G), *TGF-β1* (+869 T/C), *IL-10* (–592 C/A, –819 T/C and –1082 G/A), and *IFN-γ* (+874 T/A) between the male

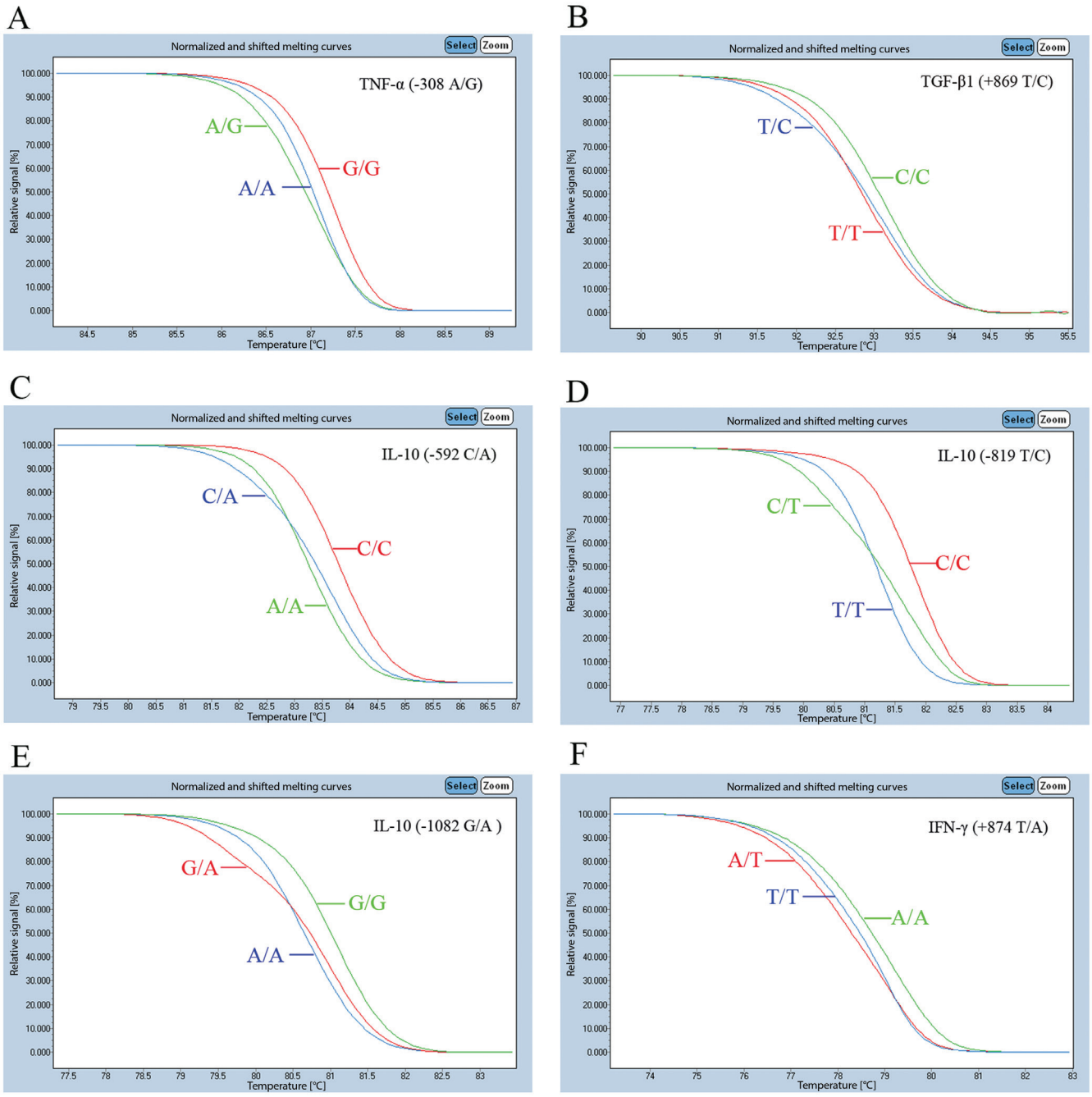


Fig. 1. Normalized and shifted melting curves for amplicon genotyping of cytokine gene obtained on a 96-well LightCycler® 480. A. *TNF-α* –308 A/G; B. *TGF-β1* +869 T/C; C. *IL-10* –592 C/A; D. *IL-10* –819 T/C; E. *IL-10* –1082 G/A; F. *IFN-γ* +874 T/A. Genotypes are labeled with a line

and female patients ($\chi^2$ test: $\chi^2 = 0.04$, $p = 0.841$; $\chi^2 = 4.37$, $p = 0.112$; $\chi^2 = 3.0$, $p = 0.223$; $\chi^2 = 3.0$, $p = 0.223$; $\chi^2 = 0.67$, $p = 0.412$; $\chi^2 = 5.80$, $p = 0.055$, respectively, at degrees of freedom (df) = 1, 2, 2, 2, 1, and 2, respectively). The data also show that there are no differences in genotype distribution of *TNF-α* (–308 A/G), *TGF-β1* (+869 T/C), *IL-10* (–592 C/A, –819 T/C and –1082 G/A), and *IFN-γ* (+874 T/A) between ≤30, 31–45, 46–60, and ≥61 years groups ($\chi^2$ test: $\chi^2 = 1.90$, $p = 0.594$; $\chi^2 = 3.96$, $p = 0.681$; $\chi^2 = 7.87$, $p = 0.247$; $\chi^2 = 7.87$, $p = 0.247$; $\chi^2 = 4.60$, $p = 0.203$; $\chi^2 = 3.49$, $p = 0.321$, respectively, at df = 3, 6, 6, 6, 3, and 6, respectively). The data confirm that the differences in gender and age composition do not lead to differences in cytokine genotype distribution.

## Alleles and genotypes distribution of *TNF-α* (–308 A/G), *TGF-β1* (+869 T/C), *IL-10* (–592 C/A, –819 T/C and –1082 G/A), and *IFN-γ* (+874 T/A) in LTRs and the control subjects

Figure 3A and 3B show the allele and genotype frequencies distribution of selective cytokine in LTRs and control subjects. The data show that there are no significant differences in the allele and genotype distribution of cytokine between

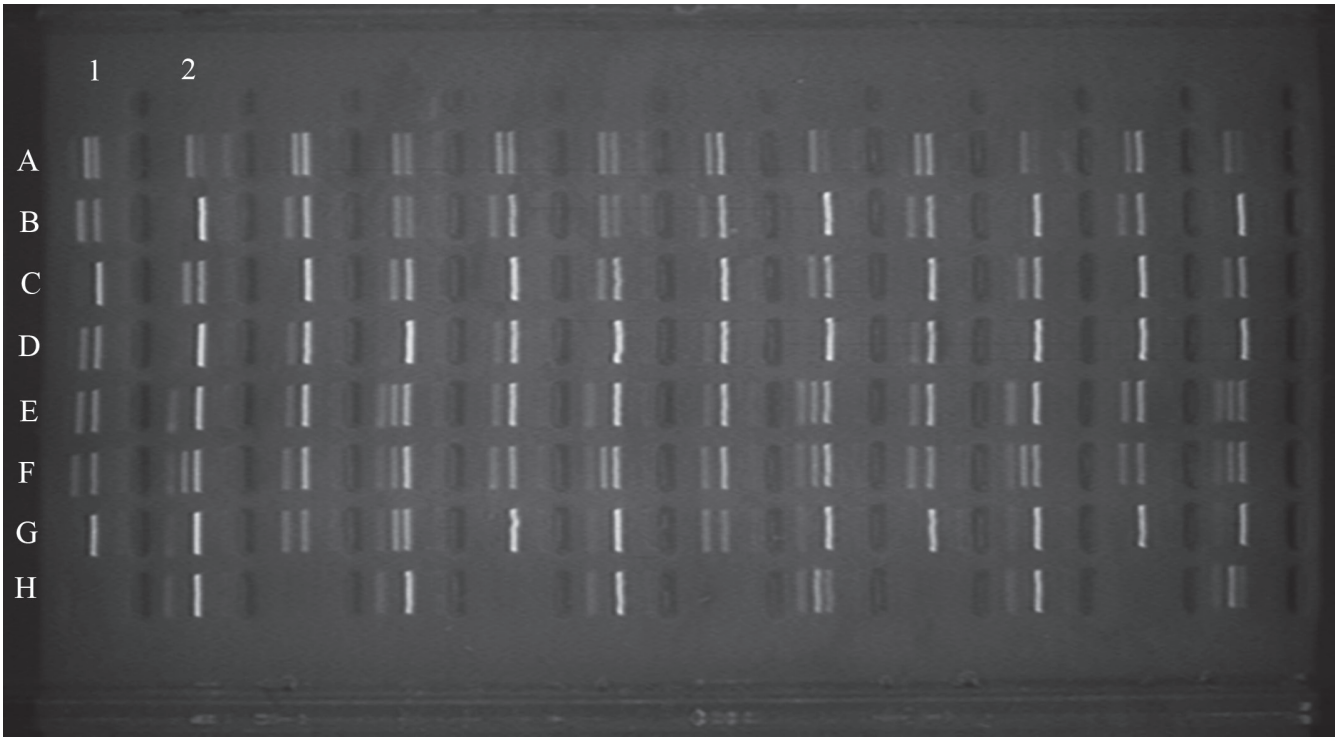


Fig. 2. Electropherogram of cytokine gene polymorphism from 6 samples obtained using the sequence-specific primer-polymerase chain reaction (SSP-PCR) method. 1H hole is negative control; 1G and 1F holes are *TNF-α* –308; 1E, 1D, 1C, and 1B holes are *TGF-β1* +869; 1A, 2H, 2G, 2F, and 2E holes are *IL-10* –592, –819 –1082; 2D and 2C holes are *IL-6* –174; 2B and 2A holes are *IFN-γ* +874

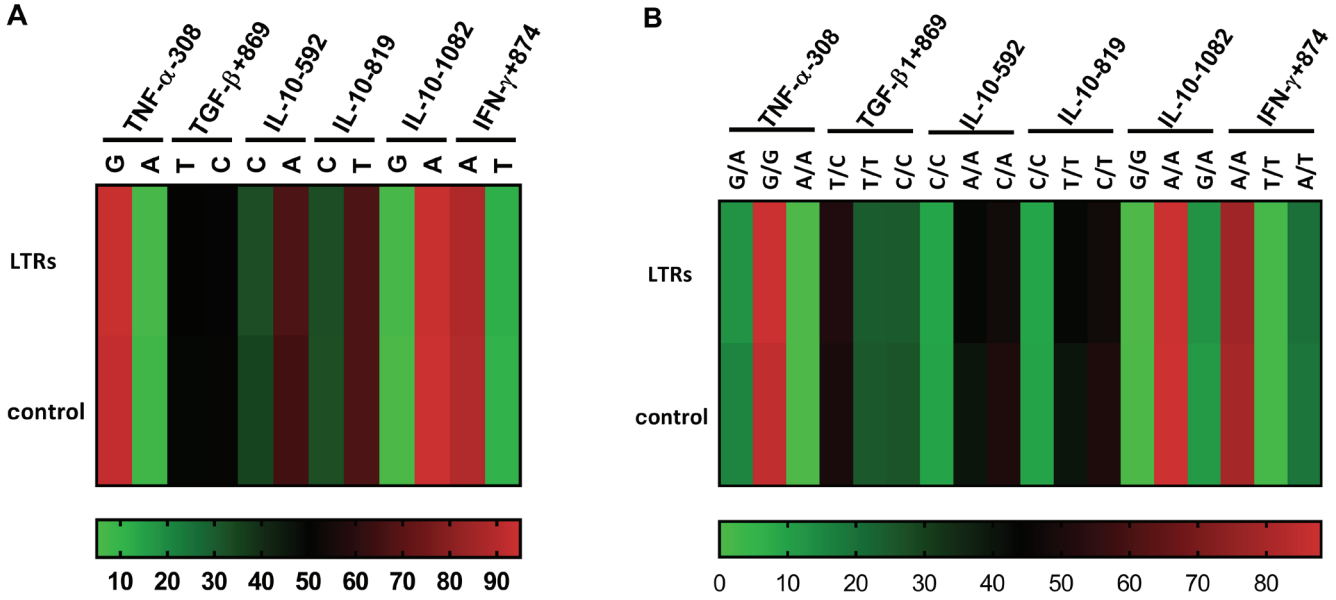


Fig. 3. The allele and genotype frequencies distribution of cytokine gene in lung transplant recipient (LTRs) and control subjects. A. The allele frequencies distribution of *TNF-α* –308, *TGF-β1* +869, *IL-10* (–592, –819, –1082), and *IFN-γ* +874 in LTRs and control subjects; B. The genotype frequencies distribution of *TNF-α* –308, *TGF-β1* +869, *IL-10* (–592, –819, –1082), and *IFN-γ* +874

the LTRs and the control subjects. As shown in Table 3, the genotype frequency of *TNF-α* –308 associated with low expression phenotype among LTRs is prevalent with 87.27%. For *TGF-β1*, combined effect of codon 10 (+869) and codon 25 (+915) determine the protein production. In Chinese population, we found that the genotype frequency of G/G at position –915 was predominant with 98%, which was obtained from the genotyping results of 100 samples using the SSP-PCR method. Therefore, we hypothesized that all LTRs had G/G genotype at position –915 and found that the genotypes associated with high expression phenotype were prevalent with 75.46%. On the contrary, as for *IL-10* and *IFN-γ*, the genotypes associated with low expression phenotype were most prevalent in the LTRs with 87.89% and 78.26%, respectively.

Table 3. Cytokine gene polymorphisms and their associated phenotypes in lung transplant recipient (LTRs)

| Cytokine gene polymorphisms | Genotype | Expression phenotype† | LTRs | |
|---|---|---|---|---|
| | | | n | % |
| *TNF-α* –308 | A/A | high | 0 | 0 |
| | G/A | intermediate | 41 | 12.73 |
| | G/G | low | 281 | 87.27 |
| *TGF-β1* +869 (+915) | T/T (G/G) | high | 78 | 24.22 |
| | T/C (G/G) | high | 165 | 51.24 |
| | C/C (G/G) | intermediate | 79 | 24.54 |
| *IL-10* (–1082, –819 and –512) | GCC/GCC | high | 0 | 0 |
| | GCC/ACC | intermediate | 6 | 1.86 |
| | GCC/ATA | intermediate | 33 | 10.25 |
| | ACC/ACC | low | 23 | 7.14 |
| | ACC/ATA | low | 121 | 37.58 |
| | ATA/ATA | low | 139 | 43.17 |
| *IFN-γ* +874 | T/T | high | 6 | 1.86 |
| | T/A | intermediate | 64 | 19.88 |
| | A/A | low | 252 | 78.26 |

† – associated level of cytokine expression with each genotype – high, intermediate, or low expression.

## Distribution of *TNF-α* (–308 A/G), *TGF-β1* (+869 T/C), *IL-10* (–592 C/A, –819 T/C and –1082 G/A), and *IFN-γ* (+874 T/A) polymorphisms in LTRs with pulmonary fibrosis, idiopathic pulmonary fibrosis and chronic obstructive pulmonary disease as primary disease

In present study, most of the primary diseases leading to lung transplantation were pulmonary fibrosis (83/322, 25.78%), followed by idiopathic pulmonary fibrosis (IPF; 66/322, 20.50%) and chronic obstructive pulmonary disease (COPD; 53/322, 16.46%). To investigate whether cytokine gene polymorphisms are associated with these diseases, we compared the distribution of cytokine polymorphisms between pulmonary fibrosis, IPF and COPD groups with normal control. The data show that there are no significant differences in the allele and genotype distribution of cytokine between the 3 disease groups and the control subjects (data not shown).

## Allele frequencies of *TNF-α* (–308 A/G), *TGF-β1* (+869 T/C), *IL-10* (–592 C/A, –819 T/C and –1082 G/A), and *IFN-γ* (+874 T/A) genes in Chinese compared with other populations

Allele frequencies of these cytokine polymorphisms in control individuals were compared to those reported in other healthy populations, including Slovak,[21] Greek Cypriot,[22] Macedonian,[23] Lebanese,[24] Iran,[25] Brazilian,[26] Mexican,[27] and Thai[28] populations (as shown in Table 4). The data show that the distribution of *TNF-α* –308 A/G polymorphism is similar in Chinese, Greek Cypriot, Lebanese, and Mexican populations, but the frequencies of TNF-α –308 A allele in Slovak, Macedonians, Iran, Brazilian, and Thai populations are higher than those in the Chinese population. For *TGF-β1* at position +869, the allele frequencies of T in Lebanese and Brazilian populations increased significantly compared to those in the Chinese population, but decreased in the Thai population. As for *IL-10* at positions –592, –819 and –1082, frequencies of the less common allele are high in Slovak, Greek Cypriot, Macedonian, Lebanese, Iran, Brazilian, and Mexican populations compared to those in the Chinese population, and they are similar in Chinese and Thai populations. Besides, the frequency of the less common T allele of IFN-γ +874 is lower in the Chinese population than those in Slovak, Greek Cypriot, Lebanese, Brazilian, and Thai populations.

# Discussion

Several SNP genotyping methods vary in terms of detection system, reaction format and allelic discrimination. However, the conventional methods for detecting cytokine SNP are time-consuming and potentially more expensive. Cytokine research urgently requires a low-cost and high-throughput genotyping technique. Therefore, we decided to develop an economic and time-, labor- and cost-saving analysis system to genotype *TNF-α* (–308 A/G), *TGF-β1* (+869 T/C), *IL-10* (–592 C/A, –819 T/C and –1082 G/A), and *IFN-γ* (+874 T/A) polymorphisms.

Table 4. Allele frequencies (n, %) of cytokine in the Chinese population compared to other populations using the $\chi^2$ test

| Cytokine | Allele | Chinese | Slovak | Greek Cypriot | Macedonian | Lebanese | Iran | Brazilian | Mexican | Thai |
|---|---|---|---|---|---|---|---|---|---|---|
| *TNF-α* –308 | A | 41 (7.71) | 37 (13.21)* | 15 (7.50) | 74 (12.29)* | 16 (7.55) | 35 (14.23)** | 55 (13.10)** | 36 (7.26) | 27 (13.24)* |
| | G | 491 (92.29) | 243 (86.79) | 185 (92.50) | 528 (87.71) | 196 (92.45) | 211 (85.77) | 365 (86.90) | 460 (92.74) | 177 (86.76) |
| *TGF-β1* +869 | T | 263 (49.44) | 153 (55.04) | 115 (57.50) | 282 (50.18) | 127 (60.10)* | 112 (50.91) | 240 (56.87)* | N/A | 80 (39.22)* |
| | C | 269 (50.56) | 125 (44.96) | 85 (42.50) | 280 (49.82) | 85 (39.90) | 108 (49.09) | 182 (43.13) | N/A | 124 (60.78) |
| *IL-10* –592 | C | 185 (34.77) | 205 (73.21)*** | 153 (76.5)*** | 425 (71.07)*** | 152 (71.84)*** | 176 (71.54)*** | 288 (68.25)*** | 301 (60.69)*** | 63 (30.88) |
| | A | 347 (65.23) | 75 (26.79) | 47 (23.50) | 173 (28.93) | 60 (28.16) | 70 (28.46) | 134 (31.75) | 195 (39.31) | 141 (69.12) |
| *IL-10* –819 | C | 185 (34.77) | 205 (73.21)*** | 153 (76.5)*** | 435 (72.74)*** | 149 (70.28)*** | 176 (71.54)*** | 288 (68.25)*** | 289 (58.27)*** | 68 (33.33) |
| | T | 347 (65.23) | 75 (26.79) | 47 (23.50) | 163 (27.26) | 63 (29.72) | 70 (28.46) | 134 (31.75) | 207 (41.73) | 136 (66.67) |
| *IL-10* –1082 | G | 30 (5.64) | 121 (43.21)*** | 76 (38.00)*** | 246 (41.14)*** | 78 (36.79)*** | 89 (43.63)*** | 163 (38.63)*** | 140 (28.23)*** | 15 (7.35) |
| | A | 502 (94.36) | 159 (56.79) | 124 (62.00) | 352 (58.86) | 134 (63.21) | 115 (56.37) | 259 (61.37) | 356 (71.77) | 189 (92.65) |
| *IFN-γ* +874 | A | 473 (88.91) | 149 (53.21)*** | 95 (47.50)*** | N/A | 106 (50.00)*** | N/A | 248 (58.77)*** | N/A | 149 (26.96)*** |
| | T | 59 (11.09) | 131 (46.79) | 115 (52.50) | N/A | 106 (50.00) | N/A | 174 (41.23) | N/A | 55 (73.04) |

* – p-value < 0.05; ** – p-value < 0.01; *** – p-value < 0.001; N/A – not applicable, abbreviation used for the lack of data in the table field.

The HRM-PCR analysis is a recently developed genotyping method, based on the characteristics of the amplicon thermal denaturation. The HRM-PCR method involves the PCR analysis of the target gene in the presence of a saturating intercalating double-stranded DNA fluorescent dye, and subsequent melting of the amplicon by gradually increasing the temperature, which results in a decrease in fluorescence caused by the release of intercalating dyes from DNA. The specific melting profile depends on the base composition, DNA sequence and amplicon length.[29,30] The HRM-PCR analysis is highly suitable for the detection of single-base variants, deletions or insertions.[31] In addition, HRM-PCR method offers several advantages over other conventional gene scanning methods, such as no post-PCR processing steps, complete closed tube format and short turnaround time.[32,33] Thus, it is an attractive technique due to the increased demand for rapid, economic, easy, and high-throughput genotyping analyses. Here, we have presented the HRM-PCR assay to identify cytokine SNPs. The data show that the differences between the 3 allelic forms of *TNF-α* (–308 A/G), *TGF-β1* (+869 T/C), *IL-10* (–592 C/A, –819 T/C and –1082 G/A), and *IFN-γ* (+874 T/A) genes are distinguishable as a result of the melting curve shape. To confirm the accuracy of the HRM-PCR assay, we randomly selected 100 samples from the LTRs and detected cytokine SNPs with the SSP-PCR method using a commercial kit. The data showed a 100% concordance between the HRM-PCR and the SSP-PCR assays for cytokine SNPs, with a Kappa test value of 1.0. All of these suggest that the HRM-PCR assay is a reliable single-tube technology for genotyping the polymorphisms of the abovementioned cytokines. In addition, HRM-PCR assay can genotype 96 samples in 1.5 h on our platform. Therefore, HRM-PCR may be a good choice for cytokines genotyping, as it is a high-throughput, cheap and time-saving method with the further advantage of no post-PCR handling.

Proinflammatory and anti-inflammatory cytokine networks lead to different responses to infection, graft tolerance or rejection. In particular, high levels of pro-inflammatory TNF-α and IFN-γ enhance cell-mediated immune response, causing allograft rejection.[34,35] In contrast, high levels of anti-inflammatory *IL-10* suppress the inflammation and are associated with tolerance.[36] Besides, high levels of *TGF-β1* with immunosuppressive properties are thought to contribute to the development of chronic allograft nephropathy.[37] The SNPs of cytokine genes mainly influence the production of proteins, which determines the microenvironment of the graft.[38,39] Pretransplant genetic testing of cytokine may provide a clinically useful means for risk stratification in solid organ transplant patients. In the present study, we explored the profiles of *TNF-α* (–308 A/G), *TGF-β1* (+869 T/C), *IL-10* (–592 C/A, –819 T/C and –1082 G/A), and *IFN-γ* (+874 T/A) SNPs in the LTRs

and the control group. Our results show that there are no significant differences in the allele and genotype distribution of cytokines between the LTRs and control groups. In addition, we found that the genotypes of *TGF-β1* +869 associated with high expression phenotype were prevalent among LTRs. On the contrary, as for *TNF-α* –308, *IL-10* and *IFN-γ*, the genotypes associated with low expression phenotype are the most prevalent in the LTRs.

The allelic frequency of a particular gene may vary significantly in different ethnic populations. Previous studies have showed the associations between ethnicity and cytokine gene polymorphisms.[20,27] In the present work, we compared the control results of cytokine gene polymorphisms with those from other national populations. We found dramatic differences in allele frequency of cytokine among different races. The data showed that there were 5, 3, 7, and 5 differences in the allele frequencies of *TNF-α* –308, *TGF-β1* +869, *IL-10* (–592, –819 and –1082), and *IFN-γ* +874 between Chinese and other 8 national populations, respectively. The differences in cytokine allelic frequencies can lead to diverse secretory profiles, responses to stimuli or susceptibility to diseases. Therefore, the studies on distribution of cytokine gene polymorphisms within populations may be helpful in understanding the observed differences in cytokine secretion profiles, which are the basis for various immunological phenomena, such as infectious, autoimmune disorders and transplant rejections. Therefore, we also explored the association between the cytokine polymorphisms and top 3 of the primary diseases leading to lung transplantation. However, we did not find a significant correlation between the cytokine polymorphisms and pulmonary fibrosis, IPF or COPD.

## Limitations

The limitations of this study should be mentioned. Firstly, the HRM technology for detecting the SNP of cytokine may not be applicable to other fluorescent PCR instruments. Secondly, in view of the limited sample size and due to the fact that the sample is limited to the Chinese population only, the conclusions may not be applied to other ethnic populations, due to the genetic differences in race.

# Conclusions

In conclusion, this study presents a rapid, low-cost and high-throughput HRM-PCR technology for genotyping *TNF-α*, *TGF-β1*, *IL-10*, and *IFN-γ* genes. It can be widely adopted in diagnostic laboratories to facilitate cytokine gene SNP screening. Moreover, our study profiles the cytokine secretion patterns in the LTRs in Chinese population, which may be utilized in optimizing drug use and improving the prognosis of LTRs.

## ORCID iDs

Hui-Jun Mu https://orcid.org/0000-0003-4352-2506
Jian Zou https://orcid.org/0000-0003-3511-8159
Ji Zhang https://orcid.org/0000-0003-4404-7524
Hai-Ping Zhang https://orcid.org/0000-0002-3841-5856

## References

1. Wilson AG, Symons JA, McDowell TL, McDevitt HO, Duff GW. Effects of a polymorphism in the human tumor necrosis factor alpha promoter on transcriptional activation. *Proc Natl Acad Sci U S A*. 1997;94(7):3195–3199. doi:10.1073/pnas.94.7.3195
2. Awad MR, El-Gamel A, Hasleton P, Turner DM, Sinnott PJ, Hutchinson IV. Genotypic variation in the transforming growth factor-beta1 gene: Association with transforming growth factor-beta1 production, fibrotic lung disease, and graft fibrosis after lung transplantation. *Transplantation*. 1998;66(8):1014–1020. doi:10.1097/00007890-199810270-00009
3. Plothow A, Benvenutti R, Contieri FL, Bicalho MG. Frequencies at three polymorphic sites of interleukin-10 gene promoter in Brazilian renal recipients. *Transplant Proc*. 2003;35(8):2908–2910. doi:10.1016/j.transproceed.2003.10.013
4. Biolo G, Amoroso A, Savoldi S, et al. Association of interferon-gamma +874A polymorphism with reduced long-term inflammatory response in haemodialysis patients. *Nephrol Dial Transplant*. 2006;21(5):1317–1322. doi:10.1093/ndt/gfk033
5. Afkari B, Babaloo Z, Dolati S, et al. Molecular analysis of interleukin-10 gene polymorphisms in patients with Behcet's disease. *Immunol Lett*. 2018;194:56–61. doi:10.1016/j.imlet.2017.12.008
6. Attar M, Mansoori M, Shahbazi M. Interleukin-6 genetic variation and susceptibility to gastric cancer in an Iranian population. *Asian Pac J Cancer Prev*. 2017;18(11):3025–3029. doi:10.22034/APJCP.2017.18.11.3025
7. Vallinoto AC, Graca ES, Araujo MS, et al. IFNG +874T/A polymorphism and cytokine plasma levels are associated with susceptibility to *Mycobacterium tuberculosis* infection and clinical manifestation of tuberculosis. *Hum Immunol*. 2010;71(7):692–696. doi:10.1016/j.humimm.2010.03.008
8. Ognjanovic S, Yuan JM, Chaptman AK, Fan Y, Yu MC. Genetic polymorphisms in the cytokine genes and risk of hepatocellular carcinoma in low-risk non-Asians of USA. *Carcinogenesis*. 2009;30(5):758–762. doi:10.1093/carcin/bgn286
9. Fang M, Huang Y, Zhang Y, Ning Z, Zhu L, Li X. Interleukin-6 -572C/G polymorphism is associated with serum interleukin-6 levels and risk of idiopathic pulmonary arterial hypertension. *J Am Soc Hypertens*. 2017;11(3):171–177. doi:10.1016/j.jash.2017.01.011
10. Wang J, Dong P, Wu W, Pan X, Liang X. High-throughput thermal stability assessment of DNA hairpins based on high resolution melting. *J Biomol Struct Dyn*. 2018;36(1):1–13. doi:10.1080/07391102.2016.1266967
11. Ousati Ashtiani Z, Mehrsai AR, Pourmand MR, Pourmand GR. High resolution melting analysis for rapid detection of PIK3CA gene mutations in bladder cancer: A mutated target for cancer therapy. *Urol J*. 2018;15(1):26–31. doi:10.22037/uj.v0i0.3987
12. Podralska M, Ziolkowska-Suchanek I, Zurawek M, et al. Genetic variants in *ATM*, *H2AFX* and *MRE11* genes and susceptibility to breast cancer in the Polish population. *BMC Cancer*. 2018;18(1):452. doi:10.1186/s12885-018-4360-3
13. Zhang Y, Zhou H, Sun H, et al. Association of peripheral blood leukocyte KIBRA methylation with gastric cancer risk: A case-control study. *Cancer Med*. 2018;7(6):2682–2690. doi:10.1002/cam4.1474
14. Girault G, Wattiau P, Saqib M, et al. High-resolution melting PCR analysis for rapid genotyping of *Burkholderia mallei*. *Infect Genet Evol*. 2018;63:1–4. doi:10.1016/j.meegid.2018.05.004
15. Wohlschlager J, Sommerwerck U, Jonigk D, Rische J, Baba HA, Muller KM. Lung transplantation and rejection: Basic principles, clinical aspects and histomorphology [in German]. *Pathologe*. 2011;32(2):104–112. doi:10.1007/s00292-010-1403-1
16. Thakkinstian A, Dmitrienko S, Gerbase-Delima M, et al. Association between cytokine gene polymorphisms and outcomes in renal transplantation: A meta-analysis of individual patient data. *Nephrol Dial Transplant*. 2008;23(9):3017–3023. doi:10.1093/ndt/gfn185

17. Goussetis E, Varela I, Peristeri I, et al. Cytokine gene polymorphisms and graft-versus-host disease in children after matched sibling hematopoietic stem cell transplantation: A single-center experience. *Cell Mol Immunol*. 2011;8(3):276–280. doi:10.1038/cmi.2011.4
18. Zhang XX, Bian RJ, Wang J, Zhang QY. Relationship between cytokine gene polymorphisms and acute rejection following liver transplantation. *Genet Mol Res*. 2016;15(2). doi:10.4238/gmr.15027599
19. Karimi MH, Ebadi P, Pourfathollah AA. Association of cytokine/costimulatory molecule polymorphism and allograft rejection: A comparative review. *Expert Rev Clin Immunol*. 2013;9(11):1099–1112. doi:10.1586/1744666X.2013.844462
20. Hoffmann SC, Stanley EM, Cox ED, et al. Ethnicity greatly influences cytokine gene polymorphism distribution. *Am J Transplant*. 2002;2(6):560–567. doi:10.1034/j.1600-6143.2002.20611.x
21. Javor J, Bucova M, Ferencik S, Grosse-Wilde H, Buc M. Single nucleotide polymorphisms of cytokine genes in the healthy Slovak population. *Int J Immunogenet*. 2007;34(4):273–280. doi:10.1111/j.1744-313X.2007.00693.x
22. Costeas PA, Koumas L, Koumouli A, Kyriakou-Giantsiou A, Papaloizou A. Cytokine polymorphism frequencies in the Greek Cypriot population. *Eur J Immunogenet*. 2003;30(5):341–343. doi:10.1046/j.1365-2370.2003.00413.x
23. Trajkov D, Trajchevska M, Arsov T, et al. Association of 22 cytokine gene polymorphisms with tuberculosis in Macedonians. *Indian J Tuberc*. 2009;56(3):117–131. PMID:20349753.
24. Mahfouz RA, Shammaa D, Harb N, et al. Distribution of cytokine gene polymorphisms in the general Lebanese population: The first report. *Genet Test Mol Biomarkers*. 2009;13(4):459–463. doi:10.1089/gtmb.2009.0013
25. Amirzargar AA, Naroueynejad M, Khosravi F, et al. Cytokine single nucleotide polymorphisms in Iranian populations. *Eur Cytokine Netw*. 2008;19(2):104–112. doi:10.1684/ecn.2008.0122
26. Visentainer JE, Sell AM, da Silva GC, et al. TNF, IFNG, IL6, IL10 and TGFB1 gene polymorphisms in South and Southeast Brazil. *Int J Immunogenet*. 2008;35(4–5):287–293. doi:10.1111/j.1744-313X.2008.00778.x
27. Vargas-Alarcon G, Ramirez-Bello J, Juarez-Cedillo T, Ramirez-Fuentes S, Carrillo-Sanchez S, Fragoso JM. Distribution of the IL-1RN, IL-6, IL-10, INF-gamma, and TNF-alpha gene polymorphisms in the Mexican population. *Genet Test Mol Biomarkers*. 2012;16(10):1246–1253. doi:10.1089/gtmb.2012.0100
28. Sodsai P, Nakkuntod J, Kupatawintu P, Hirankarn N. Distribution of cytokine gene polymorphisms in Thai population. *Tissue Antigens*. 2011;77(6):593–597. doi:10.1111/j.1399-0039.2011.01647.x
29. Reed GH, Kent JO, Wittwer CT. High-resolution DNA melting analysis for simple and efficient molecular diagnostics. *Pharmacogenomics*. 2007;8(6):597–608. doi:10.2217/14622416.8.6.597
30. Vossen RH, Aten E, Roos A, den Dunnen JT. High-resolution melting analysis (HRMA): More than just sequence variant screening. *Hum Mutat*. 2009;30(6):860–866. doi:10.1002/humu.21019
31. Druml B, Cichna-Markl M. High resolution melting (HRM) analysis of DNA: Its role and potential in food analysis. *Food Chem*. 2014;158:245–254. doi:10.1016/j.foodchem.2014.02.111
32. Montgomery J, Wittwer CT, Palais R, Zhou L. Simultaneous mutation scanning and genotyping by high-resolution DNA melting analysis. *Nat Protoc*. 2007;2(1):59–66. doi:10.1038/nprot.2007.10
33. Wittwer CT. High-resolution DNA melting analysis: Advancements and limitations. *Hum Mutat*. 2009;30(6):857–859. doi:10.1002/humu.20951
34. Xu X, Huang H, Wang Q, et al. IFN-gamma-producing Th1-like regulatory T cells may limit acute cellular renal allograft rejection: Paradoxical post-transplantation effects of IFN-gamma. *Immunobiology*. 2017;222(2):280–290. doi:10.1016/j.imbio.2016.09.012
35. Ramsperger-Gleixner M, Spriewald BM, Tandler R, et al. Increased transcript levels of TNF-alpha, TGF-beta, and granzyme B in endomyocardial biopsies correlate with allograft rejection. *Exp Clin Transplant*. 2011;9(6):387–392. PMID:22142046.
36. Li B, Tian L, Diao Y, Li X, Zhao L, Wang X. Exogenous IL-10 induces corneal transplantation immune tolerance by a mechanism associated with the altered Th1/Th2 cytokine ratio and the increased expression of TGF-beta. *Mol Med Rep*. 2014;9(6):2245–2250. doi:10.3892/mmr.2014.2073
37. Nikolova PN, Ivanova MI, Mihailova SM, et al. Cytokine gene polymorphism in kidney transplantation-impact of TGF-beta 1, TNF-alpha and IL-6 on graft outcome. *Transpl Immunol*. 2008;18(4):344–348. doi:10.1016/j.trim.2007.10.003
38. Kamel AM, Gameel A, Ebid GTA, Radwan ER, Mohammed Saleh MF, Abdelfattah R. The impact of cytokine gene polymorphisms on the outcome of HLA matched sibling hematopoietic stem cell transplantation. *Cytokine*. 2018;110:404–411. doi:10.1016/j.cyto.2018.05.003
39. Omrani MD, Mokhtari MR, Bagheri M, Ahmadpoor P. Association of interleukin-10, interferon-gamma, transforming growth factor-beta, and tumor necrosis factor-alpha gene polymorphisms with long-term kidney allograft survival. *Iran J Kidney Dis*. 2010;4(2):141–146. PMID:20404426.

# Does tumor necrosis factor alpha promoter –308 A/G polymorphism has any role in the susceptibility to sepsis and sepsis risk? A meta-analysis

Huining Niu[1,A], Fujun Li[2,A], Hua Ma[1,C], Limei Xiu[3,D], Juan Chen[1,D,E], Min Hang[4,E]

[1] Department of Hematology, Xianyang Central Hospital, China
[2] Department of Emergency Medicine, Affiliated Municipal Hospital of Xuzhou Medical University, China
[3] Department of Vasculocardiology, Chifeng Municipal Hospital, China
[4] Department of Emergency Medicine, Shanghai Pudong New Area Gongli Hospital, China

A – research concept and design; B – collection and/or assembly of data; C – data analysis and interpretation;
D – writing the article; E – critical revision of the article; F – final approval of the article

Advances in Clinical and Experimental Medicine, ISSN 1899–5276 (print), ISSN 2451–2680 (online) *Adv Clin Exp Med*. 2022;31(5):557–565

**Address for correspondence**
Min Hang
E-mail: facsmax7921@gmail.com

**Funding sources**
None declared

**Conflict of interest**
None declared

Received on July 5, 2021
Reviewed on October 8, 2021
Accepted on November 23, 2021

Published online on January 24, 2022

## Abstract

Sepsis is defined as an infection that causes the immune system to attack the body, subsequently leading to death. Some findings suggest that there is a high level of correlation between tumor necrosis factor (TNF) activity and susceptibility to sepsis. We used MEDLINE, Scopus and Web of Science databases to conduct an automated search covering the years 2000–2019. The Meta-analysis of Observational Studies in Epidemiology (MOOSE) criteria and Preferred Reporting Items for Systematic Reviews and Meta-Analyses (PRISMA) guidelines were used for the meta-analysis. The selected studies were evaluated based on their focus on the TNF-α –308 A/G polymorphism, sepsis and sepsis mortality. Based on this inclusion criterion, 24 papers out of 782 were chosen for the meta-analysis. The meta-analysis was performed using Review Manager. The comparison of TNF1 and TNF2 among the patients was calculated in the 2 groups and the odds ratio (OR) was used to construct the forest plots. The meta-analysis of the OR in Asian and Caucasian populations does not prove the influence of TNF variant on sepsis risk.

**Key words:** sepsis, tumor necrosis factor, 308A/G polymorphism, single nucleotide polymorphisms

**Cite as**
Niu H, Li F, Ma H, Xiu L, Chen J, Hang M. Does tumor necrosis factor alpha promoter –308 A/G polymorphism has any role in the susceptibility to sepsis and sepsis risk? A meta-analysis. *Adv Clin Exp Med*. 2022;31(5):557–565. doi:10.17219/acem/144198

**DOI**
10.17219/acem/144198

# Introduction

Sepsis is a serious burden to healthcare worldwide. It develops mostly in elderly patients, preterm infants or low-birth-weight infants.[1,2] An exigent factor is the association of a vital genetic component to both the risk of developing sepsis and the subsequent outcome regarding survival. Various studies have shown a connection between widespread variations in human DNA, genetic polymorphism and sepsis-related mortality.[3] Several biomarkers show elevated levels in sepsis conditions, such as *TLR4* (toll-like receptor 4) single nucleotide polymorphisms (SNPs), rs4986790, and rs4986791, but not the *SERPINE1* (serpin peptidase inhibitor, clade E (nexin, plasminogen activator inhibitor type 1), member 1) rs1799768 polymorphism.[4–8]

Tumor necrosis factor alpha (TNF-α) plays a vital role in many serious conditions, such as diabetes, cancer, etc.[9,10] The studies conducted in the past have produced mixed results on the role of TNF-α in a weakened health condition. One study reported TNF-α as a risk factor in the North Indian and Japanese populations, as well as Chinese and Turkish children. Studies in Germany and Hungary revealed a negative correlation between preterm infants and low-birth-weight infants.[8,11–21]

Several papers examining the relationship between TNF-α and sepsis risk and outcome have been published. However, various conflicting reports have emerged, and it is not easy to replicate initial studies in many cases.[22,23] We speculated that a synthesis of the results of these studies would be more understandable, as it would provide more accurate estimates of the clinical effects of the TNF-α –308 A/G polymorphism, since many studies had insufficient power to suggest that TNF2 was correlated with the development of sepsis or sepsis-related mortality.[24–26]

# Objectives

This study aimed to investigate whether having a variant TNF-α –308 genotype (TNF2 or non-G/G) is linked to a higher risk of sepsis or sepsis-related mortality.

# Materials and methods

The meta-analysis was carried out according to the Meta-analysis of Observational Studies in Epidemiology (MOOSE) guidelines. We followed the Preferred Reporting Items for Systematic Reviews and Meta-Analyses (PRISMA) normative recommendations with the registration No. XMU # SM/IRB/2020/1021.

## Data sources and searches

The keywords used were "TNF-α –308 A/G", "tumor necrosis factor", "sepsis", "septic shock", and "sepsis risk". The search was carried out in MEDLINE, Scopus, and Web of Science databases.

## Study selection

Articles from the years 2000–2019 were considered. A total of 782 articles were retrieved, out of which only 45 full-text articles were found to be eligible. Out of those, 24 were used for the purpose of the meta-analysis after their quality had been assessed.

Figure 1 shows the process of the selection of studies.

## Exclusion and inclusion criteria

The selected studies were evaluated using 2 parameters: 1) focus on TNF-α –308 A/G polymorphism; and 2) focus on sepsis and sepsis risk.

To improve the readability, we used the term "sepsis" when referring to health disorders such as sepsis, severe sepsis, septic shock, septicemia, or infection-related systemic inflammatory response syndrome.

Studies were omitted if 1) the triggers of systemic inflammatory reaction syndrome (SIRS) or multiple organ dysfunction syndrome (MODS) were specifically unrelated to infection (e.g., following heart surgery); 2) the reseached causes of sepsis were nonbacterial infections (such as parasites, fungi and viruses); or 3) there were duplicate reports. The research architecture or language used had no impact on which studies were included in the meta-analysis.

The titles and abstracts of publications found using the search strategy were reviewed by 1 reviewer (HN). Any journal that was considered to be significant; full text was downloaded. The reviewers were not blinded to study authors or outcomes. In the end, both reviewers agreed on which findings should be included in the meta-analysis. A kappa (κ) statistic was used to assess the level of agreement. A kappa (κ) value of 0.87 indicated a high level of agreement between the reviewers, and hence the selection of included studies was agreed upon (Table 1).

## Extraction of data and methodological approach

The primary outcomes were the development of sepsis and mortality among patients with sepsis. Two researchers (FL and HM) used a structured data collection form to retrieve the data.

The included studies compared G/G with G/A, G/A with A/A, and hence the meta-analysis compared the studies taking into consideration G/G with G/A or A/A allele combinations. The G/A or A/A allele combinations are referred to as TNF2 and G/G as TNF1. The meta-analysis also considered the ethnicity of the study population, as it is believed to have a confounding role in the influence of TNF on sepsis risk.

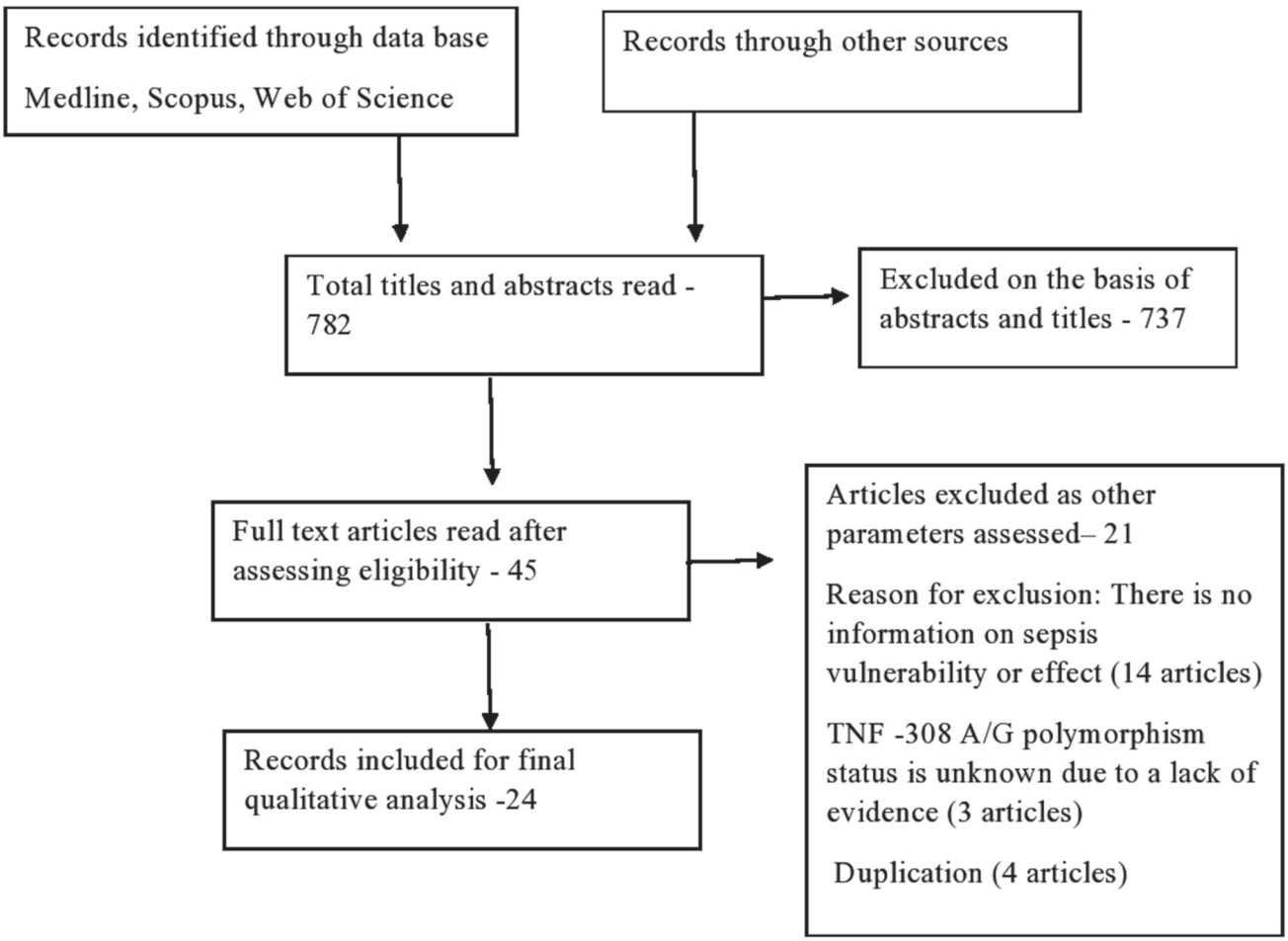


Fig. 1. The selection of studies

Patients with related symptoms or illnesses and being at risk for sepsis served as the reference population for the sepsis study. Only people with sepsis were included in the probability of mortality study. Control subjects from the general population, such as healthy blood donors or healthy volunteers, were not included in either study.

We conducted stratified analyses by variables that we believed could confound the primary analysis, including 1) ethnicity (Asian compared to Caucasian); 2) sepsis classification (sepsis, severe sepsis, and septic shock); 3) age (adults compared to pediatric patients); and 4) immune status (immune-competent compared to immune-compromised patients). In the stratified study, only results of at least 2 trials per group were considered; therefore, age, immune condition, and 2 elements relevant to methodologic accuracy (primer sequence and sepsis definition) were excluded.

## Statistical methods

The meta-analysis was performed using Review Manager v. 5 software (The Cochrane Collaboration, Copenhagen, Denmark). The comparison of TNF1 and TNF2 among patients was calculated in the 2 groups. Meta-analyses were done using a random effects model (Mantel–Haenszel method) and heterogeneity was evaluated using $I^2$ statistic. The odds ratio (OR) and 95% confidence intervals (95% CIs) were used to construct forest plots. The value of $p < 0.05$ was considered statistically significant. The publication bias was assessed using a funnel plot in which the standard error of the log of the OR was plotted against the log of the OR.

# Results

The flow diagram of trial recognition and collection is presented in Fig. 1. A total of 782 titles and abstracts were reviewed, with 24 meeting the requirements for inclusion in the final meta-analysis. The following 21 articles were excluded: 14 articles with no study on sepsis susceptibility or result, 3 articles with inadequate evidence on TNF-α –308 A/G polymorphism status and 4 articles with a secondary release.

Table 1 shows the demographic data of the patients examined in the 24 included studies. A total of 4764 patients were analyzed in 24 studies: 15 papers concerned white population, 8 Asian population and 1, a mixed population.

Table 1. Details of the included studies

| Study | Year | Ethnicity | Allele combination | Key findings |
|---|---|---|---|---|
| Song et al.[18] | 2012 | Asian | GA vs GG | OR = 1.138 (0.945 to 1.370) |
| Teuffel et al.[27] | 2010 | Asian | GA vs GG | OR = 2.187 (0.946 to 5.059) |
| Gupta et al.[16] | 2015 | Asian | GA vs GG | OR = 48.706 (10.457 to 226.86) |
| Fu et al.[30] | 2016 | Asian | GA vs GG | OR = 0.535 (0.349 to 0.820) |
| Nakada et al.[17] | 2005 | Asian | GA vs GG | OR = 0.450 (0.104 to 1.938) |
| Treszl et al.[21] | 2003 | Caucasian | GA vs GG | OR = 0.713 (0.263 to 1.934) |
| Zhang et al.[29] | 2017 | Mixed | GA vs GG and AA vs GG | OR = 3.78 (1.16, 12.30) |
| Solé-Violán et al.[31] | 2010 | Caucasian | GA vs GG | OR = 0.596 (0.472 to 0.753) |
| Solé-Violán et al.[31] | 2010 | Caucasian | GA vs GG | OR = 8.857 (4.565 to 17.184) |
| Mira et al.[32] | 1999 | Caucasian | GA vs GG | OR = 0.297 (0.119 to 0.738) |
| Gordon et al.[33] | 2004 | Caucasian | GA vs GG | OR = 2.000 (0.990 to 4.039) |
| Sipahi et al.[34] | 2006 | Caucasian | GA vs GG | OR = 0.972 (0.244 to 3.869) |
| Allam et al.[35] | 2015 | Asian | GA vs GG | OR = 0.103 (0.0456 to 0.232) |
| Duan et al.[36] | 2011 | Asian | GA vs GG | OR = 2.006 (1.199 to 3.355) |
| Paskulin et al.[37] | 2011 | Caucasian | GA vs GG | OR = 1.304 (0.859 to 1.978) |
| Jaber et al.[38] | 2004 | Caucasian | GA vs GG | OR = 1.206 (0.416 to 3.496) |
| McDaniel et al.[39] | 2007 | Caucasian | GA vs GG | OR = 1.545 (0.318 to 7.502) |
| Garnacho-Montero et al.[40] | 2006 | Caucasian | GA vs GG | OR = 0.882 (0.480 to 1.621) |
| Kothari et al.[48] | 2013 | Asian | GA vs GG | OR = 1.947 (1.280 to 2.964) |
| Susantitaphong et al.[41] | 2013 | Caucasian | GA vs GG | OR = 1.141 (0.672 to 1.939) |
| Schaaf et al.[42] | 2003 | Caucasian | GA vs GG | OR = 0.222 (0.0458 to 1.078) |
| Schueller et al.[43] | 2006 | Caucasian | GA vs GG | OR = 0.792 (0.404 to 1.550) |
| Balding et al.[44] | 2003 | Caucasian | GA vs GG | OR = 1.240 (0.869 to 1.767) |
| Majetschak et al.[45] | 2002 | Caucasian | GA vs GG | OR = 1.389 (0.385 to 5.005) |

OR – odds ratio.

Sepsis was classified as sepsis (in 8 studies), extreme sepsis (in 5 studies), septicemia (in 1 study), septic shock (in 7 studies), or 2 of the above forms of sepsis, defined as combined patient groups (in 3 studies). Fifteen researchers examined sepsis susceptibility, 5 examined sepsis death and 4 examined each of them.

In 15 studies, TNF2 (G/A or A/A) was compared to TNF1 (G/G) in 8 studies, and allele A frequency in 1 sample, the TNF 308 genotype was identified as G/G, G/A, or A/A.[29] The data from the 15 studies that reported on G/G, G/A, or A/A were translated to TNF2 (G/A or A/A) or TNF1 (G/G), yielding a total of 23 studies that could be used to assess the effect of TNF2 (Table 2,3). The data from the 15 studies that reported on G/G, G/A or A/A were translated to TNF2 (G/A or A/A) or TNF1 (G/G), yielding a total of 23 studies that could be used to assess TNF2 effect (Table 2,3).

Figure 2 shows the forest plot of the role of TNF-α during sepsis among Asian population (n = 8 studies). There was no significant effect of TNF phenotype on risk of sepsis (OR 1.21, 95% CI: [0.63; 2.30], p = 0.57, $I^2$ = 92%). The heterogeneity value $I^2$ is high (>80%) indicating inconsistency between the included studies.

Figure 3 shows the forest plot between the roles of TNF-α during sepsis among Caucasian population (n = 15 studies). There was no significant effect of the TNF phenotype on risk of sepsis (OR 1.08, 95% CI [0.73; 1.61], p = 0.69, $I^2$ = 82%). A high $I^2$ heterogeneity value (>80%) indicates the inconsistency between the studies.

Figure 4 is the funnel plot for the assessment of publication bias. The funnel plot was asymmetrical, indicating the possibility of publication bias.

However, based on the OR results of the meta-analysis, there was a higher risk of sepsis in Asian population than in Caucasian population, and there was no significant effect of TNF phenotype on sepsis risk in either population.

## Discussion

Tumor necrosis factor alpha has been identified as an important pro-inflammatory cytokine in diseases like psoriatic arthritis, rheumatoid arthritis, ulcerative colitis, Crohn's disease and other autoimmune diseases, as well an in healthy people. It is located on the p arm of chromosome 6 within the major histocompatibility complex, where genetic alterations in the TNF-α locus are known to be involved directly in high TNF-α production.[47] Many polymorphisms inside the TNF-α promoter positioned

**Table 2.** The studies presenting the role of TNF in sepsis among Asian population

| Study | TNF1 | TNF2 | OR | 95% CI | Weight (%) | |
|---|---|---|---|---|---|---|
| | | | | | fixed | random |
| Song et al.[18] | 375/727 | 560/1158 | 1.138 | [0.945; 1.370] | N/A | 15.30 |
| Teuffel et al.[27] | 34/53 | 18/40 | 2.187 | [0.946; 5.059] | N/A | 12.27 |
| Gupta et al.[16] | 23/25 | 17/89 | 48.706 | [10.457; 226.865] | N/A | 8.23 |
| Fu et al.[30] | 47/163 | 100/232 | 0.535 | [0.349; 0.820] | N/A | 14.51 |
| Nakada et al.[17] | 81/189 | 5/8 | 0.450 | [0.104; 1.938] | N/A | 8.63 |
| Allam et al.[35] | 24/69 | 57/68 | 0.103 | [0.0456; 0.232] | N/A | 12.42 |
| Duan et al.[36] | 45/131 | 36/174 | 2.006 | [1.199; 3.355] | N/A | 14.10 |
| Kothari et al.[48] | 74/169 | 64/224 | 1.947 | [1.280; 2.964] | N/A | 14.54 |
| Total (random effects) | 703/1526 | 857/1993 | 1.21 | [0.63; 2.30] | N/A | 100.00 |
| df | | | | 7 | | |
| Significance level | | | | p = 0.57 | | |
| $I^2$ (inconsistency) | | | | 92% | | |

TNF – tumor necrosis factor; OR – odds ratio; 95% CI – 95% confidence interval; df – degrees of freedom; N/A – not applicable.

**Table 3.** The studies reporting on the role of TNF in sepsis among Caucasian population

| Study | TNF1 | TNF2 | OR | 95% CI | Weight (%) | |
|---|---|---|---|---|---|---|
| | | | | | fixed | random |
| Treszl et al.[21] | 25/82 | 8/21 | 0.713 | [0.263; 1.934] | 2.01 | 5.94 |
| Solé-Violán et al.[31] | 123/1162 | 234/1413 | 0.596 | [0.472; 0.753] | 36.76 | 9.30 |
| Solé-Violán et al.[31] | 112/126 | 56/118 | 8.857 | [4.565; 17.184] | 4.57 | 7.56 |
| Mira et al.[32] | 23/54 | 25/35 | 0.297 | [0.119; 0.738] | 2.42 | 6.35 |
| Gordon et al.[33] | 39/135 | 13/77 | 2.000 | [0.990; 4.039] | 4.06 | 7.36 |
| Sipahi et al.[34] | 15/42 | 4/11 | 0.972 | [0.244; 3.869] | 1.05 | 4.41 |
| Paskulin et al.[37] | 104/349 | 42/171 | 1.304 | [0.859; 1.978] | 11.55 | 8.68 |
| Jaber et al.[38] | 19/40 | 9/21 | 1.206 | [0.416; 3.496] | 1.77 | 5.65 |
| McDaniel et al.[39] | 4/15 | 4/21 | 1.545 | [0.318; 7.502] | 0.80 | 3.77 |
| Garnacho-Montero et al.[40] | 38/224 | 19/101 | 0.882 | [0.480; 1.621] | 5.41 | 7.82 |
| Susantitaphong et al.[41] | 36/112 | 44/150 | 1.141 | [0.672; 1.939] | 7.15 | 8.19 |
| Schaaf et al.[42] | 32/48 | 18/20 | 0.222 | [0.0458; 1.078 | 0.80 | 3.78 |
| Schueller et al.[43] | 19/67 | 34/102 | 0.792 | 0.404; 1.550] | 4.44 | 7.51 |
| Balding et al.[44] | 83/183 | 156/389 | 1.240 | [0.869; 1.767] | 15.96 | 8.92 |
| Majetschak et al.[45] | 10/46 | 4/24 | 1.389 | [0.385; 5.005] | 1.22 | 4.76 |
| Total (random effects) | 682/2685 | 670/2674 | 0.978 | [0.854; 1.121] | 100.00 | 100.00 |
| df | | | | 14 | | |
| Significance level | | | | p = 0.69 | | |
| $I^2$ (inconsistency) | | | | 82% | | |

TNF – tumor necrosis factor; OR – odds ratio; 95% CI – 95% confidence interval; df – degrees of freedom.

at –1031 (T→C), –863 (C→A), –857 (C→A), –851 (C→T), –419 (G→C), –376 (G→A), –308 (G→A), –238 (G→A), –162 (G→A), and –49 (G→A) have been identified, but nucleotide position –308 directly affects TNF-α production. A SNP within the promoter of the gene for TNF-α results in 2 allelic forms, TNF1 with guanine as common allele and TNF2 with guanine substituted by adenosine.[48] The polymorphism in TNF-α –308 A/G has been associated with several pathologies like parasitic, bacterial and viral infections; autoimmune diseases like systemic lupus erythematosus, rheumatoid arthritis and ankylosing spondylitis; acute rejections for transplants[57–60]; cancers[10] and coronary artery disease.[52] It has been observed in the past that TNF-α has been involved in sepsis-induced immune depression through increased apoptosis.[49] The TNF2 allele has been linked to sepsis, but the evidence is ambigous. The present meta-analysis aimed to analyze the role of TNFα –308 genotype (TNF1 or TNF2) in a higher risk of sepsis.

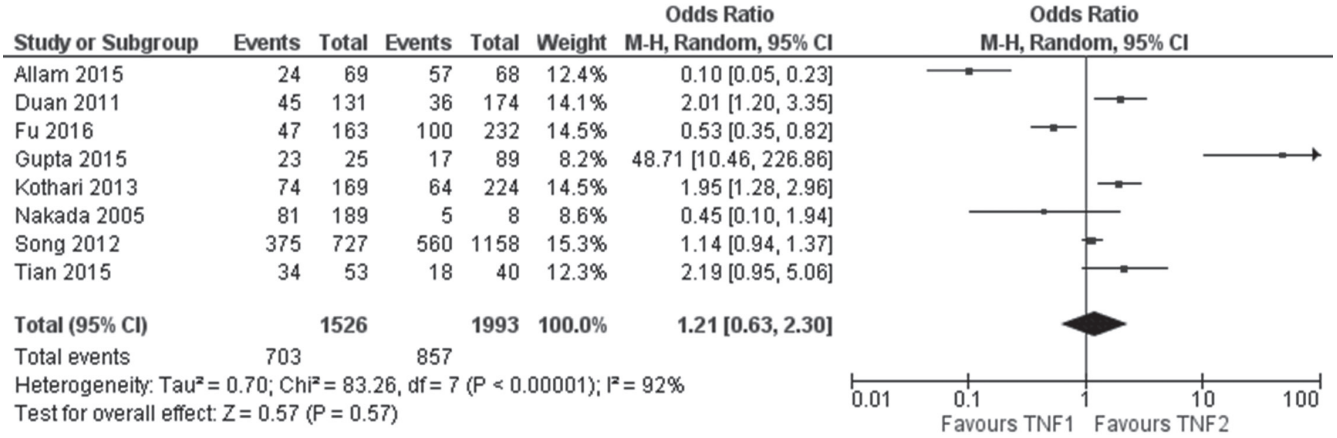


Fig. 2. The forest plot depicting the role of tumor necrosis factor alpha (TNF-α) during sepsis among the Asian population

95% CI – 95% confidence interval; df – degrees of freedom.

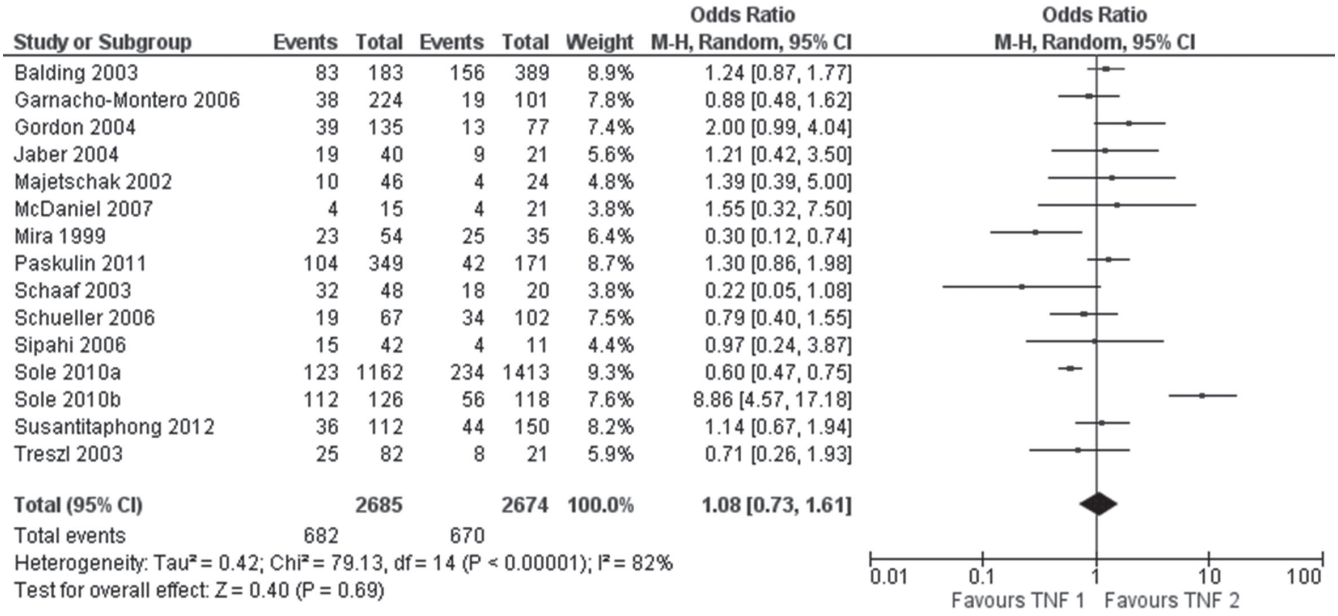


Fig. 3. The forest plot depicting the role of tumor necrosis factor alpha (TNF-α) during sepsis among the Caucasian population

95% CI – 95% confidence interval; df – degrees of freedom.

The Human Genome Project (HGP) focused on an individual's DNA sequence. The following stage was designed to compare DNA sequences from various populations. The HapMap is a collection of human genetic diversity. It was completed in 2005 and uses SNPs to discover huge blocks of DNA sequence known as haplotypes that are inherited together (Fig. 5). Researchers examine haplotypes in persons with and without certain diseases to elucidate information from the analyzed data. The haplotypes shared by persons with the disease are then analyzed in depth to search for genes that are linked to a particular condition. Scientists have already used the data in order to find a gene linked to age-related macular degeneration, a condition that causes blindness in elderly patients.[9] The International HapMap Consortium is predicted to play a significant role in finding many more disease-related genes in the future.[51]

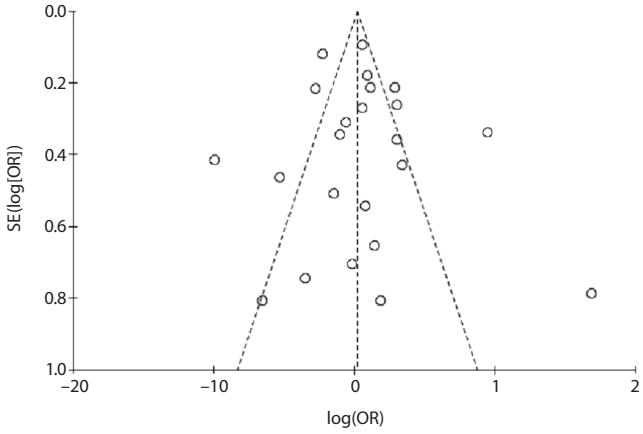


Fig. 4. Funnel plot for the assessment of publication bias

SE – standard error; OR – odds ratio.

In a small number of DNA samples, the HGP,[49] the SNP Consortium[50] and the International HapMap Project[51] found over 10 million common DNA variations, mostly SNPs. Genome-wide association studies have effectively found hundreds of unique genomic loci that have an impact on human diseases, due to the knowledge on SNPs and associated linkage disequilibrium patterns.[4]

Nonetheless, our understanding of human genetic variation in terms of variant type, frequency and population diversification is inadequate. Only common DNA variations (minor allele frequency (MAF) 5%) have been thoroughly investigated, despite the fact that low MAF variations are likely to account for a significant portion of genetic risk for common diseases. Systematic investigations of other forms of variations, particularly copy number variation, have just lately begun to shape our understanding of their frequency spectra, population distributions and linkage disequilibrium patterns.

According to Elahi et al.,[52] TNF polymorphisms are found in a region of polymorphic variation and they are in linkage disequilibrium with the human leukocyte antigen (HLA) genes and with each other. Due to the differences in the distribution of HLA alleles, there can be variation in TNF polymorphisms and various discrepancies can be associated with different geographical locations.

The current study does not demonstrate the influence of TNF variants on sepsis in Asian and Caucasian populations. However, the number of studies in Asian population is small (n = 8), thus limiting an inference to be made in general. The heterogeneity values are high (>80%), suggesting a considerable inconsistency between the studies. Potential sources of heterogeneity are age, sample size, genotyping method, and type of sepsis.

The TNF2 allele frequencies have been identified for various ethnic groups, with Asian population (TNF2 prevalence ranging from 1.7%[51] to 5.1%[54]) having a lower TNF2 allele frequency than Caucasian population (TNF2 prevalence ranging from 21.7%[55] to 23.0%[56]). To see whether the connection between TNF2 and sepsis varied by ethnicity, we conducted a stratified study. Our findings indicate that the connection between TNF2 and sepsis is not significant in the Asian community compared to other ethnic groups. Given the secondary nature of the study, this finding should be regarded as hypothesis-generating.

The authors has also researched whether the impact of TNF2 varied, based on how sepsis was defined (sepsis, extreme sepsis or septic shock) in our stratified studies. The fact that many different health conditions such as pneumonia, bacteremia, sepsis, septicemia, acute sepsis, or septic shock have been analyzed, has made it challenging to interpret past findings. The authors were able to conduct systematic review because this meta-analysis used published consensus criteria for sepsis[55] and the rest of the articles in our meta-analysis used these same definitions.

We discovered that the way sepsis was defined had little effect on the connection between TNF2 and sepsis susceptibility. Because of the limited number of trials in each subgroup, determining whether sepsis classification influenced the relationship between TNF2 and sepsis mortality is more complicated. Therefore, future research into this topic is critical. However, the present meta-analysis helped to overcome the limitations of the individual studies and thoroughly examined TNF-α role in sepsis.

One of the strengths of the study is that it was focused solely on TNF-α –308 A/G, which helped in conducting a thorough search and analysis of the impact of this single polymorphism. Other genetic variants, on the other hand, are very likely to affect sepsis risk. As a result, future experiments should examine the effects of other polymorphisms, and eventually, many polymorphisms would have to be considered.

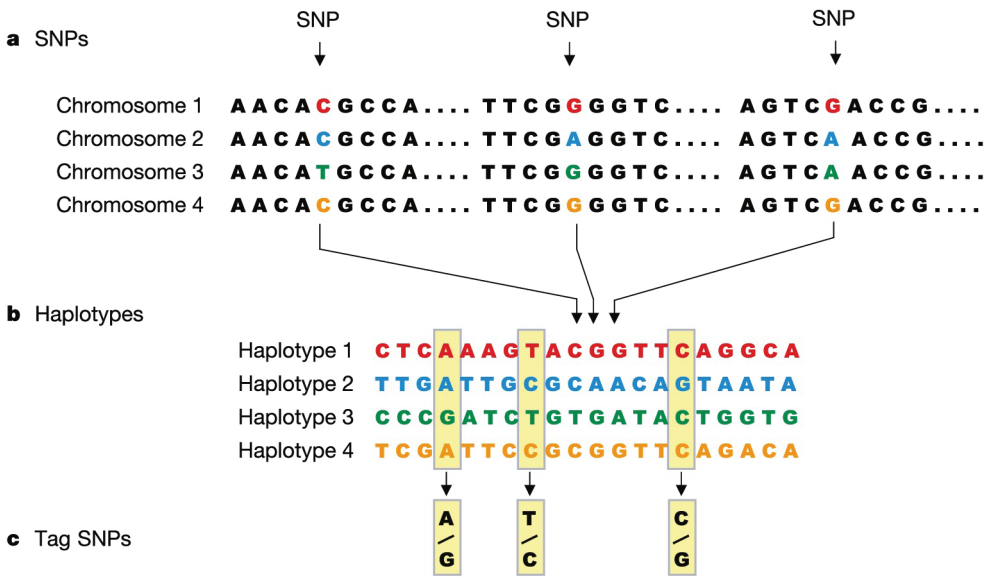


Fig. 5. Single nucleotide polymorphisms (SNPs), haplotypes and tag SNPs

In addition, the current meta-analysis reveals the possibility of obtaining a more stratified study by considering similar studies in each stratum. A meta-regression could also be carried out to examine the hidden factors affecting the phenomenon.

## Limitations

The study has a few limitations, such as limited sample size in most of the analyzed studies, that affects the statistical power. There is a high heterogeneity among the different ethnic backgrounds. Lastly, there is a strong need for more studies to determine the clarification on genetic roles and cytokine production during sepsis.

# Conclusions

The relationship between the TNF–308 G/A polymorphism and sepsis was quantitatively synthesized in this meta-analysis. It does not suggest an association between the G/A allele combination of TNF-α and sepsis risk in the Asian and Caucasian populations. We believe that integrating the effects of correlation research will help us better understand the impact of polymorphisms on disease outcomes.


### ORCID iDs

Huining Niu https://orcid.org/0000-0003-4896-9796
Fujun Li https://orcid.org/0000-0003-4842-5465
Hua Ma https://orcid.org/0000-0002-4238-5696
Limei Xiu https://orcid.org/0000-0003-2766-3683
Juan Chen https://orcid.org/0000-0002-8459-1527
Min Hang https://orcid.org/0000-0002-3259-9869


### References


1. Martín S, Pérez A, Aldecoa C. Sepsis and immunosenescence in the elderly patient: A review. *Front Med (Lausanne)*. 2017;4:20. doi:10.3389/fmed.2017.00020
2. Perner A, Rhodes A, Venkatesh B, et al. Sepsis: Frontiers in supportive care, organisation and research. *Intensive Care Med*. 2017;43(4):496–508. doi:10.1007/s00134-017-4677-4
3. Sorensen TI, Nielsen GG, Andersen PK, Teasdale TW. Genetic and environmental influences on premature death in adult adoptees. *N Engl J Med*. 1988;318(12):727–732. doi:10.1056/NEJM198803243181202
4. Ludwig KR, Hummon AB. Mass spectrometry for the discovery of biomarkers of sepsis. *Mol Biosyst*. 2017;13(4):648–664. doi:10.1039/c6mb00656f
5. Hotchkiss RS, Moldawer LL, Opal SM, et al. Sepsis and septic shock. *Nat Rev Dis Primers*. 2016;2:16045. doi:10.1038/nrdp.2016.45
6. Liu R, Mo YY, Wang HL, et al. The relationship between toll like receptor 4 gene rs4986790 and rs4986791 polymorphisms and sepsis susceptibility: A meta-analysis. *Sci Rep*. 2016;6:38947. doi:10.1038/srep38947
7. Shi Q, Mu X, Hong L, Zheng S. *SERPINE1* rs1799768 polymorphism contributes to sepsis risk and mortality. *J Renin Angiotensin Aldosterone Syst*. 2015;16(4):1218–1224. doi:10.1177/1470320315614714
8. Qiao YC, Chen YL, Pan YH, et al. The change of serum tumor necrosis factor-alpha in patients with type 1 diabetes mellitus: A systematic review and meta-analysis. *PLoS One*. 2017;12(4):e0176157. doi:10.1371/journal.pone.0176157
9. Meng N, Zhang Y, Li H, Ma J, Qu Y. Association of tumor necrosis factor alpha promoter polymorphism (TNF-α 238 G/A and TNF-α 308 G/A) with diabetic mellitus, diabetic retinopathy and diabetic nephropathy: A meta-analysis. *Curr Eye Res*. 2014;39(2):194–203. doi:10.3109/02713683.2013.834942
10. Wang Y, Yang J, Huang J, Tian Z. Tumor necrosis factor-α polymorphisms and cervical cancer: Evidence from a meta-analysis. *Gynecol Obstet Invest*. 2020;85(2):153–158. doi:10.1159/000502955
11. El-Tahan RR, Ghoneim AM, El-Mashad N. TNF-alpha gene polymorphisms and expression. *Springerplus*. 2016;5(1):1508. doi:10.1186/s40064-016-3197-y
12. Lv B, Huang J, Yuan H, Yan W, Hu G, Wang J. Tumor necrosis factor-α as a diagnostic marker for neonatal sepsis: A meta-analysis. *Scientific WorldJournal*. 2014;2014:471463. doi:10.1155/2014/471463
13. Patel HJ, Patel BM. TNF-alpha and cancer cachexia: Molecular insights and clinical implications. *Life Sci*. 2017;170:56–63. doi:10.1016/j.lfs.2016.11.033
14. Kali A. TNFerade, an innovative cancer immunotherapeutic. *Indian J Pharmacol*. 2015;47(5):479–483. doi:10.4103/0253-7613.165190
15. Iori L, Delahaye NF, Iraqi FA, Hernandez-Valladares M, Fumoux F, Rihet P. TNF as a malaria candidate gene: Polymorphism-screening and family-based association analysis of mild malaria attack and parasitemia in Burkina Faso. *Genes Immun*. 2005;6(6):472–480. doi:10.1038/sj.gene.6364231
16. Gupta DL, Nagar PK, Kamal VK, Bhoi S, Rao DN. Clinical relevance of single nucleotide polymorphisms within the 13 cytokine genes in North Indian trauma hemorrhagic shock patients. *Scand J Trauma Resusc Emerg Med*. 2015;23:96. doi:10.1186/s13049-015-0174-3
17. Nakada TA, Hirasawa H, Oda S, et al. Influence of toll-like receptor 4, CD14, tumor necrosis factor, and interleukine-10 gene polymorphisms on clinical outcome in Japanese critically ill patients. *J Surg Res*. 2005;129(2):322–328. doi:10.1016/j.jss.2005.05.020
18. Song Z, Song Y, Yin J, et al. Genetic variation in the TNF gene is associated with susceptibility to severe sepsis, but not with mortality. *PLoS One*. 2012;7(9):e46113. doi:10.1371/journal.pone.0046113
19. Sipahi T, Pocan H, Akar N. Effect of various genetic polymorphisms on the incidence and outcome of severe sepsis. *Clin Appl Thromb Hemost*. 2006;12(1):47–54. doi:10.1177/107602960601200108
20. Schueller AC, Heep A, Kattner E, et al. Prevalence of two tumor necrosis factor gene polymorphisms in premature infants with early-onset sepsis. *Biol Neonate*. 2006;90(4):229–232. doi:10.1159/000093605
21. Treszl A, Kocsis I, Szathmari M, et al. Genetic variants of TNF-[FC12]a, IL-1beta, IL-4 receptor [FC12]a-chain, IL-6 and IL-10 genes are not risk factors for sepsis in low-birth-weight infants. *Biol Neonate*. 2003;83(4):241–245. doi:10.1159/000069484
22. Wilson AG, di Giovine FS, Blakemore AI, Duff GW. Single base polymorphism in the human tumour necrosis factor-alpha (TNF alpha) gene detectable by NcoI restriction of PCR product. *Hum Mol Genet*. 1992;1(5):353. doi:10.1093/hmg/1.5.353
23. Hajeer AH, Hutchinson IV. Influence of TNFalpha gene polymorphisms on TNF alpha production and disease. *Hum Immunol*. 2001;62(11):1191–1199. doi:10.1016/s0198-8859(01)00322-6
24. Debets JM, Kampmeijer R, van der Linden MP, Buurman WA, van der Linden CJ. Plasma tumor necrosis factor and mortality in critically ill septic patients. *Crit Care Med*. 1989;17(6):489–494. doi:10.1097/00003246-198906000-00001
25. Waage A, Halstensen A, Espevik T. Association between tumour necrosis factor in serum and fatal outcome in patients with meningococcal disease. *Lancet*. 1987;1(8529):355–357. doi:10.1016/s0140-6736(87)91728-4
26. Papathanassoglou ED, Giannakopoulou MD, Bozas E. Genomic variations and susceptibility to sepsis. *AACN Adv Crit Care*. 2006;17(4):394–422. doi:10.4037/15597768-2006-4006
27. Teuffel O, Ethier MC, Beyene J, Sung L. Association between tumor necrosis factor-alpha promoter –308 A/G polymorphism and susceptibility to sepsis and sepsis mortality: A systematic review and meta-analysis. *Crit Care Med*. 2010;38(1):276–282. doi:10.1097/CCM.0b013e3181b42af0
28. Zhang M, Zhao Y, Liu Q. Tumor necrosis factor-alpha–308G/A and –238G/A polymorphisms are associated with increased risks of sepsis: Evidence from an updated meta-analysis. *APMIS*. 2017;125(5):459–467. doi:10.1111/apm.12661
29. Zhang Y, Cui X, Ning L, Wei D. The effects of tumor necrosis factor-α (TNF-α) rs1800629 and rs361525 polymorphisms on sepsis risk. *Oncotarget*. 2017;8(67):111456–111469. doi:10.18632/oncotarget.22824
30. Fu Y, Chen Y, Bai N, Liu R, Li D. Correlation of TNF-alpha gene polymorphisms with sepsis susceptibility. *Int J Clin Exp Pathol*. 2016;9:2335–2339. http://www.ijcep.com/files/ijcep0015351.pdf. Accessed January 12, 2022.

31. Solé-Violán J, de Castro F, García-Laorden MI, et al. Genetic variability in the severity and outcome of community-acquired pneumonia. *Respir Med*. 2010;104(3):440–447. doi:10.1016/j.rmed.2009.10.009
32. Mira JP, Cariou A, Grall F, et al. Association of TNF2, a TNF-alpha promoter polymorphism, with septic shock susceptibility and mortality: A multicenter study. *JAMA*. 1999;282(6):561–568. doi:10.1001/jama.282.6.561
33. Gordon AC, Lagan AL, Aganna E, et al. TNF and TNFR polymorphisms in severe sepsis and septic shock: A prospective multicentre study. *Genes Immun*. 2004;5(8):631–640. doi:10.1038/sj.gene.6364136
34. Sipahi T, Pocan H, Akar N. Effect of various genetic polymorphisms on the incidence and outcome of severe sepsis. *Clin Appl Thromb Hemost*. 2006;12(1):47–54. doi:10.1177/107602960601200108
35. Allam G, Alsulaimani AA, Alzaharani AK, Nasr A. Neonatal infections in Saudi Arabia: Association with cytokine gene polymorphisms. *Cent Eur J Immunol*. 2015;40(1):68–77. doi:10.5114/ceji.2015.50836
36. Duan ZX, Gu W, Zhang LY, et al. Tumor necrosis factor-alpha gene polymorphism is associated with the outcome of trauma patients in the Chinese Han population. *J Trauma*. 2011;70(4):954–958. doi:10.1097/TA.0b013e3181e88adf
37. Paskulin DD, Fallavena PR, Paludo FJ, et al. TNF–308G > a promoter polymorphism (rs1800629) and outcome from critical illness. *Braz J Infect Dis*. 2011;15(3):231–238. doi:10.1016/s1413-8670(11)70181-7
38. Jaber BL, Rao M, Guo D, et al. Cytokine gene promoter polymorphisms and mortality in acute renal failure. *Cytokine*. 2004;25(5):212–219. doi:10.1016/j.cyto.2003.11.004
39. McDaniel DO, Hamilton J, Brock M, et al. Molecular analysis of inflammatory markers in trauma patients at risk of postinjury complications. *J Trauma*. 2007;63(1):147–157. doi:10.1097/TA.0b013e31806bf0ab
40. Garnacho-Montero J, Aldabo-Pallas T, Garnacho-Montero C, et al. Timing of adequate antibiotic therapy is a greater determinant of outcome than are TNF and IL-10 polymorphisms in patients with sepsis. *Crit Care*. 2006;10(4):R111. doi:10.1186/cc4995
41. Susantitaphong P, Perianayagam MC, Tighiouart H, Liangos O, Bonventre JV, Jaber BL. Tumor necrosis factor-alpha promoter polymorphism and severity of acute kidney injury. *Nephron Clin Pract*. 2013;123(1–2):67–73. doi:10.1159/000351684
42. Schaaf BM, Boehmke F, Esnaashari H, et al. Pneumococcal septic shock is associated with the interleukin-10-1082 gene promoter polymorphism. *Am J Respir Crit Care Med*. 2003;168(4):476–480. doi:10.1164/rccm.200210-1164OC
43. Schueller AC, Heep A, Kattner E, et al. Prevalence of two tumor necrosis factor gene polymorphisms in premature infants with early-onset sepsis. *Biol Neonate*. 2006;90(4):229–232. doi:10.1159/000093605
44. Balding J, Healy CM, Livingstone WJ, et al. Genomic polymorphic profiles in an Irish population with meningococcaemia: Is it possible to predict severity and outcome of disease? *Genes Immun*. 2003;4(8):533–540. doi:10.1038/sj.gene.6364020
45. Majetschak M, Obertacke U, Schade FU, et al. Tumor necrosis factor gene polymorphisms, leukocyte function, and sepsis susceptibility in blunt trauma patients. *Clin Diagn Lab Immunol*. 2002;9(6):1205–1211. doi:10.1128/cdli.9.6.1205-1211.2002
46. Higuchi T, Seki N, Kamizono S, et al. Polymorphism of the 5′-flanking region of the human tumor necrosis factor (TNF)-alpha gene in Japanese. *Tissue Antigens*. 1998;51(6):605–612. doi:10.1111/j.1399-0039.1998.tb03002.x
47. Tsukamoto K, Ohta N, Shirai Y, Emi M. A highly polymorphic CA repeat marker at the human tumor necrosis factor alpha (TNF alpha) locus. *J Hum Genet*. 1998;43(4):278–279. doi:10.1007/s100380050090
48. Kothari N, Bogra J, Abbas H, et al. Tumor necrosis factor gene polymorphism results in high TNF level in sepsis and septic shock. *Cytokine*. 2013;61(2):676–681. doi:10.1016/j.cyto.2012.11.016
49. Lander ES, Linton LM, Birren B, et al. Initial sequencing and analysis of the human genome. *Nature*. 2001;409(6822):860–921. doi:10.1038/35057062
50. Sachidanandam R, Weissman D, Schmidt SC, et al. A map of human genome sequence variation containing 1.42 million single nucleotide polymorphisms. *Nature*. 2001;409(6822):928–933. doi:10.1038/35057149
51. International HapMap Consortium; Frazer KA, Ballinger DG, Cox DR, et al. A second generation human haplotype map of over 3.1 million SNPs. *Nature*. 2007;449(7164):851–861. doi:10.1038/nature06258
52. Elahi MM, Asotra K, Matata BM, Mastana SS. Tumor necrosis factor alpha –308 gene locus promoter polymorphism: An analysis of association with health and disease. *Biochim Biophys Acta*. 2009;1792(3):163–172. doi:10.1016/j.bbadis.2009.01.007
53. Huang SL, Su CH, Chang SC. Tumor necrosis factor-alpha gene polymorphism in chronic bronchitis. *Am J Respir Crit Care Med*. 1997;156(5):1436–1439. doi:10.1164/ajrccm.156.5.9609138
54. Reynard MP, Turner D, Navarrete CV. Allele frequencies of polymorphisms of the tumour necrosis factor-alpha, interleukin-10, interferon-gamma and interleukin-2 genes in a North European Caucasoid group from the UK. *Eur J Immunogenet*. 2000;27(4):241–249. doi:10.1046/j.1365-2370.2000.00227.x
55. Grove J, Daly AK, Bassendine MF, Day CP. Association of a tumor necrosis factor promoter polymorphism with susceptibility to alcoholic steatohepatitis. *Hepatology*. 1997;26(1):143–146. doi:10.1002/hep.510260119
56. Bone RC, Balk RA, Cerra FB, et al. Definitions for sepsis and organ failure and guidelines for the use of innovative therapies in sepsis. The ACCP/SCCM Consensus Conference Committee. American College of Chest Physicians/Society of Critical Care Medicine. *Chest*. 1992;101(6):1644–1655. doi:10.1378/chest.101.6.1644
57. Khurshid S, Zeb A, Bano S, et al. Association of tumour necrosis factor-alpha –308 G/A promoter polymorphism with susceptibility and disease profile of rheumatoid arthritis. *J Ayub Med Coll Abbottabad*. 2020;32(2):184–188. PMID:32583991.
58. Piotrowski P, Wudarski M, Sowińska A, Olesińska M, Jagodziński PP. TNF–308 G/A polymorphism and risk of systemic lupus erythematosus in the Polish population. *Mod Rheumatol*. 2015;25(5):719–723. doi:10.3109/14397595.2015.1008778
59. Ma HJ, Yin QF, Wu Y, Guo MH. TNF-α–308 polymorphism determines clinical manifestations and therapeutic response of ankylosing spondylitis in Han Chinese. *Med Clin (Barc)*. 2017;149(12):517–522. doi:10.1016/j.medcli.2017.04.023
60. Liu F, Li B, Wei Y, Ma Y, Yan L, Wen T. Tumor necrosis factor-alpha–308 G/A polymorphism and acute liver graft rejection: A meta-analysis. *Transpl Immunol*. 2010;24(1):45–49. doi:10.1016/j.trim.2010.09.004

# Rare causes of anemia in liver diseases

Jakub Dawidowski[1,2,A–F], Anna Pietrzak[1,2,A–F]

[1] II Gastroenterology Department, Centre of Postgraduate Medical Education, Warsaw, Poland
[2] Gastroenterology Department, Bielanski Hospital, Warsaw, Poland

A – research concept and design; B – collection and/or assembly of data; C – data analysis and interpretation;
D – writing the article; E – critical revision of the article; F – final approval of the article

Advances in Clinical and Experimental Medicine, ISSN 1899–5276 (print), ISSN 2451–2680 (online) *Adv Clin Exp Med*. 2022;31(5):567–574

**Address for correspondence**
Jakub Dawidowski
E-mail: j.dawidowski@o2.pl

**Funding sources**
None declared

**Conflict of interest**
None declared

Received on August 31, 2021
Reviewed on December 23, 2021
Accepted on January 20, 2022

Published online on March 11, 2022

## Abstract

Anemia is a common finding among patients with liver diseases. Patients who suffer from anemia are at a higher risk of liver function decompensation and hospitalization. It affects significantly their quality of life and contributes to mortality. Anemia is present in 70% of patients with liver cirrhosis and with varying incidence accompanies other liver disorders. As the etiology of anemia in liver diseases is multifactorial, various cases represent different clinical entities. Anemia accompanying hepatic disorders can be broadly divided into several types, such as anemia associated with blood loss, as well as aplastic, hemolytic and micronutrient deficiency anemia. However, it is sometimes difficult to delineate between those types in the clinical practice, as several pathophysiological causes can be present in one patient. It is reported that the most common cause of anemia in liver disease is blood loss and iron deficiency. Still, the incidence of unclear cases reaching over 50% suggests that other types of anemia can be underdiagnosed. This review comprehensively describes less frequent types of anemia associated with liver disease, namely hemolytic and aplastic anemia (AA). Hemolytic anemia can complicate autoimmune liver diseases or be a manifestation of membranopathy of red blood cells, dependent on severe hepatic function impairment or alcoholic liver disease. Aplastic anemia is best known as a sequela of viral hepatitis, but some degree of bone marrow inhibition can complicate virtually all advanced liver diseases.

**Key words:** liver, anemia, hemolytic, aplastic, hepatology

**Cite as**
Dawidowski J, Pietrzak A. Rare causes of anemia in liver diseases. *Adv Clin Exp Med*. 2022;31(5):567–574. doi:10.17219/acem/145984

**DOI**
10.17219/acem/145984

## Introduction

Anemia complicating liver diseases is a common finding in clinical practice that constitutes a significant problem, since it can have unfavorable effects on patient prognosis and quality of life. It is hypothesized that the deleterious effect of anemia is imposed through hypoxia and the promotion of hyperdynamic circulation. Cirrhotic patients with anemia were found to have a higher hospital mortality rate. They also more frequently develop complications of cirrhosis such as type 2 hepatorenal syndrome, and supposedly gastrointestinal bleeding and ascites.[1,2]

Anemia prevalence in hepatology is associated with the degree of impairment of liver function and portal hypertension. Prevalence of anemia is especially high in the context of liver cirrhosis, where decreased concentration of hemoglobin is reported to affect around 70% of patients.[3,4] As reported by Scheiner et al., more severe cases of anemia are less common. In their retrospective analysis, they found out that moderate to severe anemia was present in 28% of chronic liver disease cases.[4] Noticeably, in most cases, the etiology of anemia remains unclear. Anemia of unknown origin constituted 53% of all cases in Scheiner's cohort, followed by bleeding (25%) and iron deficiency (9%).[4] Unfortunately, the high prevalence of anemia can lead to a misconception that it is an essential feature of liver disease. In effect, less obvious reasons for anemia among patients suffering from hepatic disease tend to be overlooked or diagnosed with a significant delay. Both hemolytic and aplastic anemia (AA) are rare complications of liver disease, but clinicians should be aware of them due to the serious prognosis.

According to World Health Organization's (WHO) guideline, the thresholds for the diagnosis of anemia are set at 13 g/dL for men and 12 g/dL for women. For moderate and severe anemia, the cutoffs are <11 g/dL and <8 g/dL, respectively.[5]

Hemolytic anemia manifests itself as shorter than the normal lifespan of erythrocyte. A number of different classifications of hemolytic anemia have been implemented. The broadest, but also, due to its clinical implications, the most widely used, is a division depending on the involvement of immune-mediated mechanisms of hemolysis. The clinical picture being the most suggestive of hemolysis, can be described as an increased bilirubin concentration, high lactate dehydrogenase blood activity and a low concentration of haptoglobin in the presence of normocytic anemia with reticulocytosis.[6]

Aplastic anemia is a rare clinical entity defined as an injury to precursor hematopoietic cells. The pathomechanism of AA is considered immune-mediated, but antigens triggering the response are not fully characterized. Cytopenia tends to occur in all 3 lines of blood cells. To diagnose AA, the thresholds were established for hemoglobin at 10 g/dL, platelets at 50,000/μL and neutrophils at 1500/μL. For the diagnosis, however, bone marrow examination is necessary, as it can show hypocellularity in the absence of bone marrow infiltration or fibrosis.[7]

## Objectives

The aim of this paper is to summarize the available information about the rare causes of anemia – mainly hemolytic and aplastic – among patients with liver disease. As research on that topic is scattered, a review article seems to be the best choice to give a theoretical basis for medical practitioners who face difficulties diagnosing anemic patients with liver disorders.

## Materials and methods

A selection of available literature in PubMed, Cumulative Index to Nursing and Allied Health Literature (CINAHL) and Cochrane Library databases was performed in July 2021. The search included both original and review articles. The utilization of search terms, such as "liver disease", "liver cirrhosis", "hepatitis", "cholestasis", "liver injury", "alcoholic liver disease", "aplastic", "hypoplastic", "hemolytic", "autoimmune", "anemia", "hemolysis", "acanthocytosis", and "bone marrow aplasia" let us identify 32,825 articles. Titles and abstracts were screened from that number, which limited the number of applicable papers to 3,726 original articles and 127 review articles. We included studies that focused on hemolytic and aplastic anemia in patients with liver diseases. Studies published in other languages than English, without the abstracts available online, as well as duplications were excluded. Citations and reference lists of selected articles were analyzed in the next step, allowing to identify 185 articles for a full-text review (Fig. 1). Articles screening was performed independently by both authors, and in case of conflicting opinions papers were discussed on a case-by-case basis.

## Hemolytic anemia

Compared with bleeding or micronutrient deficiency, hemolysis is an uncommon cause of anemia in patients with liver disease. The possible mechanisms of hemolysis include immune-mediated destruction of red blood cells with the involvement of antibodies, or non-immune mechanisms, dependent mainly on acquired structural aberrations of red blood cells.

Antibody-mediated hemolysis is one of the main mechanisms of the acquired cases of hemolytic anemia in the general population. A well-described feature of liver and bile duct autoimmune diseases has a high rate of coexistence with other autoimmune diseases. In the case of autoimmune hepatitis, as many as 20–50% of patients have other

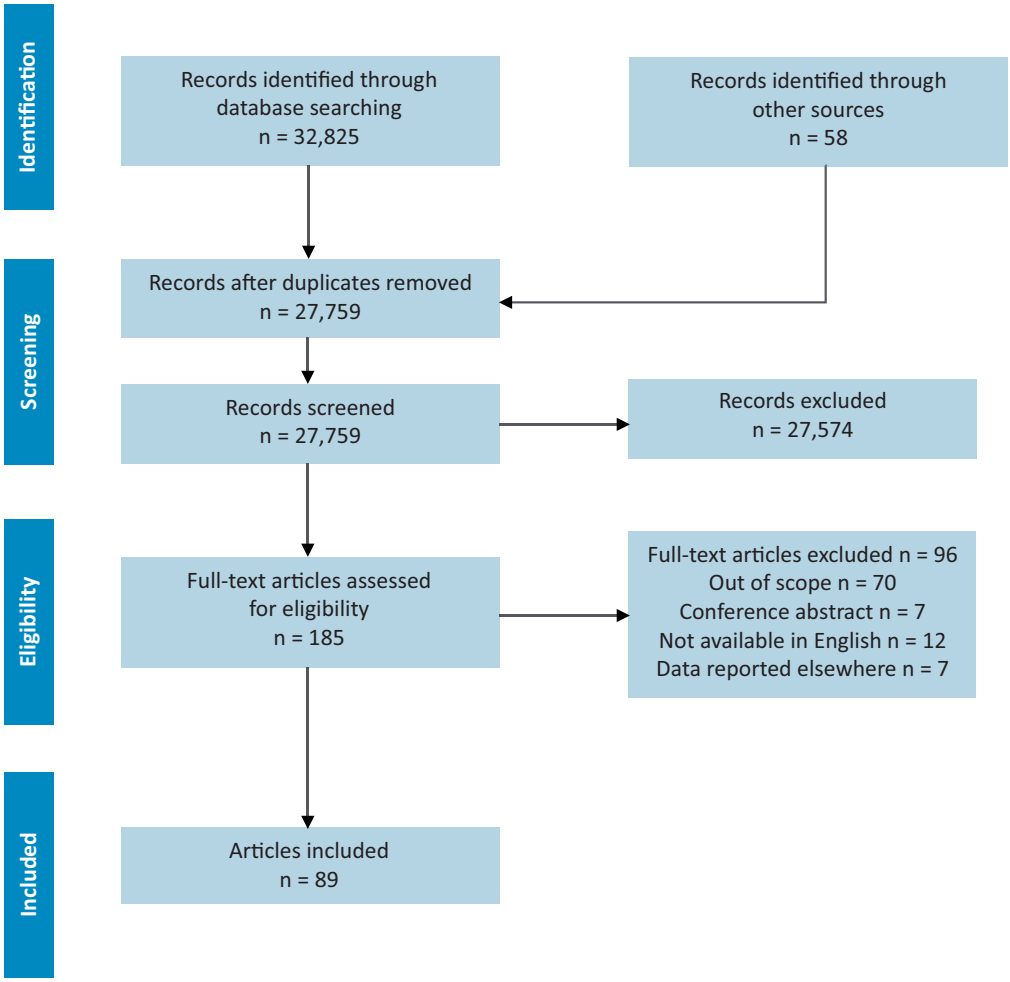


Fig. 1. Flowchart of article selection process

autoimmune disease. Those numbers can be even higher when primary biliary cholangitis (PBC) is considered, rising up to 84%, as reported by Culp et al.[8,9] Autoimmune hepatitis, PBC and primary sclerosing cholangitis (PSC) significantly differ from each other in the incidence of various extrahepatic autoimmune diseases. However, autoimmune hemolytic anemia (AIHA), characterized by a positive direct Coombs test, remains a rare comorbidity for all three. The reported prevalence of AIHA among AIH patients is less than 1%.[9] The diagnosis of AIHA complicating PBC or PSC course is even less frequent.[10,11] In fact, it is not currently clear if AIHA associated with PBC and PSC represents a distinct clinical entity or is just a coexistence of 2 independent diseases by chance. In the context of AIHA complicating autoimmune liver disease, standard treatment regimens are usually recommended. The clinical guidelines on the management of secondary AIHA, available from 2017, do not specifically discuss autoimmune liver conditions.[12] The first-line treatment includes corticosteroids and immunosuppressants, like azathioprine, cyclophosphamide or cyclosporine.[10] In cases with no satisfying improvement on corticosteroids, rituximab is a recommended option, and in the context of a limited access to rituximab, splenectomy should be considered.[13] It should, however, be noted, that the effectiveness of monotherapy with ursodeoxycholic acid (UDCA) has been described in mild cases of AIHA associated with PBC.[14]

A major portion of hemolytic anemia cases complicating liver disease is not dependent on immune-mediated mechanisms. Severe acute or chronic liver injury can lead to red blood cell membrane alternations and, in consequence, to a shortened life span of erythrocytes. The liver is an organ playing a crucial role in lipid metabolism – the insufficiency of liver functions causes lipid disturbances in cell membranes. An increasing amount of cholesterol in the erythrocyte cell membrane results in the enlargement of its surface – an effect observed as macrocytosis on complete blood count.[15] Moreover, echinocytosis and stomatocytosis of red blood cells can be an effect of phosphatidylcholine alternation, which in turn is a result of liver disease.[15] In more severe cases of liver disease, spur cell anemia (acanthocytosis) can develop. Spur cell anemia is a rare complication of liver disease, but its association with the liver function impairment is well described in the literature. Spur cell anemia especially often accompanies cases of alcoholic liver disease.[16] The name of the disease is derived from the characteristic morphology of erythrocytes, which are enlarged and develop thorny-like processes. The primary mechanism behind

spur cell anemia are changes in cholesterol to phospholipid ratio. In effect, the erythrocyte cell membrane loses its normal elastic properties. Deformed erythrocytes become prone to sequestration and destruction by macrophages in spleen. Interestingly, the aberration in lipid cell membrane composition is clearly acquired; red blood cells that were transfused to cirrhotic patients tend to gradually change their lipid composition and have a shortened lifespan.[17] Data from pediatric cohorts suggest that besides cell membrane lipid disturbances, vitamin E deficiency can play a major role in the pathogenesis of hemolytic anemia in the context of liver disease.[18]

The risk of spur cell anemia development is 2 times higher in women with alcoholic liver disease.[16] Patients who, besides alcoholic liver disease, have other comorbidities, especially chronic obstructive pulmonary disease (COPD), are at a higher risk of spur cell anemia. Tariq et al. hypothesize in their study that COPD and alcoholic liver disease can have common destructive mechanisms of action towards red cell membranes through increased reactive oxygen species (ROS) production in both diseases.[16]

Spur cell anemia is associated with a poor prognosis and a reported average survival time of 1 year.[19] Scarce reports suggest that liver transplantation can play a curative role in both liver disease and spur cell anemia.[20] Data on splenectomy usefulness in spur cell anemia treatment are insufficient. Early data showed that spur cells transferred to healthy asplenic recipients had normal survival.[17] However, decreasing spleen blood flow by placing a transjugular intrahepatic portosystemic shunt (TIPS) has not been observed to affect the disease course positively.[20]

Zieve's syndrome represents another clinical entity, which essential feature is non-immune mediated hemolytic anemia, strongly associated with alcoholic liver disease. The syndrome is rare, and only several hundred cases have been reported so far; however, it seems to be underreported due to a limited awareness of clinicians.[21] Zieve's syndrome, besides transient hemolytic anemia, is characterized by jaundice and hyperlipidemia. Hemolytic anemia associated with Zieve's syndrome has similar pathomechanism to spur cell anemia in cases of chronic liver failure. The most important distinctive feature of hemolytic anemia associated with Zieve's syndrome is its temporary character. Significant disturbances that are believed to play a role in the pathogenesis of hemolysis in Zieve's syndrome are lysolecithin and lysocephalin induction, and their accumulation in red cell membranes – changes which are dependent on vitamin E deficiency.[21] The symptoms of Zieve's syndrome tend to wear off after several weeks (usually 4–6). Since this syndrome is usually caused by excessive alcohol consumption, abstinence can shorten the time to subsiding of symptoms. Due to the rarity of this clinical entity, well-designed studies concerning optimal treatment are lacking. The awareness of Zieve's syndrome can have important clinical implications, as hemolysis resulting from it can influence the Maddrey score, prompting the initiation of corticosteroid treatment. Because of the fact that Zieve's syndrome is believed not to be an immune-mediated type of hemolysis, glucocorticoid therapy is regarded of little value, and may result in an increased risk of iatrogenic complications.[21]

Non-immune mediated hemolysis is a common feature of Wilson's disease (WD), which relatively often can be a presenting symptom leading to diagnosis. Such a course of WD is frequently reported in a younger population.[22,23] The mechanism behind hemolysis in WD is multifactorial. In case of massive necrosis of hepatocytes, a significant load of copper is released to the bloodstream and causes oxidative stress to cell membranes.[24] Other possible mechanisms include the sodium pump function impairment and the alternation of cell membrane composition.[23] Hemolysis subsides when the pharmacotherapy of WD is introduced, or when the patient undergoes liver transplantation.

Patients with liver disease can also develop anemia due to their medication. The best-documented example of anemia due to medications used in hepatology is ribavirin-induced hemolytic anemia (RIHA). According to the summary of product characteristics, anemia is a very common adverse reaction to ribavirin (>10% of patients), and hemolytic anemia is common (>1% of patients).[25] Unfortunately, in the available clinical research, the mechanism of decrease in hemoglobin concentration was not analyzed. A decline of 3 g/dL was observed in 54% of patients taking standard ribavirin dose, and in around 8%, it was greater than 5 mg/dL.[26] Data presented in the summary of product characteristics come from the trials of ribavirin combined with peginterferon, which is also known to cause hemolytic anemia by itself. When ribavirin is co-administered with direct-acting antivirals (DAA) instead of peginterferon, RIHA rate ranges between 5% and 40%.[27] However, more severe cases of RIHA constitute less than 10% of all cases.[28] Exact pathophysiological mechanism of RIHA is unknown. It is postulated that the active form of ribavirin causes cellular shortage of adenosine triphosphate (ATP) in erythrocytes, the consequence of which is impaired glycolysis and oxidative stress, an effect that is dose-related.[26,29] Hemolysis was also observed in other species exposed to ribavirin.[30] Reducing a dose of ribavirin or discontinuation is usually an adequate action. The need for blood transfusions is sporadic (0.1%), assuming correct laboratory results monitoring.[28]

## Aplastic anemia

Aplastic anemia is another rare type of anemia, both in the general population and among patients with liver disease. It has been reported to complicate 2% of cases of chronic liver disease,[31] but the majority of clinical cases described in literature come from the context of acute liver disease. Aplastic anemia is defined by pancytopenia,

accompanied by decreased bone marrow cellularity in the absence of bone marrow infiltration or marrow fibrosis.[7] Diagnostic criteria include at least 2 of the following: hemoglobin concentration less than 10 g/dL, platelet count less than 50,000/μL, or neutrophil count below 1500/μL.[32] Immune-mediated pathologies are important factors in the development of many AA cases, but very often the exact mechanism of AA remains unclear.

In cirrhotic patients, bone marrow inhibition may contribute to existing anemia. However, anemia itself may not meet the criteria of an aplastic one. Bihari et al. conducted a complex comparison of bone marrow in cirrhotic and control individuals.[33] They have found that the number of $CD34^+$ progenitor cells has decreased in advanced cirrhosis. There was a significant correlation of this effect with model for end-stage liver disease (MELD) and Child–Pugh scores, but not with the etiology of cirrhosis. Besides that, the overall cellularity of bone marrow was decreased in cirrhosis; however, some degree of erythroid hyperplasia was observed. The changes in the number of hematopoietic cells can be linked to altered bone marrow microenvironment, with decreased population of niche cells, nerve fibers and Schwann cells, all of which are important in hematopoiesis. On the other hand, the inhibition of hematopoiesis can be linked to an increased concentration of proinflammatory cytokines and a decreased concentration of hematopoietic cell growth factors.[33] The awareness of bone marrow functioning impairment led to attempts of setting it as a therapeutic target. A randomized controlled trial, conducted by Anand et al. showed that cirrhotic individuals benefit from therapy with erythropoietin combined with granulocyte colony-stimulating factor. The response was more pronounced in patients in early cirrhosis stages and without a deep depletion of hemopoietic cells in the bone marrow.[34]

In liver disease, AA is mainly associated with infectious causes. So far, many infectious factors have been linked to AA. The cases of hepatitis-associated aplastic anemia (HAAA) were described after virtually all hepatotropic viral infections, including hepatitis A virus (HAV), hepatitis B virus (HBV), hepatitis C virus (HCV), hepatitis D virus (HDV), and hepatitis E virus (HEV). Besides that, less frequent causes noted in the literature are Epstein–Barr virus (EBV) and cytomegalovirus (CMV) infections. The HBV and HCV acute infections are most common in cases with established causative factor.[35] However, the majority of patients are seronegative for known hepatotropic viruses.[36] The HAAA associated with nonviral hepatitis, including drug and vaccine-induced hepatitis, has also been reported.[37,38] Distinct clinical picture can be elicited by parvovirus B19 infection, which is a well-known causative factor for the development of AA. It is worth noting that parvovirus B19 has a predilection to erythroid lineage cells; therefore, bone marrow biopsy can show cellularity within reference range, with depletion of erythropoietic cells.[39] In fact, an association of parvovirus B19 with AA is much stronger than with hepatitis, but it can cause both clinical entities. Pure red cell aplasia, instead of AA, is also commonly described in the context of HAV infections.

The HAAA was described to accompany 2–5% of hepatitis cases in Western Europe, and 1–5% of AA cases are associated with HAAA.[40] It was found to be relatively more common in areas with a high prevalence of human immunodeficiency virus (HIV) infections, suggesting the influence of comorbidities on the occurrence rate of the disease.[36] Some authors report higher HAAA prevalence in children than adults, especially among adolescent boys.[36] However, other series of cases do not show any association with age or sex, similarly to what is observed in the general AA patients population.[41] The HAAA can complicate both mild and severe cases of hepatitis, and the onset of hepatitis preceding HAAA can be both fulminant or insidious.[36,38]

The onset of the disease varies, but it is typically observed after 2–3 months after hepatitis.[36,38] However, an earlier onset is not uncommon in literature, and patients can still have laboratory features of acute hepatitis on presentation with HAAA.[42] In fact, according to a study in bone marrow transplant patients by Safadi et al., around 40% of patients who develop HAAA still have the laboratory markers of hepatitis on diagnosis.[41] At the opposite extreme, HAAA can also be observed in 10% of patients after more than 1 year from a hepatitis episode.[41] However, in such a scenario, the causal relationship with previous hepatitis is more controversial.

The reported symptomatology is similar to symptoms of AA in general population, which include fatigue, pallor, bleeding, easy bruising, and infections. Those symptoms can present in various combinations, depending on the degree of damage to particular cell lines, like anemia, thrombocytopenia and leukopenia, and can differ in severity. The diagnosis has to be confirmed by the aplastic or hypoplastic bone marrow in bone marrow biopsy or aspirate examination.

It is suspected that cytotoxic T lymphocytes play a key role in the pathogenesis of HAAA. Ikawa et al. suggest that $CD8^+$ lymphocytes recognize similar antigen patterns of liver and hematopoietic cells.[43] In vitro studies have shown that in some cases, the presence of $CD8^+$ lymphocytes in bone marrow correlates with the impairment of cell colonies formation.[44] A similar inhibitory effect on colony forming in bone marrow was linked to the increased interferon gamma (IFNγ) concentration,[45] which can be produced by $CD8^+$ lymphocytes infiltrating bone marrow. Interferon gamma plays a multidirectional role in bone marrow functioning. It can stimulate bone marrow stem cells in the short term by promoting their differentiation, but in a longer perspective, it plays an inhibitory role by intensifying apoptosis, decreasing the self-renewal of stem cells and disturbing the interaction of stem cells with the bone marrow microenvironment.[46]

The outcome of HAAA, when untreated, remains fatal in the majority of cases. The HAAA is considered an indication for hematopoietic stem cell transplantation, especially in younger patients with human leukocyte antigen (HLA)-matched siblings. Patients with HAAA are often erythrocyte-dependent and platelet transfusion-dependent, but restrictive thresholds for transfusion should be observed to avoid sensitization before bone marrow transplantation.[36] Results of stem cell transplantation from HLA-matched unrelated donors have inferior results.[37] When stem cell transplantation is not an available option, or the patient is over 40 years old, the immunosuppressive treatment should be implemented. Cyclosporine and antithymocyte immunoglobulin (ATG) are the treatments of choice.[37,42] Cases of simultaneous improvement of hepatitis features and pancytopenia after the initiation of immunosuppressive treatment imply that the exact immune-mediated mechanism can be responsible for both hepatic and bone marrow injury.[37] Clinical data seem to confirm that, compared with the general population of patients with AA, patients with HAAA have similarly favorable results of bone marrow transplantation and immunosuppressive therapy.[47]

Interestingly, HAAA relatively often complicates liver transplantations performed due to hepatitis with fulminant organ failure, affecting 28% of patients in the pediatric population. The HAAA following liver transplantation can be diagnosed from 1 to 7 weeks after surgery. Earlier studies usually implemented a reduction of immunosuppression after the diagnosis of post-transplant HAAA to reduce the risk of severe infections.[48] However, more recent data suggest very good results of the treatment with ATG in combination with cyclosporine A.[49]

Drug-induced AA can be caused by several pharmaceuticals used in hepatological practice, including interferon, azathioprine, propranolol, or spironolactone. Interferon treatment is known to cause immune-mediated side effects. Regarding the hematopoietic system, the most clinically significant phenomenon are cases of autoimmune hemolytic anemia. However, endogenous interferon is usually regarded as an important element of pathological pathways, leading to AA of other causes. Myelosuppression and AA have been also reported to complicate the administration of interferon in the treatment of chronic viral hepatitis.[50,51] Such reports are extremely rare, and with a declining indication for interferon use in hepatology, interferon-induced AA remains a marginal problem.

## Summary

Anemia associated with liver disease is most frequently ascribed to blood loss from the gastrointestinal tract or micronutrient deficiency, with less common occurrence of hemolytic or aplastic anemia. However, both latter types of anemia require clinicians' attention, as they can pose a significant threat to the patients if misdiagnosed and untreated. It is also important to remember that the diagnosis of one type of anemia does not preclude overlapping of other reasons for a decreased hemoglobin concentration. Therefore, a lack of improvement after the initial diagnosis and treatment of micronutrient deficiency or blood loss should trigger further diagnostics.

Hemolytic anemia is reported to complicate 1–14% of cases of advanced liver disease,[1,4] but in some clinical entities can be much more prevalent. Cases of immune-mediated hemolytic anemia can complicate autoimmune liver diseases, such as autoimmune hepatitis, PBC and PSC. Non-immune mediated hemolytic anemia in the context of liver disease can develop as acquired membranopathy of red blood cells. It can accompany virtually every severe liver disease. However, especially often, it can complicate alcohol liver disease. Non-immune mediated hemolysis can also be the first clinical manifestation of WD, particularly among younger patients. Non-immune mediated cases of hemolytic anemia caused by ribavirin are becoming less frequent due to a decreasing number of indications for the use of ribavirin in hepatology.

Aplasia occurring in the context of liver disease is a rare finding. However, cases associated with hepatitis are a well-recognized clinical entity. Viral agents most commonly trigger hepatitis-associated AA, but other noninfectious causes are also involved in the pathogenesis of AA.

## Limitations

This review is burdened with several limitations that are typical for the methodology used. In comparison to systematic reviews, narrative reviews are regarded to have a more subjective character. However, authors have made every effort to avoid any bias in the process of paper selection. Moreover, this literature review was limited only to papers written in English, which could have affected its completeness. Since database search provided us with a very high number of potential matches to the topic of our review, we implemented strict rules of title and abstract selection. There is a risk that some articles rejected based on the title and abstract screening would provide valuable information if they were included.

As aplastic and hemolytic anemia are rarely diagnosed in liver disease, the available data are scarce and often of limited quality. The abovementioned clinical entities are frequently characterized based on series of case reports, and their treatment options are not tested in randomized clinical trials. Further research is needed to fully understand the prevalence of hemolytic and aplastic anemia in liver disease, and the peculiarities of their treatment.

## Conclusions

Step-by-step approach to anemic patient with liver disease requires initially ruling out the most common underlying disorders. They include mainly blood loss and

micronutrient deficiency. However, a considerable proportion of patients remain without a clear diagnosis even after that. In such cases, less common causes of anemia should be investigated, like hemolytic anemia and AA. Both are not homogenous clinical entities but umbrella terms for various diseases. Immune-mediated hemolytic anemia is known to complicate a number of autoimmune disorders, and is an uncommon finding among patients with AIH, PBC and PSC. Non-immune mediated hemolysis is usually regarded as more probable among patients with liver disease, and is often caused by acquired membranopathy of red blood cells. It should always be suspected in alcoholic liver disease and severe liver failure. When anemia complicates hepatitis of infectious origin, the evaluation toward AA may be indicated. Moreover, when hemolytic or AA is considered in differential diagnosis, the pharmacotherapy of a patient should be thoroughly analyzed, as many drugs have been associated with discussed hematological disorders.

## ORCID iDs

Jakub Dawidowski https://orcid.org/0000-0001-9945-5811
Anna Pietrzak https://orcid.org/0000-0001-9394-4470

## References

1. Bizid S, Yacoub H, Mohamed G, et al. Does anemia have a potential effect on type 2 hepatorenal syndrome? *Can J Gastroenterol Hepatol*. 2020;2020:1134744. doi:10.1155/2020/1134744
2. Les I, Doval E, Flavià M, et al. Quality of life in cirrhosis is related to potentially treatable factors. *Eur J Gastroenterol Hepatol*. 2010; 22(2):221–227. doi:10.1097/MEG.0b013e3283319975
3. Privitera G, Meli G. An unusual cause of anemia in cirrhosis: Spur cell anemia, a case report with review of literature. *Gastroenterol Hepatol Bed Bench*. 2016;9(4):335–339. PMID:27895861. PMCID:PMC5118860.
4. Scheiner B, Semmler G, Maurer F, et al. Prevalence of and risk factors for anaemia in patients with advanced chronic liver disease. *Liver Int*. 2020;40(1):194–204. doi:10.1111/liv.14229
5. World Health Organization (WHO). Haemoglobin concentrations for the diagnosis of anaemia and assessment of severity. Vitamin and Mineral Nutrition Information System. http://www.who.int/vmnis/indicators/haemoglobin.pdf. Accessed August 1, 2021.
6. Phillips J, Henderson AC. Hemolytic anemia: Evaluation and differential diagnosis. *Am Fam Physician*. 2018;98(6):354–361. PMID:30215915.
7. Killick SB, Bown N, Cavenagh J, et al. Guidelines for the diagnosis and management of adult aplastic anaemia. *Br J Haematol*. 2016;172(2): 187–207. doi:10.1111/bjh.13853
8. Culp KS, Fleming CR, Duffy J, Baldus WP, Dickson ER. Autoimmune associations in primary biliary cirrhosis. *Mayo Clin Proc*. 1982;57(6): 365–370. PMID:6896227.
9. Wong GW, Heneghan MA. Association of extrahepatic manifestations with autoimmune hepatitis. *Dig Dis*. 2015;33(Suppl 2):25–35. doi:10.1159/000440707
10. Tian Y, Wang C, Liu JX, Wang HH. Primary biliary cirrhosis-related autoimmune hemolytic anemia: Three case reports and review of the literature. *Case Rep Gastroenterol*. 2009;3(2):240–247. doi:10.1159/000229189
11. Kawaguchi T, Arinaga-Hino T, Morishige S, et al. Prednisolone-responsive primary sclerosing cholangitis with autoimmune hemolytic anemia: A case report and review of the literature. *Clin J Gastroenterol*. 2021;14(1):330–335. doi:10.1007/s12328-020-01256-8
12. Hill QA, Stamps R, Massey E, et al. Guidelines on the management of drug-induced immune and secondary autoimmune, haemolytic anaemia. *Br J Haematol*. 2017;177(2):208–220. doi:10.1111/bjh.14654
13. Hill A, Hill QA. Autoimmune hemolytic anemia. *Hematology Am Soc Hematol Educ Program*. 2018;2018(1):382–389. doi:10.1182/asheducation-2018.1.382
14. Fuller SJ, Kumar P, Weltman M, Wiley JS. Autoimmune hemolysis associated with primary biliary cirrhosis responding to ursodeoxycholic acid as sole treatment. *Am J Hematol*. 2003;72(1):31–33. doi:10.1002/ajh.10252
15. Morse EE. Mechanisms of hemolysis in liver disease. *Ann Clin Lab Sci*. 1990;20(3):169–174. PMID:2188563.
16. Tariq T, Karabon P, Irfan FB, Sieloff EM, Patterson R, Desai AP. National trends and outcomes of nonautoimmune hemolytic anemia in alcoholic liver disease: Analysis of the nationwide inpatient sample. *J Clin Gastroenterol*. 2021;55(3):258–262. doi:10.1097/MCG.0000000000001383
17. Douglass CC, McCall MS, Frenel EP. The acanthocyte in cirrhosis with hemolytic anemia. *Ann Intern Med*. 1968;68(2):390–397. doi:10.7326/0003-4819-68-2-390
18. Fernández-Zamorano A, Arnalich F, Codoceo R, et al. Hemolytic anemia and susceptibility to hydrogen-peroxide hemolysis in children with vitamin E-deficiency and chronic liver disease. *J Med*. 1988;19(5–6): 317–334. PMID:3204329.
19. Cooper RA, Kimball DB, Durocher JR. Role of the spleen in membrane conditioning and hemolysis of spur cells in liver disease. *N Engl J Med*. 1974;290(23):1279–1284. doi:10.1056/NEJM197406062902303
20. Chitale AA, Sterling RK, Post AB, Silver BJ, Mulligan DC, Schulak JA. Resolution of spur cell anemia with liver transplantation: A case report and review of the literature. *Transplantation*. 1998;65(7):993–995. doi:10.1097/00007890-199804150-00021
21. Liu MX, Wen XY, Leung YK, et al. Hemolytic anemia in alcoholic liver disease: Zieve syndrome. A case report and literature review. *Medicine (Baltimore)*. 2017;96(47):e8742. doi:10.1097/MD.0000000000008742
22. Walia BN, Singh S, Marwaha RK, Bhusnurmath SR, Dilawari JB. Fulminant hepatic failure and acute intravascular haemolysis as presenting manifestations of Wilson's disease in young children. *J Gastroenterol Hepatol*. 1992;7(4):370–373. doi:10.1111/j.1440-1746.1992.tb01000.x
23. Walshe JM. The acute haemolytic syndrome in Wilson's disease: A review of 22 patients. *QJM*. 2013;106(11):1003–1008. doi:10.1093/qjmed/hct137
24. Stremmel W, Merle U, Weiskirchen R. Clinical features of Wilson disease. *Ann Transl Med*. 2019;7(Suppl 2):S61. doi:10.21037/atm.2019.01.20
25. European Medicines Agency. Summary Of Product Characteristics. https://www.ema.europa.eu/en/documents/product-information/ribavirin-teva-epar-product-information_en.pdf. Accessed August 7, 2021.
26. Krishnan SM, Dixit NM. Ribavirin-induced anemia in hepatitis C virus patients undergoing combination therapy. *PLoS Comput Biol*. 2011; 7(2):e1001072. doi:10.1371/journal.pcbi.1001072
27. Jimmerson LC, Clayton CW, MaWhinney S, et al. Effects of ribavirin/sofosbuvir treatment and ITPA phenotype on endogenous purines. *Antiviral Res*. 2017;138:79–85. doi:10.1016/j.antiviral.2016.12.005
28. Devine EB, Kowdley KV, Veenstra DL, Sullivan SD. Management strategies for ribavirin-induced hemolytic anemia in the treatment of hepatitis C: Clinical and economic implications. *Value Health*. 2001; 4(5):376–384. doi:10.1046/j.1524-4733.2001.45075.x
29. De Franceschi L, Fattovich G, Turrini F, et al. Hemolytic anemia induced by ribavirin therapy in patients with chronic hepatitis C virus infection: Role of membrane oxidative damage. *Hepatology*. 2000; 31(4):997–1004. doi:10.1053/he.2000.5789
30. Gonzalez-Casas R, Jones EA, Moreno-Otero R. Spectrum of anemia associated with chronic liver disease. *World J Gastroenterol*. 2009; 15(37):4653–4658. doi:10.3748/wjg.15.4653
31. Özatli D, Köksal AS, Haznedaroglu IC, et al. Erythrocytes: Anemias in chronic liver diseases. *Hematology*. 2000;5(1):69–76. doi:10.1080/10245332.2000.11746489
32. Camitta BM, Rappeport JM, Parkman R, Nathan DG. Selection of patients for bone marrow transplantation in severe aplastic anemia. *Blood*. 1975;45(3):355–363. PMID:1090310.
33. Bihari C, Anand L, Rooge S, et al. Bone marrow stem cells and their niche components are adversely affected in advanced cirrhosis of the liver. *Hepatology*. 2016;64(4):1273–1288. doi:10.1002/hep.28754
34. Anand L, Bihari C, Kedarisetty CK, et al. Early cirrhosis and a preserved bone marrow niche favour regenerative response to growth factors in decompensated cirrhosis. *Liver Int*. 2019;39(1):115–126. doi:10.1111/liv.13923
35. Rauff B, Idrees M, Shah SA, et al. Hepatitis associated aplastic anemia: A review. *Virol J*. 2011;8:87. doi:10.1186/1743-422X-8-87

36. Gonzalez-Casas R, Garcia-Buey L, Jones EA, Gisbert JP, Moreno-Otero R. Systematic review. Hepatitis-associated aplastic anaemia: A syndrome associated with abnormal immunological function. *Aliment Pharmacol Ther.* 2009;30(5):436–443. doi:10.1111/j.1365-2036.2009.04060.x
37. Sawada K, Takai A, Yamada T, et al. Hepatitis-associated aplastic anemia with rapid progression of liver fibrosis due to repeated hepatitis. *Intern Med.* 2020;59(8):1035–1040. doi:10.2169/internalmedicine.4072-19
38. Qureshi K, Sarwar U, Khallafi H. Severe aplastic anemia following acute hepatitis from toxic liver injury: Literature review and case report of a successful outcome. *Case Reports Hepatol*. 2014;2014:216570. doi:10.1155/2014/216570
39. Chisaka H, Morita E, Yaegashi N, Sugamura K. Parvovirus B19 and the pathogenesis of anaemia. *Rev Med Virol*. 2003;13(6):347–359. doi:10.1002/rmv.395
40. Alshaibani A, Dufour C, Risitano A, de Latour R, Aljurf M. Hepatitis-associated aplastic anemia [published online as ahead of print on November 10, 2021]. *Hematol Oncol Stem Cell Ther.* 2020;S1658-3876(20)30168-0. doi:10.1016/j.hemonc.2020.10.001
41. Safadi R, Or R, Ilan Y, et al. Lack of known hepatitis virus in hepatitis-associated aplastic anemia and outcome after bone marrow transplantation. *Bone Marrow Transplant*. 2001;27(2):183–190. doi:10.1038/sj.bmt.1702749
42. Gonçalves V, Calado R, Palaré MJ, Ferrão A, Morais A. Hepatitis-associated aplastic anaemia: A poor prognosis. *BMJ Case Rep*. 2013;2013:bcr2012007968. doi:10.1136/bcr-2012-007968
43. Ikawa Y, Nishimura R, Kuroda R, et al. Expansion of a liver-infiltrating cytotoxic T-lymphocyte clone in concert with the development of hepatitis-associated aplastic anaemia. *Br J Haematol.* 2013;161(4):599–602. doi:10.1111/bjh.12259
44. Young NS. Hematopoietic cell destruction by immune mechanisms in acquired aplastic anemia. *Semin Hematol*. 2000;37(1):3–14. doi:10.1016/s0037-1963(00)90026-x
45. Young NS. Pathophysiologic mechanisms in acquired aplastic anemia. *Hematology Am Soc Hematol Educ Program*. 2006;72–77. doi:10.1182/asheducation-2006.1.72
46. Morales-Mantilla DE, King KY. The role of interferon-gamma in hematopoietic stem cell development, homeostasis, and disease. *Curr Stem Cell Rep*. 2018;4(3):264–271. doi:10.1007/s40778-018-0139-3
47. Brown KE, Tisdale J, Barrett AJ, Dunbar CE, Young NS. Hepatitis-associated aplastic anemia. *N Engl J Med*. 1997;336(15):1059–1064. doi:10.1056/NEJM199704103361504
48. Tzakis AG, Arditi M, Whitington PF, et al. Aplastic anemia complicating orthotopic liver transplantation for non-A, non-B hepatitis. *N Engl J Med*. 1988;319(7):393–396. doi:10.1056/NEJM198808183190702
49. Delehaye F, Habes D, Dourthe ME, et al. Management of childhood aplastic anemia following liver transplantation for nonviral hepatitis: A French survey. *Pediatr Blood Cancer.* 2020;67(4):e28177. doi:10.1002/pbc.28177
50. Young NS, Calado RT, Scheinberg P. Current concepts in the pathophysiology and treatment of aplastic anemia. *Blood.* 2006;108(8):2509–2519. doi:10.1182/blood-2006-03-010777
51. Ioannou S, Hatzis G, Vlahadami I, Voulgarelis M. Aplastic anemia associated with interferon alpha 2a in a patient with chronic hepatitis C virus infection: A case report. *J Med Case Rep.* 2010;4:268. doi:10.1186/1752-1947-4-268

# Ambulatory pulse pressure and its contributors in autosomal dominant polycystic kidney disease

Agata Koska-Ścigała[1,B–D], Magdalena Jankowska[2,A–D], Anna Szyndler[3,E], Krzysztof Narkiewicz[3,E,F], Alicja Dębska-Ślizień[2,E,F]

[1] Department of Neurology, Regional Hospital in Elbląg, Poland
[2] Department of Nephrology, Transplantology and Internal Medicine, Faculty of Medicine, Medical University of Gdańsk, Poland
[3] Department of Hypertension and Diabetology, Faculty of Medicine, Medical University of Gdańsk, Poland

A – research concept and design; B – collection and/or assembly of data; C – data analysis and interpretation;
D – writing the article; E – critical revision of the article; F – final approval of the article

Advances in Clinical and Experimental Medicine, ISSN 1899–5276 (print), ISSN 2451–2680 (online) *Adv Clin Exp Med*. 2022;31(5):575–578

**Address for correspondence**
Magdalena Jankowska
E-mail: maja@gumed.edu.pl

**Funding sources**
A grant from National Science Centre, Kraków, Poland (No. 2018/30/M/NZ5/00480).

**Conflict of interest**
None declared

Received on May 17, 2021
Reviewed on March 16, 2022
Accepted on April 21, 2022

Published online on May 11, 2022

## Abstract

**Background.** Pulse pressure (PP) is a pulsatile component of blood pressure (BP), strongly correlated with arterial stiffness (AS) and impacting prognosis. Disproportionally increased PP values in individuals with autosomal dominant polycystic kidney disease (ADPKD) should be expected, given the multifactorial cardiovascular involvement in the natural course of this disease.

**Objectives.** To investigate ambulatory PP in a group of ADPKD patients, and to examine the impact of age, sex, kidney function, hypertension, circadian rhythm, and antihypertensive drugs (AH) on studied parameters.

**Materials and methods.** A total of 130 ADPKD patients (median age 41 years, 35% men) who underwent 24-hour BP measurement with portable oscillometer Spacelabs 90217, were included in the study and their recordings were retrospectively analyzed. Demographic data and the medical history including antihypertensive treatment were collected, ADPKD was diagnosed based on the criteria by Pei et al., and estimated glomerular filtration rate (eGFR) was calculated according to the Chronic Kidney Disease Epidemiology Collaboration (CKD-EPI) equation.

**Results.** Pulse pressure in the whole group was 46 (IQR: 42–53) mm Hg and it was significantly higher in men than in women and during the day compared to nighttime. There was a negative correlation of PP with eGFR and a positive correlation with age. Pulse pressure was not different in ADPKD patients with or without a diagnosis of hypertension.

**Conclusions.** Ambulatory PP is not substantially increased in ADPKD patients across different stages of CKD. It follows a regular pattern of being increased with age, male sex, daytime, and decreasing eGFR, but not with the diagnosis of hypertension.

**Key words:** hypertension, ADPKD, pulse pressure

**Cite as**
Koska-Ścigała A, Jankowska M, Szyndler A, Narkiewicz K, Dębska-Ślizień A. Ambulatory pulse pressure and its contributors in autosomal dominant polycystic kidney disease. *Adv Clin Exp Med*. 2022;31(5):575–578. doi:10.17219/acem/149373

**DOI**
10.17219/acem/149373

## Background

Pulse pressure (PP) is defined as an arithmetic difference between systolic blood pressure (SBP) and diastolic blood pressure (DBP).[1] However, being easily accessible and extremely simple to obtain, it seems not appreciated highly enough in the clinical settings, given that PP surpasses many other indices, including mean arterial pressure (MAP), as a predictor of cardiovascular complications. Pulse pressure is also an established risk factor for unfavorable cardiovascular and kidney outcomes in patients with chronic kidney disease (CKD).[2–4]

Arterial stiffness (AS) is a consequence of arteriosclerosis, loss of elastin, collagen replacement, calcification, thickening of the artery wall, and impaired endothelium-dependent vasodilatation.[5] It leads to high PP with disturbed perfusion flow, causing hypertrophy and/or hyperplasia of smooth muscles in the arterial wall, and end organ damage.[6]

Interestingly, patients with autosomal dominant polycystic kidney disease (ADPKD), the most common genetic cause of kidney failure, present with all the abovementioned contributors to increased PP and AS. Progressive renal dysfunction in ADPKD is caused by an enlargement of cysts, and it often leads to a dependence on renal replacement therapy (RRT).[7] Endothelium damage occurs in the early stages of the disease.[8] Also, abnormal function of polycystins, products of genes directly involved in the pathogenesis of ADPKD, is responsible for vascular damage.[9,10]

## Objectives

The aim of the study was to investigate ambulatory PP in a group of ADPKD patients and to examine the impact of age, sex, kidney function, hypertension, circadian rhythm, and antihypertensive drugs (AH) on studied parameters.

## Materials and methods

Patients older than 18, recruited from a single outpatient center, with an established diagnosis of ADPKD based on clinical criteria by Pei et al., were referred to ambulatory blood pressure monitoring (ABPM) between 2014 and 2018.[11] Renal function was assessed by estimating creatinine clearance using the Chronic Kidney Disease Epidemiology Collaboration (CKD-EPI) equation. Hypertension was diagnosed based on prior medical history or the use of AH agents. The exclusion criteria included diabetes mellitus and other comorbidities influencing the vascular phenotype.

For ambulatory 24-hour BP monitoring, portable oscillometer was used – Spacelabs 90217 (Spacelabs Healthcare Company, Issaquah, USA). Monitors were programmed to obtain readings at 15-minute intervals during daytime (6:00–22:00) and 30-minute intervals during nighttime (22:00–6:00). The arm cuff was positioned on the nondominant upper limb. Pulse pressure was calculated as SBP–DBP. Mean arterial pressure was calculated as DBP plus 1/3 of PP.

The collection and analysis of blinded data were approved by Ethical Committee of the Medical University of Gdansk, Poland (approval No. NKBBN 429/2019).

### Statistical analyses

For statistical analysis, we used STATISTICA v. 10 (StatSoft Inc., Tulsa, USA). The normality of distribution was tested using the Shapiro–Wilk test. Data did not follow a normal distribution and were expressed as medians and interquartile range (IQR). We compared groups with the Mann–Whitney U test or Kruskal–Wallis analysis of variance (ANOVA) by ranks, as appropriate. Correlations were expressed as Spearman's coefficients. Differences and associations were considered significant for $p < 0.05$.

## Results

Data of 24-hour ABPM from 130 ADPKD patients were collected. The median age of the study group was 41 (33–51) years and there were 46 men (35%). Mean estimated glomerular filtration rate (eGFR) in the whole group was 79 (54–90) mL/min/1.73 m$^2$. Median SBP was 126 (120–133) mm Hg and median DBP was 74 (75–84) mm Hg. Characteristics of the group stratified according to the CKD stage are displayed in Table 1. A majority (68%) of patients were in G1 or G2 CKD stage.

Pulse pressure in the whole group was 46 (42–53) mm Hg, and it was significantly higher in men than in women (49 (44–55) mm Hg compared to 44 (41–51) mm Hg, respectively, $Z = -2.77$; $p_{Mann–Whitney} = 0.005$). Also, there was a significant diurnal difference in PP: 47 (42–54) mm Hg during the day compared to 45 (41–52) mm Hg at night, $Z = 3.60$; $p = 0.001$. Figure 1 displays a comparison of PP according the CKD grade Kruskal–Wallis H test ((KW-H) (4; 129) = 7.2042; $p = 0.126$ (we excluded CKD G5 patients from this analysis as there was only 1 such patient in this group)). We found a weak correlation (Spearman's test) between PP and age ($r = 0.210$; $p < 0.05$).

Pulse pressure was not different in patients with or without a diagnosis of hypertension.

Eighty-seven patients were treated with AH. We analyzed the impact of the number and class of AH on the PP value (Table 2). Pulse pressure was not different between patients non-treated or treated with a different number of AH (1–4 drugs, Fig. 2). Pulse pressure was higher in a group of patients that received blockers of α1-adrenergic receptors (AB) (54 (51–61) mm Hg in non-treated patients compared to 46 (42–53) mm Hg in treated ones; $p_{Mann–Whitney} = 0.038$). The AB treatment was not significantly associated with a different MAP (97 mm Hg compared to 95 mm Hg; $Z = -0.94$; $p_{Mann–Whitney} = 0.344$) for treated and non-treated patients, respectively.

Table 1. Characteristics of study group regarding CKD stage

| Stage (n) | Age [years] | Men, n (%) | MAP [mm Hg] | PP [mm Hg] | AH [%] |
|---|---|---|---|---|---|
| G1 (42) | 31 (23–37) | 12 (26) | 93 (88–99) | 44 (40–49) | 35 |
| G2 (47) | 43 (34–53) | 19 (41) | 95 (89–101) | 45 (41–53) | 47 |
| G3a (15) | 46 (35–63) | 5 (10) | 94 (93–100) | 49 (42–54) | 87 |
| G3b (15) | 50 (42–61) | 5 (10) | 99 (95–102) | 46 (42–52) | 87 |
| G4 (10) | 52 (38–61) | 5 (10) | 94 (91–97) | 53 (43–60) | 90 |
| G5 (1) | 46 | 0 | 99 | 53 | 100 |
| All (130) | 41 (33–51) | 46 (35) | 95 (90–100) | 46 (42–53) | 60 |

Data are expressed as median (Q1–Q3) unless indicated otherwise. CKD – chronic kidney disease; MAP – mean arterial pressure; PP – pulse pressure; AH – antihypertensive drugs.

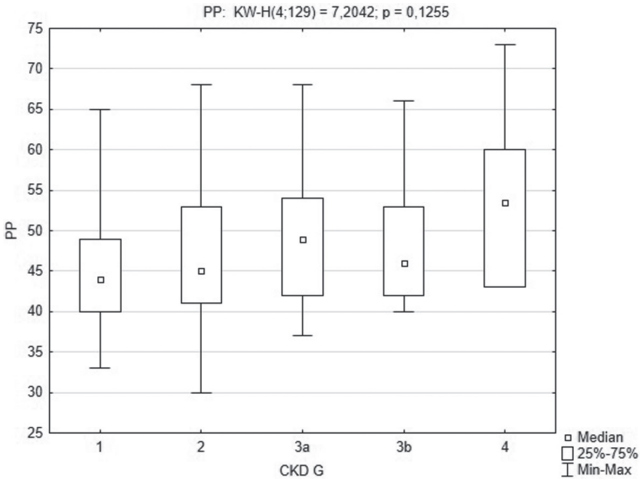


Fig. 1. Box and whisker plot of pulse pressure (PP) by stage of chronic kidney disease (CKD)

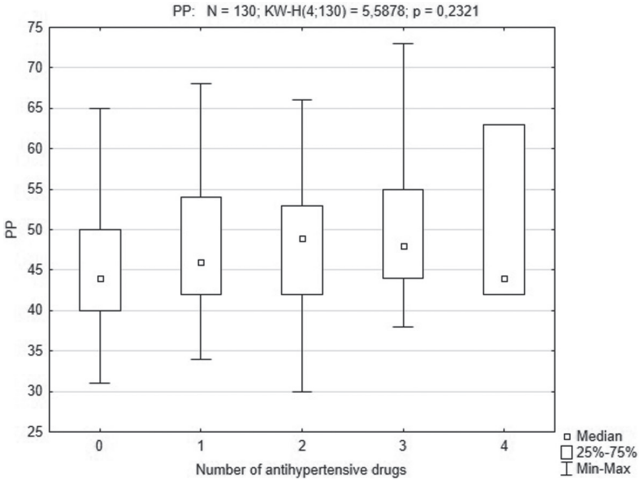


Fig. 2. Box and whisker plot of pulse pressure (PP) according to the number of prescribed antihypertensive drugs

Table 2. Comparison of PP (Mann–Whitney test) regarding the class of antihypertensive medication used in the treatment (only treated patients included, n = 78)

| Variable | ACEI | ARB | ACEI/ARB | CCB | Diuretics | BB | AB |
|---|---|---|---|---|---|---|---|
| PP* [mm Hg] treated | 47 (42–54) | 47 (42–53) | 46 (42–53) | 48 (42–54) | 49 (42–54) | 47 (43–56) | 54 (51–61) |
| PP* [mm Hg] non-treated | 46 (42–53) | 45 (44–60) | 49 (43–54) | 48 (43–54) | 44 (42–51) | 49 (42–54) | 46 (42–53) |
| Z | 0.35 | –1.13 | 1.12 | –1.79 | –0.08 | –1.46 | –2.40 |
| p-value | 0.7251 | 0.2584 | 0.2601 | 0.0734 | 0.9327 | 0.1418 | **0.0161** |

* Data are expressed as median (IQR). Values in bold are statistically significant. PP – pulse pressure; ACEI – angiotensin-converting enzyme inhibitors; ARB – angiotensin receptor blockers; CCB – calcium channel blockers; BB – β-blockers; AB – α1-blockers; IQR – interquartile range.

# Discussion

High PP is strongly correlated with stiffened arteries which cannot dampen pulsatile flow and may cause the destruction of the arterial walls, microvascular remodeling and microinfarcts, particularly in high-flow organs like the brain and kidneys, sensitive to PP.[12] Furthermore, AS increases left ventricular pulsatile work, wall stress and myocardial oxygen consumption, and causes left ventricular hypertrophy (LVH).[13] The LVH preceding hypertension has been described in early ADPKD and could be explained by several rationales.[14] Polycystin 1 and polycystin 2 are present in endothelial cells, vascular smooth muscle cells, cardiomyocytes, and fibroblasts. Insufficient polycystin dosage leads to the reduced availability of nitric oxide synthase in the vascular endothelium and results in insufficient vasodilatation.[9] This is observed also in people with ADPKD without hypertension or renal decline.[15] Vasoconstriction in ADPKD is also supported by a high level of endothelin I.[8] In this way, the balance between vasodilatation and vasoconstriction is impaired and causes vascular remodeling. Interestingly, also the mechanism of bone formation and vascular calcification may be at play in ADPKD and influence AS across different stages of ADPKD.[16]

Given the results of the HALT Progression of Polycystic Kidney Disease (HALT-PKD) study,[17] one might expect disproportionally increased PP values in ADPKD individuals. However, it seems not to be the case. The median value of 24-hour PP in a group of 130 patients with ADPKD was 46 (42–53) mm Hg. Although the exact target PP value has

not been established, it is known that individuals in the highest tenth of the 24-hour PP distribution had a significantly higher-than-average cardiovascular risk in multivariable-adjusted models.[18] We stratified PP in our group according to age and sex, as PP is known to be higher in men and to increase with age. Both statements held true in our cohort, although the rate of PP rise accelerates after attaining 50 years of age, and our group was relatively young (median: 41 years). In a recently published study analyzing the results from the International Database on Ambulatory Blood Pressure in Relation to Cardiovascular Outcome (IDACO) that comprises over 11,000 participants, the mean PP was higher (49.7 ±10.0 mm Hg).[19] Also, median PP in adults >50 years of age from our study (50 mm Hg) fits into the low-middle PP category (41.17–51.19 mm Hg) from IDACO.[19] This may come as a surprise, given the aforementioned facts imposing a substantial risk of AS and vascular resistance on ADPKD patients. On the other hand, this finding goes in line with the excellent prognosis and low mortality rate in RRT patients with ADPKD, as compared to other etiologies.

Patients treated with AB had higher 24-hour PP values, although we found no difference in MAP between AB receivers and non-receivers. This fact can be explained by the effects of sympathetic vascular tone on arterial pressure and its involvement in the wave reflection and modulation of the aortic PP. However, the most probable explanation of this finding is older age and lower eGFR in patients treated with AB. The best practice remains using renin–angiotensin–aldosterone (RAA) blockade as the therapy of the first choice in different stages of ADPKD, as reflected in both arms of the HALT-PKD study.[17,20]

## Limitations

The first limitation of the study is a cross-sectional design. We were able to infer about associations but not of any causative relations between analyzed groups of AH and PP. Second, only a single ABPM measurement was performed and we might have missed some fluctuations in PP with time. Finally, we did not have a control group of individuals without ADPKD for comparisons. Adjusting for age, hypertension and stage of CKD would be very difficult in such a group. Third, we report only a single-center experience. However, due to a reliable protocol of measurement and verified equipment, we believe that our results are easily replicable in other centers.

# Conclusions

Ambulatory PP is not substantially increased in ADPKD patients across different stages of CKD. It follows a regular pattern of being increased with age, male sex, daytime, and decreasing eGFR, but not with the diagnosis of hypertension.


## ORCID iDs

Agata Koska-Ścigała https://orcid.org/0000-0002-4832-160X
Magdalena Jankowska https://orcid.org/0000-0002-2432-6350
Anna Szyndler https://orcid.org/0000-0002-5720-128X
Krzysztof Narkiewicz https://orcid.org/0000-0001-5949-5018
Alicja Dębska-Ślizień https://orcid.org/0000-0001-8210-8063


## References


1. Gillebert TC. Pulse pressure and blood pressure components: Is the sum more than the parts? *Eur J Prev Cardiol*. 2018;25(5):457–459. doi:10.1177/2047487318755805
2. Klassen PS, Lowrie EG, Reddan DN, et al. Association between pulse pressure and mortality in patients undergoing maintenance hemodialysis. *JAMA*. 2002;287:1548–1555. doi:10.1001/jama.287.12.1548
3. Wang Z, Yu D, Cai Y, et al. Optimal cut-off threshold in pulse pressure predicting cardiovascular death among newly diagnosed end-stage renal disease patients: A prospective cohort study. *Medicine (Baltimore)*. 2019;98(27):e16340. doi:10.1097/MD.0000000000016340
4. Low S, Moh A, Ang SF, et al. The role of pulse pressure in navigating the paradigm of chronic kidney disease progression in type 2 diabetes mellitus. *J Nephrol*. 2021;34(5):1429–1444. doi:10.1007/s40620-020-00954-3
5. Bakris GL, Laffin LJ. Assessing wide pulse pressure hypertension: Data beyond the guidelines. *J Am Coll Cardiol*. 2019;73(22):2856–2858. doi:10.1016/j.jacc.2019.03.494
6. Safar M, Nilsson P, Blacher J, et al. Pulse pressure, arterial stiffness and end-organ damage. *Curr Hypertens Rep*. 2012;14(4):339–344. doi:10.1007/s11906-012-0272-9
7. Cornec-Le Gall E, Alam A, Perrone RD. Autosomal dominant polycystic kidney disease. *Lancet*. 2019;393(10174):919–935. doi:10.1016/S0140-6736(18)32782-X
8. Ecder T, Schrier RW. Cardiovascular abnormalities in autosomal-dominant polycystic kidney disease. *Nat Rev Nephrol*. 2009;5(4):221–228. doi:10.1038/nrneph.2009.13
9. Kuo IY, Chapman AB. Polycystins, ADPKD, and cardiovascular disease. *Kidney Int Rep*. 2019;5(4):396–406. doi:10.1016/j.ekir.2019.12.007
10. Kang YR, Ahn JH, Kim KH, et al. Multiple cardiovascular manifestations in a patient with autosomal dominant polycystic kidney disease. *J Cardiovasc Ultrasound*. 2014;22:144–147. doi:10.4250/jcu.2014.22.3.144
11. Pei Y, Hwang YH, Conklin J, et al. Imaging-based diagnosis of autosomal dominant polycystic kidney disease. *J Am Soc Nephrol*. 2015;26:746–753. doi:10.1681/ASN.2014030297
12. Adji A, O'Rourke MF, Namasivayam M. Arterial stiffness, its assessment, prognostic value, and implications for treatment. *Am J Hypertens*. 2011;24(1):5–17. doi:10.1038/ajh.2010.192
13. Ecder T, Schrier RW. Hypertension in autosomal-dominant polycystic kidney disease: Early occurrence and unique aspects. *J Am Soc Nephrol*. 2001;12(1):194–200. doi:10.1681/ASN.V121194
14. Vaccarino V, Holford TR, Krumholz HM. Pulse pressure and risk for myocardial infarction and heart failure in the elderly. *J Am Coll Cardiol*. 2000;36(1):130–138. doi:10.1016/s0735-1097(00)00687-2
15. Raptis V, Loutradis C, Sarafidis PA. Renal injury progression in autosomal dominant polycystic kidney disease: A look beyond the cysts. *Nephrol Dial Transplant*. 2018;33(11):1887–1895. doi:10.1093/ndt/gfy023
16. Jankowska M, Haarhaus M, Qureshi AR, et al. Sclerostin: A debutant on the autosomal dominant polycystic kidney disease scene? *Kid Int Rep*. 2017;2(3):481–485. doi:10.1016/j.ekir.2017.01.001
17. Schrier RW, Abebe KZ, Perrone RD, et al. Blood pressure in early autosomal dominant polycystic kidney disease. *N Engl J Med*. 2014;371:2255–2266. doi:10.1056/NEJMoa1402685
18. Gu YM, Thijs L, Li Y, et al. Outcome-driven thresholds for ambulatory pulse pressure in 9938 participants recruited from 11 populations. *Hypertension*. 2014;63(2):229–237. doi:10.1161/HYPERTENSIONAHA.113.02179
19. Melgarejo JD, Thijs L, Wei DM, et al. Relative and absolute risk to guide the management of pulse pressure, an age-related cardiovascular risk factor. *Am J Hypertens*. 2021;34(9):929–938. doi:10.1093/ajh/hpab048
20. Torres VE, Abebe KZ, Chapman AB, et al. Angiotensin blockade in late autosomal dominant polycystic kidney disease. *N Engl J Med*. 2014;371(24):2267–2276. doi:10.1056/NEJMoa1402686